Industria Textilă

ISSN 1222-5347

1/2019

Revistă **cotată ISI** și inclusă în **Master Journal List** a Institutului pentru Știința Informării din Philadelphia – S.U.A., începând cu vol. 58, nr. 1/2007/

ISI rated *magazine, included in the* ***ISI Master Journal List*** *of the Institute of Science Information, Philadelphia, USA, starting with vol. 58, no. 1/2007*

Editată în 6 nr./an, indexată și recenzată în:

Edited in 6 issues per year, indexed and abstracted in:

Science Citation Index Expanded (SciSearch®), Materials Science Citation Index®, Journal Citation Reports/Science Edition, World Textile Abstracts, Chemical Abstracts, VINITI, Scopus, Toga FIZ technik ProQuest Central

Editată cu sprijinul Ministerului Cercetării și Inovării

Recunoscută în România, în domeniul Științelor inginerești, de către **Consiliul Național al Cercetării Științifice din Învățământul Superior** (C.N.C.S.I.S.), în **grupa A** /

Aknowledged in Romania, in the engineering sciences domain, by the ***National Council of the Scientific Research from the Higher Education*** *(CNCSIS), in* ***group A***

Contents

EDITORIAL STAFF

Editor-in-chief: Dr. eng. Emilia Visileanu
Graphic designer: Florin Prisecaru
e-mail: industriatextila@certex.ro

Journal edited in colaboration with **Editura AGIR**, 118 Calea Victoriei, sector 1, Bucharest, tel./fax: 021-316.89.92; 021-316.89.93;
e-mail: editura@agir.ro, www.edituraagir.ro

Influence of dye structure and temperature on the adsorption of acid dyes onto polyamide 6 knitwear

DOI: 10.35530/IT.070.01.1400

MATEJA KERT
INES BESEDIČ
ČRTOMIR PODLIPNIK

REZUMAT – ABSTRACT

Influența structurii colorantului și a temperaturii asupra adsorbției coloranților acizi pe tricoturile din poliamidă 6

A fost studiată influența structurii colorantului și a temperaturii de vopsire asupra adsorbției coloranților acizi pe tricoturile din poliamidă 6 (PA 6). Au fost utilizați trei coloranți acizi cu conținut diferit de grupări sulfonice, și anume C. I. roșu acid 88, C. I. roșu acid 14 și C. I. roșu acid 18. Vopsirea a fost efectuată cu aparatul Launder-ometer la 40°C și 60°C, la pH 4. Probele au fost scoase din aparat la intervale diferite de timp. Rezultatele au arătat că atât structura colorantului, cât și temperatura de vopsire au afectat adsorbția coloranților acizi pe tricoturile din PA 6. Rata și cantitatea de adsorbție au crescut odată cu creșterea temperaturii de vopsire și cu scăderea numărului de grupări sulfonice din coloranți.

Cuvinte-cheie: colorant acid, poliamidă 6, vopsire, adsorbție

Influence of dye structure and temperature on the adsorption of acid dyes onto polyamide 6 knitwear

In this research, the influence of dye structure and dyeing temperature on the adsorption of acid dyes onto polyamide 6 knitwear (PA 6) was studied. Three acid dyes with different amounts of sulphonic groups, namely C. I. Acid Red 88, C. I. Acid Red 14, and C. I. Acid Red 18 were used. Dyeing was performed in a Launder-ometer apparatus at 40°C and 60°C, at pH 4. The samples were taken out of the apparatus at different time intervals. The results showed that both dye structure and dyeing temperature affected the adsorption of acid dyes onto PA 6 knitwear. The rate and quantity of adsorption increased with an increase in dyeing temperature and a decrease in the number of sulphonic groups in dyes.

Keywords: acid dye, polyamide 6, dyeing, adsorption

INTRODUCTION

The adsorption of acid dyes onto polyamide 6 fibres is affected by a number a factors such as: dye structure, dye concentration, dyeing agents (e.g., levelling agents), liquor-to-goods ratio, dyeing temperature, dyeing time, and pH value of the dyebath [1–3]. In the process of dyeing, acid dyes migrate from the dyebath onto a fibre surface as a consequence of different attractive intermolecular forces between dyes and fibres. These attractive forces usually depend on both the chemical structure of dyes and the presence of functional groups on fibre surface that are mostly pH-dependent. During dyeing, the concentration of dyes on the fibre surface increases with dyeing time, whilst that in the dyebath decreases. Equilibrium is reached at the interface fibre-dyebath, when the concentration of dyes on the fibre does not change with time. At this point the adsorption rate of dyes from the dyebath is equal to the desorption rate of dyes from the fibre surface [4]. One of the factors that affect the adsorption of dyes onto fibres is the chemical structure of dyes. The studies done so far showed that the number of sulphonic groups in acid dyes affects the adsorption onto the cationic textile substrate [5–8], to which polyamide belongs in an acidic pH. The dyes containing more sulphonic groups are adsorbed by polyamide and wool fabrics to lesser extent in comparison to those containing fewer sulphonic groups. Studies showed that the acid dyes containing one sulphonic group exhibit good adsorption capability for a polyamide at high pH values, whilst the satisfactory adsorption of acid dyes with multiple sulphonic groups is obtained only at very low pH values [5]. The number of sulphonic groups in acid dyes also affects the overdyeing process of polyamide. Numerous studies [5–6, 8] showed that overdyeing appeared on the polyamide when acid dyes with higher affinity were used, and when dyes included a lower number of sulphonic groups in the structure. The highest overdyeing of polyamide was achieved with dyes containing one sulphonic group, followed by the dye containing two sulphonic groups, then the dye with three sulphonic groups, whilst the dye C. I. Acid Red 41 – containing four sulphonic groups – showed no trends toward overdyeing [8]. In the area of overdyeing, the acid dyes with two or three sulphonic groups are not able to form a bridge between amido groups of adjacent chains, meaning that acid dyes with a higher amount of sulphonic groups behave similarly as dyes with only one sulphonic group [5].

The purpose of this research is to investigate the influence of both the structure of acid dyes and the dyeing temperature on the adsorption of acid dyes on polyamide 6 warp knitwear in weakly acidic conditions. The dyeing was performed with three anionic acid dyes, containing different quantities of sulphonic groups, at two dyeing temperatures (40°C and 60°C), and at pH 4. It was assumed that the exhaustion of dye to polyamide 6 knitwear is affected by the dye structure, dyeing temperature, and dyeing time.

EXPERIMENTAL

Materials

The polyamide 6 (PA 6) warp knitwear was supplied by AquafilSLO, Ljubljana, which has the following specifications: a density of 31 lines/cm, 29 columns/cm, and mass per square metre 72 g/m^2. Before dyeing, PA 6 knitwear was soaped for 30 minutes at 45–50 ºC in a solution containing 0.5 g/l nonionic detergent (Teopon 100; Orka, Ljubljana) using a liquor-to-goods ratio of 20:1, and was thoroughly rinsed, and air-dried. Prior to dyeing, the conditioning of samples in the standard conditions (SIST EN ISO 139:2005) was carried out. The weight of each sample was 2.0 g.

The dyes used in the research were C.I. Acid Red 88 (AR88), C.I. Acid Red 14 (AR14), and C.I. Acid Red 18 (AR18). All dyes were Sigma Aldrich products and used as received. Citric acid and disodium hydrogen phosphate were of laboratory grade and purchased from Sigma Aldrich products. The structures of acid dyes are presented in figure 1.

Dyeing

The dyeing of PA 6 samples was performed in the Launder-ometer apparatus using a liquor-to-goods ratio 150:1 at pH 4. A McIlvain buffer consisting of citric acid and disodium hydrogen phosphate was used to prepare a buffer solution of pH 4. Before dyeing, the pH of the buffered solution was measured using the MA 5740 pH-metre (Iskra, Ljubljana). The buffer solution was prepared directly before dyeing. Knitwear was dyed with 1% o.m.f dyes. Dyeing was conducted at 40 °C and 60 °C in two replicates. Before dyeing, the dyebath was warmed up to the dyeing temperature and the samples were introduced into the beakers. The samples were then taken out of the beakers at the following time intervals (t): 5, 10, 20, 30, 45, 60, 90, 120, 150, 200, 240, and 360 minutes. The dyed samples were dried on a flat surface in the open air at room temperature of 23 °C.

ANALYSIS OF DYEING

Determination of the dyebath exhaustion

The calibration curve (absorbance vs. dye concentration) of each dye was prepared in a buffered solution of pH 4 at 25°C, using a 1-cm path length quartz cell housed in an UV-VIS spectrophotometer Cary 1E (Varian, Australia). From the calibration curves the concentrations of dyes in the dyebath before and after dyeing were determined at the maximum absorption wavelength (λ_{max} = 506 nm for AR88, 515 nm for AR14, and 507 nm for AR18). The percentage of exhaustion (E), which is a function of dyeing time and temperature, was calculated using the following equation [4]:

$$E(\%) = 100 \times \frac{C_o - C_d}{C_o} \quad (1)$$

where C_o and C_d are the concentrations of dyes in the dyebath before and after dyeing.

Colorimetric measurements

The reflectance value (R) at the maximum absorption wavelength (λ_{max}) and CIELAB colour values of the dyed fabric were measured in a standard atmosphere (SIST EN ISO 139:2005) using the SF600 PLUS-CT spectrophotometer (Datacolor, Switzerland). The measurements were conducted using illuminant D_{65}, measuring geometry d/8°, 10° standard observer, and a 9 mm aperture. An eight-layer sample was employed to avoid the transmission of light. For each dyed sample, 10 measurements were performed and a mean value was presented as a result. From the values of R the Kubelka-Munk values (K/S) was calculated according to equation 2, in order to express colour strength.

$$\frac{K}{S} = \frac{(1-R)^2}{2R} \quad (2)$$

where K is the absorption coefficient and S – the scattering coefficient for a coloured substrate at a specific wavelength. R is the fractional reflectance value of the dye on the substrate at the λ_{max}.

Adsorption kinetics

To describe the adsorption kinetics of the studied dyes a pseudo-second order model was used, based on the following differential equation:

$$\frac{dC_e}{dC_t} = k(C_e - C_t)^2 \quad (3)$$

By the integration of equation 3 for boundary conditions t = 0 to t = t and C_t = 0 to C_t = C_t the following equation is given:

$$\frac{1}{(C_e - C_t)} = \frac{1}{C_e} + kt \quad (4)$$

where C_e (mg g^{-1}) is the amount of dye adsorbed on PA6 knitwear at equilibrium, C_t – the amount of dye

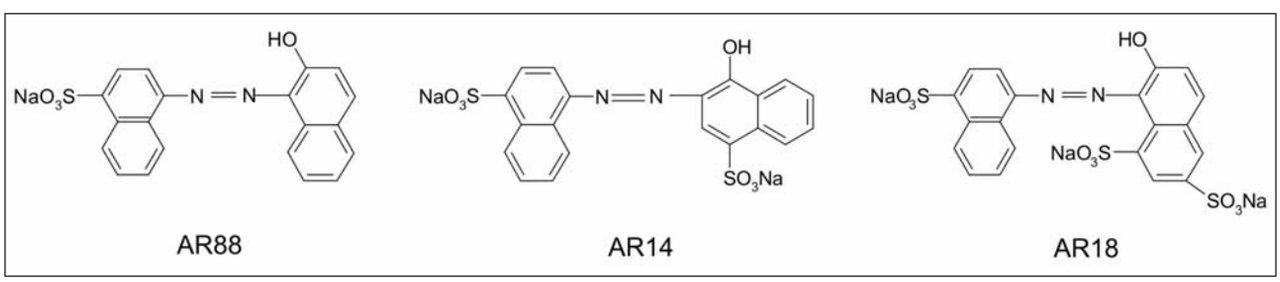

Fig. 1. Structure of the dyes used in the research

adsorbed on PA 6 knitwear at time t, and k (g mg^{-1} min^{-1}) – the adsorption rate constant.
Equation 4 can be rearranged into:

$$\frac{t}{C_t} = \frac{1}{kC_e^2} + \frac{1}{C_e}t \quad (5)$$

From the linear function of plot t/C_t versus t the adsorption parameters k and C_e, and the correlation coefficient, r^2, were calculated.

Determination of octanol-water partition and distribution coefficient

The octanol-water partition coefficient, expressed in its logarithmic form (log P), is the most widely used accepted measure of lipophilicity. It refers to the partitioning of the same species of a substance between octanol and aqueous phase (equation 6).

$$\log P_{octanol/water} = \log\left(\frac{[solute]_{octanol}}{[solute]^{un\text{-}ionized}_{water}}\right) \quad (6)$$

In the case, when substances, which contain ionogenic functions, may exist as a mixture of the dissociated and undissociated forms at different pH values, the distribution coefficient (mostly used as log D) is more appropriate [9]. It refers to more complex partitioning equilibria. Distribution coefficient is the ratio of the sum of the concentrations of all species of the compound in octanol to the sum of the concentrations of all species of the compound in water (equation 7).

$$\log D_{octanol/water} = \log\left(\frac{[solute]_{octanol}}{[solute]^{ionized}_{water} + [solute]^{neutral}_{water}}\right) \quad (7)$$

In the research the values of log P and log D of studied dyes was calculated by the use of MarvinSketch version 17.22, calculation module developed by ChemAxon [10], where log D was predicted from the dyes structures. The calculation is based on model, expressed in details at reference [9]. From values of log D an approximation of hydrophilic or hydrophobic performance of acid dyes can be given.

RESULTS AND DISCUSSION

The influence of acid dye structure (AR88, AR14, and AR18) on adsorption on PA 6 knitwear was spectrophotometrically evaluated by the determination of the dye concentration in the dyebath after dyeing and the colour strength (*K/S*) of the dyed samples. In figure 2 the percentage of exhaustion (E) vs. dyeing time (t) is presented, whilst in figure 3 the colour strength (*K/S*) vs. dyeing time (t) is presented.
It can be seen from figure 2 that the percentage of exhaustion was strongly influenced by dyeing temperature, dyeing time, and dye structure. The values of E increased with the increase of both dyeing time and dyeing temperature. For all studied dyes the higher value of E was obtained at 60°C rather than at 40°C. Wen et al. confirmed the same phenomenon for the dyeing of wool powders with acid dyes [10]. The percentage of exhaustion increased by prolongation of the dyeing time until equilibrium was

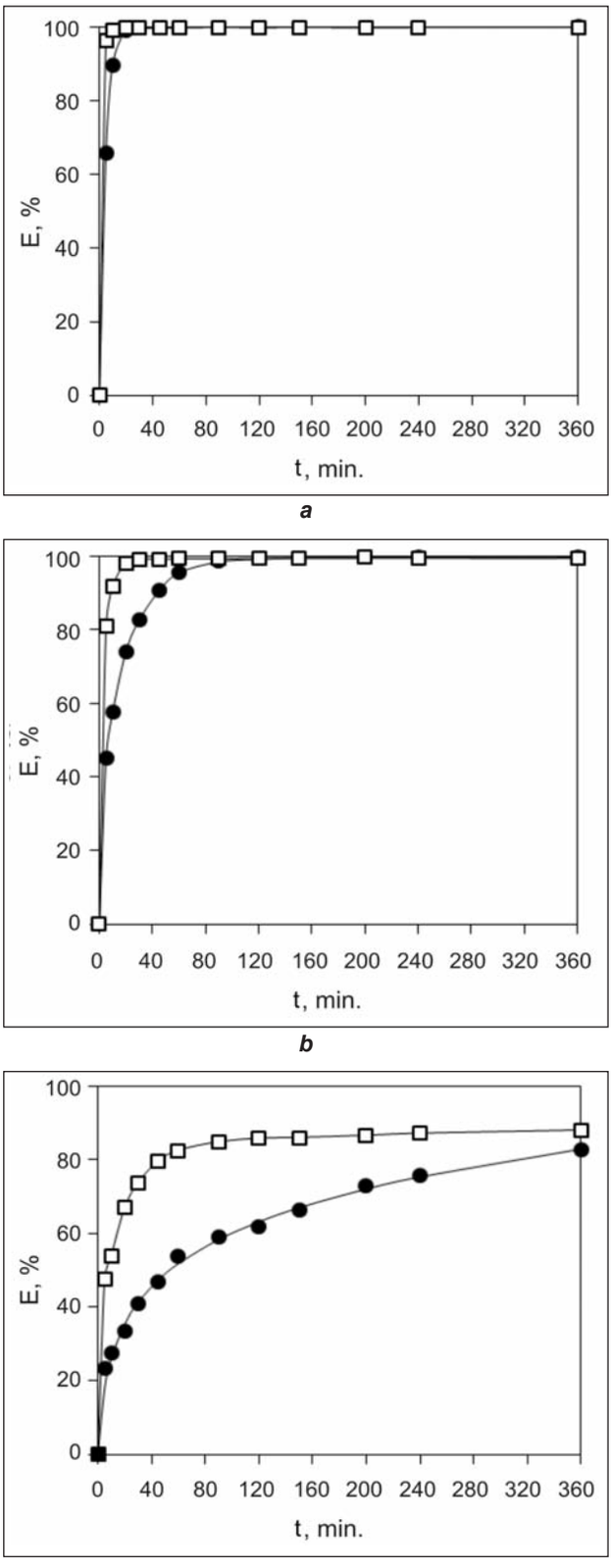

Fig. 2. Percentage of exhaustion as a function of dyeing time for the PA 6 knitwear dyed with AR88 (a), AR14 (b), and AR18 (c) at two temperatures. ● – 40°C, □ – 60°C

reached, where no change of E with t was noticed. Figure 2, *a* shows that for the dye AR88 the equilibrium was reached after 40 minutes of dyeing at 40°C, whilst at 60°C the equilibrium was reached even after a shorter time, i.e. 20 minutes of dyeing. Using the dye AR14 (figure 2, *b*) the equilibrium was reached

after 120 minutes of dyeing in comparison to the dye AR18 (figure 2,*c*), where equilibrium was not reached even after 360 minutes of dyeing at 40°C. The latter indicates that the dye uptake is strongly affected by the dye structure. Since the dyes AR88 and AR18 are structurally very similar and differ only in the number and position of sulphonic groups, it can be assumed that the number of sulphonic groups affects dye adsorption on PA 6 knitwear. Among the studied dyes, the dye AR18 has the highest number of sulphonic groups. It contains three sulphonic groups, followed by the dye AR14 with two, whilst the dye AR88 contains only one sulphonic group. The latest discoveries show that the solubility of dyes in an aqueous medium increases along with an increased in the number of sulphonic groups in the dye molecule, whilst the substantivity of dyes decreases at a given value of pH [11]. This is confirmed by the results presented in this paper (among the studied dyes, dye AR18 is more soluble in water than dye AR88). The binding of acid dyes to PA 6 involves different intermolecular interactions and forces, including electrostatic interactions between the anionic sulphonic group of dye ($-SO_3^-$) in dyes and the protonated terminal amino groups ($-NH_3^+$) in PA 6, hydrogen bonding, van der Waals forces, and hydrophobic interactions. The latter plays an important role on the uptake of dyes by fibres and the wet fastness of dyes on fibre [2].

The comparison of the *E* values for the studied dyes AR88, AR14, and AR18 (figure 2) showed that the dye AR88 exhausted on PA 6 knitwear to the greatest extent, followed by the dye AR14, whilst the dye AR18 showed the smallest percentage of exhaustion. It should be emphasised that the hydrophobic/hydrophilic ratio of AR88 molecule in comparison with those of the dyes AR14 and AR18 is more on the hydrophobic side. The values of computational determination of log *P* and log *D* show that the log *P* for studied dyes are 3.02 (AR88), –0.44 (AR14), and –3.91 (AR18) when dyes are in ionic form, and 5.28 (AR88), 4.06 (AR14), and 2.88 (AR18) when dyes are in non-ionic form, respectively. Values of log *D,* which are pH dependant, are 2.86 (AR88), –0.34 (AR14), and –3.53 (AR18) at pH 4. This confirms, that the hydrophilicity of dyes decreased in the following order AR88<AR14<AR18, and vice versa the hydrophobicity of dyes increases in the following order AR88>AR14>AR18. Thus, it can be concluded, that the dyes with the higher number of sulphonic groups tend to stay in aqueous phase, i.e. the dyebath at the studied pH value of the dyebath. In contrast to the dyes AR14 and AR18, the dye AR88, which is the most hydrophobic among the studied dyes, tends to migrate to the fibre surface. The latter is understandable, since water molecules do not form attractive intermolecular interactions with the hydrophobic part of the dye molecule, but need to rearrange themselves around the hydrophobic part of the dissolved dye. Thus, it can be concluded that when the dye AR88 migrates to the fibre surface more willingly, this influences the energy stability of the system.

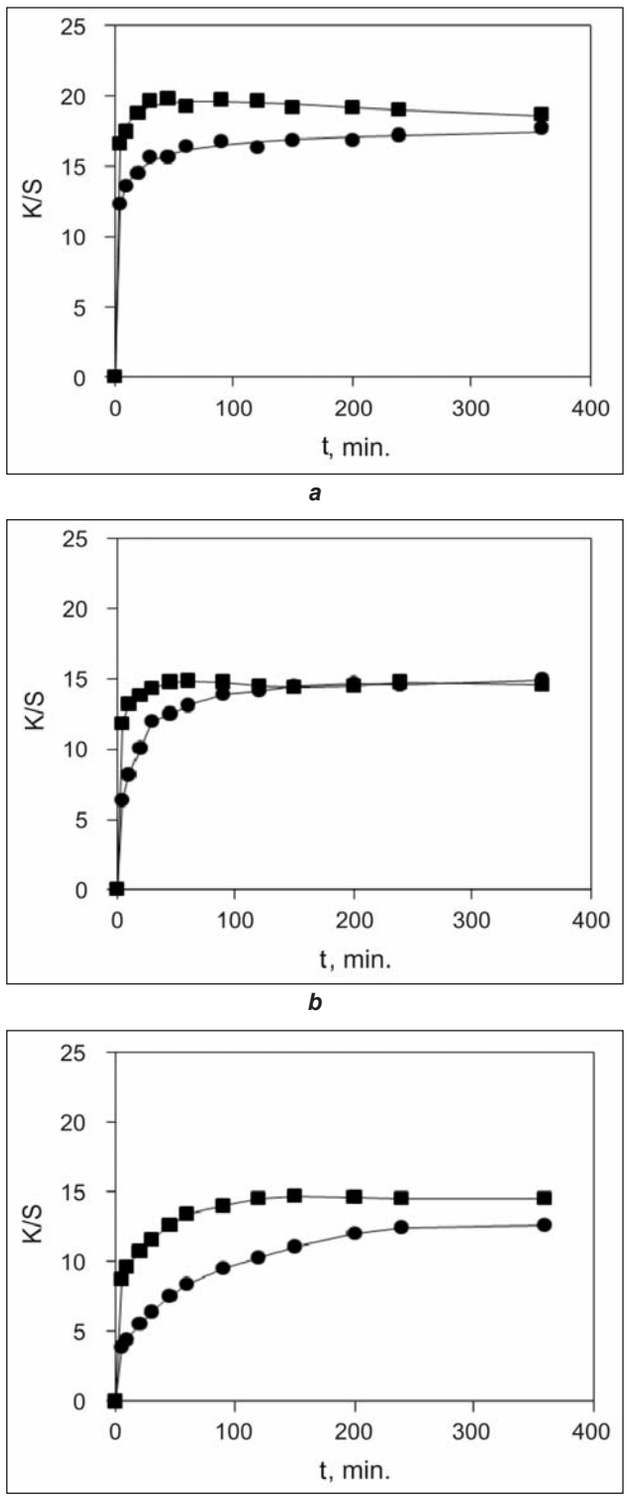

Fig. 3. Colour strength as a function of dyeing for the PA 6 knitwear dyed with AR88 (a), AR14 (b), AR18 (c) at two temperatures. ● – 40°C, □ – 60°C

The colour strength as a function of time, illustrated in figure 3, was influenced by dyeing time, dyeing temperature, and dye structure, similarly as the percentage of dye exhaustion. The values of *K/S* increased with the increase of both the percentage of exhaustion and the dyeing temperature.

Table 1

PARAMETERS OF ADSORPTION KINETICS FOR STUDIED DYES

Dye	T (°C)	C_e (mg·g^{-1})	k (g·mg^{-1}·min^{-1})	r^2
AR88	40	9.82	0.16	1
	60	11.47	0.80	1
AR14	40	9.26	0.02	0.9997
	60	9.04	0.24	1
AR18	40	8.85	0.003	0.9903
	60	9.04	0.02	1

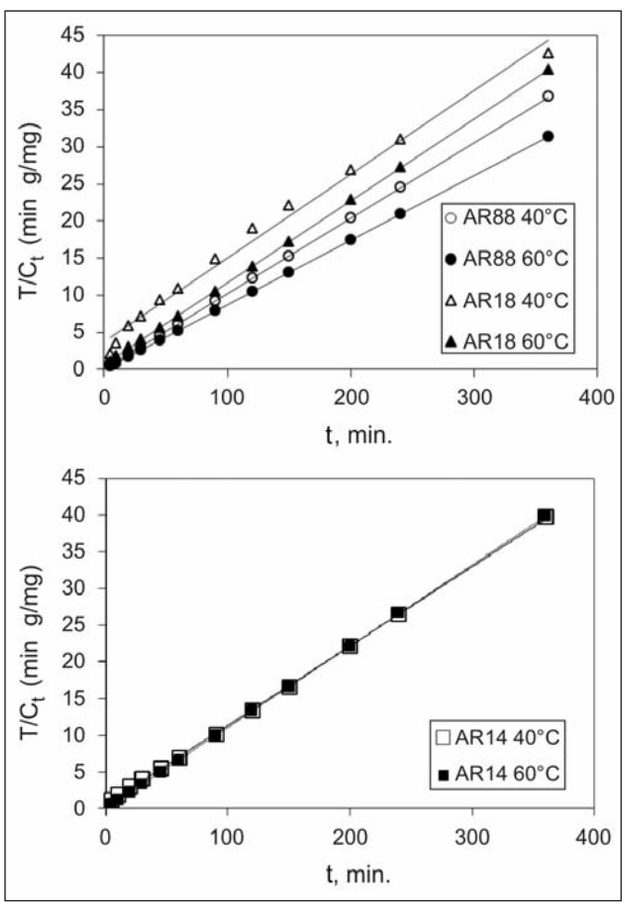

Fig. 4. Plots of t/c_t versus t of studied dyes at two dyeing temperatures

The results of adsorption kinetics are presented in table 1 and figure 4.

Linear plots of t/c_t versus t (figure 4) show the suitability of pseudo-second order rate equation for the AR88, AR14, and AR18 at two dyeing temperatures. The calculated adsorption rate constant (k) confirms that the rate of adsorption decreases with the increase of both number of sulphonic groups in the dye molecule and dyeing temperature. The concentration of dye adsorbed at equilibrium (c_e) is the highest in the case of AR88, and the lowest in the case of AR18, irrespective of the dyeing temperature. The results of spectrophotometric measurements of dyed samples are presented in figure 5.

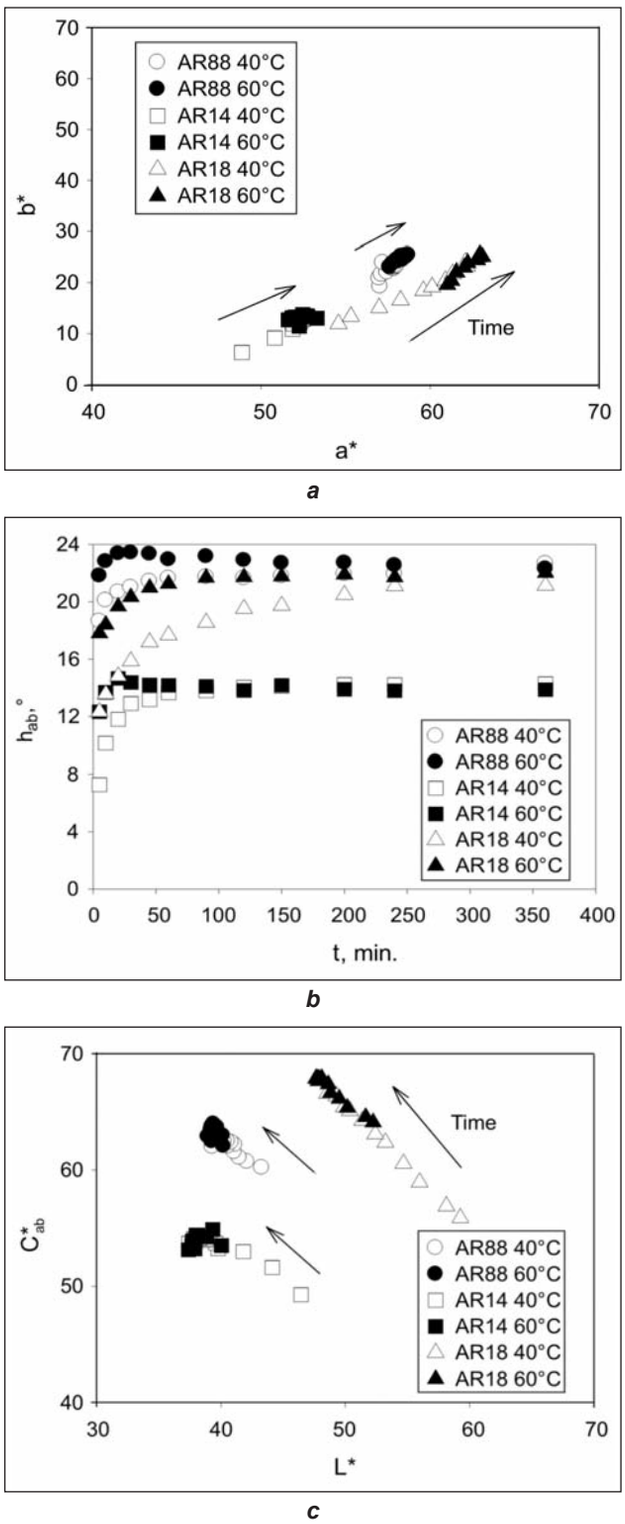

Fig. 5. Changes in the colour parameters of the PA6 knitwear in the process of dyeing: (a) a^* vs. b^*, (b) h_{ab} vs. t, (c) C^*_{ab} vs. L^*

From figure 5, *a* it can be seen that both values a^* and b^* are positive, and increased with dyeing time irrespective of selected dye. This indicates that the knitwear becomes redder and less blue by prolonging the dyeing time. At the dyeing temperature of 60°C, samples become even redder and less blue. PA 6 knitwear, dyed with AR18 has the highest values of a^*, followed by PA6 dyed with AR88, whilst PA6 knitwear, dyed with AR14 are less red than knitwear,

dyed with the other two dyes. From figure 5, *a* it can be also seen that the values of *a** are more grouped at the dyeing temperature 60°C, and more scattered at the dyeing temperature 40°C where a progressive increase of *a** is noticed for PA6 samples, dyed with AR14 and AR18. Also, for the PA6 sample, dyed with AR88, a very sudden increase of *a** is noticed. At 60°C, the values of *a** are less dependent on increase in dyeing time. At equilibrium (*t* = 360 min), the values of *a** and *b** are almost equal for the individual dye, irrespective of dyeing temperature. The values of h_{ab} (figure 5, *b*) increase with the increasing of both dyeing time and dyeing temperature. The highest value of h_{ab} is obtained on samples dyed with AR88, followed by AR18, whilst samples, dyed with AR14 have the lowest value of h_{ab}. At a shorter dyeing time of up to 60 minutes, a very dramatic increase of h_{ab} is noticed, but from 100 minutes of dyeing till 360 minutes almost no change in h_{ab} values is detected for the selected dyed sample. From figure 5, *c* it can be seen that the CIE lightness (*L**) decreased with the increase of both dyeing temperature and time for all studied dyes, indicating that the samples become darker during the dyeing process. At 40°C, a more progressive decrease of *L** is noticed for samples dyed with AR18 and AR14 than for samples dyed with AR88, whilst at 60°C the stepwise decrease of *L** with the increase of dyeing time is less pronounced, especially in samples, dyed with AR88 and AR14. This suggests that the adsorption of dye AR88 onto PA 6 knitwear occurs faster in comparison with dyes AR14 and AR18. Since chroma (C^*_{ab}) is derived from values *a** and *b**, its increase with the increase of *T* and *t* of dyeing is expected. Thus, the colour of PA 6 samples becomes more saturated.

CONCLUSIONS

According to the obtained results, the following can be concluded:

- A higher percentage of exhaustion of studied acid dyes is obtained at 60°C than at 40°C.
- The exhaustion of studied acid dyes onto PA 6 knitwear increases with the increasing dyeing time until the equilibrium is reached, at which no changes of exhaustion are noticed. At higher dyeing temperatures the exhaustion is reached in a shorter time.
- At a given pH value of the dyebath, the acid dye with the higher number of sulphonic groups in its structure exhausts on PA 6 knitwear to a lesser extent than that with a lower number of sulphonic groups, irrespective of dyeing temperature and dyeing time.

ACKNOWLEDGEMENTS

This work was financially supported by the Slovenian Research Agency (Programme P2-0213 Textiles and Ecology).

BIBLIOGRAPHY

[1] Burkinshaw, S.M. *Chemical principals of synthetic fibre dyeing*, In: 1st edition, Blackie Academic & Professional, Glasgow, 1995, pp. 77–156.
[2] *Synthetic fibre dyeing*, Edited by C. Hawkyard, Society of Dyers and Colourists, Bradford, 2004, pp. 82–120.
[3] Suganuma, K. *The relation between the number of sulphonic groups in acid dyes and the yield stress of dyed nylon monofilament,* In: Text. Res. J., 51, nr. 10, 1981, p. 626.
[4] *The theory of coloration of textiles,* Edited by A. Johnson, 2nd edition, Society of Dyers and Colourists, Bradford, 1989, p. 256.
[5] Atherton, E., Downey, D.A., Peters, R.H. *Studies of the dyeing of nylon with acid dyes: Part I: Measurement of affinity and the mechanism of dyeing,* In: Text. Res. J., 25, nr. 12, 1955, p. 977.
[6] Naebe, M., Cookson, P.G., Rippon, J., Brady, R.P., Wang, X. *Effects of plasma treatment of wool on the uptake of sulfonated dyes with different hydrophobic properties,* In: Text. Res. J., 80, nr. 4, 2010, p. 312.
[7] Lewis, D.M. *Dyestuff-fibre interactions,* In: Rev. Prog. Color, 28, nr. 1, 1998, p. 12.
[8] Viallier, P., Jordan, C. *Nylon 6.6 dyeing behaviour for fibres of different levels of fineness,* In: Color. Technol., 117, nr. 1, 2001, p. 30.
[9] Csizmadia, F., Tsantili-Kakoulidou, A., Panderi, I., Darvas, F. *Prediction of distribution coefficient from structure. 1. Estimation method,* In: J. Pharm. Sci., 86, nr. 7, 1997, p. 865.
[10] MarvinSketch version 17.22, (www.chemaxon.com/products/marvin/marvinsketch/2017)
[11] Wen, G., Cookson, P.G., Liu, X., Wang, X.G., *The effect of pH and temperature on the dye sorption of wool powders,* In: J. Appl. Polym. Sci., 116, nr. 4, 2010, p. 2216.
[12] Aspland, J.R. *Chapter II/Part 1: Anionic dyes and their application to ionic fibers: dyeing nylon with acid dyes,* In: Text. Chem. Color., 25, nr. 4, 1993, p. 19.

Authors:

MATEJA KERT[1], INES BESEDIČ[1], ČRTOMIR PODLIPNIK[2]

[1]University of Ljubljana, Faculty of Natural Sciences and Engineering, Department of Textiles, Graphic Arts, and Design, Aškerčeva 12, Ljubljana, Slovenia

[2]University of Ljubljana, Faculty of Chemistry and Chemical Technology, Večna pot 113, Ljubljana, Slovenia

Corresponding author:

MATEJA KERT
e-mail: mateja.kert@ntf.uni-lj.si

The relationship between earnings and labour productivity in textile industry

NORINA POPOVICI
CAMELIA MORARU
IRENA MUNTEANU

REZUMAT – ABSTRACT

Relația dintre venituri și productivitatea muncii în industria textilă

Veniturile și productivitatea muncii sunt indicatori economici importanți, relațiile dintre acestea fiind analizate de economiști, angajatori și factorii de decizie. Relația dintre venituri și productivitatea muncii este importantă pentru fiecare regiune sau sector economic, deoarece aceasta influențează standardul de viață și distribuția veniturilor între muncă și capital. Lucrarea analizează legătura dintre salariul mediu brut și productivitatea muncii din industria textilă în perioada 2005–2016, în România. Rezultatele analizei evidențiază că există o corelație pozitivă, dar moderată, între salariul mediu brut și productivitatea muncii. În acest scop, au fost utilizate metodele statistico-econometrice pentru a verifica normalitatea distribuției seriilor de date și existența unei corelații între indicatorii analizați.

Cuvinte-cheie: câștig, eficiență, industria textilă, câștiguri salariale medii brute, productivitate

The relationship between earnings and labour productivity in textile industry

Earnings and labor productivity are important economic indicators, the relationship between them being analyzed by economists, employers and policy makers. The relationship between earnings and labor productivity is important for each region or economic sector, because it influences the living standard and the distribution of income between labor and capital. This paper analyzes the link between gross average earning and labor productivity in the textile industry during 2005–2016 in Romania. The results of the analysis show that there is a positive, but moderate correlation between gross average earning and labor productivity. For this purpose were used statistical-econometric methods to verify the normality of data series distribution and the existence of a correlation between the indicators analyzed.

Keywords: earning, efficiency, textile industry, gross average earnings, productivity

INTRODUCTION

Wages are the main source of living for employees, accounting most of the revenues achieved and having a decisive effect on the standard of living of the employee and its family. Labor productivity is one of the indicators that show how effective the workforce is. Of all the factors of production, human capital (meaning labor) is one of the most important factors that impose effects on productivity. Increasing labor productivity means that a larger quantity of goods has been produced over a period of time in a sector or across one country.

The main objective of this paper is to verify one of the fundamental correlations in the economy, namely the link between earnings and labor productivity.

Starting from the hypothesis that there is a connection between these two indicators, the test results used in this paper confirmed a modest correlation between the two indicators, insufficient to generate the normality required in the analyzed industrial sector: the evolution of earnings to be based on the evolution of labor productivity in the textile manufacturing sector.

The paper contains a review of literature on the subject, the statistical analysis of the indicators and discussions on the results of the research and the conclusions of these results, part which is a starting point for adoption of economic policies meant to ensure high labor productivity, with positive effects on earnings within a national economy.

REVIEW OF LITERATURE

Afrooz et all (2010), in a study entitled “An analysis of gender, age and education effects on wages and productivity” noted that there is a positive relationship between productivity and real wages. Similarly, there was an increase in wage bonus with years of schooling and higher education proved to generate higher productivity [1].

Gupta (1975), in his study regarding stimulating the workforce of the Indian iron and steel industry, found that monetary incentives are the best motivations that lead to better motivation and higher labor productivity [2].

Hind (1990) claimed that direct monetary benefits, together with greater accountability and autonomy in decision-making process, had strong motivations compared to other advantages. However, non-monetary incentives are probably more important for directors, especially those who are senior positions [3].

Huizinga and Broer (2004), referring to the example in Netherlands, said that only on short term, wage growth will increase labor productivity, but on the long term it will have no impact [4].

Klein’s study (2012) showed that the absence of a strong relationship between wages and labor productivity in some countries can be explained by macroeconomics and/or institutional factors. These factors tend to create a barrier between the two variables, which means that earnings from labor productivity do

not fully lead to an increase of real wages (or vice versa) on short or long term [5].

ANALYSIS AND DISCUSSION

The database for the analysis of the relationship between gross average earning and labor productivity in the textile manufacturing industry in Romania includes data with annual frequency and was built during 2005–2016. The information and statistical data related to the monthly gross average earnings and labor productivity were taken from the National Statistics Institute, based on tempo-online data series. For empirical research, the 2005–2016 period was chosen in order to achieve meaningful and reliable results.

In order to capture the link between gross average earning and labor productivity, but also to understand the methodological approach, we considered necessary to present the dynamics of the explanatory variables during the analyzed period (table 1 and table 2) [6].

Another step in the econometric analysis is the presentation of the statistical descriptions of the instrumental variables included in the model.

Thus, based on the data from tables 1 and 2, we have presented for the two indicators analyzed the descriptive statistics (standard deviation, Skewess and Kurtosis indicators to see the deviation of the empirical distribution in relation to a symmetric distribution around the mean and the degree of flattening or sharpening of data distribution), as can be seen in table 3 [7].

We checked the distribution normality using as instruments graphical tools as Q-Q Plot and Kolmogorov-Smirnov (as parametric methods) and graphs as

Table 1

MONTHLY GROSS AVERAGE EARNINGS IN TEXTILE INDUSTRY
Unit: Lei

Year	Jan	Feb	Mar	Apr	May	Jun	Jul	Aug	Sep	Oct	Nov	Dec
2005	590	592	622	620	629	659	677	675	667	683	710	758
2006	667	660	707	686	737	755	765	778	767	788	812	838
2007	814	833	880	843	892	921	924	927	936	983	1015	1068
2008	979	972	1008	1043	1045	1095	1132	1084	1106	1158	1129	1205
2009	1157	1155	1240	1249	1261	1288	1283	1197	1289	1343	1363	1490
2010	1352	1394	1486	1389	1425	1468	1491	1416	1470	1528	1515	1784
2011	1523	1519	1623	1561	1560	1624	1609	1503	1590	1607	1624	1786
2012	1559	1554	1608	1595	1631	1683	1671	1578	1688	1691	1721	1815
2013	1605	1632	1719	1733	1732	1850	1841	1708	1764	1774	1831	2010
2014	1767	1802	1876	1839	1858	1960	1979	1821	1883	1893	1986	2129
2015	1809	1835	1922	1890	1883	1992	2030	1847	1947	1978	2110	2253
2016	2011	2042	2140	2130	2214	2357	2343	2264				

Table 2

LABOR PRODUCTIVITY IN TEXTILE INDUSTRY
Unit: percent

Year	Jan	Feb	Mar	Apr	May	Jun	Jul	Aug	Sep	Oct	Nov	Dec
2005	63.8	68.3	74.8	69.0	67.6	78.4	67.1	56.1	76.6	74	75.1	59.1
2006	68	65.8	81.3	60.4	71.1	71.3	62	52.5	65.3	74.7	76.1	64.0
2007	82.4	81.8	87.6	69.7	82.6	75.9	86.6	58.6	76.9	87.8	87.7	65.2
2008	76.7	89.8	83.2	80.9	76.5	89.0	90.5	68.0	90.5	94.8	89.6	78.4
2009	77.7	74.7	83.5	76.7	76.2	76.6	79.0	67.5	98.7	112.1	104.2	90.8
2010	94.7	107	117.9	99.6	89.0	93.6	92.3	75.0	108.1	112.4	119.4	89.8
2011	110.1	106.7	118.5	100.6	103.7	88.9	85.7	75.0	102.4	101.6	107.3	91.5
2012	98.2	114.1	110.2	85.7	100.0	87.9	74.9	66.1	91.1	110.2	110.0	77.3
2013	99.5	108.3	115.8	101.9	88.3	80.1	86.1	72.8	100.9	107.0	104.5	89.2
2014	109.70	103.60	99.30	86.70	99.10	89.30	85.20	64.20	93.10	94.50	92.90	77.30
2015	82.2	85.0	86.9	74.4	66.2	69.5	76.1	51.8	84.1	90.3	84.9	71.2
2016	78.4	83.8	85.4	72.1	72.5	72.1	66.4	59.1				

Table 3

DESCRIPTIVE ANALYSIS OF VARIABLES GROSS AVERAGE EARNINGS AND LABOR PRODUCTIVITY									
	N	Min	Max	Mean	Std. Deviation	Skewness		Kurtosis	
	Statistic	Statistic	Statistic	Statistic	Statistic	Statistic	Std. Error	Statistic	Std. Error
Gross average earning	140	590.00	2357.00	1412.7071	476.47261	–.141	.205	–1.102	.407
Labour productivity	140	51.80	119.40	84.9214	15.52712	.228	.205	–.629	.407
Valid N (listwise)	140								

Boxplot (1, 2, 3) to identify aberrant values in data series.

Figure 1 presents the Q-Q Plot for gross average earnings data series and it can be seen that the values of earnings variable closely follow the normal distribution (the deviations observed are insignificant).

Figure 2 presents the Q-Q Plot for labor productivity data series and it also can be noticed that the values of the productivity labour variable follow closely the normal distribution (the deviations observed are insignificant).

The hypothesis that the gross average earnings and labour productivity variables are normal is strengthened by the Kolmogorov-Smirnov test (p values are much higher than 0.01–0.210 for gross average earnings and 0.377 for labour productivity), as can be seen in table 4.

From QQ plot analysis (figure 1 and figure 2), boxplots (figure 3) and the significance levels obtained in the KS test (0.210 and 0.377) we deduce that there is insufficient data to conclude that the gross average earnings and labor productivity variables would not be normally distributed. So, for the current analysis, we can assume that the gross average earnings and labor productivity variables are normally distributed, with the parameters estimated in the table above.

Next, we want to identify the existence of linear associations between the gross average earnings and labor

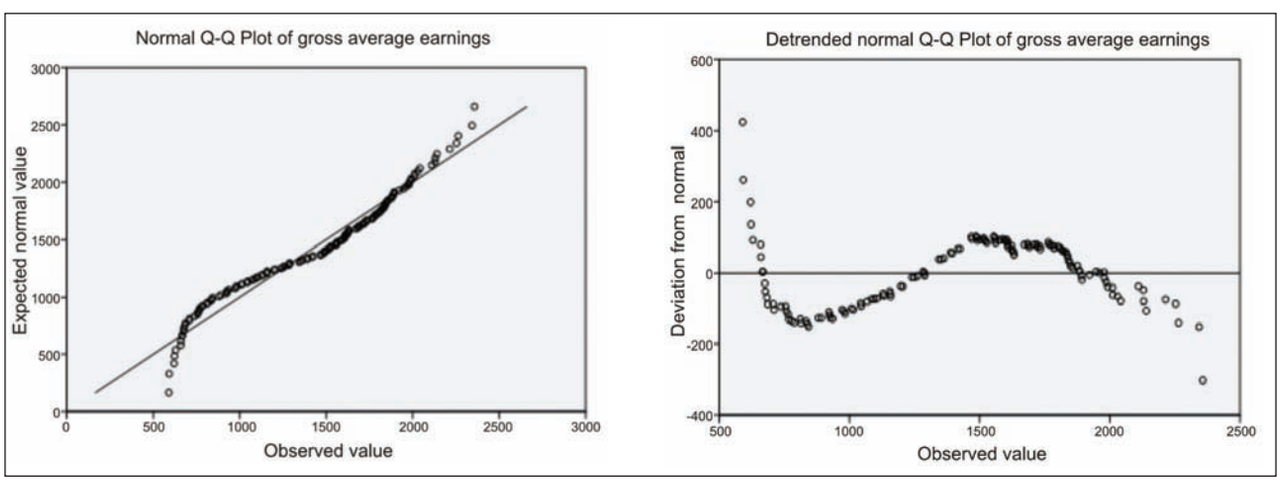

Fig. 1. Q-Q plot for Gross average earnings variable

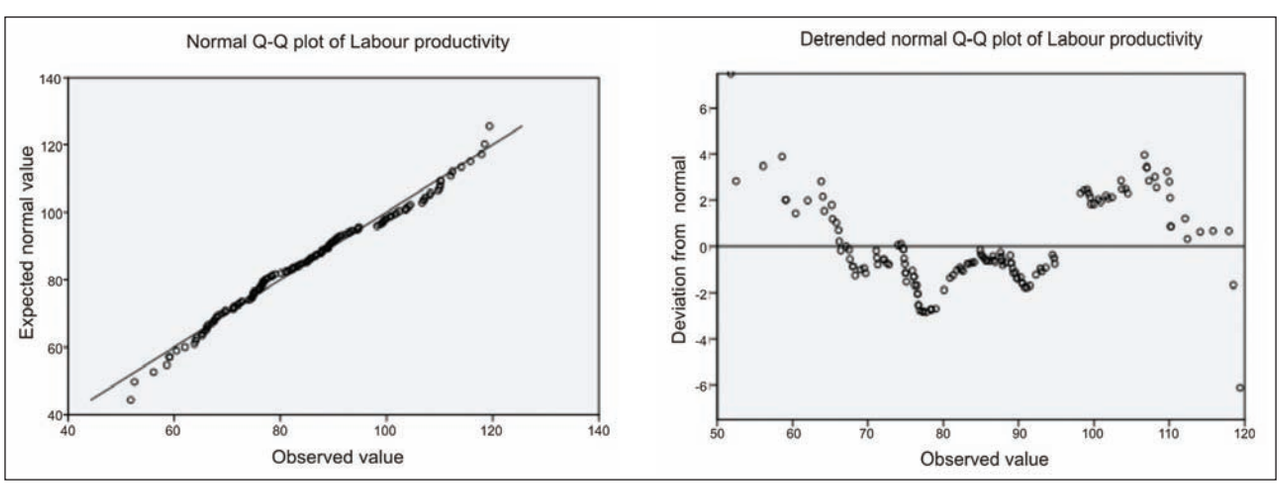

Fig. 2. Q-Q plot for Labour productivity variable

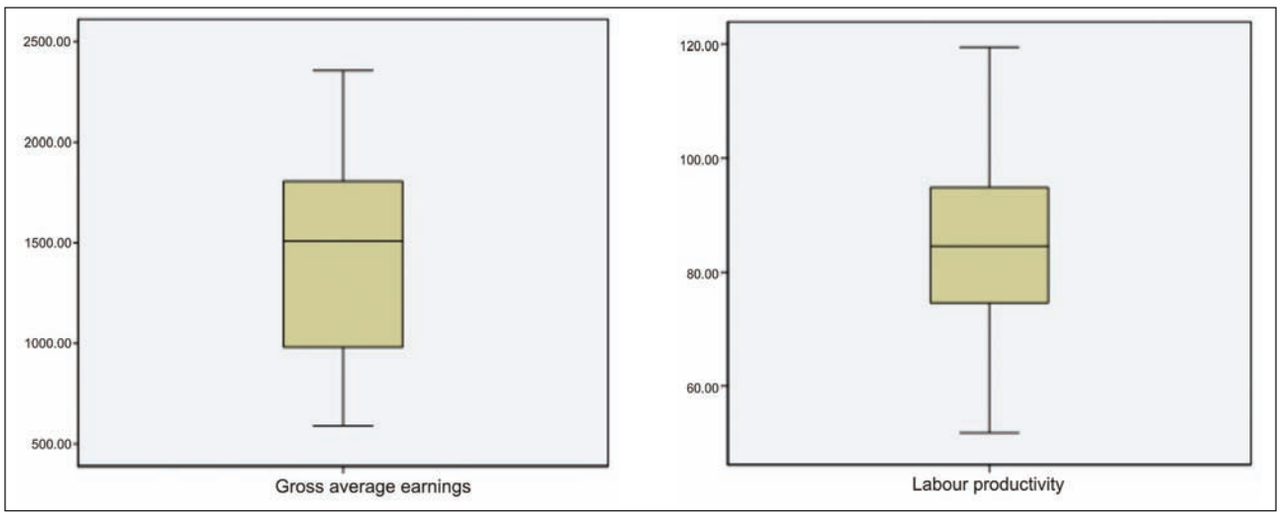

Fig. 3. Boxplots for the gross average earnings and labor productivity variables

Table 4

RESULTS OF THE KOLMOGOROV-SMIRNOV TEST			
		Gross average earnings	**Labour productivity**
N		140	140
Normal parameters[a,b]	Mean	1412.7071	84.9214
	Std. Deviation	476.47261	15.52712
Most extreme differences	Absolute	.090	.077
	Positive	.077	.077
	Negative	–.090	–.048
Kolmogorov-Smirnov Z		1.061	.912
Asymp. Sig. (2-tailed)		.210	.377

[a] Test distribution is Normal.
[b] Calculated from data.

productivity variables in textile industry. Therefore, in the following it is analyzed the value of Pearson correlation coefficient, used to measure and describe the degree of linear association between two normally distributed variables.

According to the data presented in table 5, Pearson correlation coefficient is 0.335. The significance level is <0.05, so the correlation coefficient is significant. Variables are positively correlated, but not strongly correlated. We can deduce that there is a linear association between the two variables, but there may also be non-linear associations. Association is positive (gross average earning tends to grow along with labour productivity), but the magnitude of the association is moderate.

Starting from all the statistical data analyzed above, we can identify a correlation between gross average earning and labor productivity by estimating an econometric model. The result of the linear regression model for gross average earnings depending on labor productivity is represented in figure 4.

As we have shown, association is a positive one (gross average earning tends to grow along with labour productivity), but the magnitude of the association is moderate. Therefore, we also take into consideration the nonparametric correlation coefficients Kendall and Spearman. These indicators aim to highlight the degree of association between the analyzed variables.

Table 5

PEARSON CORRELATION COEFFICIENT			
	Correlations	**Gross average earnings**	**Labour productivity**
Gross average earnings	Pearson Correlation	1	.335**
	Sig. (1-tailed)		.000
	Sum of Squares and Cross-products	3.156E7	344456.179
	Covariance	227026.151	2478.102
	N	140	140
Labour productivity	Pearson Correlation	.335**	1
	Sig. (1-tailed)	.000	
	Sum of Squares and Cross-products	344456.179	33511.716
	Covariance	2478.102	241.091
	N	140	140

** Correlation is significant at the 0.01 level (1-tailed).

Table 6

ANALYSIS OF KENDALL AND SPEARMAN CORRELATION COEFFICIENTS				
	Correlations		**Gross average earnings**	**Labour productivity**
Kendall's tau_b	Gross average earnings	Correlation Coefficient	1.000	.207**
		Sig. (1-tailed)	.	.000
		N	140	140
	Labour productivity	Correlation Coefficient	.207**	1.000
		Sig. (1-tailed)	.000	.
		N	140	140
Spearman's rho	Gross average earnings	Correlation Coefficient	1.000	.311**
		Sig. (1-tailed)	.	.000
		N	140	140
	Labour productivity	Correlation Coefficient	.311**	1.000
		Sig. (1-tailed)	.000	.
		N	140	140

** Correlation is significant at the 0.01 level (1-tailed).

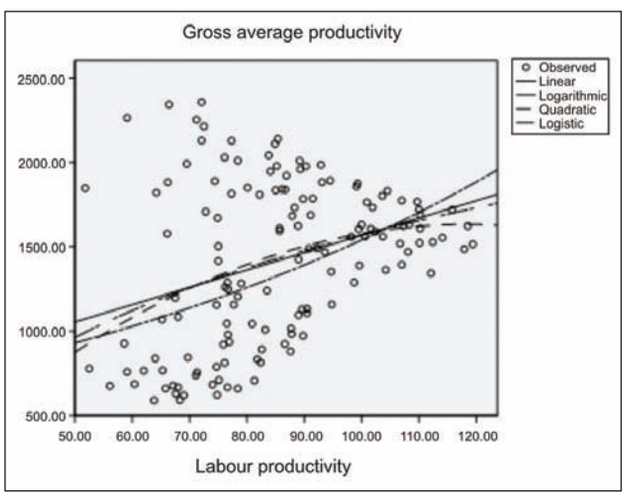

Fig. 4. The linear regression model for gross average earnings according to labour productivity

According to the data from table 6, the nonparametric correlation coefficients, Kendall and Spearman, are also positive and statistically significant ($p < 0.01$), but do not denote a strong correlation between the two variables (they do not approach value 1).

CONCLUSIONS

In this paper we wanted to analyze whether one of the fundamental correlations in the economy – the correlation between gross average earnings and labor productivity – was respected in the textile industry.

Following the analysis of the two indicators, we can say that there is a positive association between gross average earnings and labor productivity, but the magnitude of the association is moderate, thus concluding that the evolution of earnings in the textile manufacturing industry was not based closely on the evolution of labor productivity. There is a moderate association between gross average earnings and labor productivity, so a correlation, but the evolution of gross average earnings was based on other causes and not, as it should have, on labor productivity. This has negative effects on inflation, living standards, economic equilibrium.

The link between labor productivity and wage has a positive effect on the economy, as it provides an incentive for workers to increase production. An increase in productivity leads to a higher supply on the market, which determines lower prices. Therefore, this would also influence consumers in a beneficial way. Increasing productivity would increase exports. This would also be beneficial to a country's economy. If wages are related to qualitative productivity, the quality of production would also be high.

In a future paper, we intend to study the bilateral relationship between the two variables analyzed in the present paper and to identify the factors that underlie the evolution of earnings in the economy, by testing the intensity of the relationship between them and the analyzed indicator.

BIBLIOGRAPHY

[1] Afrooz, A., Rahim, K.B.A., Noor, Z.B.M., Chin, L. *A review of effects of gender, age, and education on wage and productivity*, In: International Research Journal of Finance and Economics, 2010, vol. 2, no 4, pp. 47–51.

[2] Gupta, B. *Labour incentive in India of iron and steel industry,* In: Research Abstract Quarterly, 1975, pp. 171–176.

[3] Hind, M. *Developing the employment package: Attracting and retaining the best employees,* In: Management Decision, 1990, vol. 28, no 6.

[4] Huizinga, F., Broer, P. *Wage moderation and labour productivity*, In: Netherlands Bureau for Economic Policy Analysis, Series CPB Discussion, 2004, Papers 28, pp. 28–34.

[5] Klein, N. *Real wage, labour productivity and employment trends in South Africa: a closer look*, In: IMF Working Paper, 2012, No.12/92, pp. 1–27.

[6] INSSE Monthly Statical Bulletin, 2016 [online] Available at http://statistici.insse.ro/shop/index.jsp?page=tempo3&lang=ro&ind=FOM107D

[7] IBM Corp. Released 2013. IBM SPSS Statistics for Windows, Version 22.0. Armonk, NY: IBM Corp.

Authors:

NORINA POPOVICI[1], CAMELIA MORARU[2], IRENA MUNTEANU[3]

[1,3] "Ovidius" University, Faculty of Economic Sciences, Department of Business Administration, University Alley, No.1, Campus, 900470, Constanta, Romania

e-mail: norinapopovici@yahoo.com, irena.munteanu@yahoo.com

[2] "Dimitrie Cantemir" Christian University, Faculty of Tourism and Commercial Management, Department of Business Administration, Dezrobirii Street, No 90A, 900372, Constanta, Romania

e-mail: cami.moraru@yahoo.com

Corresponding author:

NORINA POPOVICI

e-mail: norinapopovici@yahoo.com

Effect of textile woven fabric parameters on its thermal properties

SABRI HALAOUA
ZOUHAIER ROMDHANI
ABDELMAJID JEMNI

REZUMAT – ABSTRACT

Efectul parametrilor țesăturilor asupra proprietăților termice ale acestora

Acest studio urmărește să investigheze relația dintre proprietățile de construcție a țesăturii și proprietățile termice. În acest scop, au fost utilizate trei structuri de legătură de bază, trei compoziții fibroase, cinci mase de suprafață și patru grosimi. S-au determinat rezistența termică la convecție R_{CV}, rezistența la conductivitate termică R_{CD}, puterea adiatermică și conductivitatea termică a țesăturilor. În cadrul acestui studiu, legătura pânză a prezentat cele mai mari proprietăți termice, în timp ce legăturile diagonal și atlaz au prezentat cele mai scăzute caracteristici termice. Tipul de fibră afectează foarte mult proprietățile termice într-un mod foarte diferit. Creșterea masei și a grosimii suprafeței a fost direct legată de puterea adiatermică, rezistența termică și conductivitatea termică.

Cuvinte-cheie: proprietățile țesăturii, rezistența termică, puterea adiatermică, conductivitatea termică

Effect of textile wovenfabricparameters on its thermal propert

This paper aims to investigate the relationship between fabric construction properties and its thermal properties. For this aim three basic weave structures, three fiber compositions, five surface mass and four thicknesses were used. The thermal convection resistance R_{CV}, thermal conduction resistance R_{CD}, adiathermic power and thermal conductivity of all fabric samples were determined. In this research the plain weave structure showed the highest thermal properties while the twill and satin weave depicted the lowest thermal characteristics. The fiber type affects deeply different thermal properties. The increase of the surface mass and thickness was directly bound to the adiathermic power, thermal resistance and the thermal conductivity.

Keywords: fabric properties, thermal resistance, adiathermic power, thermal conductivity

INTRODUCTION

Different Standards had defined the thermal comfort as being “that condition of mind which expresses satisfaction with the thermal environment” (ISO 2005; ASHRAE 1974). To reach the thermal comfort two conditions must be fulfilled; a sensation of thermal neutrality between the skin and the body’s core temperature and the body’s energy balance (Häusler and Berger, 2002). Therefore, the comfort can be defined as ‘a pleasant state of psychological and physical harmony between a human being and the environment’ (Das and Ishtiaque, 2004). In addition, the physiological comfort and the garment role may be summarized in the figure 1. In this fact, the Physiological comfort is deeply dependent on the used garment properties. The clothing parameters are the used materials nature and its structure such as porosity, the air permeability, the thermal conductivity, the effective resistance and the thermal efficiency [6, 7].
Many several studies investigated the effect of the garment structure on the physical and thermal properties. This paper studied the effect of the weave structure, the fiber composition, the surface mass and the thickness of the woven fabric on its thermal property. The comfort of the woven structure depends on the external climatic and the weave structure (Saville, 1999). The effect of the weave structure affects deeply the porosity of woven textile fabric which leads to the variation of the thermal property (Matusiak and Sikorski, 2011). Therefore, it is found that plain fabrics have the highest value of thermal resistance (Frydrych et al., 2002). Every linear structure has its special characteristic; therefore, these properties influence the porosity which results in decreased thermal conductivity (Varshney et al.,

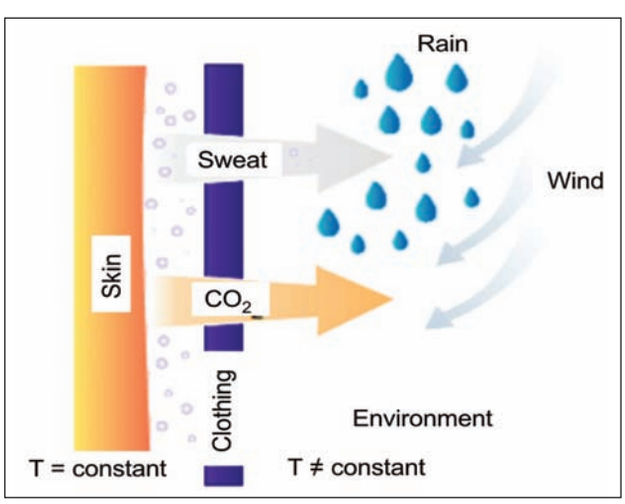

Fig. 1. The body’s thermoregulatory mechanism (Grażyna et al., 2016)

2010). The effect of the fiber type on the thermal resistance properties fabrics was studied by Afzal (Afzal et al., 2014). Then, the effect of fibre morphology, yarn and fabric structure on thermal comfort properties of fabric was investigated (Pac et al., 2001). Therefore, Khoddami et al. (2009) showed that the thermal resistance of woven fabric increases while increasing the sample thickness. Thus, many researches (Havenith, 2002; Milenkovic et al., 1999) demonstrated that heat resistance increases by increasing the fabric thickness.

The relationship between thermal properties and the textile woven structures has been studied by several researchers (Matusiak, 2006; Süle, 2012). It was reported that the entrapped air layer within fabrics was of great importance in determining heat flux. Finally, the fabric properties determine the thermal resistance and thermal conductivity. Par definition, the thermal conductivity expresses the ease of conduction of heat through a porous medium. The heat is transmitted mainly by conduction, in the solid phase of the fibrous materials, and by conduction, convection, and radiation in its fluid phase. The flux of heat transfer is:

$$ø_T = ø_{cond} + ø_{conv} + ø_{rad} \quad (1)$$

where: $ø_{cond}$ is the conductive flux, $ø_{conv}$ – the convective flux, $ø_{rad}$ – the radiative flux.

It is experimentally demonstrated the existence of relationship between the heat flux ø and the temperature gradient through a solid medium.

$$ø = -\lambda \text{ grad } T \quad (2)$$

In this field, many models were examined and mathematical models given (Militky and Kremenakova, 2010; Wang et al., 2008; Eucken, 1940; Maxwell, 1954; Levy, 1981) respectively by equation (3), (4), (5) and (6) which were put in as shown in table 1, where:

P is the volume fraction of material 1;

K_e – effective thermal conductivity;

K_p and K_s – thermal conductivity with parallel and series arrangement;

K_i and v_i – the thermal conductivity and volume fraction of i material;

v_1 and v_2 – the volume fraction of materials 1 and 2;

K_1 and K_2 – the thermal conductivity of materials 1 and 2.

Table 1

EFFECTIVE THERMAL CONDUCTIVITY EQUATION	
Series – parallel 1	$K_e = \frac{(K_p + K_s)}{2}$ (3) $K_p = PK_1 + (1-P)K_2$ $K_s = \frac{K_1K_2}{PK_2 + (1-P)K_1}$
Series – parallel 2	$K_e = K_s/2\left(\sqrt{1 + 8K_p/K_s} - 1\right)$ (4) $K_p = \sum_{i=1}^{N} K_i v_i,\ K_s = 1/\sum_{i=1}^{N} \frac{v_i}{K_i}$
Maxwell Eucken	$K_e = K_1 \frac{2K_1 + K_2 - 2(K_1 - K_2)v_2}{2K_1 + K_2 + (K_1 - K_2)v_2}$ (5)
Levy's	$K_e = K_1 \frac{2K_1 + K_2 - 2(K_1 - K_2)F}{2K_1 + K_2 + (K_1 - K_2)F}$ (6) $F = \frac{2/G - 1 + v_2 - \sqrt{(2/G - 1 + v_2)^2 - 8v_2/G}}{2}$ $G = \frac{(K_1 - K_2)^2}{(K_1 + K_2)^2 + K_1K_2/2}$

MATERIALS AND METHODS

In this study, three basic textile fiber was used: the cotton, the blend cotton–polyester and the polyester. Then, three weaving concepts are utilized to evaluate the effect of investigated factors on the physical and thermal properties. These weaves are the plain weave which consists of yarns interlaced in an alternating fashion one over and one under every other yarn. The second is the twill weave which is more pliable than the first and it has better drapability while maintaining more fabric stability. The last pattern is the satin weave which is a very pliable weave and is used for forming over curved surfaces. The textile structures weaves, the mass per area and the thickness used for this study with their characteristics are shown in table 2.

The fabric weight and thickness values were measured according to ASTM D3776 (2011) and to ASTM D1777-96 (2007) respectively. The measurement of the adiathermic power is carried out with a heating body covered with the sample to be tested as shown in figure 2. The test environment must have a

Table 2

PROPERTIES OF THE TESTED TEXTILE FABRICS

Material	Weave	Nm (Weft)	Nm (Warp)	Warp count	Weft count
Cotton (100%)	Plain	52	48	34	28
	Twill	52	48	34	28
	Satin	52	48	34	28
Cotton / Polyester	Plain	48	50	34	28
Polyester (100%)	Plain	48	50	34	28
Surface mass (g/m²)					
Cotton (100%)	140	155	170	180	200
Thickness (mm)					
Cotton (100%)	0,46	0,49	0,52		

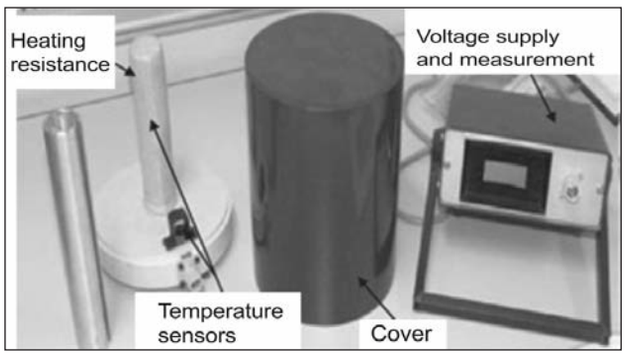

Fig. 2. Experimental device of the adiathermic property determination

perfectly controlled temperature and humidity (20 °C ± 2 °C and Relative Humidity 65% ± 2%).

RESULTS AND DISCUSSION

Effect of constructional parameters on adiathermic power

In this section, the effect of weave structure, the fiber type, the thickness and the mass area on comfort properties are investigated. As the comfort properties are generally related to adiathermic power, the thermal resistance and thermal conductivity, these parameters are discussed. These observed parameters contributed to the thermo-physiological comfort of the fabrics.

The adiathermic power is defined as the capacity of the fabric to oppose the pass of the heat flux into its structure. In this part, this thermal property was discussed. According to the experimental results, it can be noted that different woven parameters structure had significant effect on the adiathermic power. First, each weave structure has a specific pattern of yarn interlacing points between the warp and the weft. It can be concluded from the experimental graphs that the adiathermic power value is related to the density of yarn interlacing points. The lower density gives important porosity and air permeability which means lower adiathermic power. Therefore, the plain weave has the highest adiathermic power. This can be explained that this weave has the maximum yarn interlacing points between warp and weft. On the contrary, while decreasing the yarn interlacing points between warp and weft, the adiathermic power decreases. This result is given by the twill and satin weave. The figure 3 indicated that the satin weave has the lowest value of adiathermic power, which is understandable, because this fabric is characterized by the lowest mass per square meter and relatively small thickness.

It is known from the literature that the polyester fibers indicate much lower thermal insulation than the cotton fibers. This is may explained the thermal properties (the adiathermic power, the thermal resistance and the thermal conductivity) behavior for the fabric manufactured of 100% cotton. For the fabric consisting of 100% polyester, it shows that the thermal properties are very important than each compound of

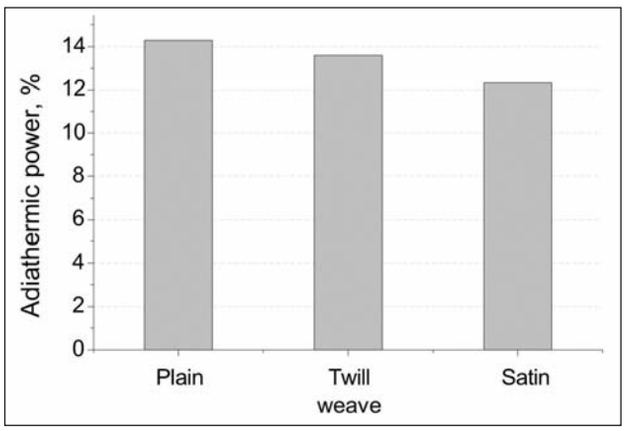

Fig. 3. Variation of the adiathermic power according to weave structure of woven fabric

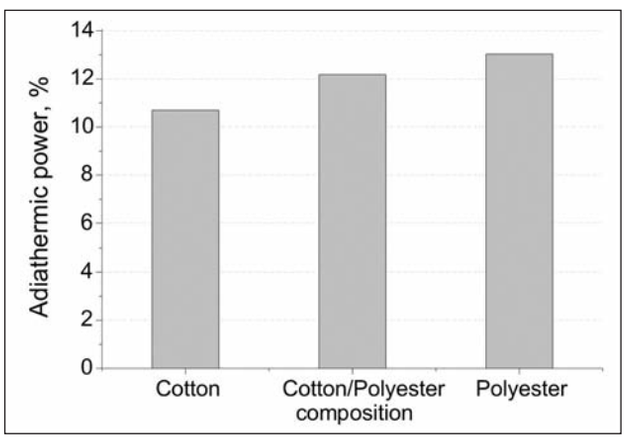

Fig. 4. Variation of the adiathermic power according to fiber composition

blend cotton/polyester which indicates the effect of insulation properties of the cotton. Therefore, the thermal behavior of the blend fabric (cotton/polyester) is in relation of the percent high content of polyester fibers in the sample as shown in figure 4. Hence, with the higher content of cotton fibers indicates the higher thermal properties.

The adiathermic power increases due to increase in mass area and fabric thickness as well as shown in figure 5. This is explained on the fact that by increase

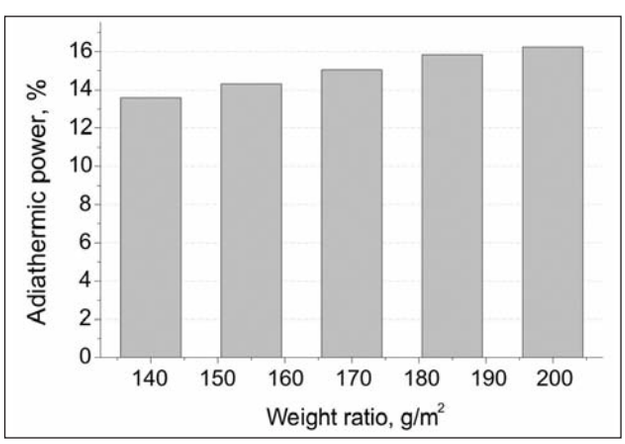

Fig. 5. Variation of the adiathermic power according to mass per area of woven fabric

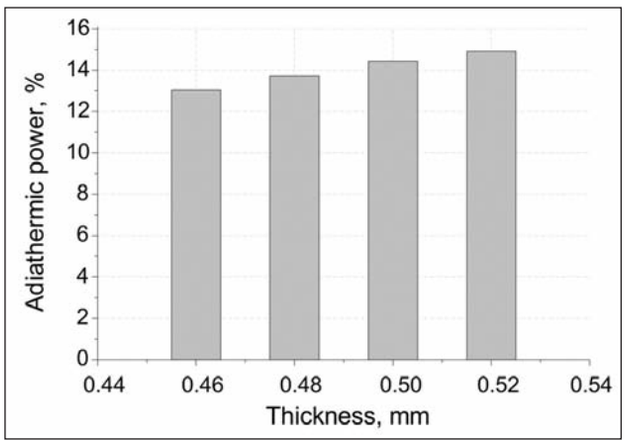

Fig. 6. Variation of the adiathermic power according to thickness of woven fabric

in fabric thickness, the fiber weight per unit area increases. This increase in fibrous material, having a higher thermal property than air, increases their contact points with each other and influences the convenient heat flow across the fabric.

The experimental results show that fabric thickness is in direct proportion with adiathermic power of the fabric as shown in figure 6. When the fabric thickness increases, the air gaps in the fabric structure increases. As the air is a good thermal insulator, therefore by increasing fabric thickness the thermal properties and the adiathermic power increases as well.

In the same consideration, as the fabric thickness increases also the weft count (Nm) or the higher yarn diameter increase. Hence, increases in the adiathermic power of the fabric.

Effect of constructional parameters on thermal resistance and conductivity

The thermal property of woven fabrics was deeply affected by surface properties, which were determined by geometric structure. This geometry was given by the weaving technique, the yarn properties (composition, size, twist and diameter), weft count and warp density. This property was discussed as the thermal conduction resistance R_{CD} and the thermal conductivity. The thermal resistance of a fabric refers to its ability to resist the heat flow through it. The lower the thermal resistance, the better will be the comfort for hot climatic conditions. The thermal conductivity was defined as the measure of conducted heat pass though unit thickness under 1°C heat difference. These two factors were discussed as function of the weave type, the fiber composition, the surface mass and the thickness of woven fabric.

First, the plain weave has many intersections which make this weave very denser and stiffer. Contrarily, the twill weave has less intersections and the satin has important floats which create a shiny surface. These weave properties provide the highest value of thermal conductivity and the lowest thermal resistance for the plain weave. While increasing the yarn float, the thermal resistance increases and thermal conductivity decreases. The variation of these properties was due to bigger pores in the fabric which helps getting more air entrapped into the fabric structure. This more quantity of air will be trapped into the structure and play important role in the variation of these thermal properties.

Second, the fiber composition had important effect on thermal resistance and conductivity. Hence, the thermal conductivity of woven polyester fabric was slightly lower than cotton and blend cotton/polyester fabric. Materials with a lower thermal conductivity have higher resistance to heat flux. This result can be explained by the yarn structure of cotton composition. In third part, the increase of the mass area of woven fabric generates the incrementing of the thermal conduction resistance and the decrease of the thermal conductivity which is explained by the entrapped air in the woven structure. Therefore, the increase of the woven surface area leads to increase of air in the structure. Hence, air has important insulation property, there are its increase in the structure leads to lower thermal conductivity and the highest thermal resistance as shown in table 3.

Table 3

EXPERIMENTAL PROCEDURE PARAMETERS				
		R_{CV} (m^2.K/W)	**R_{CD}** (m^2.K/W)	**TC** (W/K.m)
Woven structure	Plain	5.74	0.6	0.029
	Twill	5.74	0.8	0.027
	Satin	5.74	0.96	0.024
Fiber nature	Cotton	5.74	0.6	0.032
	Co/PES	5.74	0.86	0.029
	PES	5.74	0.93	0.026
Surface mass (g/m^2)	140	5.74	0.62	0.195
	155	5.74	0.84	0.189
	170	5.74	0.91	0.183
	185	5.74	0.97	0.18
	200	5.74	1.08	0.178
Thickness(mm)	0,46	5.74	0.86	0.034
	0,48	5.74	0.883	0.031
	0,5	5.74	0.92	0.029
	0,52	5.74	0.957	0.026

Legend:
Thermal convection resistance: R_{CV}
Thermal conduction resistance: R_{CD}
Thermal conductivity: TC
Cotton/ Polyester: Co/ PES

Finally, these same results of thermal properties obtained in the case of the variation of the surface mass are valid and confirmed in the case of the variation of the woven thickness and explained by the entrapped air in the textile structure.

CONCLUSIONS

To obtain an acceptable satisfaction and physiological comfort it is obligatory to analyze the impact of various fabric parameters on their thermal properties. This research showed that the fabric manufactured with the plain weave and each having the important mass per square and the thickness presents the best thermal properties. These properties decrease for samples presenting the highest porosity and important polyester fiber composition which are known to have low thermal insulation. However, the analysis of physical parameters of fabrics shows that the woven textile fabric having the plain weave, the highest mass per area and the thickness had the important adiathermic power and the lowest thermal resistance and thermal conductivity.

Thus, theses thermal properties are deeply related to the air permeability and fabric porosity. This is due to the increase or decrease in the structure in contact point and yarn density. In second part, the variation in air gap results in improved thermal properties.

BIBLIOGRAPHY

[1] International Organization for Standardization (ISO), (2005) Ergonomics of the thermal environment – analytical determination and interpretation of thermal comfort using calculation of the PMV and PPD indices and local thermal comfort criteria (Standard No. ISO 7730: 2005). Geneva, Switzerland: ISO.

[2] American Society of Heating, Refrigerating and Air-Conditioning Engineers (ASHRAE) (1974), Thermal environmental conditions for human occupancy (Standard No. ASHRAE 55-74). Atlanta, GA, USA: ASHRAE.

[3] Häusler, T., Berger, B. (2002) *Determination of thermal comfort and amount of daylight*. In: Besler GJ, editor. Proceedings of the 10th International Conference on Air Conditioning, Air Protection & District Heating.Wrocław, Poland: PZITS; pp. 227–32.

[4] Das, A., Ishtiaque, S. *Comfort characteristics of fabrics containing twist-less and hollow fibrous assemblies in weft*. JTATM 3: 1-7, 2004.

[5] Grażyna, B., Iwona, F., Agnieszka, G. (2016) *Fabric selection for the reference clothing destined for ergonomics test of protective clothing: physiological comfort point of view*, In: AUTEX Research Journal 16(4), pp. 256–261.

[6] Fourt, L., Holies, N. (1970) *Clothing: comfort and function*. Marcel Dekker (New York).

[7] Song, G., *Improving comfort in clothing,* In: Woodhead Publishing (Cambridge), 2011.

[8] Saville, B.P., *In physical testing of textiles,* In: England, Woodhead Publishing Ltd., 1999, pp. 209–243.

[9] Matusiak, M., Sikorski, K. (2011) I*nfluence of the structure of woven fabrics on their thermal insulation properties.* In: FibresTexEast Eur 19(5), pp. 46–53, 2011.

[9a] Frydrych, I., Dziworska, G., Bilska, J. (2002) *Comparative analysis of the thermal insulation properties of fabrics made of natural and man-made cellulose fibers*. In: FibresTex East Eur 39(4), pp. 40-44.

[10] Varshney, R., Kothari, V., Dhamija, S. (2010) *A study on thermo physiological comfort properties of fabrics in relation to constituent fibre fineness and cross-sectional shapes.* In: J TextI 101(6), pp. 495–505.

[11] Afzal A, Hussain T, Mohsin M, et al (2014),*Statistical models for predicting the thermal resistance of polyester/cotton blended interlock knitted fabrics.*In: Int J ThermSci85: 40-46

[12] Afzal, A., Hussain, T., Mohsin, M., et al (2014) *Statistical model for predicting the air permeability of polyester/ cotton-blended interlock knitted fabrics*. In: J Text I 105(2), pp. 214–222.

[13] Pac, M.J., Bueno, M.A., Renner, M. (2001) *Warm-cool feeling relative to tribological properties of fabrics*. In: Text Res J 71(9), pp. 806–812.

[14] Khoddami, A., Carr, C.M., Gong, R.H. (2009) *Effect of hollow polyester fibres on mechanical properties of knitted wool/ polyester fabrics.* In: Fiber Polym 10(4), pp. 452–460.

[15] Havenith, G. (2002) *Interaction of clothing and thermoregulation*. In: Exogenous Dermatology, 1(5), pp. 221–230.

[16] Milenkovic, L., Skundric, P., Sokolovic, R., Nikolic, T. (1999) *Comfort properties of defence protective clothing.* In: The Scientific Journal Facta Universitatis, 1(4), pp. 101–106.

[17] Matusiak, M. (2006) *Investigation of the thermal insulation properties of multilayer textiles*. In: FibresTex East Eur. 14, pp. 98–102.

[18] Süle, G. (2012) *Investigation of bending and drape properties of woven fabrics and the effects of fabric constructional parameters and warp tension on these properties*. In: Text Res J 82, pp. 810–819.

[19] Militky, J., Kremenakova, D. (2010) *In Prediction of fabrics thermal conductivity,* In: 5th International textile, clothing & design conference – Magic World of Textiles, Dubrovnik, Croatia, Dubrovnik, Croatia, pp. 1–6.

[20] Wang, J., Carson, J.K., North, M.F. (2008) *A new structural model of effective thermal conductivity for heterogeneous materials with co-continuous phases*. In: Int J Heat Mass Transfer 51 (9-10), pp. 2389–2397.

[21] Eucken, A. (1940) Allgemeine Gesetzmabigkeiten fur das Warmeleitvermogenverschiedener Stoffarten und Aggregatzustande. In: Forschung Gabiete Ingenieur,11, pp. 6–20.

[22] Maxwell, J.C. (1954) *A treatise on electricity and magnetism,* (3rd ed), New York, Dover Publications Inc.

[23] Levy, F.L. (1981) *A modified Maxwell-Eucken equation for calculating the thermal conductivity of two-component solutions or mixtures*. In: IntJ Refrig 4 (4), pp. 223–225.

[24] ASTM D3776, (2011) *Standard Test Methods for Mass per Unit Area (Weight) of Fabric*.

[25] ASTM D1777-96, (2007) *Test Method for Thickness of Textile Materials*.

Authors:

SABRI HALAOUA[1], ZOUHAIER ROMDHANI[1], ABDELMAJID JEMNI[2]

[1]Unit of Textile Research Material and Process (MPTex), University of Monastir, ENIM, Tunisia

[2]Laboratory of study of the Thermal and Energy Systems (LESTE), University of Monastir, ENIM, Tunisia

Corresponding author:

ZOUHAIER ROMDHANI

e–mail: romdhanizouhaier@gmail.com

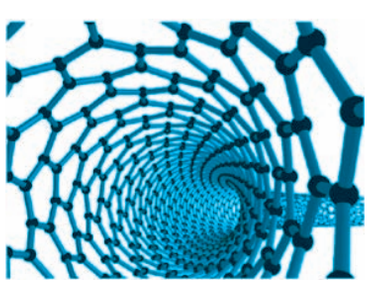

Textile cosmetic pads based on psyllium and protein colloid in combination with the horsetail extract

OLIVERA ŠAUPERL
JULIJA VOLMAJER VALH
LIDIJA FRAS ZEMLJIČ
JASNA TOMPA

REZUMAT – ABSTRACT

Textile funcționalizate pe bază de psyllium și substanță proteică coloidală în combinație cu extract de coada calului, pentru cosmetică

Scopul principal al acestei lucrări de cercetare a fost de a dezvolta produse cosmetice pentru îngrijire/vindecare, în care a fost selectată apa cu extract de coada calului, în calitate de compus de vindecare/îngrijire. Împreună cu aceasta, psyllium și cheratina (substanța proteică coloidală) au fost utilizate în calitate de compuși naturali capabili să formeze o structură de tip gel în mediile apoase, fiind explorate ca: i) purtători ai unui compus de îngrijire/vindecare (extract de coada calului) și ii) "liant" (datorită viscozității relativ înalte) între compusul de vindecare și substratul textil (de exemplu, viscoza nețesută). Un astfel de sistem de funcționalizare a fost aplicat relativ ușor pe substratul de viscoză nețesut. Astfel, a fost creat produsul final, adică produsul cosmetic, care prezintă o bună activitate antioxidantă, stabilitate la depozitare și biodegradabilitate. Ultima proprietate este extrem de importantă pentru produsele ecologice.

Cuvinte-cheie: produse cosmetice, psyllium, coada calului, cheratină, vindecare/îngrijire

Textile cosmetic pads based on psyllium and protein colloid in combination with the horsetail extract

The basic purpose of this research work was to develop a care/healing cosmetic pads where a horsetail water extract was selected as a healing/care compound. Together with this, psyllium and keratin (protein colloid) were used as natural compounds capable to form a gel-like structure in aqueous media, so they were explored as i) carriers of a care/healing compound (horsetail extract), and as ii) "binding element" (due to relatively high viscosity) in-between the healing compound and the textile substrate (i.e. non-woven viscose) itself. Such functionalization system was relatively easily applied onto the non-woven viscose substrate. In this way the final product i.e. the cosmetic pad was created showing good ant oxidative activity, storage stability and biodegradability. The latest is extremely important for environmentally friendly products.

Keywords: viscose pads, psyllium, horsetail, keratin, healing/care

INTRODUCTION

Different natural and chemical compounds in the form of hydrogels, hydrocolloids, bio-films, foams, silicone, etc. are suitable as carriers of the healing substances [1–2]. Alternatively, such compounds can also be applied to any of the textile material, e.g. viscose, which is otherwise a leading substrate in the field of sanitation and medicine [1–2]. Satisfactorily antimicrobial [3], antioxidant, etc. action can be achieved with so called fiber functionalization. A modern concept of textile functionalization introduces natural compounds in the field of textile finishing due to the fact that they have no adverse impact on the potential user and the environment. Here, various plant extracts, or other natural active substances are of particular interest [1–2]. All these compounds must be skin-friendly in order to avoid possible side effects, water pollution, etc. [4]. Arising from these findings the aim of presented work was to create viscose nonwoven natural cosmetic/healing pads by using functionalization based on the horsetail extract as a main healing compound, individually, or in combination with psyllium and keratin. Both, psyllium and keratin colloids are very suitable for various uses, as they intensively swell in aqueous medium [5–11]. High swelling capacity rate possess also animal keratin-based adhesives [11–14]. These protein colloids (keratins) are interesting for water treatment applications [12], and also in the textile industry where are used as adhesives, especially in the field of leather industry, to replace conventional toxic substances [13]. Horsetail is rich source of silicon, and as such contributes to the form, resilience, and flexibility of all connective tissues [15]. All mentioned was the reason why it was used as the main part of the cosmetic pads in order to possibly reduce the skin redness, skin spots, or other skin inconvenience. In order to obtain hydrophilic colloidal systems, horsetail extract was combined with psyllium and keratin. To the best of our knowledge, in such form, this colloidal system was not used until now for viscose fiber functionalization. The obtained coating systems/adsorbates were analyzed from the viscosimetric point of view, supported with testing of their anti-microbial and anti-oxidant activity, biodegradability, followed by "in vivo" bioactive approach (preliminary visual testing). From practical point of view, ant oxidative properties are very important for medical textiles, since ant oxidative

agents are known to cause reduced production of free radicals that increase oxidative stress, leading to DNA damage. Moreover, ant oxidative properties may also contribute to the anti-inflammatory effect [16].

EXPERIMENTAL

Materials and procedures

Dried horsetail plant, commercial psyllium, commercial keratin (rabbit skin glue binder), stabilizer sodium lactate ($C_3H_5O_3Na$, Sigma Aldrich), non-woven viscose obtained by the process of carding, laying and needling, with a surface weight of 165 g/m^2, ready-to-use in the form of a 45 mm-width tape, on the back side combined with polypropylene (PP) (Producer Tosama d.o.o.) were used within experiment. **Horsetail extract**: The extract was prepared according to the following procedure: 20 g of dried horsetail plant was poured with 500 mL of demineralized water, then treated for 4 h at 100 °C, and finally left overnight to slowly cool down at the room temperature. **Functionalization medium (coating systems)**: Psyllium in combination with demineralized water, and psyllium in combination with the horsetail extract were prepared in ratio of 200 mL of demineralized water: 3 g of psyllium, while keratin (rabbit skin glue binder) in combination with demineralized water, and keratin in combination with the horsetail extract in ratio of 200 mL of demineralized water: 20 g of rabbit skin glue binder. **Viscose functionalization**: Non-woven viscose was functionalized according to the conventional impregnation method by using a two-roller foulard (W. Mathis); Conditions: 2 bar pressure, material transfer rate 2 m/min, and add-on 90–100 %. Before squeezing, the non-woven viscose was thoroughly soaked (1 hour) with all functionalization formulations as pointed out in the table 1.

Methods

Viscosimetry: The viscosity of prepared liquid functionalization formulations in mPas was determined by using viscometer FUNGILAB Smart Serial.

Antimicrobial activity: Antimicrobial testing was carried out in accordance with the standard AATCC 147 (test organism: *S aureus,* ATCC No 25923).

Antioxidant activity: Antioxidant activity of functionalized non-woven viscose was evaluated by using the $ABTS^{\bullet+}$ method (2,2'-azino-bis-3-ethylbenzothiazoline-6-sulfonic acid, Sigma Aldrich). The radical $ABTS^{\bullet+}$ occurs during the oxidation of ABTS, and potassium persulfate absorbing in the visible region at a wavelength of 734 nm. This is determined spectrophotometrically (eq. 1).

$$\text{Inhibition} = (A_{starting} - A_{sample})/A_{sample} \times 100/\% \quad (1)$$

where: $A_{starting}$ is absorbance, measured at starting concentration of $ABTS^{\bullet+}$, A_{sample} – absorbance, measured at the rest concentration of $ABTS^{\bullet+}$ [16].

Determination of biodegradability: Textiles-determination of the resistance of cellulose-containing textiles to micro-organisms-Soil burial test – Part 1: Assessment of rot-retardant Finishing (ISO 11721-1: 2001). **In vivo preliminary testing**: Preliminary *in vivo* testing was performed on population of four volunteers suffering from the skin problems.

RESULTS AND DISCUSSION

Viscosimetry: Results of the average viscosity (3 replicates) of the functionalization formulations used within research are collected in table 1.

Table 1

FVISCOSITY IN mPas OF SEPARATE FUNCTIONALIZATION FORMULATION	
Functionalization formulation	**Viscosity** (m*Pas*)
Psyllium + demineralized water (reference)	2923.4
Psyllium + horsetail extract	377.7
Rabbit skin glue binder + demineralized water (reference)	1336.3
Rabbit skin glue binder + horsetail extract	840.0

Psyllium and protein colloid (rabbit skin glue binder) have high swelling ability in the aqueous medium so, they were selected to determine whether either of these compounds provides better properties in terms of stickiness and the ability to retain the horsetail extract in a gel-like structure. The interest was therefore, to achieve optimal viscosity in terms of the functionalization formulations practical use following optimal ratio between the solvent and the solute. On the basis of preliminary tests it was determined the optimal targeted viscosity which is in the case of psyllium of about 350 mPas, and in the case of a rabbit skin glue binder about 800 mPas. Based on this, the ratio between the solvent and the solute was defined: 200 mL of solvent: 3 g of psyllium i.e. ratio 67:33 (v:m) and 200 mL of the solvent: 20 g of rabbit glue binder i.e. ratio 10:1 (v:m). **Antimicrobial activity**: The bacterial strain *Staphylococcus aureus* (Gram-positive bacteria, ATCC No 25923) was used as the test organism. This type of micro-organism was selected on the basis of the assumption that it is a micro-organism that is present in most environments. An insufficient anti-microbial activity (AATCC standard 147) on *Staphylococcus aureus* is seen with all functionalized samples (no zone of inhibition). However, not only antimicrobial properties are essential for medical textiles development, but also **antioxidant activity** [18–19]. Functionalization of viscose with combination of psyllium and the horsetail extract proved to be more effective if compared to viscose, functionalized with combination of protein colloid (keratin) in combination with the horsetail extract. Anyway, it can be seen from results that functionalization where horsetail extract was used as a solvent for psyllium and the protein colloid (keratin), increased the antioxidant activity from 81 % to 95 % in the case of psyllium (if deionized water was used as a solvent) and in the case of a keratin from 55.9 %

to 71.5 % (if deionized water was used as a solvent). Results show also good antioxidative activity of viscose, functionalized with psyllium in combination with deionized water (81 %), indicating that psyllium itself has good antimicrobial activity. Certain antioxidant activity (55.9 %) possesses also viscose, functionalized with keratin in combination with deionized water, which is related to the antioxidant activity of protein colloid (keratin) itself due to the presence of amino acid cysteine in its structure [20]. Antioxidant results are shown in figure 1.

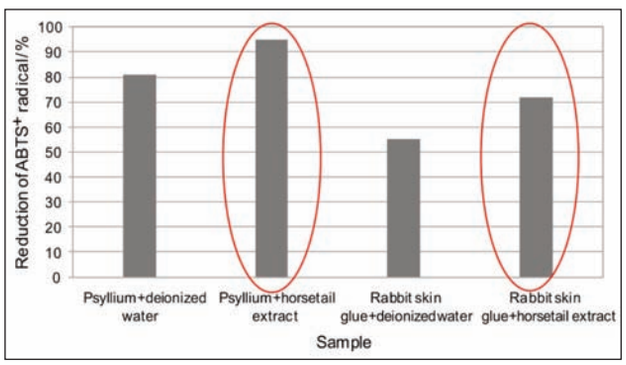

Fig. 1. Antioxidativity (reduction of radical $ABTS^{\bullet+}$) of functionalized non-woven viscose in dependence on functionalization formulation

Fig. 2. Biodegradability of functionalized viscose samples after seven days of burial in the soil

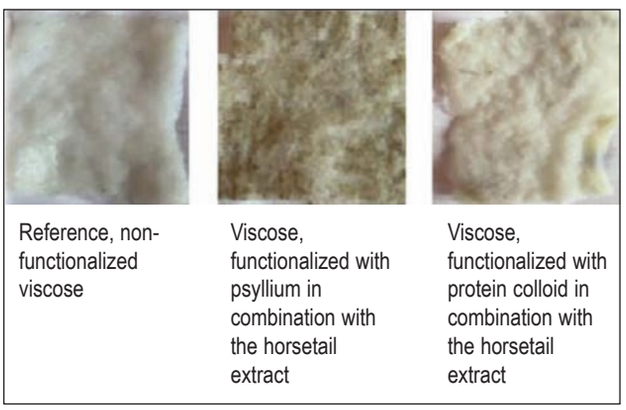

Fig. 3. Biodegradability of functionalized viscose samples with added stabilizer after seven days of burial in the soil

Biodegradability and aging: Results show a significant degree of biodegradability of horsetail extract based functionalized samples after seven days of burial in the soil. In the case of viscose, functionalized with keratin in combination with horsetail extract, the appearance of biodegradability was even more pronounced than in the case of functionalization using psyllium in combination with the horsetail extract (figures 2–3).

After fourteen days, the cosmetic pads were completely decomposed. Thus, this product is also very friendly from environmentally point of view. In order to check the stability of prepared cosmetic pads under real storage conditions the cosmetic pads were packed in polyethylene (PE) bags and stored in a refrigerator which not proves to be effective, as after a few days a mould appeared and fully covered the surface of the pads. In this respect, appropriate solution based on the drying of the pads at room temperature was found as a good approach. These were subsequently rehydrated by the addition of about 5 ml of distilled water, thereby establishing the original state of functionalized samples. In order to achieve certain stability of the functionalized samples even in wet conditions, 5 % of natural stabilizer (Na lactate) was added to the separate functionalization formulation; the samples remained in perfect condition (visual estimation) after thirty days of storage in the refrigerator. Antioxidativity of samples remained almost the same.

Testing in vivo-preliminary study: The study included 4 test persons-volunteers who treated the various parts of the body they considered as a skin problematic. In all cases, after one day of care, a significant improvement in the appearance of spots on certain parts of the body and the appearance of redness on the face and forehead was confirmed (figure 4 second line).

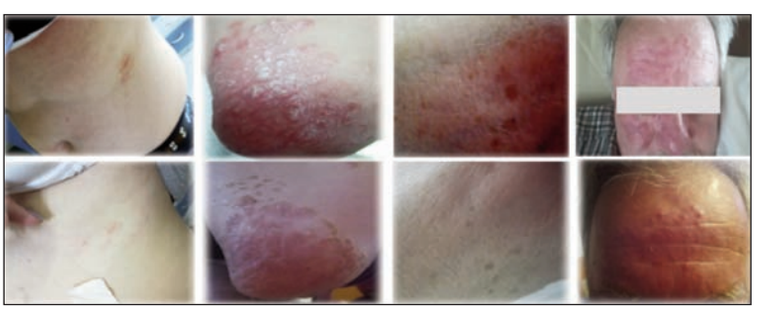

Fig. 4. Results in-vivo-preliminary visual testing

CONCLUSIONS

Psyllium and protein colloid (rabbit skin glue binder) were used as *i*) the carriers of the care/healing compound (horsetail extract) and as *ii*) the binding elements between the active substance (horsetail extract) and the textile (non-woven viscose). Great attention was paid to optimizing adequate viscosity for optimal coating of the samples. *S. aureus* is insufficiently reduced by all functionalized samples. On the other hand, high antioxidant activity of functionalized viscose samples with integrated horsetail extract is seen with all tested samples. Besides this, prepared pads are excellent biodegradable. The storage stability of textile pads in the refrigerator is prolonged

when the stabilizer (Na-lactate) is part of the functionalization formulation. A great potential for the production of psyllium and protein colloid based textile pads with incorporated horsetail extract is confirmed with the research; preliminary in-vivo results showed extremely promising results.

BIBLIOGRAPHY

[1] Šauperl, O., Kralj Kunčič, M., Tompa, J., Fras Zemljič, L., Volmajer Valh J. *Functionalization of non-woven viscose with formulation of chitosan and honey for medical applications*, In: Fibres & textiles in Eastern Europe, 2017, in progress.

[2] Šauperl, O., Tompa, J., Volmajer Valh, J. *Influence of the temperature on the efficiency of cellulose treatment using copolymer chitosan-eugenol*, In: Journal of engineered fibers and fabrics, 2014, vol. 9, no. 3, pp. 107–114.

[3] Fras Zemljič, L., Šauperl, O. *Chitosan and its derivatives as an adsorbate for cellulose fibres' anti-microbial functionalizations*, In: Industria textila, 2012, vol. 63, no. 6, pp. 296–301.

[4] Joshi, M., Ali, S.W., Purwar, R., Rajendran, S., *Ecofriendly antimicrobial finishing of textiles using bioactive agents based on natural products*, In: Indian Journal of Fibre & Textile Research, 2009, vol. 34, pp. 295–304.

[5] Milton, H., Fiscera, A., Nanxiong Yu, B., et al. *The gel-forming polysaccharide of psyllium husk (Plantago ovata Forsk)*, In: Carbohydrate Research, 2014, vol. 339 (11), pp. 2009–2017.

[6] Banasaz, S., Hojatoleslami, M., Razavi, S., et al. *The effect of psyllium seed gum as an edible coating and comparison to Chitozan on the textural properties and color changes of res delicious apple*, In: International Journal of Farming and Allied Sciences, 2013, vol. 2 (18), pp. 651–657.

[7] Farahnaky, A., Askari, H., Majzoobi, M., Mesbahi, G.H. *The impact of concentration temperature and pH on dynamic rheology of psyllium gels*, In: Journal of Food Engineering, 2010, vol. 100 (2), pp. 294–301.

[8] Moreaux, S., Nichols, J., Bowman, J. GP., Hatfield, P.G. *Psyllium lowers blood glucose and insulin concentration in horses*, In: Journal of Equine Veterinary Science, 2011, vol. 31 (4), pp. 160–165.

[9] Anand, S., Kennedy, J., Miraftab, M., Rajendranet, S. *Medical and healthcare textiles*, In: Woodhead Publishing, 2010, vol. 560, pp. 249–250.

[10] Cavallaria, C., Brigidib, P., Finia, A. *Ex-vivo and in-vitro assessment of mucoadhesive patches containing the gel-formig polysacharide psyllium for buccal delivery of chlorhexidine base*, In: International Journal of Pharmaceutics, 2015, vol. 496 (2), pp. 593–600.

[11] Singht, B. *Psyllium as therapeutic and drug delivery agent*, In: International Journal of Pharmaceutics, 2007, vol. 334 (1-2), pp. 1–14.

[12] Wattie, B. *Synthesis of keratin-based hydrogels and cryogels destined for environmental applications*, In: Department of Bioresource Engineering, Faculty of Agricultural and Environmental Sciences, Macdonald Campus of McGill University Ste-Anne-de-Bellevue, Quebec, Canada, Bryan Wattie, 2016

[13] Sedliačik, J., Matyašovský, J., Smidriakov, M., Sedliacikova, M., Jurkovič, P. *Application of collagen colloid from chrome sharings for innovative polycondensation adhesives*, In: Journal of the American leather chemists association, 2011, vol. 106 (11), pp. 332–340.

[14] Manzano, E., Romero-Pastor, J., Navas, N., Rodríguez-Simón, L. R., Cardell, C. *A study of the interaction between rabbit glue binder and blue copper pigment under UV radiation: A specroscopic and PCA approach*, In: Vibrational Spectroscopy, 2010, vol. 53 (2), pp. 260–268.

[15] Nagai, T., Myoda, T., Nagashima, T. *Antioxidative activities of water extract and ethanol extract from field horsetail (tsukushi) Equisetum L.*, In: Food chem., 2005, vol. 91, pp. 389–394.

[16] Fras Zemljič, L., Peršin, Z., Šauperl, O., Rudolf, A., Kostić, M. *Medical textiles based on viscose rayon fabrics coated with chitosan encapsulated iodine: antibacterial and antioxidant properties*, In: Textile research journal, First Published August 13, 2017, pp. 1–13.

[17] Ohba, R., Deguchi, T., Kishikawa, M., Arsyad, F., Morimura, S., Kida, K. *Physiological functions of enzymatic hydrolysates of collagen or keratin contained in livestock and fish waste*, In: Food Science and Technology Research, 2003, vol. 9 (1), pp. 91–93.

[18] Ristić, T., Hribernik, S., Fras Zemljič, L. *Electrokinetic properties of fibres functionalised by chitosan and chitosan nanoparticles*, In: Cellulose (2015), vol. 22 (6), pp. 3811–3823.

[19] Ristić, T., Zabret, A., Fras Zemljič, L., Peršin, Z. *Chitosan nanoparticles as a potential drug delivery system attached to viscose cellulose fibers*, In: Cellulose (2017), vol. 24 (2), pp. 739–753.

[20] Di Bernardini, R., Harnedy, P., Bolton, D., Kerry, J., O'Neill, E., Mullen, A.M., Hayes, M. *Antioxidant and antimicrobial peptidic hydrolysates from muscle protein sources and by-products*, In: Food Chemistry, 2011, vol. 124 (4), pp. 1296–1307.

Authors:

OLIVERA ŠAUPERL, LIDIJA FRAS ZEMLJIČ, JULIJA VOLMAJER VALH, JASNA TOMPA

University of Maribor, Faculty of Mechanical Engineering,
Smetanova ulica 15, SI-2000, Maribor, Slovenia
e-mail: olivera.sauperl@um.si, lidija.fras@um.si, julija.volmajer@um.si, jasna.tompa@um.si

Corresponding authors:

OLIVERA ŠAUPERL
e-mail: olivera.sauperl@um.si

Eco-friendly route for dyeing of cotton fabric using three organic mordants in reactive dyes

RIAZ BAIG
DILSHAD HUSSAIN
MUHAMMAD NAJAM-UL-HAQ
ABDUL WAQAR RAJPUT
RANA AMJAD

REZUMAT – ABSTRACT

Soluție ecologică pentru vopsirea țesăturilor din bumbac utilizând trei mordanți organici în coloranți reactivi

Coloranții textile și agenții de fixare care sunt utilizați în procesul de vopsire contribuie în mare măsură la poluarea mediului. În studiul de față, trei tipuri diferite de mordanți organici (citrat de sodiu, acetat de amoniu și acetat de potasiu) sunt utilizați la vopsirea prin epuizare, ca mordanți. Efectul concentrațiilor de mordanți este studiat pe baza proprietăților de rezistență a culorii (modificarea culorii, rezistența la frecare și rezistența la lumină) a bumbacului vopsit cu coloranți reactivi utilizând acești mordanți organici. Compararea acestor mordanți cu agentul de fixare convențional (NaCl) este, de asemenea, studiată pentru a evalua diferența dintre proprietățile de rezistență a culorii sărurilor convenționale și organice utilizate în acest studiu. S-a constatat că proprietățile de rezistență a culorii sărurilor convenționale și organice sunt comparabile, precum și încazul citratului de sodiu. În mod similar, intensitatea culorii țesăturii după vopsirea cu săruri organice și anorganice a fost măsurată utilizând Datacolor. Rezultatele au confirmat că valorile mai ridicate ale K/S sunt obținute pentru sărurile organice prin utilizarea unei concentrații mai scăzute de sare organic în comparație cu sarea convențională. Scăderea totalului solidelor dizolvate (TDS) ale efluenților colorați se situează între 6% și 29% pentru trei săruri organice în comparație cu sarea convențională.

Cuvinte-cheie: coloranți reactivi, proprietăți de rezistență a culorii, mordanți organici, țesătură din bumbac, totalul solidelor dizolvate

Eco-friendly route for dyeing of cotton fabric using three organic mordants in reactive dyes

The textile dyes and fixing agents that used in dyeing process are major contributor to environmental pollution. In the present study, three different organic mordants (Sodium Citrate, Ammonium Acetate, and Potassium Acetate) are used in exhaust dyeing as mordants. Effect of mordant concentrations is studied on fastness properties (color change, rubbing fastness & light fastness) of cotton dyed with reactive dyes using these organic mordants. Comparison of these mordants with conventional fixing agent (NaCl) is also studied in order to evaluate the difference between fastness properties of conventional and organic salts used in this study. We found that the color fastness properties of conventional and organic salts are comparable, better in case of sodium citrate. Similarly color depth on fabric after dyeing with organic as well as inorganic salts is measured using data color. Results confirm that higher values of K/S are obtained for organic salts by using lower organic salt concentration compared to conventional salt. Reduction in total dissolved solids (TDS) of dye effluents is obtained from 6% to 29% for three organic salts as compared to conventional salt.

Keywords: reactive dyes, fastness properties, organic mordants, cotton fabric, total dissolved solids

INTRODUCTION

Dyeing and finishing processes are integral part of textile industry. Variety of methods is being used in textile industry to improve the dyeing process [1]. Exhaust dyeing is one of all these processes used in textile dyeing. It has good fatness properties due to dye fibre chemical bonding as compare to other dyeing processes. Due to the presence of xenobiotic compounds in textile waste of this process, it contributes a lot in creating environmental pollution [2]. Textile effluents usually contain alkalis, organic acids, organic dyes, finishing agents and non-biodegradable inorganic salts [3, 4]. These textile waste materials are harmful for aquatic life as well as it is responsible for many diseases in humans [5]. For treatment of these toxic compounds many methods have been developed which include adsorption, oxidation, anaerobic decolourization, catalysis, ion exchange, membrane filtration, flocculation and ozonation [6–8]. All these methods have certain drawbacks, they can reduce the pollution but they are expensive. Another major issue is the disposal of solid waste produced during such treatments [9]. One obvious solution of this problem could be the use of better chemicals and improve the processing technology in order to reduce pollution problems.

Reactive dyes are mostly used in textile industry to produce bright colours. These reactive dyes also impart fastness properties to the dyed fabrics due to the strong covalent bonding under alkaline conditions between natural fibre and dye [10]. It is well known that reactive dyes have low degree of fixation on the textile fabric [11]. For any type of dying process, usually surfactants, inorganic salts and alkalis are required during dyeing process in order to fix the dye into fibre under suitable alkaline conditions [12–13].

These salts and alkalis, after dyeing process are drained along with effluents. Due to incorporation of salts and alkalis in the waste effluents, value of dissolved solids increases into the effluent in the form of Total Dissolved Solids (TDS) which also produces environmental pollution [14–15]. Improvement in dyeing techniques, machinery and use of more improved structural dyes has helped in reduction of organic salts and ultimately TDS in the effluents [16–19].
Use of organic salts instead of conventional inorganic salt could reduce the pollution problem because the removal and degradation of organic salts is easier. In the present work an attempt has been made to replace the conventional inorganic salts with organic salts. Effect of using reduced concentration of organic salts on the dyeing properties, colour depth and K/S values has been studied. It has been observed that reduced concentration of organic salts under the same dyeing conditions not only helps to decrease the TDS in textile effluents, but also improves colour depth.

EXPERIMENTAL

Chemicals and reagents

Cotton twill fabric having 200 g/m^2, 160 ends/inch and 60 picks/inch was used in this study. Reactive dyes C.I. Reactive Blue 250, C.I. Reactive Red 195, C.I. Reactive Yellow 145 & C.I. Reactive Black 5 were used. Organic mordants used in this study were mono sodium citrate, ammonium acetate and potassium acetate supplied by Sigma Aldrich. All these chemicals were of analytical grade and were used without any further pre-treatment.

Dyeing procedure

Commercially scoured and bleached Twill fabric was used for exhaust dyeing. IR dyer (D400IR) was used to dyecotton fabric. 0.4% aqueous solution of each dye was prepared and then fed into the IR dyer along-with fabric. Liquor ratio (1:10) was adjusted according to fabric weight. 2 g commercially available salt of sodium chloride and 3 g sodium bicarbonate was added into the container. Similarly, 2 g of each organic salt & 3 g sodium bicarbonate was separately weighed and feed into already labeled separate containers of IR Dyer having dye solution and fabric. The details of the dyeing conditions arementioned in table 1.

Table 1

Dying Process	Exhaust dying
Dyeing Temperature	70 °C
Dyeing Time	30 minutes
Baths rotational speed	40 rpm
Dye Depth Shade	2% shade

At the completion of dyeing procedure, contents of IR dyer were drain out leaving dyed fabric. Fabric was washed and rinsed with hot water (95 °C) and then with water at room temperature till desorption of dye [20].
Samples were removed from IR Dyeing machine D400IR, washed, dried and conditioned then, evaluated for fastness properties (fastness to light on weathero meter Ci 3000, crocking on AATCC Crockmeter, and laundering on Washtec-p Launder o meter) by using standard testing methods.
The dyeing parameters such as the effect of concentration of organic salts on the dyeing properties, color depth and K/S values were also studied using similar procedure.

RESULTS AND DISCUSSION

Evaluation of fastness properties

Fastness properties of dye are considered as an important parameter in dying process. Fasteners are basically binding agents which bind the reactive dyes to the cellulose fibers and improve the binding strength during wet treatments. Fastening agents improve the production rate by reducing the washing baths and process time. We also studied the fastening properties of four dyes using organic mordants. For comparison, the effect of traditional inorganic salt (NaCl) is also applied to the same dyes under similar conditions. We applied different standard methods to evaluate the fastness properties including (BO5 for fastness to light, AATCC 8 for fastness to dry and wet crocking, AATCC 61 for fastness to laundering). Results of fastness properties using conventional as well as organic salt for all the dyes are shown in table 2.
Results confirm that all organic salts show better fastness properties for all the methods compared to conventional salt i.e. NaCl. Different types of cotton fibers were also tested to further justify the hypothesis but these mordants show better results in all types of fibers. Better colour change has also been observed in all dyes by applying organic mordants. This may be attributed to the better association of citrate and acetate groups to the cotton fibers. Among organic salts, sodium citrate showed better fastness properties than ammonium acetate and potassium acetate. These results prove that organic salts can be used as potential replacements for conventional inorganic mordants due to their better fastening properties and eco-friendly nature. This leads to the decrease in TDS in the effluent water normally caused by the use of sodium chloride. With further optimization these mordants could be applied at industrial scale.

Optimization of salt concentration vs color yield

With increasing salt concentration, dye levelness improves and resultant color yield [21–22]. Initially we optimized the effect of concentration of inorganic salt on the color yield of the fabric using 2% dye solution and varying concentrations of inorganic salt from 1% to 5% using liquor ratio of (1:10). Results show that for C.I Reactive Blue 250 using 5% Sodium Chloride (NaCl), maximum value of color yield is obtained.

Table 2

Dye 20 gm/l	Mordants	Colour fastness to accelerated laundering AATCC 61							Color fastness to crocking (AATCC 8)		CF to light (ISO 105BO2)
		Staining						Col change	Dry	Wet	
		Ace	Co	Ny	Po	Acr	Wo				
C.I Reactive Blue 250	Sodium Chloride	4–5	4–5	4	4–5	4–5	3–4	4	4–5	4	7–8
	Potassium Acetate	3–4	3–4	3–4	4–5	4–5	3–4	4	3–4	3–4	4–5
	Ammonium Acetate	4–5	4–5	4–5	4–5	4–5	4–5	3–4	4–5	3–4	5
	Sodium Citrate	4–5	4–5	4–5	4–5	4–5	4	4–5	4–5	4–5	8
C.I Reactive Red 195	Sodium Chloride	4–5	4–5	4–5	4–5	4–5	4–5	4–5	4–5	4–5	8
	Potassium Acetate	4–5	4	4–5	4–5	4–5	4	4	3–4	4–5	5–6
	Ammonium Acetate	4–5	4–5	4–5	4–5	4–5	4–5	3–4	4–5	4	5–6
	Sodium Citrate	4–5	4–5	4–5	4–5	4–5	4–5	4–5	4–5	4–5	7–8
C.I Reactive Yellow 145	Sodium Chloride	4–5	4–5	4	4–5	4–5	4–5	4	4–5	3–4	7–8
	Potassium Acetate	4–5	3–4	4–5	4–5	4–5	4	3–4	4–5	4–5	6–7
	Ammonium Acetate	4–5	4	4	4–5	4–5	4–5	4–5	4–5	3–4	5–6
	Sodium Citrate	4–5	4	4–5	4–5	4–5	4	4–5	4–5	4–5	8
C.I Reactive Black 5	Sodium Chloride	4–5	5	4	4–5	4–5	4–5	4–5	4–5	4	7–8
	Potassium Acetate	4–5	4–5	4–5	4–5	4–5	4–5	4	4–5	3–4	6–7
	Ammonium Acetate	4–5	4–5	4–5	4–5	4–5	4–5	3–4	4	4	5–6
	Sodium Citrate	4–5	5	4–5	4–5	4–5	4	4–5	4–5	4–5	6

Similarly changing the alkali concentration also affected the color yield. Changing the concentration from 0.5% to 3%, using 2% solution of C.I Reactive Blue 250 under same dyeing conditions as mentioned above. Results show that maximum color yield is obtained at 1.5% alkali solution, using 5%. Effect of salt concentration on color yield is shown in figure 1.

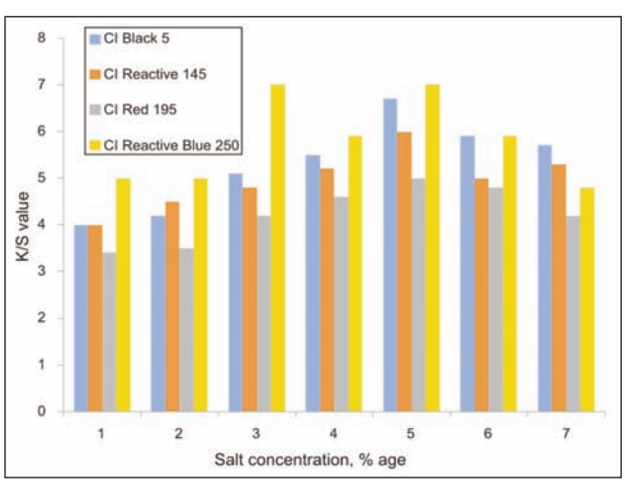

Fig. 1. Color yield vs salt concentration (%)

Similarly, dyeing is performed using 2% reactive dyes, by taking each of 2% organic salts including potassium acetate, ammonium acetate and sodium citrate. Color strength for each dyed fabric is taken using data color (SF650X). Results show that greater values of color ratio (K/S) are obtained using lower concentration of organic salts for different reactive dyes compared to conventional inorganic salts which required higher concentration for fixation of dyes on fabric. This shows that inorganic salts are better substitute of inorganic salt. This lower concentration of organic mordants is also helpful in lowering of total dissolved solids in effluents of dyeing in textile industry. Results showing the effect of organic salt concentration on K/S value are shown in figure 2.

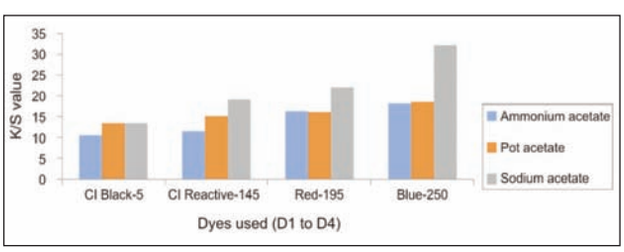

Fig. 2. Effect of organic salt concentration on K/S value on cotton fabric using reactive dyes

Effluent analysis

Purpose of this study is to reduce the TDS of dye effluent by using alternative biodegradable electrolyte. Table 3 shows that the use of Sodium Citrate reduce nearly 17%–29% TDS of effluents for all dyes as compare to conventional inorganic salt Sodium Chloride. Similarly TDS of effluents was reduced 6%–20% by using organic salts Potassium Acetate and Ammonium Acetate. Reduction in TDS due to use of sodium citrate the lower level in total dissolved salt for all the dyes are because of the lower concentration of the sodium citrate for the better color fixation and better color yield. This gives better color yield for all the used dyes. It shows that in the effluent the unfixed dye ratios is reduced and make the Sodium Citrate an ecofriendlysalt for dyeing. Further, it provided significantly higher color yields for all dyes. The ratio of unfixed dye in the effluent remarkably reduced and a Sodium Citrate salt is environment friendly.

Table 3

Dyes used (20 g/l)	Effluent samples (diluted 100 times)	TDS (mg/l)
C.I Reactive Blue 250	Sodium Citrate (40 g/l)	1010
	Potassium Acetate (40 g/l)	1145
	Ammonium Acetate	1280
	Sodium chloride (50 g/l) Sodium bicarbonate (15 g/l)	1380
C.I Reactive Red 195	Sodium Citrate (40 g/l)	990
	Potassium Acetate (40 g/l)	1110
	Ammonium Acetate	1295
	Sodium chloride (50 g/l) Sodium bicarbonate (15 g/l)	1400
C.I Reactive Yellow 145	Sodium Citrate (40 g/l)	1140
	Potassium Acetate (40 g/l)	1215
	Ammonium Acetate	1250
	Sodium chloride (50 g/l) Sodium bicarbonate (15 g/l)	1390
C.I Reactive Black 5	Sodium Citrate (40 g/l)	1130
	Potassium Acetate(40 g/l)	1220
	Ammonium Acetate	1325
	Sodium chloride (50 g/l) Sodium bicarbonate (15 g/l)	1420

CONCLUSION

In this research, for the first time, we evaluated the effect of three organic salts on dying of cotton fabric using four reactive dyes. We studied the effect of organic mordants on different dying parameters such as fastness properties, color yield and K/S value. From the results, we can conclude that the organic salts including sodium citrate, potassium acetate and ammonium acetate show comparable fastness properties as obtained in case of using conventional salts. Out of these three salts sodium citrate show better fastness properties as compared to other salts. Furthermore, at lower concentration organic salts show higher K/S values.

The use of these biodegradable salts during the dyeing process helps in decreasing TDS which is ultimately reduction in environmental pollution.

Effluents analysis shows that 6% – 29% reduction in TSD is observed by using all three organic salts as mordants as compare to Conventional salt Sodium Chloride. So, we can predict that after further optimization these mordants could be potential replacement of traditional inorganic salts in textile industry.

BIBLIOGRAPHY

[1] Robinson, T., McMullan, G., Marchant R., and Nigam, P. *Remediation of dyes in textile effluent: a critical review on current treatment technologies with a proposed alternative,* In: Bioresource technology, Volume 77, Issue 3, pp. 247–255.

[2] Akhtar, S., Baig, S. F., Saif, S., Mahmood, A., and Ahmad, S. R. *Five year carbon footprint of a textile industry: A podium to incorporate sustainability,* In: Nature Environment and Pollution Technology, Volume16, Issue 1, pp. 125–132.

[3] Bilińska, L., Gmurek, M., and Ledakowicz, S. *Comparison between industrial and simulated textile wastewater treatment by AOPs – Biodegradability, toxicity and cost assessment,* In: Chemical Engineering Journal, Volume 306, pp. 550–559.

[4] Zhang, W., Liu, W., Zhang, J., Zhao, H., Zhang, Y., Quan, X., and Jin, Y. *Characterisation of acute toxicity, genotoxicity and oxidative stress posed by textile effluent on zebrafish,* In: Journal of environmental sciences, Volume 24, pp. 2019–2027.

[5] Khan, S., and Malik, A. *Environmental deterioration and human health: Natural and anthropogenic determinants*, eds. A. Malik, E. Grohmann and R. Akhtar, In: Springer Netherlands, Dordrecht, 2014, pp. 55–71.

[6] Pekakis, P. A., Xekoukoulotakis, N. P., and Mantzavinos, D. *Treatment of textile dyehouse wastewater by TiO_2 photocatalysis,* In: Water research, Volume 40, pp. 1276–1286.

[7] Sarayu, K., and Sandhya, S. *Current technologies for biological treatment of textile wastewater – A review,* In: Applied biochemistry and biotechnology, Volume 167, pp. 645–661.

[8] Husaain, D., Najam-ul-Haq, M., Saeed, A., Jabeen, F., Athar, M. and Naeem Ashiq, M. *Synthesis of poly GMA/DVB and its application for the removal of Malachite Green from aqueous medium by adsorption process,* In: Desalination and Water Treatment, Volume 53, pp. 2518–2528.

[9] Garg, V., Kaushik, P., and Dilbaghi, N. *Vermiconversion of wastewater sludge from textile mill mixed with anaerobically digested biogas plant slurry employing Eiseniafoetida,* In: Ecotoxicology and environmental safety, Volume 65, pp. 412–419.

[10] Khatri, A., Peerzada, M. H., Mohsin, M., and White, M. *A review on developments in dyeing cotton fabrics with reactive dyes for reducing effluent pollution,* In: Journal of Cleaner Production, Volume 87, pp. 50–57.

[11] Nabil, G. M., El-Mallah, N. M., and Mahmoud, M. E. *Enhanced decolorization of reactive black 5 dye by active carbon sorbent-immobilized-cationic surfactant (AC-CS),* In: Journal of industrial and engineering chemistry, Volume 20, pp. 994–1002.

[12] Ferreira, A. M., Coutinho, J. A., Fernandes, A. M., and Freire, M. G. *Complete removal of textile dyes from aqueous media using ionic-liquid-based aqueous two-phase systems,* In: Separation and Purification Technology, Volume 128, pp. 58–66.

[13] Moreira, S., Milagres, A. M., and Mussatto, S. I. *Reactive dyes and textile effluent decolorization by a mediator system of salt-tolerant laccase from Peniophoracinerea,* In: Separation and Purification Technology, Volume 135, pp. 183–189.

[14] Vajnhandl, S., and Valh, J. V. *The status of water reuse in European textile sector,* In: Journal of environmental management, Volume 141, pp. 29-35.

[15] Balapure, K., Bhatt, N., and Madamwar, D. *Mineralization of reactive azo dyes present in simulated textile waste water using down flow microaerophilic fixed film bioreactor,* In: Bioresource technology, Volume 175, pp. 1–7.

[16] Kharat, *D. Treatment of textile industry effluents: limitations and scope,* In: Journal of Environmental Research and Development, 2015, Volume 9, p. 1210.

[17] Noroozi, B., and Sorial, G. A. *Applicable models for multi-component adsorption of dyes: A review,* In: Journal of Environmental Sciences, Volume 25, pp. 419–429.

[18] Kongahge, D., Foroughi, J., Gambhir, S., Spinks, G. M., and Wallace, G. G. *Fabrication of a graphene coated nonwoven textile for industrial applications,* In: RSC Advances, Volume 6, pp. 73203–73209.

[19] Dasgupta, J., Sikder, J., Chakraborty, S., Curcio, S., and Drioli, E. *Remediation of textile effluents by membrane based treatment techniques: A state of the art review,* In: Journal of environmental management, Volume 147, pp. 55–72.

[20] Li, Y., Ren, J., Chen, S., Fan, F., Shen, Q., and Wang, C. *Cationic superfine pigment dyeing for wool using exhaust process by pH adjustment,* In: Fibers and Polymers, Volume 16, pp. 67–72.

[21] Haji, A. and Qavamnia, S. S. *Response surface methodology optimized dyeing of wool with cumin seeds extract improved with plasma treatment,* In: Fibers and Polymers, Volume 16, pp. 46–53.

[22] Javaid Mughal, M., Saeed, R., Naeem, M., Aleem Ahmed, M., Yasmien, A., Siddiqui, Q., and Iqbal, M. *Dye fixation and decolourization of vinyl sulphone reactive dyes by using dicyanidiamide fixer in the presence of ferric chloride,* In: Journal of Saudi Chemical Society, Volume 17, pp. 23–28.

Authors:

RIAZ BAIG[1],
DILSHAD HUSSAIN[1],
MUHAMMAD NAJAM-UL-HAQ[1],
ABDUL WAQAR RAJPUT[2]
RANA AMJAD[3]

[1]Division of Analytical Chemistry, Institute of Chemical Sciences, Bahauddin Zakariya University, Multan 60800, Pakistan

[2]Technical Textile Research Group, BZU College of Textile Engineering, Multan, Pakistan

[3]Applied Chemistry Research Center, PCSIR Laboratories Complex, Ferozpur Road, Lahore, Pakistan

e-mail: raiz_baig2009@yahoo.com,shad3233@yahoo.com, najamullhaq@bzu.edu.pk, waqar.rajput@bzu.edu.pk, amjadayubbhatti@gmail.com

Corresponding author:

ABDUL WAQAR RAJPUT
e-mail: waqar.rajput@bzu.edu.pk

Comparative study between two types of electrolyte used in the reactive dyeing of cotton

AYDA BAFFOUN

REZUMAT – ABSTRACT

Studiu comparativ între două tipuri de electroliți utilizați în vopsirea cu coloranți reactivi a bumbacului

Scopul acestui studiu a fost de a compara eficiența a două tipuri de electroliți în vopsirea țesăturilor de bumbac cu coloranți reactivi. S-au studiat factorii care afectează capacitatea de vopsire, cum ar fi concentrația de săruri și performanțele de rezistență a culorii, cum ar fi concentrația substanțelor alcaline. Randamentul tinctorial K/S și rezistența culorii țesăturii vopsite folosind sulfat de sodiu au fost comparabile cu cele obținute cu clorură de sodiu. Cu toate acestea, epuizarea și timpul de fixare au fost mai scurte, iar coeficientul de difuzie a fost mai mic în cazul sulfatului de sodiu.

Cuvinte-cheie: colorant reactiv, țesătură din bumbac, electrolit, epuizare

Comparative study between two types of electrolyte used in the reactive dyeing of cotton

The aim of this paper was to compare the efficiency of two type of electrolyte in the dyeing of cotton fabrics with reactive dyes. Factors affecting dye ability such as salt concentration, and fastness performances such as alkaliconcentrationwere studied. The colouryield K/S and colour fastness of the dyed fabric using sodium sulfate were comparable to those obtained with sodium chloride. However, the exhaustion and the fixation timewere shorter and the diffusion coefficient was lower in the case of sodium sulfate.

Keywords: reactive dye, cotton fabric, electrolyte, exhaustion

INTRODUCTION

Cotton is the most natural fibreused in textile industry because it is globally inexpensive, absorbent, breathable and soft. However, different chemical modifications have been studied to improve its wettability, dye ability, chemical affinity, crease recovery, hydrophilicity, and its functional properties. Cotton fibres can be dyed using anionic dyes easily, but usually the common processes of cotton dyeing require large amounts of salt and alkali which mostly remain in the dye bath after the dyeing and may harm the environment [1–3].

Reactive dyes are quite often used for dyeing of cotton fabric as they produce bright and brilliant colour in various shade ranges with excellent colour fastness and are applicable with various application methods. Reactive dyes are applied to cotton in two stages that are exhaustion and fixation. Exhaustion is achieved using salt, preferably Glauber's salt (Na_2SO_4) or common salt (NaCl) to overcome the negative zeta potential of cotton and promote increased dye-uptake [4–6]. In fact, when cotton fibre is immersed into water, its surface due to hydroxyl ions become also anionic, hence the dye particles and the cellulosic fibre tend to repel each other. The addition of salt creates an electrical positive double layer which hides negative electrostatic charge of cotton surface. This allows the dye to approach the fibre; so that H-bonding and other short-range dye–fibre forces of attraction can operate. The organic dye molecules will have a greater affinity for the fabric than the aqueous solution [7]. The required amount of salt is greater than that required for the adsorption of direct dyes because the reactivedyes have low affinity for the fibre [8]. The quantities of present electrolyte can vary up to 100 g/l depending on the required colour deepness, the structure of the dyes or the dyeing recipe [9].The exhausted dyes are fixed to the cotton fabric by using alkalis such as sodium hydroxide (NaOH) and/or sodium carbonate (Na_2CO_3). Under alkaline conditions reactive dyes react with hydroxyl groups of cellulose, mostly by neucleophilic substitution or addition, to form the covalent bonds.

These strong bonds would be expected to lead to excellent colour fastness laundering. However, the dyes can also react with hydroxyl groups of water so that they are no longer able to react with cellulose. The addition of salt and alkali depends on the deepness of the shade to be produced [10–11]. In reactive dyeing, the process is too lengthy, due to the heat control of dye bath and to portion wise addition of salt and alkali in order to avoid uneven dyeing and maximizing the exhaustion and fixation.

In the present work, a comparative study about two types of salts is elaborated in order to identify their influence in dyeing conditions of cotton fabrics with reactive dye. Different factors affecting dye ability and colour fastness were thoroughly investigated, such as salt and alkali concentrations and type, dyeing temperature and dyeing time.

EXPERIMENTAL WORK

Materials

We have used a Woven twill cotton fabric, scoured, bleached and ready for dyeing with a weight per unit area of 210 g/m^2.
The Sumifix Supra Yellow E-XF, a bifunctionnal reactive dye, was provided by Sumitomo Chemical Co., Ltd (Japan). Its chemical formula is specified in figure 1.
The wetting agent and all other reagents, namely sodium chloride, sodium sulfate, sodium hydroxide and sodium carbonate were supplied by the society Chimitex Plus (Tunisia) and were commonly used laboratory reagent grade.

Dyeing process

Cotton fabric weighing 5.0 g was dyed with a liquor-to-goods ratio of 10:1 in a dyebath containing 1% owf of dyes. Dyeing was performed in Ahiba Laboratory dyeing machine (DataColor – USA). The dyeing profile is shown in figure 2.
After dyeing, all the samples were hot rinsed, neutralized with 1mL/L acetic acid during 10 min at 50°C, soaped with 2 mL/L soap powder solution for 10 min at 90°C and then rinsed thoroughly with tap water and air-dried at room temperature [12].

Conductivity measurements

The conductivity was measured using the conductivity meter Sension+ EC71 (Hach – USA) and recorded in mS/cm.

Colour measurements

The relative colouryield of dyed fabrics expressed as K/S was measured by the light reflectance technique using the Kubulka-Munk equation. The reflectance of dyed fabrics was measured on Spectra Flash SF600 spectrophotometer with data Master 2.3 software (Data Color International, USA).
The dye exhaustion rate (%E) was calculated according to the following equation:

$$\%E = \left[\frac{A_0 - A_f}{A_0}\right] \times 100 \quad (1)$$

Where A_0 and A_f are, respectively, the absorbance of the dyebath before and after dyeing at λ_{max} of the dye used. The absorbance was measured on Biochrom Libra S6 visible spectrophotometer.

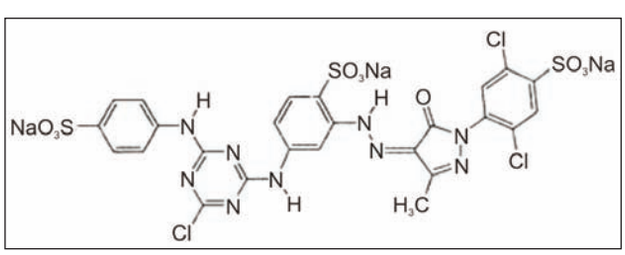

Fig. 1. Chemical structure of the used dye (λ_{max} = 418 nm)

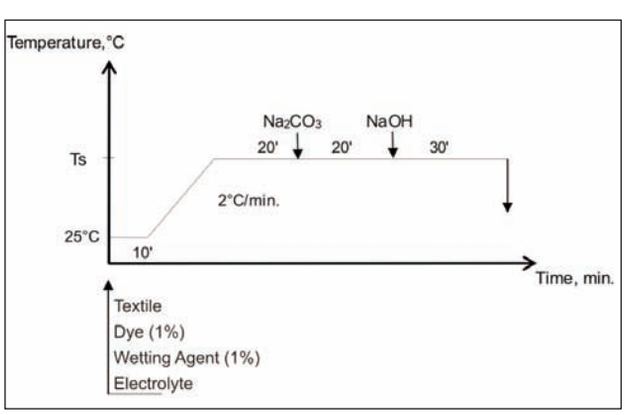

Fig. 2. Dyeing process of cotton fabric with reactive dye

Colour fastness testing

The dyed samples were tested for colour fastness according to standard methods: 1°) ISO 105-C06: 2010 Colour fastness to domestic and commercial laundering, 2°) ISO 105-X12:1987colour fastness to rubbing, and 3°) ISO 105-B02:2014: Colour fastness to artificial light: Xenon arc fading lamp test.

Dyeing Kinetic study

The study of the Kinetics concerns the mechanism by which the dyeing processes attempts to reach the equilibrium state and how long it takes. One of the most fundamental processes that control the rate at which many distinct periods or stages in the whole process occur is the diffusion.
In our case, considering that "C" stands for the concentration of dye particles which is described as:

$$C(x, y, z, t) \quad (2)$$

"J" stands for the course density of dye particles which is described as:

$$J(x, y, z, t) \quad (3)$$

The Fick's law is empirical in that it assumes proportionality between the diffusion flux and the concentration gradient [13]. It describes the diffusion processes of the dye by the following equation:

$$J = -D \text{ grad } C \quad (4)$$

Or, we know that the conservation of the particles gives the following mathematical equation:

$$\text{div}J = -\frac{\partial C(x, y, z, t)}{\partial t} \quad (5)$$

Combining equation 3 and 4, we obtain the following mathematical model:

$$\frac{\partial C(x, y, z, t)}{\partial t} = D\Delta C \quad (6)$$

In order to resolve this equation, Crank proposed a simplified solution to this Fick's law of diffusion [14]. The specific surface of the fibre appears in this solution:

$$\frac{C_{f,t}}{C_{f,\infty}} = A\sqrt{t} \quad (7)$$

where:

$$A = \frac{4}{r\sqrt{\pi}}\sqrt{D} \quad (8)$$

D (cm²/s) is the diffusion coefficient, C is the dye concentration and r is the radius of the fibre (m).
In the case of the cotton reactive dyeing, the equation can be simplified as following:

$$\frac{E_t}{E_\infty} = \frac{4}{r\sqrt{\pi}}\sqrt{D}(t^{1/2}) \quad (9)$$

In our study, we use the Equation (9) to determine the diffusion coefficient. It is sufficient to determine the slope of the curve of E_t/E_∞ versus $t^{1/2}$ to calculate the diffusion coefficient D. [15]

RESULTS

Effect of dyebath temperature on exhaustion

Figures 3 and 4 show, respectively, the effect of dyeing temperature on dyebath conductivity and on exhaustion of the dye on the fibres. The conductivity increases with the temperature and stabilize from 50 °C. As temperature increases, the energy gained by the molecules in the medium (electrolyte) increases and hence the ions are in a higher energy state. This energy will be converted into kinetic energy and so, the mobility increases. Hence the conductivity increases. The conductivity of Sodium Sulfate is higher than that of Sodium Chloride irrespective the temperature. In fact, conductivity depends on the concentration of charge carriers (ions) in the aqueous solution. When one mole of NaCl dissolves it produces two ions. But when one mole of Na_2SO_4 dissolves it produces three ions. Thus fewer moles of ions are produced by the NaCl solution and so we would expect its conductivity to be smaller.

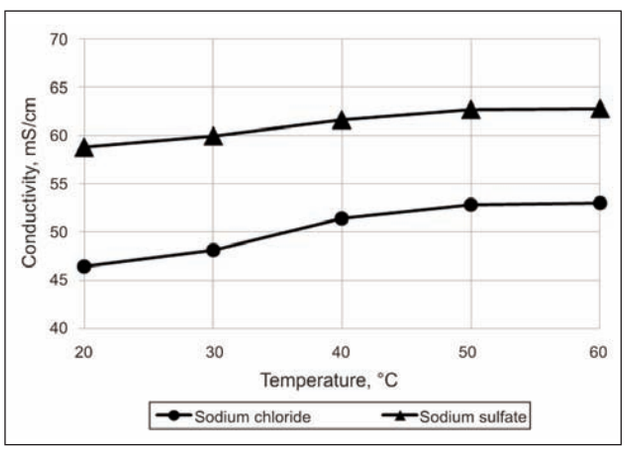

Fig. 3. Effect of dyeing temperature on bath conductivity

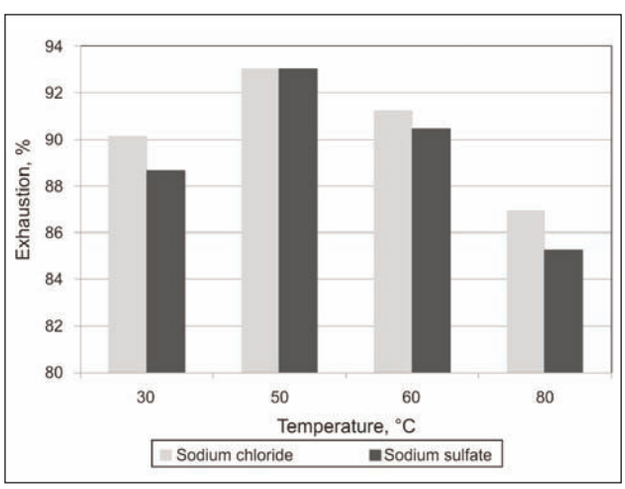

Fig. 4. Effect of dyeing temperature on the exhaustion of the dye on cotton fabric

An increase in the dye exhaustion on cotton fabric is observed as the dyeing temperature increased from 30 to 50 °C. However, increasing the temperature from 50 to 80 °C was accompanied by a successive decrease in the exhaustion values for both electrolytes. It is known that increasing temperature favours cotton fibre swelling, which leads to a higher dye uptake. The Exhaustion is slightly better when sodium chloride is used as electrolyte.
These results indicate that 50 °C is the suitable temperature for this reactive dye, above which the hydrolysis of the dye occurs resulting in a decrease in the dye uptake. This vinyl sulfone dye, actually, belongs to the group of alkali-controllable reactive dyes, which display optimum fixation temperature between 40 and 60 °C and which are characterized by low exhaustion in electrolyte solution before the addition of alkali. Such dyes have high reactivity and require careful alkali addition (portion wise) to achieve level dyeing [16]. This temperature will be considered as optimal for the rest of the study.

Optimization of electrolyte and alkali concentrations

Different factors can affect the dye ability and fastness properties of reactive dyeing of cotton fabrics. The most important ones are electrolyte concentration and alkali concentration. A factorial experimental design was used to study the main effects and the interaction effects between these two operational parameters. The experimental design and the statistical analysis of experiments were carried out using the statistical software Minitab 14. The analysis of variance was applied to evaluate the significance of the effect of all variables and their interactions on the response. P-values lower than 0.05 indicate that the model and the terms are statistically significant [17].
The factors considered in this study are: Electrolyte concentration (20 and 40 g/L), Sodium carbonate concentration (3 and 7 g/L) and Sodium hydroxide concentration (0.7 and 1 mL/L). These minimum and maximum values are indicated by the technical data sheet of the dye. The experimental result or the response to treat is the colour yield parameter (K/S). The study was realized for the two electrolytes: Sodium Sulfate and Sodium chloride
The experimental surface plan to modelize is described in table 1.
A main effect occurs when the mean response changes across the levels of a factor. Main effects plots could be used to compare the relative strength of the effects across factors. Main effect diagrams described in figures 5 and 6 show the behaviour of

Table 1

LEVELS OF STUDIED VARIABLE			
Test N°	**Electrolyte (g/L)**	**Na_2CO_3 (g/L)**	**NaOH (mL/L)**
1	20	3	0.7
2	20	3	1
3	20	7	0.7
4	20	7	1
5	40	3	0.7
6	40	3	1
7	40	7	0.7
8	40	7	1

Table 2

VARIANCE ANALYSIS FOR THE COLOUR YIELD PARAMETER (K/S), WITH NaCl AS A SALT					
Source	**DL**	**Adj SS**	**Adj MS**	**F**	**P**
Model	3	1.7204	0.57348	22.72	0.006
Linear	3	1.7204	0.57348	22.72	0.006
[NaCl]	1	0.8320	0.83205	32.97	0.005
[Na_2CO_3]	1	0.1922	0.19220	7.62	0.041
[NaOH]	1	0.6962	0.69620	27.59	0.006
Error	4	0.1010	0.2524		
Total	7	1.8214			

the response through the different variations of factors. This behaviour varies from one response to another. But, it is clear that Electrolyte concentration has the highest effect on the dyeing quality and this for the two type of salt. Sodium carbonate and sodium hydroxide concentration have also an effect on colour yield which is non-negligible in the case where NaCl is used as an exhaustion agent.

An interaction between factors occurs when the change in response from the low level to the high level of one factor is different from the change in response at the same two levels of a second factor. Hence, the effect of one factor is dependent upon a second factor. Interactions plots could be used to compare the relative strength of the effects across factors. As seen in figures 7 and 8, there is no interaction between different parameters. The only obvious interaction was between the two alkalis in the case where Na_2SO_4 was used as a salt.

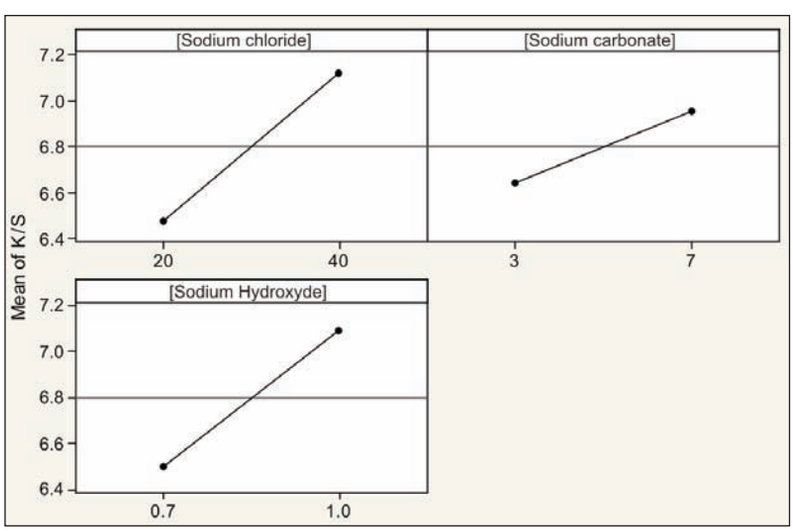

Fig. 5. Analysis of main effects plot of the colour yield (K/S) in the case where NaCl is used as electrolyte

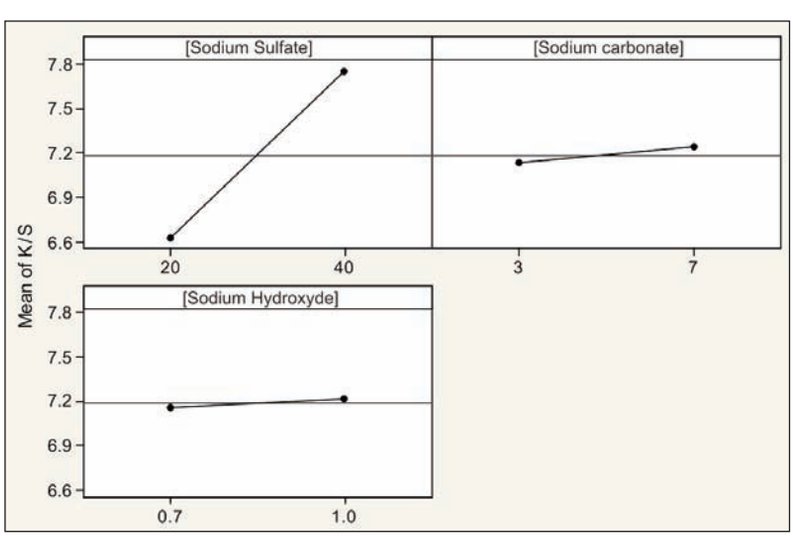

Fig. 6. Analysis of main effects plot of the colour yield (K/S) in the case where Na_2SO_4 is used as electrolyte

In the case of NaCl as a salt, the regression analysis of the experimental surface plan by a quadratic model leads to the following equation:

$$K/S = 3.773 + 0.03225\ [NaCl] + 0.0775\ [Na_2CO_3] + + 1.967\ [NaOH]$$

For the regression equation of the dyeing quality parameter (K/S), it was found that the squared multiple correlation coefficient R^2 is equal to 94.46%. It can be deduced that the model obtained has a very good predictability. According to table 2, the variance analysis (ANOVA) proves that, for the dyeing parameter, the regression model obtained is highly significant (p = 0.006). Moreover, there is a significant linear effect (p = 0.006) When Sodium Sulfate was used as a salt, the following equation is obtained:

$$K/S = 5{,}212 + 0.05650\ [Na_2SO_4] + + 0.0250\ [Na_2CO_3] + 0.183\ [NaOH]$$

For the regression equation of the dyeing quality parameter (K/S), the interaction between the two alkalis was neglected because the value of p

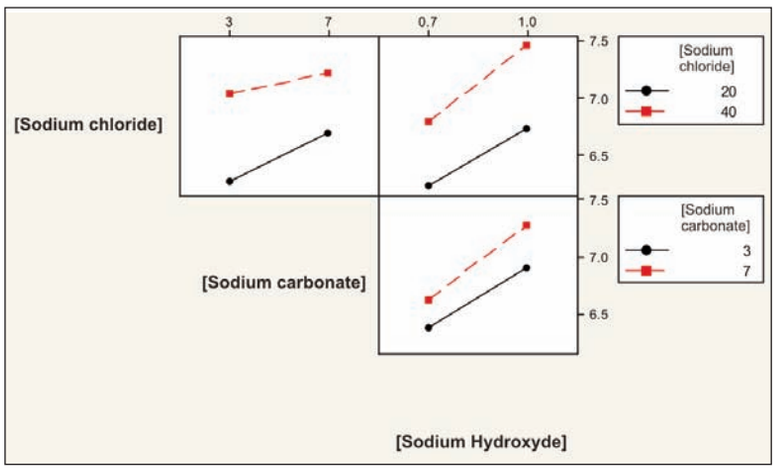

Fig. 7. Analysis of interaction plot of the colour yield (K/S) in the case where NaCl is used as electrolyte

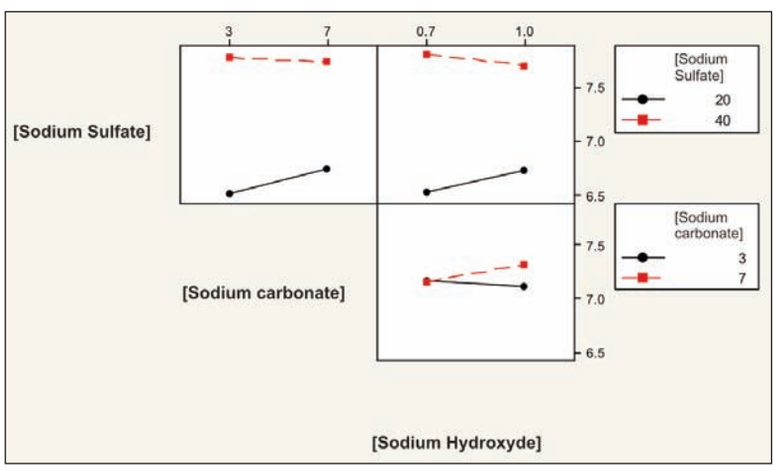

Fig. 8. Analysis of interaction plot of the colour yield (K/S) in the case where Na_2SO_4 is used as electrolyte

was superior to 0.005. The model obtained has a very good predictability as the squared multiple correlation coefficient R^2 was equal to 93.21%.

According to table 3, the variance analysis (ANOVA) proves that, for the dyeing parameter, the regression model obtained is highly significant (p = 0.008). Moreover, there is a significant linear effect (p = 0.008).

Many designed experiments involve determining optimal conditions that will produce the "best" value for the response. Response optimizer provides an optimal solution for the input variable combinations [18]. The desired Response optimization described in figures 9 and 10 shows that optimal experimental conditions for obtaining the highest colouryieldare a salt concentration of 40 g/L, Na_2CO_3 concentration of 7 g/L and NaOH concentration of 1 ml/L.

Table 3

VARIANCE ANALYSIS FOR THE COLOUR YIELD PARAMETER (K/S), WITH Na_2SO_4 AS A SALT

Source	DL	Adj SS	Adj MS	F	P
Model	3	2.57985	0.85995	18.31	0.008
Linear	3	2.57985	0.85995	18.31	0.008
[Na_2SO_4]	1	2.55380	2.55380	54.37	0.002
[Na_2CO_3]	1	0.02000	0.02000	0.43	0.048
[NaOH]	1	0.00605	0.00605	0.13	0.038
Error	4	0.18790	0.04698		
Total	7	2.76775			

Dyeing kinetics study

The slope of a dyeing exhaustion curve defines the rate of dyeing at any instant during the dyeing process. Equilibrium is reached when no more dye is taken up by the fibres. There is a balance between the rate of dye absorption and desorption. Figure 11 shows the evolution of the % exhaustion of the reactive dye versus dyeing time for the two type of salt. The maximal exhaustion is obtained after 70 minutes at 50°C. The dyeing exhaustion rate is slightly better when sodium sulfate is used as a salt. Dyeing conditions that can be recovered from these curves are described in table 4. The half-dyeing time (t½), which is the time taken for the fibre to adsorb half as much dye as is adsorbed at equilibrium, is considered as a convenient measure of the velocity of dyeing [19]. It can allow the determination of Exhaustion and Fixation time. The exhaustion rate is better when sodium sulfate is used as electrolyte.

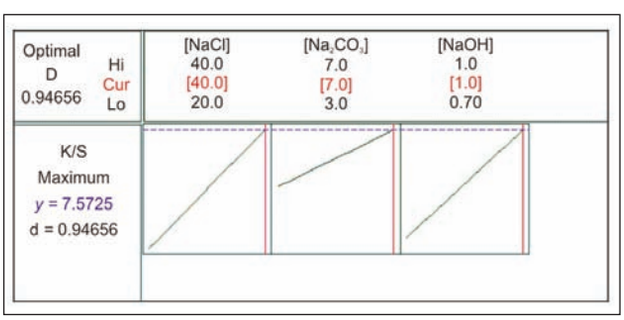

Fig. 9. Response optimization of the colour yield (NaCl as a salt)

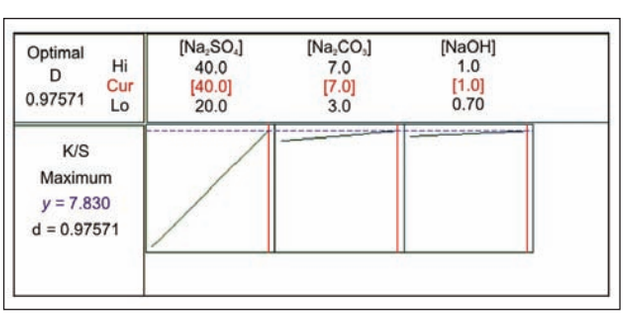

Fig. 10. Response optimization of the colour yield (Na_2SO_4 as a salt)

Table 4

DYEING TIME FOR THE TWO SALTS					
Type of salt	**Exhaustion (%)**	**$t_{1/2}$ (min)**	**Exhaustion time (min)**	**Fixation time (min)**	**D_{moy} cm²/s) 10^{-11}**
[NaCl]	88.52	6	12	24	0,7989
[Na_2SO_4]	90.66	5	10	20	0,8160

Table 5

COLOUR FASTNESS					
		ISO 105-C06 (C1S test method)	**ISO 105-X12**		**ISO 105-B02**
		Washing (60°C)	**Dry Rubbing**	**Wet Rubbing**	**Light**
Electrolyte	NaCl	5	4/5	4	5
	Na_2SO_4	5	4/5	4	5

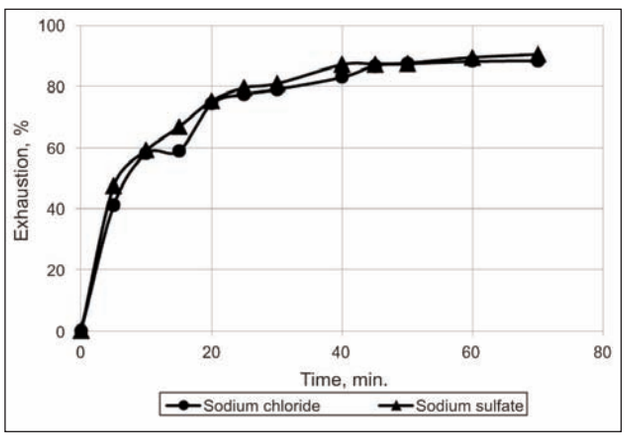

Fig. 11. Dyeing exhaustion curves for the two type of salt (NaCl and Na_2SO_4)

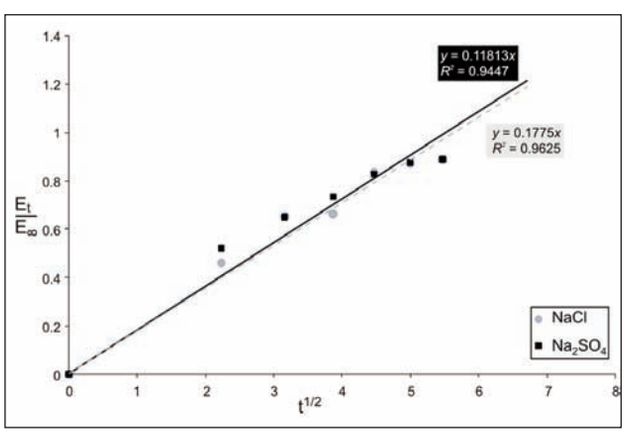

Fig. 12. Influence of salt type (NaCl and Na_2SO_4) on the coefficient of diffusion of the dye

The exhaustion and fixation time are shorter in this case.

The diffusion coefficient D can be deduced from figure (12). It is clear that the diffusion is better in the case of Sodium Sulfate as electrolyte. The probable explanation is that addition of the sodium sulfate lowers the repulsion more than the sodium chloride by imparting more quantity of oppositely charged ion with the charged dye anion. Compared to sodium chloride, the presence of the sodium sulfate in the dyebath decreases much more the membrane potential of cellulose which reduces of the repellency of cellulose and dye particles with the same charges and consequently improves dye ability.

Colour fastness results

The results summarized in table 5 demonstrate that whatever the nature of electrolyte, no difference in colour fastness was observed.

CONCLUSIONS

The influence of two types of electrolyte (sodium sulfate and sodium chloride) on the quality of a reactive dyeing on cotton fabric was studied. Obtained results have shown that the colour yield K/S and colour fastness of the dyed fabric using sodium sulfate were comparable to those obtained with sodium chloride. Sodium sulfate overcomes more efficiently the negative zeta potential of cotton than sodium chloride; that is why the diffusion coefficient is lower in this case, and the exhaustion time is shorter. Response surface methodology was employed to model, analyze and optimize electrolyte and alkali concentration. The optimum concentrations for obtaining highest colour yield on reactive dyeing of cotton fabric were a salt concentration of 40 g/L, Na_2CO_3 concentration of 7 g/L and NaOH concentration of 1 ml/L.

ACKNOWLEDGEMENTS

The author would like to express sincere gratitude to the direction and the staff of Chimitex Plus for their support and help.

BIBLIOGRAPHY

[1] Hajji, S.A., Qavamnia, S., & Bizhaem, F.K. *Salt free neutral dyeing of cotton with anionic dyes using plasma and chitosan treatments.* In: Industria Textila, 2016, vol. 67, pp. 109–113.

[2] Zhang, F., Chen, Y., Lin, H., Wang, H., Zhao, B., *HBP-NH_2 grafted cotton fibre: Preparation and salt-free dyeing properties*. In: Carbohydrate Polymers, 2008, vol. 74, issue 2, pp. 250–256

[3] Haji, A., *Eco*-Friendly Dyeing and Antibacterial Treatment of Cotton. In: Cellulose Chemistry and Technology, 2013, vol. 47, pp. 303–308.

[4] Trotman, E.R. *Dyeing and chemical technology of textile fibres*, Nottingham: 6th ed, 1984.

[5] Tarbuk, A., Grancaric, A. and Leskovac, M. *Novel cotton cellulose by cationisation during the mercerisation process – Part 1: Chemical and morphological changes*. In: Cellulose, 2014, vol. 21, pp. 2167–2179.

[6] Ristic, N. & Ristic, L. *Cationic modification of cotton fabrics and reactive dyeing characteristics*. In: Journal of Engineered fibers and fabrics, 2012, vol. 7, pp. 113–121.

[7] Cocket, S. & Hilton, K. *Dyeing of cellulose fibre and related Process,* London: Leonard Hill books Ltd, 1961, p. 212.

[8] Lim, S. & Hudson, S.H. HYPERLINK "http://onlinelibrary.wiley.com/doi/10.1111/j.1478-4408.2004.tb00215.x/full" *Application of a fibre-reactive chitosan derivative to cotton fabric as a zero-salt dyeing auxiliary*. In: *Coloration Technology,* 2004, vol. 120, issue 3, pp. 108–113.

[9] Madaras, G.W., Parish, G. & Shore, J. *Batchwise dyeing of woven cellulosic fabric*s, Bradford: SDC, 1993.

[10] Agarwal, B. & Bhattacharya, S. *Possibilities of polymer-aided dyeing of cotton fabric with reactive dyes at neutral pH*. In: Journal of applied polymer science, 2010, vol. 118, pp. 1257–1269.

[11] Chinta, S. & Vijayakumar, S. *Technical facts and figures of reactive dyes used in textiles*. In: International Journal of Managment Science, 2013, vol. 4, pp. 308–312.

[12] Hamdaoui, M., Turki, S., Romdhani, Z. & Halaoua, S. *Effect of reactive dye mixtures on exhaustion values*. In: Indian Journal of fibre & Textile Research, 2013, vol. 38, pp. 405–409.

[13] Fick, A. *Ueber diffusion.* In: Annalen der Physik, 1855, vol. 170, p. 59.

[14] Crank, J. & Park, G., *Diffusion in polymers*, London: Academin Press, 1968.

[15] Hamdaoui, M., Charfi, A. & Khoffi, F. *Study of the dyeing kinetics: Influence of pre-treatments and woven fabric structure*. In: *Open Acces Scientific Reports,* 2012, vol. 1, Issue 10.

[16] Burkinshaw, S. *Physico-chemical aspects of textile coloration*, Bradford: John Wiley & Sons in association with the Society of Dyers and Colorists, 2016.

[17] Haji, A. and Qavamnia, S.S., *Response surface methodology optimized dyeing of wool with cumin seeds extract improved with plasma treatmen*t. In: Fibers and Polymers, 2015, vol. 16, pp. 46–53.

[18] Meyers, R. & Montgomery, D. *Response surface methodology: Process and Product Optimization using designed experiments*, New York: John Wiley & sons, 1995.

[19] Boulton, J. & Reading, B. *Classification of direct dyes with respect to the production of level dyeings on viscose rayon*. In: Journal of the society of dyers and colourists, 1934, vol. 50, pp. 381–385.

Authors:

AYDA BAFFOUN

University of Monastir
Textile Materials and Processes Research Unit MPTex
National Engineering School of Monastir
Monastir, Tunisia

e-mail: aydabaffoun@gmail.com

Recycling of cellulose from vegetable fiber waste for sustainable industrial applications

UMIT HALIS ERDOGAN
FIGEN SELLI
HICRAN DURAN

REZUMAT – ABSTRACT

Reciclarea celulozei din deșeuri de fibre vegetale pentru aplicații industriale sustenabile

Recent, două subiecte au devenit importante pentru industria textilă, și anume "asigurarea sustenabilității prin reutilizarea deșeurilor textile" și "dezvoltarea unor materii prime textile noi cu valoare ridicată". Celuloza, care este un polimer fascinant, a fost utilizată de ani de zile ca materie primă pentru a obține diverse produse, cum ar fi: hârtia, fibrele și peliculele. În acest studiu, se urmărește asigurarea durabilității prin reciclare a celulozei din deșeurile de fibră de iută, ținându-se cont de cantitatea de deșeuri de fire de bătătură din iută eliberată în procesul de producție a covoarelor. În acest scop, la început, s-a efectuat curățarea preliminară a deșeurilor de fibră, apoi s-a realizat extracția celulozei și, în final, s-a efectuat caracterizarea celulozei reciclate. Metoda de extracție cu acid organic a fost eficientă pentru izolarea celulozei din deșeurile de fibre, cu un randament de 43,65%. Analizele microscopic și experimentale au confirmat faptul că partea ne-celulozică a deșeurilor de fibre a fost îndepărtată cu succes, iar celuloza reciclată are o structură similară cu proba martor de celuloză. Rezultatele sugerează că reziduurile de fibre vegetale pot fi utilizate ca sursă potențială de celuloză. Celuloza reciclată poate fi utilizată în producția de hârtie, compozite, fibre de celuloză regenerată și alte aplicații industriale.

Cuvinte-cheie: deșeuri de fibre, reciclabil, celuloză, extracție, sustenabilitate

Recycling of cellulose from vegetable fiber waste for sustainable industrial applications

Recently two significant topics that became important for textile industry namely 'providing sustainability by reusing of textile wastes' and 'developing high-valued new textile raw materials. Cellulose, which is a fascinating polymer, has been used for years as a raw material to obtain various products such as papers, fibers and films. In this study, it is aimed to provide sustainability with recycling of cellulose from waste jute fibers, considering the amount of waste jute weft yarns released in the production process of machine carpets. For this purpose, pre-cleaning of waste fibers was carried out at first, and then extraction of cellulose was accomplished, and finally characterization of recycled cellulose was performed. Organic acid extraction method was effective for isolation of cellulose from waste fibers with 43.65% yield performance. Microscopic and experimental analyses confirmed that non-cellulosic part of waste fibers were removed successfully and recycled cellulose has similar structure with control cellulose. Our results suggest that, waste vegetable fibers can be used as a potential source for cellulose. Recycled cellulose can be used in the production of paper, composites, regenerated cellulose fibers and other industrial applications.

Keywords: waste fibers, recycle, cellulose, extraction, sustainability

INTRODUCTION

Natural fibers have been used as textile raw materials since antiquity. Today each year approximately 35 million tons of natural fibers are harvested by farmers from a wide range of plants and animals [1]. These renewable and sustainable fibers are still raw materials of apparel, home textiles and technical textiles. Among the natural fibers, vegetable fibers such as cotton, jute, hemp and flax have high annual production. Vegetable fiber wastes in the forms of fiber, yarn and fabric release during production processes and after usage of textiles. These vegetable fiber wastes include valuable polymers such as cellulose and lignin which can be recycled and used as a raw material of composites, papers and anew textiles. Therefore, in the recent years, researches have focused on recycling and sustainability in the textile sector in conjunction with the other branches of industry [2]. Limited resources and increasing consumption make the recycling and waste management a necessity instead of a choice.

Cellulose, which is a fascinating polymer, has been used for years as a raw material to obtain various products such as papers, fibers and films. Plants are the major source of cellulose and numerous studies have been carried out to extract cellulose and/or nano-cellulose from several plants and itsderivate by using different methods [3–4]. For instance, the physicochemical characterization of the cellulose extracted from the forestry residue of ficus leaves using chemical method was carried out by Reddy et al. In the study, detailed chemical composition of the ficus leaf fibers and extracted cellulose was discussed [5]. Besides, numbers of studies also increase on recycling cellulose from waste materials [6–7]. Kopania et al. present the results of cellulose fiber extraction from waste plant biomass including: rape, hemp and flax straws [8]. Vegetable fibers contain high amount of cellulose, which can be extracted and

reused as a raw material in various industry. Moran et al. studied on extraction of cellulose and preparation of nano-cellulose from sisal fibers. Feasibility of extracting cellulose from sisal fiber, by means of two different procedures was carried out and compared [9]. Acid hydrolysis extraction of nano-crystalline cellulose from coir fiber and its application in composite films was investigated by Azeredo and colleagues [10]. Jute, one of the common agro-fiber, was also used as raw material for the preparation of microcrystalline cellulose [11]. Turkey is one of the leading textile producers, therefore vegetable fiber wastes having high cellulose content release in the different steps of textile production processes. Recycling of these wastes and reusing them as a raw material offer economic and social benefits to the country. Hence, in our previous studies extraction and characterization of cellulose from waste of various vegetable fibers were also considered [12–14].

In this study, it is aimed to provide sustainability with recycling of cellulose from waste jute fibers, considering the amount of waste jute weft yarns released in the production process of machine carpets. For this purpose, pre-cleaning of waste fibers was carried out at first, and then extraction of cellulose was accomplished via organic acid extraction, and finally characterization of recycled cellulose was performed. The structures and properties of recycled and control cellulose were compared and discussed.

MATERIALS AND METHOD

Materials

In this study waste jute yarns, which is released during machine carpet production, were used to extract cellulose. Commercial cellulose was purchased from Sigma-Aldrich for the comparison of analyse results. Other chemical agents such as formic acid (98–100%), hydrogen peroxide (35%), ethanol, benzene, ethylenediaminetetraacetic acid (EDTA), hydrochloric acid (37%), sulfuric acid, acetone and copper (II) ethylenediamine solution (CUEN) were also supplied from Sigma-Aldrich.

Methods

Determination of chemical composition

Chemical composition of the waste fibers was determined to confirm the high cellulose content of jute considering the China Textile Industry Standard [15]. At first, waste fibers were dried in vacuum oven for 8 hours at 105°C in order to achieve dry weight of samples, and then pectin composition of samples was determined with 0.5 % EDTA solution. Hydrochloric acid (0.5 M) was used to obtain the hemicellulose content and sulfuric acid (72% v/v) was used to determine both the cellulose and klason lignin content of the samples.

Extraction of cellulose

In our study; at first pre-cleaning of waste fibers with hot distilled water were carried out to remove water soluble contents. Waste fibers are cut into 1–2 cm small pieces and washed for 3 hours at boiling temperature. Afterwards, fibers were dried in an oven for 8 hours at 105°C for further process. For the removal of water insoluble content of waste fibers such as wax and lipophilic materials, another treatment was carried out. Washed and dried fiber bundles were placed in a soxhlet apparatus and treated with a mixture of 2:1 benzene/ethanol at 80°C for 6 hours. The remaining solution was stored to reuse. After soxhlet-extraction, fiber material was washed to remove possible residues with ethanol and acetone, respectively. For the final step of cleaning, fibers were rinsed with distilled water and dried at room temperature [12].

Extraction of cellulose was performed by using organic acid pulping and hydrogen peroxide bleaching [11,13–14]. Organic acid pulping can be effectively used to obtain cellulose from soft wood materials [16]. In organic acid pulping formic acid and peroxyformic acid were used for delignification, respectively. Firstly, formic acid in 90% concentration was used to remove the non-cellulosic materials of waste fibers. Peroxoacids are synthesized using a carboxylic acid and hydrogen peroxide according to the following reaction

$$RCOOH + H_2O_2 \rightleftarrows RCOOH + H_2O \quad (1)$$

If a strong mineral acid is not used as a catalyst for the proton donation, this reaction is reversible and slow. However, strong mineral acids such as sulfuric acid cause deterioration of the pulp and decrease dramatically the degree of polymerization of cellulose [17]. Considering these disadvantages of sulfuric acid, formic acid and hydrogen peroxide were used to synthesize the peroxyacid in this study. Following the formic acid treatment, peroxyformic acid treatment with hydrogen peroxide 35% concentration was carried out to improve delignification. Samples are washed with peroxyformic acid for 150 minutes and then dried. Finally, bleaching of obtained material was performed with hydrogen peroxide for 75 minutes at 60°C. Lignin-hemicellulose bonds and hemicellulose itself were also hydrolyzed with this method [18]. During extraction of cellulose, the weight loss of the starting material was also noted down after every process step to calculate yield ratio. Starting material (waste jute fibers), pulping process and the extracted material (recycled cellulose) can be seen in figure 1.

Characterization of recycled cellulose

Experimental analyses were carried out to characterize the recycled cellulose and to make a comparison with control cellulose. The degree of polymerization (DP) was calculated by viscosity method. Viscosity measurement was carried out with ViscoSytem AVS470 at 20°C with iron (III) sodium tartrate complex (EWNN mod NaCl) solution. Method is adapted from DIN 54270-3 standard. Structural analyses of recycled cellulose and reference cellulose were carried out by using Fourier Infrared Spectroscopy (FTIR) and X-Ray Diffraction (XRD) methods. FTIR measurements were performed by using Perkin Elmer Spectrum BX instrument, wavelength 400–4000 cm^{-1}, 2 cm^{-1} resolution (% absorbance) and XRD analyses

Fig. 1. Waste jute fibers, pulping process and recycled cellulose

by Rigaku D/MAX200 X-Ray diffractometer using CuKα radiation and operating at 40 kV and 36 mA. The diffraction intensities of the reference cellulose and extracted cellulose were recorded between 3° and 90° (2θ). The crystallinity indexes of cellulose samples were calculated considering peak height method [19]. Thermal stability analysis of samples were carried out using Perkin Elmer Simultaneous Thermal Analyzer (STA) 6000, in nitrogen medium and scanned between 25–600°C at a heating rate of 10°C per minute. Gravimetric method was used to determine the moisture content of cellulose samples. Solubility of the extracted cellulose was observed with optical microscope (Olympus BX43) using CUEN solution. Colour measurement of the various cellulosic samples was performed with Minolta 3600D CM spectrophotometer (D65 illuminant specular included, 10° observer angle) for comparison. The spectrophotometer, having a software, that could calculate CIEL*a*b*C*h^0. The software also gives data about color strength (K/S) values from the reflectance values at the appropriate λ_{max} for each sample.

RESULTS AND DISCUSSION

Chemical composition and pulp yield

Chemical composition of the waste jute fibers and pulp yield are summarized in table 1. The high cellulose content of waste fibers with 63.60 % enhances the variety of utilization and sustainability. Pulp yield also shows that organic acid extraction method is effective for the extraction of cellulose from waste fibers.

Degree of polymerization and moisture contents

Polymerization degree and moisture content of recycled (r-cell) and control cellulose (a-cell) can be seen in table 2. DP of recycled cellulose is higher than reference cellulose; this is most probably due to the extraction method applied to waste fibers. Besides, DP of natural fibers is most variable as nature of cellulose formation. Moisture content of both sample are high and close to the moisture content of commercial cellulosic fibers [20]. Moisture content of recycled cellulose is less than control cellulose as a result of different DP and crystal structure of samples.

Table 1

Constituent	Content %
Cellulose	63.60
Hemicellulose	20.10
Lignin	13.80
Pectin	2.60
Pulp Yield	43.65±0.25

Table 2

Sample	DP	Moisture content (%)
r-cell	1106.0 ± 117.5	7,78 ± 0.14
a-cell	872.0 ± 87.0	8.44 ± 0.15

Structural analysis

FTIR results which were performed to analyze and compare the functional groups and bond energies of recycled and control cellulose, are given in figure 2. As it can be seen in FTIR spectra of the recycled and control cellulose (fig. 2), similar peaks between absorption bands 700–1800 cm^{-1} and 2400–3600 cm^{-1} were observed. The absorption bands at around 3300 and 1028 cm^{-1} in FTIR spectra of the cellulose samples are assigned to O–H stretching vibrations and cyclic alcohol groups, respectively. The peak at around 2900 cm^{-1} absorption band, which is assigned to CH_2 and CH_3 vibrations, is similar for both samples. The band at 1228 cm^{-1} noticed in FTIR spectra of the samples is attributed to axial asymmetric strain of =C–O–C groups which are observed in ether, ester, and phenol groups [21].

XRD patterns of recycled and control cellulose are shown in figure 3. The diffraction peaks at 2θ = 22–23° (002) and 2θ = 18–19° (110) indicate the typical diffractions of cellulose [21]. Crystallinity indexes of recycled and control cellulose samples were calculated as 78.87% and 74.41 %, respectively. XRD patterns of the samples show the same intensity peaks at the same diffraction angles.

Thermo gravimetric analysis (TGA) was conducted to investigate the effect of extraction on thermal behavior

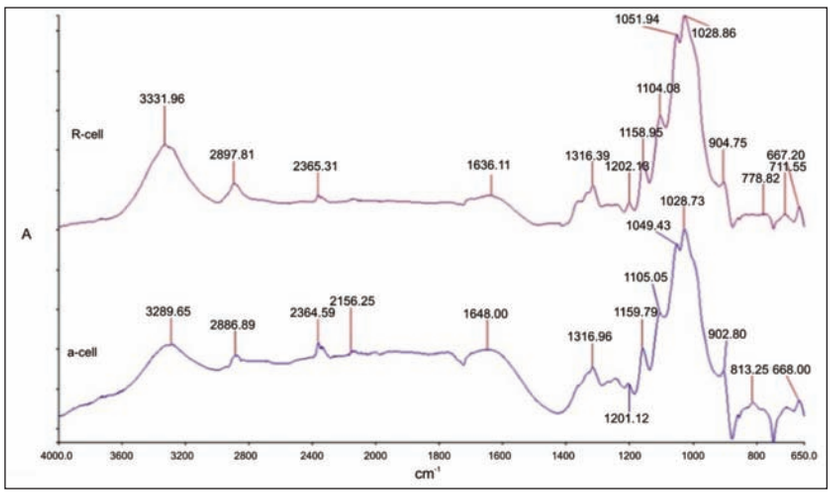

Fig. 2. FTIR spectra of the cellulose samples

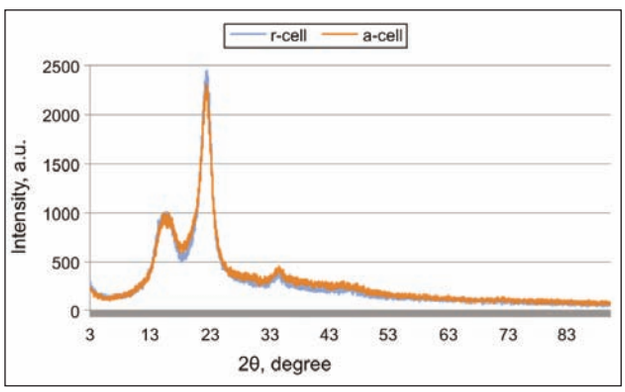

Fig. 3. XRD patterns of the cellulose samples

of recycled cellulose. TGA curves of the cellulose samples are presented in figure 4. The initial weight loss, which represents the evaporation of water, was observed between 50 and 100°C. Weight losses in samples between these temperatures are compatible with moisture absorption values of samples indicated in table 2. The second weight loss was recorded between 260°C and 320°C which is related to the decomposition of hemicellulose and the glycosidic linkages of cellulose. The third weight loss was detected between 320°C and 390°C corresponds to the decomposition of cellulose [22]. After that, the weight loss was pursued until 600°C with a loss rate of about 92%. Initial, maximum and the final degradation

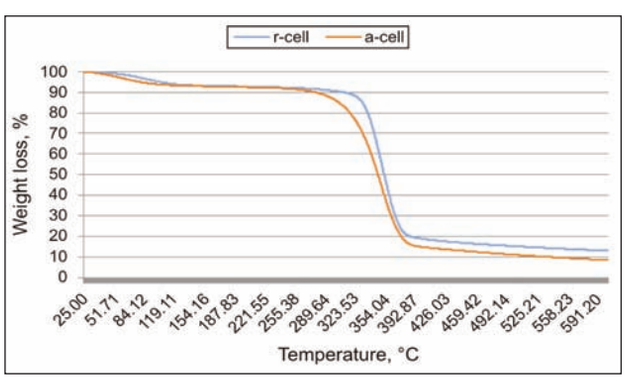

Fig. 4. TGA curves of the cellulose samples

temperature of recycle cellulose is a little bit higher than control cellulose. This can be due to higher DP and crystallinity of recycled cellulose.

Microscopic observations and color measurement

Solubility of recycled cellulose was also observed with an optical microscope by using CUEN solution. CUEN is a well-known chemical which is used to solve cellulose in viscosity measurements.

Dissolution behavior of the recycled cellulose under microscope can be seen in figure 5. As it can be seen from digital images of recycled cellulose, it began to fragmentize with the addition of CUEN and then completely dissolved by the time (approximately within one minute).

The colorimetric values of the waste jute fiber, viscose and recycled cellulose are summarized in table 3. Since, the control cellulose is in powder form, color of it was not measured and considered in this test. Waste jute has the highest yellowness (b*) and lowest lightness (L) value as it is expected. Similar yellowness (b*) and lightness (L) values were obtained for the recycled cellulose and viscose fiber. K/S and R% which indicate the color strength and reflectance values of samples are also given in table 3.

Fig. 5. Solubility of recycled cellulose under microscope with CUEN solution (50x)

Table 3

Sample	L	b*	%R (min) (400 nm)	K/S (max) (400 nm)
r-cell	91.542	4.736	67.75	0.0768
waste jute	61.393	18.130	12.12	3.186
viscose fiber	93.934	2.222	77.73	0.0319

CONCLUSION

In this study, extraction and characterization of cellulose was considered from waste jute fibers which release in machine carpet production. Thus recycling of a valuable polymer was achieved. Organic acid extraction method was effective for the regaining of cellulose from waste fibers with 43.65 % yield performance. Microscopic and experimental analyses confirmed that non-cellulosic part of waste fibers were removed successfully and recycled cellulose has similar structure with control cellulose. Our results suggest that, waste vegetable fibers can be used as a potential source for cellulose. Recycled cellulose can be used in the production of paper, composites

and regenerated cellulose fibers. Moreover, micro and nano crystalline cellulose may be produced from recycled cellulose and they can be used as a raw material of packaging industry. Consequently, the results of this project are important for both environmental and economic perspective since cellulose is a valuable biopolymer for various industries. Further study is now carried out by our research group to spin functional regenerated cellulose fiber using the recycled cellulose obtained in this study.

Acknowledgement

The authors gratefully acknowledge the funding by Scientific and Technological Research Council of Turkey (TÜBİTAK) under grant 115M736. We also thank machine carpet companies Atlantik, Serko and Mutaş for their supports and technical assistances.

BIBLIOGRAPHY

[1] Kozłowski, R.M. *Handbook of natural fibres*, Elsevier, 2012.
[2] Muthu, S.S. *Textiles and clothing sustainability: Recycled and upcycled textiles and fashion*, Springer Singapore, 2017.
[3] Klemm, D., Heublein, B., Fink, H-P., Bohn, A. *Cellulose: Fascinating biopolymer and sustainable raw material*, In: Angew and the Chemie International Edition, 2005, Vol. 44, no. 22, pp. 3358–3393.
[4] Islam, M.T., Alam, M.M., Patrucco, A., Montarsolo, A., Zoccola, M. *Preparation of nanocellulose: A review*, In: AATC Journal of research, 2014, Vol. 1, no. 5, pp. 17–23.
[5] Reddy, K.O., C. Maheswari U., E. Shukla M.M., Varada Rajulu, A. *Extraction and characterization of cellulose from pretreated ficus (Peepal Tree) leaf fibers*, In: Journal of Natural Fibers, 2016, Vol. 13, no. 1, pp. 54–64,
[6] Johar, N., Ahmad, I., Dufresne, A. *Extraction, preparation and characterization of cellulose fibres and nanocrystals from rice husk*, In: Industrial Crops and Products, 2012, vol. 37, no. 1, pp. 93–99.
[7] Elanthikkal, S., Gopalakrishnapanicker, U., Varghese, S., Guthrie, J. *Cellulose microfibres produced from banana plant wastes: Isolation and characterization*, In: Carbohydrate Polymers, 2010, vol. 80, no. 5, pp. 852–859.
[8] Kopania, E., Wietecha, J., Ciechańska, D..*Studies on Isolation of Cellulose Fibres from Waste Plant Biomass*, In: Fibres& Textiles in Eastern Europe, 2012, vol. 20, no 96, pp. 167–172.
[9] Moran, J.I., Alvarez, V.A., Cyras, V.P., Vazquez, A. *Extraction of cellulose and preparation of nanocellulose from sisal fibers*, In: Cellulose, 2008, vol. 15, no. 1, pp. 149–159.
[10] Azeredo, H.M.C., Imam, S.H., Figueire, M.C.B., Nascimento, D.M., and Morsyleide, F.R. *Handbook of polymer nanocomposites. Processing, performance and application – Volume C: Polymer nanocomposites of cellulose nanoparticles*, Springer, 2014.
[11] Jahan, S.M., Saeed, A., He, Z., Ni Y. *Jute as raw material for the preparation of microcrystalline cellulose*, In: Cellulose, 2010, vol. 18, no. 2, pp. 451–459.
[12] Erdoğan, U.H., Duran, H. *Cellulose from waste jute fibers: Extraction and characterization,* In: IFATCC XXIV International Congress Book of Abstracts, Czech Republic, Pardubice, 2016, pp. 161–164
[13] Erdogan, U.H., Selli, F., Duran, H. *Banana plant waste as raw material for cellulose extraction*. In: Fiber and Textiles, 2017a, vol. 24, no. 3, pp. 48–52.
[14] Erdogan, U.H., Selli, F., Duran, H. *Using sisal fiber wastes to isolate cellulose*, In: 8th TEXTEH International Conference. Bucharest, Romania, 2017b, pp. 19–20.
[15] Zhang, J., Zhang, H., Zhang, J. *Evaluation of liquid ammonia treatment on surface characteristics of hemp fiber*, In: Cellulose, 2013, Vol. 21, no. 1, pp. 569–579.
[16] Jahan, M.S., Lee, Z.Z., Jin, Y., *Organic acid pulping of rice straw. I: Cooking*, In: Turkish Journal of Agriculture and Forestry, 2006, vol. 30, no. 3, pp. 231–239.
[17] Kham, L., Bigot, Y., Delmas, M., Avigno, G. *Delignification of wheat straw using a mixture of carboxylic acids and peroxoacids*. In: Industrial Crops and Products, 2005, vol. 21, no. 1, pp. 9–15.
[18] Muurinen, E., *Organosolv pulping: a review and distillation study related to peroxyacid pulping*. In: Department of Process Engineering, University of Oulu, 2000.
[19] Park, S., Baker, J.O., Himmel, M.E., Parilla, P.A., and Johnson, D.K. *Cellulose crystallinity index: measurement techniques and their impact on interpreting cellulase performance*, In: Technology for Biofuels 2010, vol. 3, no. 1, pp. 1–10.
[20] ASTM D 1909-04, Standard Table of Commercial Moisture Regains for Textile Fibers, 2004
[21] Erdoğan, U.H., Seki, Y., Aydogdu, G., Kutlu, B., Aksit, A. *Effect of different surface treatments on the properties of jut*, In: Journal of Natural Fibers, 2016, vol. 13, no. 2, pp. 158–171.
[22] Kılınç, A.Ç., Köktaş, S., Seki, Y., Atagür, M., Dalmış, R., Erdoğan, U.H., Göktaş, A.A., Seydibeyoğlu, M.Ö. *Extraction and investigation of lightweight and porous natural fiber from Conium maculatum as a potential reinforcement for composite materials in transportation*, In: Composites Part B, 2018, vol. 140, pp. 1–8c.

Authors:

UMIT HALIS ERDOGAN, HICRAN DURAN, FIGEN SELLI

Dokuz Eylul University, Department of Textile Engineering, 35390,Tınaztepe Campus, Buca, Izmir, Turkey

e-mail: umit.erdogan@deu.edu.tr, duran.hicran@gmail.com, figenselli@gmail.com

Corresponding author:

UMIT HALIS ERDOGAN

e-mail: umit.erdogan@deu.edu.tr

Basic researchabout corncob residue as Lyocell spinning material

CHENG WANG
RONGHUAN HAN
LIXIA HU
FUMEI WANG

REZUMAT – ABSTRACT

Cercetare de bază asupra reziduurilor de știuleți de porumb ca material de filare al fibrei Lyocell

Au fost utilizate reziduurile de știuleți de porumb ca material sursă nou, mai ieftin pentru tehnologia de filare a fibrei Lyocell. În această lucrare au fost investigate proprietățile chimice ale reziduurilor de știuleți de porumb după extracția hemicelulozei și ligninei. Compoziția principală a reziduului de știuleți de porumb este celuloza, însoțită de o ușoară hemiceluloză și o cantitate foarte mică de component insolubile pentru filare. În comparație cu pulpa de lemn, reziduul de știuleți de porumb are o masă moleculară a numărului mediu similară, o masă molecular medie ușor mai mare, o masă molecular relativă mai mică și o polidispersie mai mare. Toate aceste proprietăți sugerează că acest tip de reziduu de știuleți de porumb are un potențial mare de utilizare ca material de filare pentru fibrele celulozice regenerate. A fost produs un nou tip de fibră din reziduu de știuleți de porumb, utilizând tehnologia de filare a fibrei Lyocell. Au fost analizate proprietățile mecanice ale fibrelor din reziduuri de știuleți de porumb. Fibrele din reziduuri de știuleți de porumb au o valoare a rezistenței la tracțiune între cea a fibrei de viscoză și cea a fibrei Lyocell, indicând perspectivele sale bune de aplicare. Cu toate acestea, fibrele din reziduuri de știuleți de porumb au o cristalinitate ridicată și o valoare de orientare cu o densitate liniară mare de fibră, ceea ce sugerează că tehnologia de filare trebuie îmbunătățită în continuare.

Cuvinte-cheie: reziduuri din știuleți de porumb, tehnologia de filare a fibrei Lyocell, fibră din reziduuri de știuleți de porumb, fibră Lyocell

Basic research about corncob residue as Lyocell spinning material

Using the corncob residue as a new cheaper source material for Lyocell spinning technology. Chemical properties of the corncob residue after extraction of hemicellulose and lignin were investigated in this paper. It was found that the main composition of corncob residue is cellulose, accompanied by slight hemicellulose and very tiny amount of spinning insoluble components. Compared to wood pulp, corncob residue has a similar number-average molecular weight, a slightly larger weight-average molecular weight, a lower peak-relative molecular weight, and a larger polydispersity. All those properties suggest that this kind of corncob residue has big potential to be used as spinning material for regenerated cellulose fiber. A new type corncob residue made fiber was produced, using the Lyocell spinning technology. Mechanical properties of the corncob residue fiber were analyzed. The corncob residue fiber has a tensile strength value between that of viscose fiber and Lyocell fiber, indicating its good application prospects. However, the corncob residue fiber has a high crystallinity and the orientation value with large fiber linear density, suggesting that the spinning technology needs to be further improved.

Keywords: corncob residue, Lyocell spinning technology, corncob residue fiber, Lyocell fiber

INTRODUCTION

Corncob is the central core of an ear of maize, whose weight accounting for 20%~30% of the maize. Corncob contains 32%~36% cellulose, 35%~40% hemicellulose, 25% lignin and very little amount of insoluble ash [1]. Usually, Corncob is considered an agricultural waste with an annual production of approximately 40 million tons in China [2]. Corncob is rich in nutrients and easy to collect. However, only small amount of the corncobs are utilized for furfural xylitol production. Most of them are burned directly, causing environmental pollution and a waste of their economic value [3]. After extraction of hemicellulose and delignification processes, the main composition of the corncob residue should be cellulose. If using the corncob residue produces something, it will benefit not only the economy but also the society.

The development of viscose products is limited because of the by-products produced during the production process which may cause environmental pollution. In the1980s, a new type of green environmental process, Lyocell process was invented. In the Lyocell process, a solution named N-methyl morpholine oxide (NMMO) is used to dissolve wood-pulp cellulose. Then, the mixed solution is spun to form a filament. Finally the solvent extracted during the washing process of the fibers. The Lyocell manufacturing process is simple and environmentally friendly, using a non-toxic solvent with a 99% recycle rate. Fibers, produced using Lyocell process, have superior mechanical properties comparing with viscose fibers [4].

The production of the Lyocell, using wood pulp cellulose as raw materials, has realized industrialization [5]. Large numbers of wood were cut for producing pulp material, leading to the increasing environmental problems. Usually, a tree has a growth cycle ranging from a few years to decades. Consequently, the

cost of producing the pulp material is relatively high, which limits the production and development of regenerated cellulose fibers [6]. As a result, much attention has recently been paid to find a cheaper, renewable, abundantly available resource. Compared to woods, bamboo has a shorter growth cycle and the production of bamboo pulp material carries a lower cost. Yang investigated the bamboo Lyocell fiber and found that this kind of fiber has better mechanical properties than those of bamboo viscose fiber, obvious negative ion effects, and antimicrobial activities [7]. Uddin produced a new cheaper regenerated cellulose fiber, the bagasse fiber, using the Lyocell process [8]. They studied effects of different coagulants on the fiber properties and found that the bagasse fiber has similar physical properties with commercial Lyocell fiber.

The main objective of our research is to find a cheaper source of material for regenerated cellulose fiber production. This paper innovates in using corncob residue as raw materials for spinning. Corncob residue fibers were produced through a conventional Lyocell spinning process by using corncob residue. In this study, the main components of corncob residue were first detected. Internal structure, mechanical properties, and application value of corncob residue fibers were analyzed.

MATERIALS AND METHODS

Materials

I) Corncob residue

The corncob residue after extraction of hemicelluloses (used for xylitol production) and lignin was provided by Shandong Yingli Industrial Co. Ltd, China as shown in figure 1.

Fig. 1. Corncob residue

II) Corncob residue fiber

Corncob residue fiber is a new regenerated cellulose fiber. Corncob residue fibers analyzed in this research are manufactured by Shandong Yingli Industrial Company, China, using Corncob residue as materials by Lyocell spinning technology and equipments.

III) Contrast samples

The contrast samples are shown in table 1. The data of structural properties of Lenzing fibers and Tencel A100 were collected from others' studies [9–12]. The chemical structure and mechanical properties of other fibers and the raw materials are tested using the same methods.

Table 1

Sample	Manufacturer
Raw material for Incell fiber	Shandong Yingli Company
Incell fiber	
Viscose fiber	Lenzing Company
Lyocell fiber	
Tencel A100	Courtaulds Company

Methods

Fourier transform infrared spectroscopy measurements (FT-IR)

The FTIR spectra were obtained using the U.S. Nicolet Nexus 670 Fourier Transform Infrared-Raman Spectrometer. The wavelength range is 4000 cm^{-1} ~ 600 cm^{-1} with a resolution of 4 cm^{-1}, and each spectrum has 128 scans.

Gel permeation chromatography measurements (GPC)

The molecular weight and molecular weight distribution of corncob residues and corncob residue fibers were determined using gel permeation chromatography (GPC). The large numbers of intramolecular and intermolecular hydrogen bonds in crystalline cellulose make it difficult to be dissolved in general solvent, which led to the limited application of GPC in cellulose than in polymer [13]. In 1979, McCormick found cellulose could be dissolved in a Dimethylacetamide (DMAc) solution containing 5%~10% LiCl without any degradation [14]. Since then, the GPC method using LiCl/DMAc as solvent and mobile phase becomes widely used for characterizing molecular weight of cellulose [15].

After preparation of cellulose solution [16], a Waters 1525 liquid chromatograph equipped with GPC was used to measure the relative molecular weight distribution of cellulose in the fiber.

X-ray diffraction measurements (XRD)

The crystallinity (X_c) and crystal orientation (f_c) of corncob residue fibers, Incell fibers, viscose fibers, Lyocell fibers and Tencel A100 were analyzed using an X-ray diffractometer (Rigaku D/max-2550 PC, Rigaku Corporation, Japan). The powder samples were scanned using Cu-Kα radiation operated at 40 kV and 200 mA, in a 2θ range from 5° to 60° at a speed of 10°/min.

The crystallinity (X_c) of all fibers were calculated from the following equation:

$$X_C = \frac{I_C}{I_C + I_A} \quad (1)$$

Where I_C is the intensity of the crystalline peak, and I_A is the intensity of amorphous peak.
The crystal orientation (f_c) of all fibers was calculated according to Herman's crystal orientation functions with equations below:

$$I_C = \frac{3\langle\cos^2\theta\rangle - 1}{2} \quad (2)$$

where

$$\langle\cos^2\theta\rangle = \frac{\int_0^{\frac{\pi}{2}} I_{(\phi)} \cos^2\phi \sin\phi \, d\phi}{\int_0^{\frac{\pi}{2}} I_{(\phi)} \sin\phi \, d\theta}$$

Where ϕ is azimuthal angle and $I(\phi)$ is the relational expression between the intensity of diffraction peak and azimuthal angle.

Mechanical properties

The linear density of the fibers was measured following the China National Standard GB/T 14335-2008.
The moisture regain of the fibers was tested according to the China National Standard GB/T 6503-2008. All samples were tested in duplicate.
Tensile properties of the fibers were tested following the China National Standard GB/T14337-2008. All measurements were repeated 50 times.

RESULTS AND DISCUSSION

FTIR analysis

The infrared spectra of corncob residue fiber, corncob residue, and cotton fiber are shown in figure 2. All spectra show the same characteristic absorption bands of cellulose, such as O–H stretching vibration absorption band near 3335 cm^{-1}, peaks around 1060 cm^{-1} in the fingerprint region, C-H stretching vibration absorption band in a wave number of 2895 cm^{-1}.

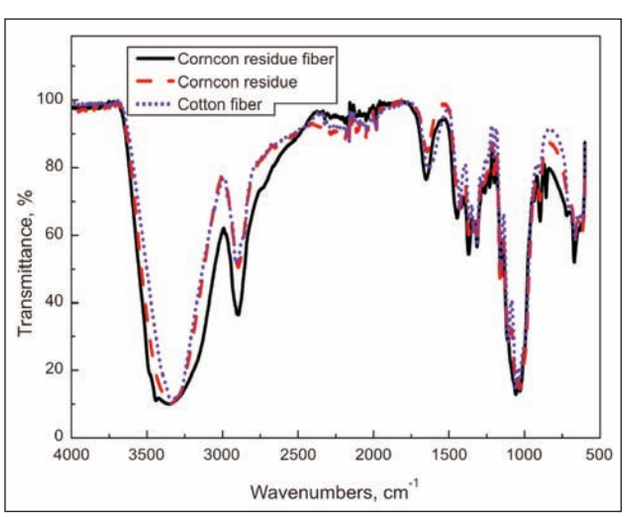

Fig. 2. The infrared spectra of corncob residue fiber, corncob residue, and cotton fiber

There were no obvious characteristic absorbency peaks of lignin for all spectra, such as the peak of carbonyl group of carboxyl and ester group near 1740 cm^{-1}, the peak of C=C aromatic ring around 1600 cm^{-1}, the peak of aromatic ring in a wave number of 1510 cm^{-1}, the peak of C–O stretching of lignin near 1240 cm^{-1}. Those all demonstrate that the composition of corncob fiber is cellulose but no lignin.
Infrared spectra of cotton fiber and corncob residue are similar, which illustrates the similar main components and content of each component in these two samples. However, infrared spectra of corncob residue fiber and corncob residue show a little difference in intensity at the same absorption peak, due to the content change of functional groups of cellulose in the spinning process.

GPC analysis

Molecular weight and its polydispersity of corncob residues and raw material for Incell fibersare shown in table 2. There is no difference in number average molecular weight (Mn) between corncob residues and raw material for Incell fibers. The peak relative molecular weight (Mp) of the corncob residue is slightly lower than that of raw material for Incell fiber. Polydispersity is the ratio of the average molecular weight to the number average molecular weight. The values of weight average molecular weight (Mw) and polydispersity for the corncob residue are slightly higher.

Table 2

Sample	Mn	Mw	Mp	Poly-dispersity
Raw material for Incell fiber	58331	203471	167858	3.49
Corncob residue	58287	215920	159856	3.70

Figure 3 shows the GPC curves of corncob residue and raw material for Incell fiber. Both curves are asymmetrical. It is mainly because both of them contain a small amount of hemicellulose, resulting in the relative molecular weight distribution curve is skewed, and has poor symmetry, large polydispersity [17]. The hemicellulose acts as a plasticizer, making it easy to improve the spinnability [18]. But the main peak of GPC curve of corncob residue is lower than that of wood pulp raw material for Incell fiber, indicating that the corncob residue has a larger polydispersity.
Combined with infrared spectrum analysis, it can be found that corncob residue has the same main components with the wood pulp raw material for Incell fiber, which is consist of are cellulose and a small amount of hemicellulose. What's more, relative molecular weight distribution curves of both materials above are similar, suggesting that the corncob residue in this study has potential to be used as the material for spinning instead of wood pulp.

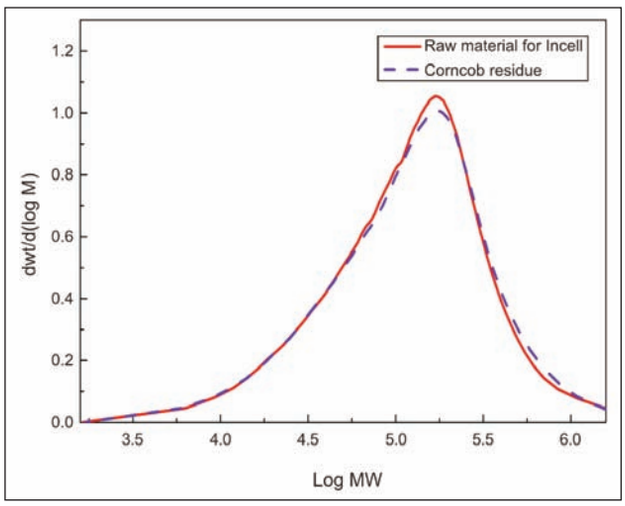

Fig. 3. The relative molecular weight distribution curve measured using GPC

When the solution was preparing in GPC method, the corncob residue is not completely dissolved and there is a tiny amount of undissolved flocculent substance at the bottom of the container. The substance could probably be the very tiny amount of ash impurities, which suggests the corncob residue solution need to be filtrated and purified before the spinning process.

XRD analysis

The crystallinity (X_c) and crystal orientation (f_c) of all fibers were measured by Wide-angle X-ray diffraction (WAXD) measurements. The X_c and f_c of all fibers are listed in table 3.

The crystallinity degree of corncob residue fiber is higher than that of any other fibers in this study, shown in table 3. The crystal orientation degree of corncob residue fiber is higher than that of Viscose fiber and Lyocell fiber, however, a litter bit lower than that of Incell fiber. Those all directly suggest that draft radio of corncob residue fiber is relatively high during the spinning process. In order to obtain flexible fibers, the draft radio should be reduced when manufacturing corncob residue fibers.

Linear density analysis

The average linear density of the corncob residue fiber is 10.33 dtex, which is too high if the fiber is used for textile. For further industry application, the linear density of the fiber must be reduced.

Table 3

Sample	Degree of crystallinity, X_c (%)	Degree of crystal orientation, f_c (%)
Corncob residue fiber [a]	61.9	79.5
Incell fiber [a]	51.7	80.4
Viscose fiber [a]	27.0	58.0
Lyocell fiber [b]	44.0	71.0
Tencel A100 [c]	53.6	—

[a] New data in this study; [b] Data collected from Carrillo's research [9]; [c] Data collected from Wu's study [10].

Moisture regain analysis

The moisture regains of the corncob residue fiber measured by oven method is 9.31%, which is slightly higher than moisture regains of cotton and much greater than that of synthetic fiber, such as polyester. But the moisture regains of corncob residue fiber are lower than moisture regain of regular viscose fiber (12%~14%) and Lyocell fiber (11%~13%) [19], which is possible because of that the degree of crystallinity and crystal orientation of corncob residue fiber is relatively high.

Mechanical properties analysis

The mechanical properties of corncob fibers, Incell fibers, viscose fiber, Lyocell fiber and Tencel A100 are listed in table 4. The load-elongation curve of Corncob residue fiber Incell fiber and Viscose fiber are shown in figure 4.

The tensile strength of corncob residue fiber was significantly higher than that of viscose fiber, suggesting that corncob residue fiber has broad application prospects and will play an important role in reducing the cost of production, effective utilizing of industrial and agricultural waste, and reducing of environmental pollution.

The tensile strength of four kinds of fibers produced by Lyocell spinning technology is generally higher than that of viscose fiber, which due to the Lyocell process technology. Except for viscose fiber, other fibers have the same spinning technology principle, but different parameters and raw materials. The

Table 4

Sample	Tensile strength		Elongation at break		Initial Modulus	
	average (cN/dtex)	CV (%)	average (%)	CV (%)	average (cN/dtex)	CV (%)
Corncob fiber [a]	2.72	6.54	8.01	28.7	112	8.90
Incell fiber [a]	3.75	11.9	11.9	16.8	72.4	28.9
Viscose fiber [a]	1.82	13.2	19.6	10.5	22.3	31.2
Lyocell fiber [d]	3.17	—	12.5	—	35.4	—
Tencel A100 [e]	3.97	—	12.6	—	41.4	—

[a] New data in this study; [d] Data collected from Kreze's research [11]; [e] Data collected from Lou's study [12].

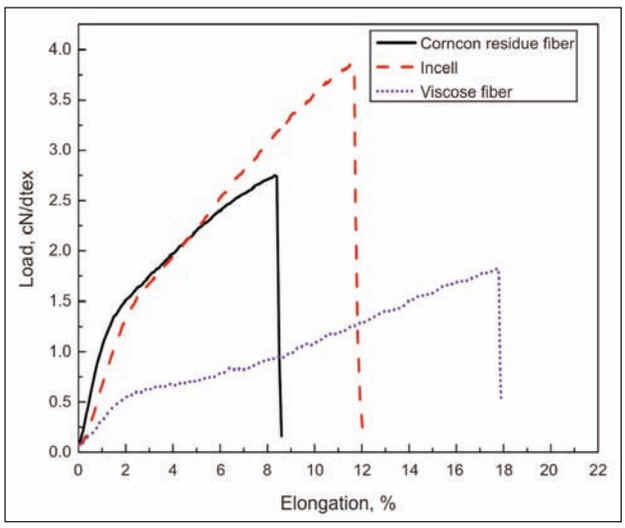

Fig. 4. Load-elongation curve of three kinds of fibers

degree of crystallinity and orientation can reflect differences of the spinning process parameters. Corncob residue fiber has high crystallinity and orientation degree, indicating that it should have high strength and modulus, smaller elongation. However, corncob residue fiber manufactured in this study has high modulus and low elongation characteristics but did not get a high strength, mainly because that the raw material has slightly large dispersion in molecular weight and the tiny amount of impurities. The purification of corncob residue and reduction of its cellulose dispersion inside should be an important research subject to improve fiber strength.

Among these five kinds of fibers, elongation of viscose fiber is the highest, followed by that of Tencel A100, Lyocell fiber, and Incell fiber, and the elongation of corncob residue fiber is the lowest. When draft ratio increases, the breaking elongation will decrease [20]. The initial modulus of corncob residue fiber is the highest, followed by that of Incell fiber and Tencel A100, and initial modulus of viscose fiber is the lowest. This is because of the high crystallization of corncob residue fiber, leading to its high rigid and low flexibility. Those evidences above all suggest that it is necessary to decrease the draft ratio in the future producing process. The coefficient of variation of extension at break of corncob residue fiber is higher than that of Incell fiber, which may because of the uneven line density of corncob residue fiber.

CONCLUSIONS

Corncob residue fiber is a new regenerated cellulose fiber manufactured by Shandong Yingli Industrial Co. Ltd., China with corncob residue as main raw materials using Lyocell spinning technology. With analysis of chemical properties of corncob residue, mechanical properties of corncob residue fiber, the conclusions are shown as follows:

(1) Main compositions of corncob residue are cellulose, slight hemicellulose and very tiny amount of spinning insoluble components. These components can be dissolved in the same solvent when dissolving wood pulp. Similar relative molecular weight distribution curves of corncob residue and wood pulp suggestthat corncob residue can replace wood pulp as raw material for spinning in a certain extent. Compared to wood pulp, corncob residue has a similar number-average molecular weight, a slightly larger weight-average molecular weight, a lower peak-relative molecular weight, and a larger polydispersity.

(2) The breaking strength of corncob residue fiber produced by Lyocell technology is 2.72 cN/dtex, which is higher than that of viscose fiber, slightly lower than that of Lyocell fiber and Tencel A100, indicating corncob residue fiber has broad application prospects.

(3) The line density of corncob residue fiber is 10.33 dtex. The crystallinity of corncob residue fiber is higher than that of viscose fiber, Incell fiber, Lyocell fiber and Tencel A100. The degree of orientation of corncob residue fiber is higher than the other fibers, which lead that the standard moisture regain of corncob residue fiber is lower than that of the other fibers. The initial modulus of corncob residue fiber is higher than that of other fibers. Those all tell that a great effort should be taken in optimizing of manufacturing technology of corncob residue fiber.

BIBLIOGRAPHY

[1] Wang, L., Yang, M., Fan, X. *An environmentally friendly and efficient method for xylitol bioconversion with high-temperature-steaming corncob hydrolysate by adapted Candida tropicalis*, In: Process Biochemistry, 2011, vol. 46, no. 8, pp. 1619–1626.

[2] Fang, J., Liu, H.J., Zhang, G.G. *Preparation of carboxymethyl cellulose from corncob*, In: Procedia Environmental Sciences, 2016, vol. 31, no. 1, pp. 98–102.

[3] Jia, F., Liu, H.J., Zhang, G.G. *Physicochemical properties and possible applications of waste corncob fly ash from biomass gasification industries of China*, In: BioResources, 2016, vol. 11, no. 2, pp. 3783–3798.

[4] Wooding, C. *Regenerated Cellulose Fibres*, Woodhead Publishing Ltd, Cambridge, 2001, Chapter 4, pp. 62–87.

[5] Mi K.Y., Reza M.S., Kim I.M. *Physical properties and fibrillation tendency of regenerated cellulose fiber dry jet-wet spun from high-molecular weight cotton linter Pulp/NMMO solution*, In: Fibers and Polymers, 2015, vol. 16, no. 8, pp. 1618–1628.

[6] Zhang, H.R., Liu, X., Li, D. *Effect of oligosaccharide accumulated in the coagulation bath on the lyocell fiber process during industrial production*, In: Journal of Applied Polymer Science, 2009, vol. 113, no. 1, pp. 150–156.

[7] Yang, G., Zhang, Y., Shao, H. *A comparative study of bamboo Lyocell fiber and other regenerated cellulose fibers 2nd ICC 2007, Tokyo, Japan, October 25–29, 2007*, In: Holzforschung, 2008, vol. 63, no. 1, pp. 18–22.

[8] Uddin, A.J., Yamamoto, A., Gotoh, Y. *Preparation and physical properties of regenerated cellulose fibres from sugarcane bagasse*, In: Textile Research Journal, 2010, vol. 80, no. 80, pp. 1846–1858.

[9] Carrillo, F., Colom, X., Valldeperas, J. *Structural characterization and properties of lyocell fibers after fibrillation and enzymatic defibrillation finishing treatments*, In: Textile Research Journal, 2003, vol. 73, no. 11, pp. 1024–1030.

[10] Wu, Q., Pan, D., *A new cellulose based carbon fiber from a Lyocell precursor*, In: Textile Research Journal, 2002, vol. 72, no. 5, pp. 405–410.

[11] Kreze, T., Malej, S. *Structural characteristics of new and conventional regenerated cellulosic fibers*, In: Textile Research Journal, 2003, vol. 73, no. 8, pp. 675–684.

[12] Lou, L.Q. *Performance test of Lyocell fiber*, In: Silk, 2003, vol. 1, pp. 36–38.

[13] Eremeeva, T. *Size-exclusion chromatography of enzymatically treated cellulose and related polysaccharides: a review*, In: Journal of Biochemical & Biophysical Methods, 2003, vol. 56, no. 1–3, pp. 253–264.

[14] Mccormick, C.L., Lichatowich, D.K. *Homogeneous solution reactions of cellulose, chitin, and other polysaccharides to produce controlled-activity pesticide systems*, In: Journal of Polymer Science Part C Polymer Letters, 2003, vol. 17, no. 8, pp. 479–484.

[15] Bikova, T., Treimanis, A. *Problems of the MMD analysis of cellulose by SEC using DMA/LiCl: a review*, In: Carbohydrate Polymers, 2002, vol. 48, no. 1, pp. 23–28.

[16] Jerosch, H., Lavédrine, B., Cherton, J.C. *Study of the stability of cellulose-holocellulose solutions in N, N-dimethylacetamide-lithium chloride by size exclusion chromatography*, In: Journal of Chromatography A, 2001, vol. 927, no. 1–2, pp. 31–38.

[17] Zhang, H.H., Zhang, S.J., Shao, H.L. *Validate the feasibility of predicting the molecular weight distribution of cellulose by using rheological method*, In: Journal of Donghua University Natural Science, 2004, vol. 30, no. 5, pp. 82–85.

[18] Zhang, H.H., *Study on the improvement of mechanical properties of Lyocell fiber used as precursor of carbon fiber*. In: Materials Science, Donghua University, 2005.

[19] Ibbett, R.N., Hsieh, Y.L. *Effect of fiber swelling on the structure of Lyocell fabrics*, In: Textile Research Journal, 2001, vol. 71, no. 2, pp. 164–173.

[20] Mortimer, S.A., Péguy, A.A., Ball, R.C. *Influence of the physical process parameters on the structure formation of lyocellfibres*, In: Cellulose Chemistry & Technology, 1996, vol. 30, no. 3, pp. 251–266.

Authors:

CHENG WANG[1], LIXIA HU[1], RONGHUAN HAN[2], FUMEI WANG[1, 3]

[1]Donghua University, College of Textiles,
201620, Shanghai, China

[2]Shandong Yingli Industrial Co. LTD,
262700, Shandong, China

[3]Donghua University, Key Laboratory of Textile Science & Technology, Ministry of Education,
201620, Shanghai, China

e-mail: wc19930127@yahoo.com

Corresponding author:

FUMEI WANG
e-mail: wfumei@dhu.edu.cn

Research on achieving a meteorological monitoring system to increase efficiency in the execution and operation of solar installations and to reduce environmental pollution

NICOLAE DIACONU
ANDREEA ROXANA UNGUR (POPESCU)
MARIN SILVIU NAN
DANUT GRECEA
OLIMPIU STOICUTA
MARIUS RAZVAN POPESCU

REZUMAT – ABSTRACT

Cercetări privind realizarea unui sistem de monitorizare meteorologică pentru creșterea eficienței în execuția și exploatarea instalațiilor solare și pentru reducerea poluării mediului

Protecția mediului alături de economie și coeziunea socială sunt principalii piloni în dezvoltarea durabilă a unei țări. În acest context, strategia de dezvoltare a sectoarelor industriale din România trebuie să promoveze tehnologiile moderne cu un impact cât mai redus asupra mediului. Prin urmare, stabilirea modului de dispersie a poluanților, cât și identificarea fenomenelor meteorologice ce produc stagnarea poluanților în atmosferă, reprezintă o necesitate în cadrul zonelor industriale. Pe de altă parte, creșterea eficienței conversiei fotovoltaice, prin mărirea gradului de utilizare a radiației solare, atât din punctul de vedere al execuției, cât și al exploatării instalațiilor fotovoltaice, poate fi realizată în urma unor analize amănunțite asupra parametrilor și fenomenelor meteorologice ce definesc zona în care urmează a fi amplasat parcul fotovoltaic. Astfel, în cadrul acestui articol se prezintă un sistem meteorologic compus din șase stații meteorologice și un computer destinat salvării datelor achiziționate. Fiecare stație meteorologică achiziționează, din locul unde este montată, informații cu privire la următoarele variabile: temperatura mediului, intensitatea radiației solare, umiditate, presiune barometrică, altitudine, viteza vântului, direcția vântului și cantitatea de precipitații.

Cuvinte-cheie: protecţia mediului, sistem meteorologic, radiaţie solară

Research on achieving a meteorological monitoring system to increase efficiency in the execution and operation of solar installations and to reduce environmental pollution

Environmental protection alongside the economic and social cohesion are key pillars in the sustainable development of a country. In this context, the strategy of development of industries in Romania should promote modern technologies with as reduced environmental impact as possible. Therefore, determining how dispersion of the pollutants and identify weather events that cause the stagnation of pollutants in the atmosphere are a necessity in the industrial areas. On the other hand, the increased photovoltaic conversion efficiency by increasing the use of solar radiation, both in terms of execution as well as the operation of photovoltaic installations can be achieved as a result of detailed analysis of parameters and meteorological phenomena that define the area where the photovoltaic park will be located. Thus, this article presents a weather system consisting of six weather stations and a computer for keeping the data acquired. Each weather station acquires from where is assembled, information on the following variables: ambient temperature, solar radiation intensity, humidity, barometric pressure, altitude, wind speed, wind direction and rainfall.

Keywords: environmental protection, meteorological system, solar radiation

INTRODUCTION

The pollutants mode dispersion in the atmosphere is influenced by meteorological phenomena and parameters in the area where the pollution source is located. To find the best methods to minimize the quantities of pollutants released into the environment, the sources of pollution must be continuously monitored [1].

On the other hand, to increase the photovoltaic conversion efficiency by increasing the use of solar radiation, both in terms of execution as well as the operation of photovoltaic systems, requires a thorough analysis of the parameters and meteorological phenomena that define the area where the photovoltaic park will be located.

In this context, the paper presents the design of a system of six meteorological weather stations and a central computer for saving the acquired data.

The Meteorological System presented in this article is intended for continuous monitoring of meteorological parameters in the industrial areas that are sources of pollution in the areas where the photovoltaic parks will be located.

The meteorological stations acquire, from where they are located, information on the following variables: ambient temperature, solar radiation intensity, humidity, barometric pressure, altitude, wind speed, wind direction and rainfall.

DESCRIPTION OF THE METEOROLOGICAL SYSTEM

The Meteorological system proposed consists of six weather stations and a computer. Data transmission between system components meteorological 7 is via GSM modems. Each weather station acquires information on the following variables: ambient temperature,

solar radiation intensity, humidity, barometric pressure, altitude, wind speed, wind direction and rainfall. The parameters listed above are taken using specialized sensors that are connected to a Arduino Uno development platform, and then via a GSM modem are transmitted to the personal computer, where these parameters are stored.
In the meteorological system architecture shown in figure 1, the personal computer acts as a master device, while the other six meteorological stations play the role of SLAVE type devices.

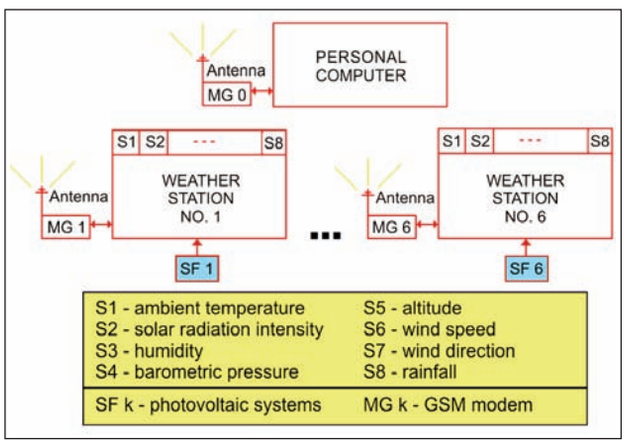

Fig. 1. The Architecture of the Meteorological System

The data reading provided by the meteorological stations it is made in an order initially set via the acquisition program running on the personal computer (PC).
Each modem has in its part a phone card with a phone number.
The exchange of information between personal computer and the composition of the modem from the weather stations is made via short message service (SMS).
The personal computer is powered from the mains power supply of 220 Vac through a backup power system.
Each station is has autonomous energy. The electricity supply units with equipment from the composition of a meteorological station are via an autonomous photovoltaic system with energy storage, where the consumers have continuous current.
The main elements of the composition of autonomous photovoltaic systems are described below.

THE PHOTOVOLTAIC SYSTEM

The block diagram of a photovoltaic system is shown in figure 2.
The photovoltaic system is made up of a photovoltaic panel TPS-103, a charge controller and a battery.
All photovoltaic system from the 6 meteorological stations are identical.
The photovoltaic panel TPS-103, used in the photovoltaic system is one of amorphous silicon, with a maximum output of 6W [2].

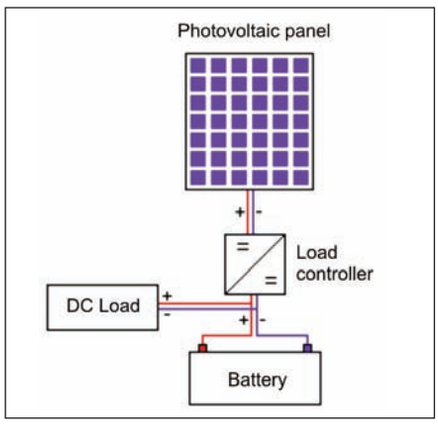

Fig. 2. Block diagram of the photovoltaic system

Current – power and voltage – the voltage of the photovoltaic panel TPS-103 characteristics are shown in figures 3 and 4.

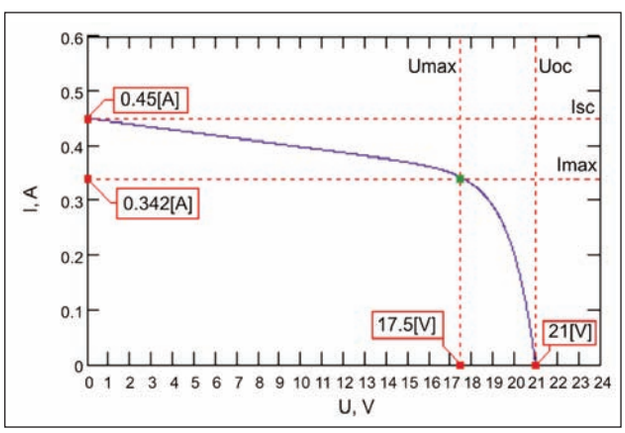

Fig. 3. Current-voltage of the photovoltaic panel TPS-103 characteristic

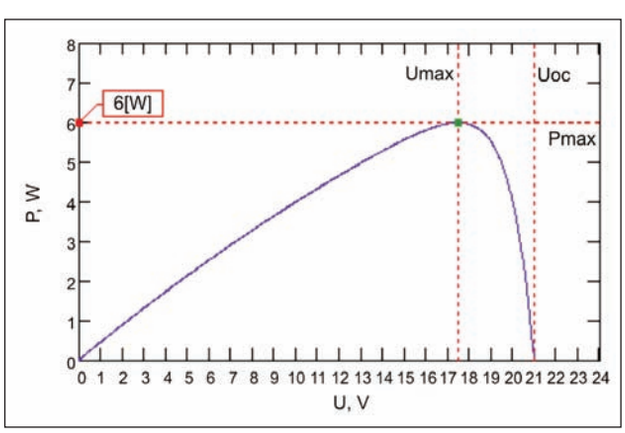

Fig. 4. Power-tension of the photovoltaic panel TPS-103 characteristic

The characteristics shown in figuress 3 and 4 are obtained in Mathcad, based on electrical parameters of the TPS-103 photovoltaic panel, supplied by the manufacturer company.
The load controller used in the photovoltaic system is Conrad 12 V/4 A. The load regulator is one type

series that aims to make the energy flow within the photovoltaic system.
The load controller controls the battery charging current, so the voltage across the battery voltage does not exceed the maximum load.
Among the most significant technical data of the Conrad load controller, we mention here the following [3]: the nominal voltage is 12 V, the maximum battery charging voltage is 13.8 V, the maximum current of photovoltaic panel and maximum battery charging current is 4 A and maximum power consumption of the controller load is 1.5 mA.
On the other hand, the battery constituting the photovoltaic system is S12 / 6.6S, type Pb - gel.
Among the most significant technical data of the battery [4], it is noted the following: the nominal voltage across the battery is 12 V, nominal capacity 6.6 Ah and the discharge current is 0.06 A. The variation in proportion to the time of the discharge current of the battery is defined by the following relation:

$$i(t) = a_1 + a_2 \cdot t + a_3 \cdot e^{a_4 \cdot t} \quad (1)$$

where: $a_1 = 0.397186$; $a_2 = -0.003356$;
$a_3 = 3.641273$; $a_1 = -0.374555$.

Equation (1) is obtained from the technical data of the battery using the exponential regression. The variation in proportion to time of the discharge current of the battery is shown in figure 5.

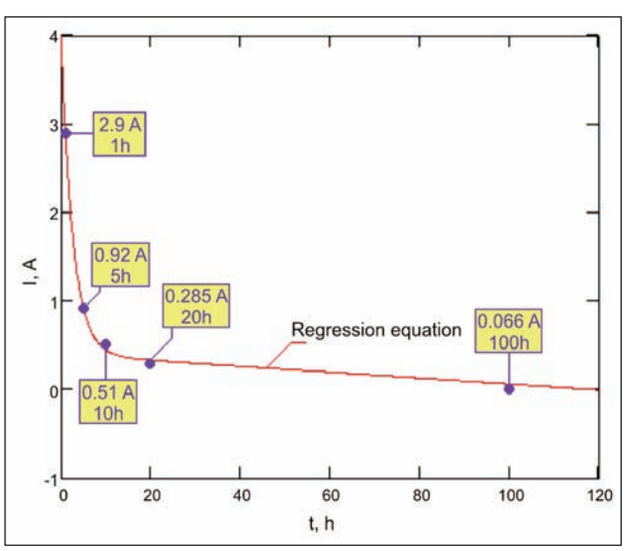

Fig. 5. The variation in proportion to time of the discharge current

According to technical specifications, battery S12/S 6.6 is designed to support up to 800 full discharge cycles (100%) and 3000 cycles of discharge of 30%.

DATA ACQUISITION SYSTEM

The data acquisition in the composition of meteorological stations is built around the development platform Arduino Uno, and eight sensors that aim to measure the following quantities: ambient temperature, solar radiation intensity, humidity, barometric pressure, altitude, wind speed, the wind direction and the amount of rainfall.
All sensors except the anemometer, rain gauge, wind vane and the pyranometer are placed in a metal box fitted with side holes. All items listed above, plus photovoltaic system and GSM modem, forms the basic structure of a weather station. The meteorological station is shown in figure 6.

Fig. 6. The meteorological stations

In the metal box in addition to those mentioned above, are mounted the battery and the load controller from the composition of the photovoltaic system.
The Arduino Uno Development Platform is a system built around the microcontroller ATMega328P.
The main features of the platform Arduino Uno platform are: the voltage of the platform is the range 7 Vdc – 12 Vdc, the total number of digital inputs and outputs are 14, of which 6 are PWM outputs, the platform has 6 analog inputs, has a Flash memory of 32 KB, a SRAM memory of 2 KB, EEPROM memory of 1 KB and the quartz frequency is 16 MHz.
The microcontroller of the Arduino Uno development platform composition is programmed via a USB cable using the specialized software Arduino 1.6.6, which is compatible with Windows operating systems.
The reading, processing and transmission of the weather data from the 8 sensors is based on a software program written in Arduino 1.6.6.
Once checked, this program is included in the composition of microcontroller memory ATMega328P Arduino platform.
The Arduino Uno platform is supplied with 12 Vdc directly to the battery from the composition of the photovoltaic system (see figure 2).The sensors used in a meteorological station were chosen so that they

be compatible with the development platform. The main features of the elements constituting the meteorological system and how to connect them are presented below [5–16]:

- **The barometric pressure sensor**. In order to measure the barometric pressure in the meteorological station, using a piezoresistive sensor, very accurate, BMP180, manufactured by Bosch Company. To offset the effects of temperature on the pressure, the BMP180 sensor is composed of a temperature sensor as well. This sensor is compatible with Arduino Uno platform and is powered by 3.3 Vdc directly on the platform Arduino. How to connect the Arduino Uno platform BMP180 sensor is shown in figure 7. The barometric pressure measurement range is from 300 HP to 1100 hPa.

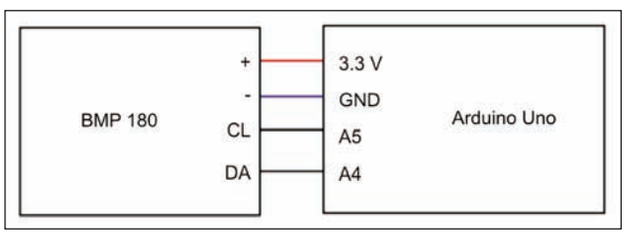

Fig. 7. How to connect the Arduino Uno sensor platform BMP180

The altitude is calculated using the following barometric formula:

$$A = 44330 \cdot \left(1 - \left(\frac{p}{p_0}\right)^{\frac{1}{5.255}}\right) \quad (2)$$

where p_0 = 1013.25 [hPa] is the pressure of the sea level, A [m] – altitude, and p [hPa] – the pressure measured with the use of BMP180 sensor.

Data communication between sensor and BMP 180 Arduino Uno platform development is based on I2C communication protocol.

- **The humidity and temperature sensor**. Temperature and humidity sensor, used in a SHT15 meteorological station, produced by Sensirion Company [17, 18]. SHT15 sensor platform is compatible with the Arduino Uno, being charged to 5 Vdc directly on Arduino platform. How to connect the sensor to the platform SHT15 Arduino Uno is shown in figure 8.

The humidity measuring range is between 0 [%RH] and 100 [%RH], with a precision of ±2 [%RH]. On the other hand, the measurement range of the temperature is between –40 °C and +123.8 °C, with a precision of ±0.3 °C.

The communication of the data between SHT15 sensor and the Arduino Uno development platform is a made on serial protocol.

Pins 4 and 5 of the Arduino Uno platform structure (see figure 8) are digital input pins.

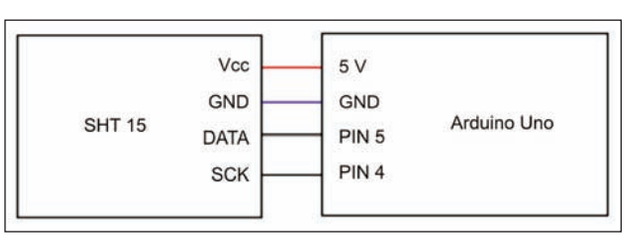

Fig. 8. The way the SHT15 sensor is connected to the Arduino Uno platform

- **The measuring element of the wind speed**. Wind speed measurement is done using a N96FY anemometer. The anenometer used is conducted around three hemispheric cups mounted on a shaft, which are driven by the air currents. According to the technical specifications the anenometer is conducted around a reed relay which closes from a second to another, when the wind speed is 2.4 km/h. The way the anemometer is connected to the Arduino platform is shown in figure 9.

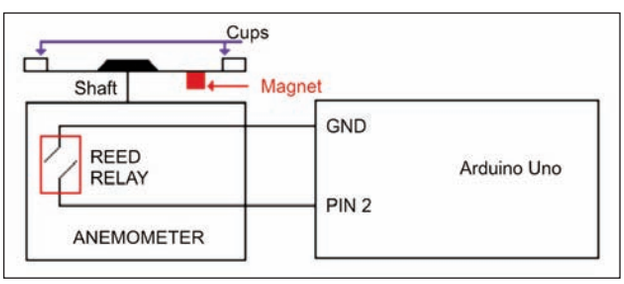

Fig. 9. The way the anemometer is connected to the Arduino Uno platform

Pin 2 of the Arduino platform structure (see figure 9) is a digital input pin. Pin 2, in the application, is configured to trigger an external interrupt on a falling edge of the input pulse.

The reverse logic counting of the pulses arriving on pin 2 is due to pull-up resistor that connects via terminal 2 at 5 Vdc supply voltage of the composition of Arduino Uno platform.

- **The element of measuring the wind direction**. The wind direction, within a meteorological station is measured using a wind vane. The wind vane is made by means of eight resistances and 8 reed relays as in figure 10.

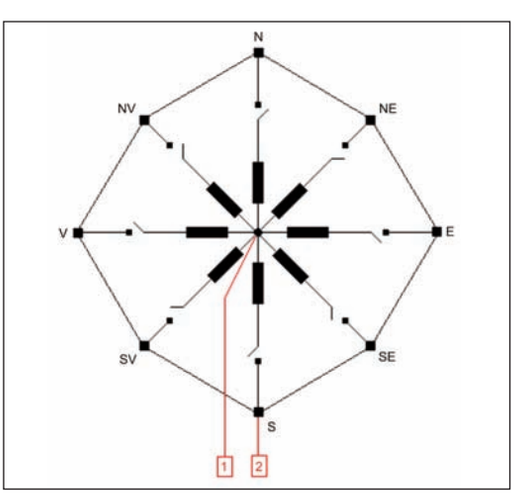

Fig. 10. The internal structure of the wind vane

According to technical specifications, the wind vane is able to show 16 distinct directions of the wind. Besides the 8 resistors, the wind vane contains a fixed resistance, which together with the 8 resistors, form a resistive divider.
In these conditions, for every wind direction, the wind vane provides a voltage that is read on one of the analog inputs of the Arduino platform. How to connect a wind vane Arduino platform is shown in figure 11.

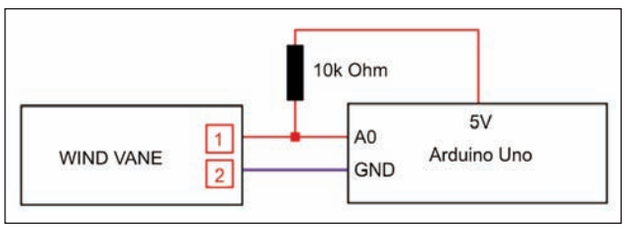

Fig. 11. Connection of the wind vane to the Arduino Uno platform

The A0 pin used for connecting the wind vane to the Arduino Uno platform, it is an analog one.

- **The measurement element of the precipitations**. The amount of precipitation that falls in a given area is monitored using a rain gauge. According to the technical specifications, the rain gauge is designed around a reed relay, which is activated every 0.2794 [mm]. The amount of precipitations is measured in [mm] thick layer of water (a thick layer 1 [mm] corresponds to a quantity of 1 [L] of water, spread evenly over an area of 1 [m^2]). The way the rain gauge is connected to the Arduino Uno platform is shown in figure 12.

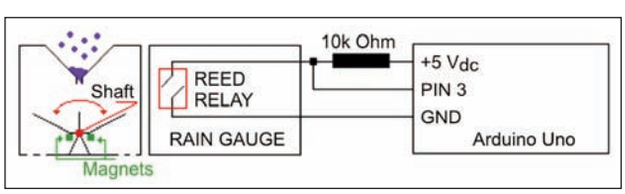

Fig. 12. The way the rain gauge is connected to the Arduino Uno platform

The pin 3 of the Arduino Uno platform structure (see figure 12) is a digital input pin and is configured as pin 2 in connection from the anenometer scheme (see figure 9).

- **The measurement element of the solar radiation**. The solar radiation measurement is made through a pyranometer, LP Silicon – PYRA 04, manufactured by Delta OHM, Italy. According to technical specifications, the feature of the pyranometer is a linear one with deviations of less than 1%. The voltage provided by the PYRA 04 pyranometer is amplified in a voltage range (0…5) [V] through HD978TR4 circuit. The range measurement of the solar radiation sensor specific of the PYRA 04 is (0…2000) [W/m^2] having a sensitivity of 20 [μV/(W/m^2)]. According to technical specifications, the static characteristic of HD978TR4 circuit is a linear one. The resolution of HD978TR4 circuit is 20 [μV] and the input voltage range is (0…20) [mV]. The way the pyranometer is connected through HD978TR4 circuit to the Uno Arduino platform is shown in figure 13.

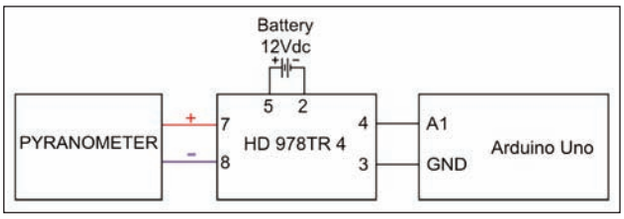

Fig. 13. The way the pyranometer is connected through HD978TR4 circuit to the Uno Arduino platform

The A1 pin used for connecting the PYRA 04 pyranometer to the Arduino Uno platform is an analog pin. The Arduino Uno platform analogues pins are connected to an analog-digital converter that has a resolution of 10 bits.

- **The GSM modem in the composition of a weather station.** Data transmission measured by sensors in the composition of meteorological station to the central computer is done via a GSM modem. The GSM modem used in a GSM weather station is a-gsm v2.064. This modem is compatible with Arduino Uno platform and connects directly to the terminal platform (the connection is via the 16-father pins of the modem that plugs directly into the mother pins of the Arduino Uno platform). The modem is fed through +5 [V] and GND pins of the Arduino Uno platform. Transmitting data from a weather station to the GSM modem of central computer componence is made using SMS messages. Data transmission is done when a transmission command is received from the modem of the central computer component. The data transmission is done every hour.
- **The GSM modem of the central computer constituent.** The data reading from all the weather stations is made using a GSM modem connected to a computer. The data obtained from the weather stations are stored on the central computer's hard disk, within Excel documents. The GSM modem from the constituent of the central computer is BGS2T Cinterion, manufactured by Germalto Company in Germany. The supply voltage of the modem is between (8…30) [V_{dc}] and the communication between the modem and the computer is via RS232 serial interface. The antenna used for modem BGS2T is one of nickel, of 2 dB, covering the frequency bands 850, 950 and 1900 MHz with an impedance of 50 [Ω]. The data acquisition program provided by the weather stations is conducted in Matlab and based on AT commands of the BGS2T modem.

DESCRIPTION OF THE SOFTWARE

The monitoring and transmission of data from sensors in the constituent of the meteorological stations

is implemented in the ATMega328P microcontroller, constituting the development platform Arduino Uno.
Each station of the meteorological system is identified by the telephone number of the GSM modem a-gsm v2.064.
On the other hand, the central computer system from the weather is identified by the telephone number of the modem BGS2T composition.
The data acquisition from a specified weather station and their transmission to the central computer is done only when the ATMega328P microcontroller receives a command transmission in this regard.
The order of transmission is an SMS message as follows: “TRANSMISSION START”.
Upon receiving an order from meteorological data transmission program of the ATMega328P microcontroller constituent, it verifies that the phone number from which the message was received is identical to the composition BGS2T modem, connected to the central computer.
If the phone number is the same, it proceeds to the purchase, and then data transmission to the central computer via SMS.
The program of the ATMega328P microcontroller constituent is based on the flowchart in the following figure.

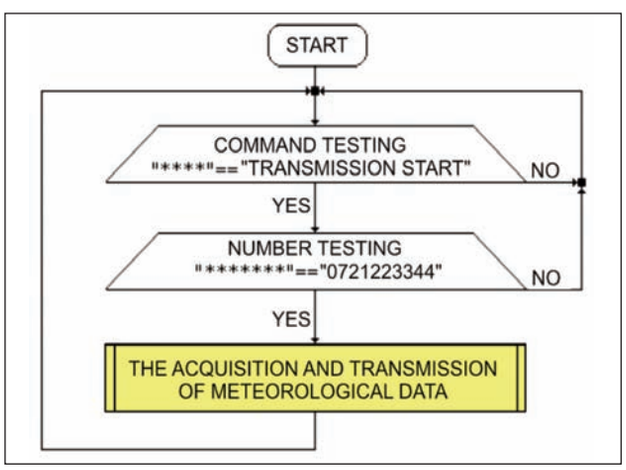

Fig. 14. The program flow diagram of the ATMega328P microcontroller constituent

The constituting elements of the weather stations are interrogated in a certain order.
On the other hand, the SMS message containing all of the data acquired from a specific weather station is composed of the values of the acquired placed in the message in the following order: the ambient temperature, intensity of solar radiation, humidity, barometric pressure, altitude, wind speed, wind direction and rainfall.
Each value in the composition of SMS is followed by an empty space. On the other hand, the monitoring of all the weather stations, running on the central computer, is based on the following flowchart.
From figure 15, it is noted that the reading and saving of the data constituent from a weather station, is the result of tests consisting of the verification telephone

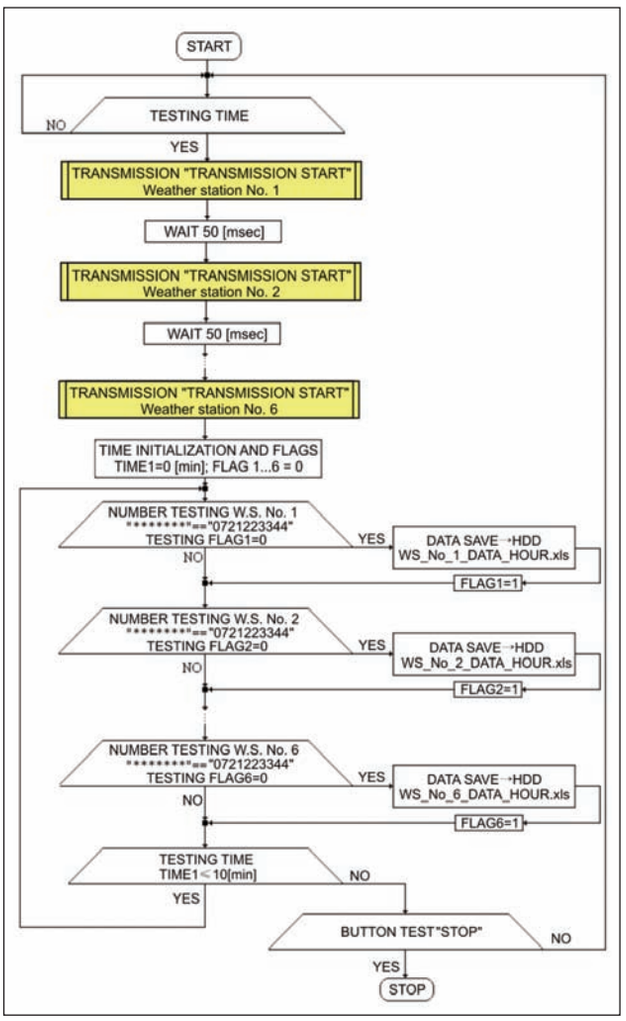

Fig. 15. The flowchart of the program constituting the central computer

number from the constituent of the meteorological station and of a flag.
The procedure for reading and saving the weather data is done in a loop that lasts 10 minutes.
The meteorological data are saved on the central computer’s hard disk in some Excel documents. The name of the Excel documents it is given by the meteorological station, followed by the date and time the data is saved.
Meteorological data acquisition program can be stopped if the button “STOP” of the user interface is pressed.
The user interface and procurement program is realized in Matlab [19].
The meteorological data acquisition program is an executable type that can be installed on any Windows operating system of 32-bit.
The executable program is based on the MATLAB command “*deploytool*”.
The user interface of the meteorological data acquisition program is shown in figure 16.
Starting the acquisition of meteorological data is done via the START button in the user interface structure (see figure 16).
The user interface is designed to monitor six meteorological stations.

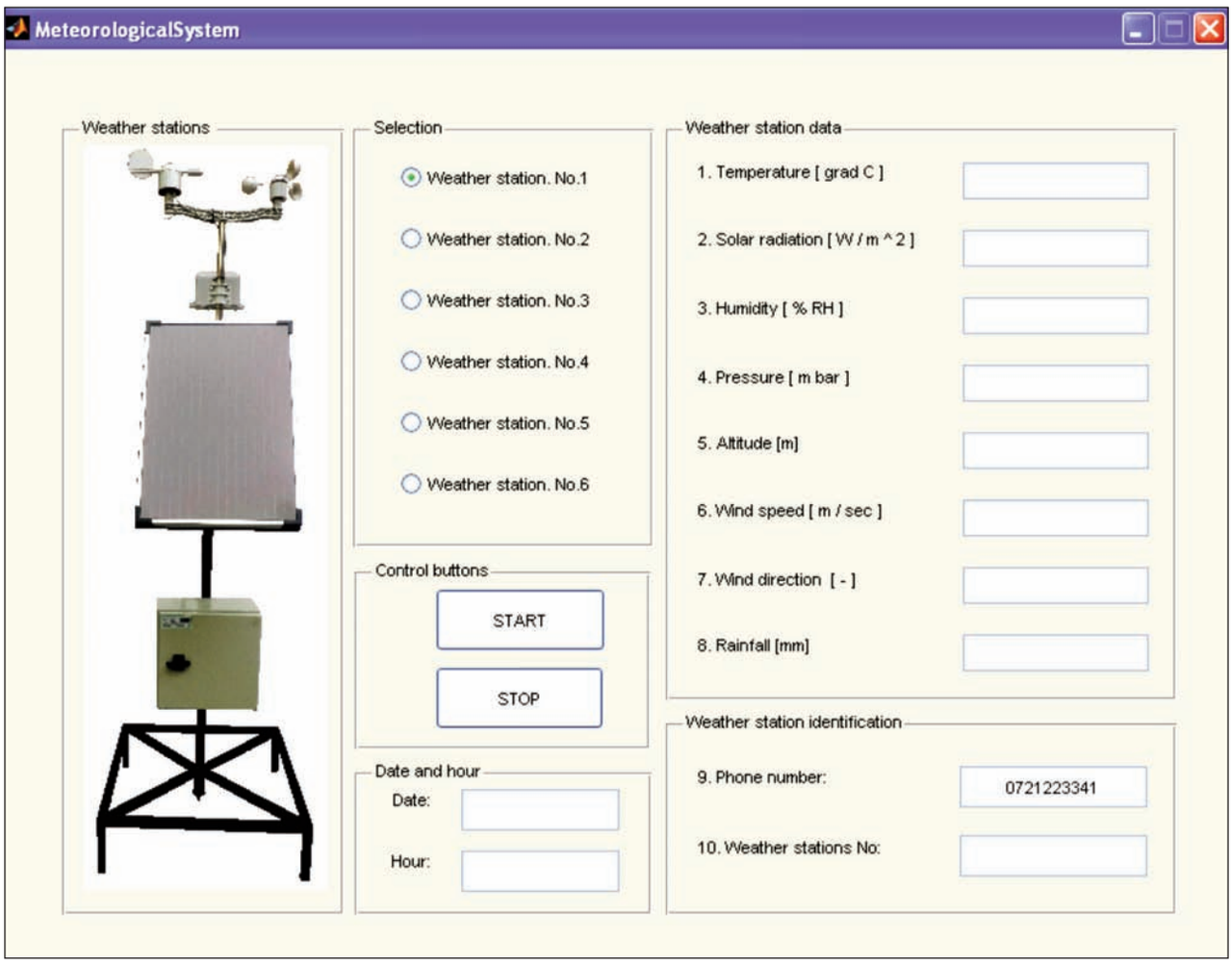

Fig. 16. The user interface of the software purchase

To view the latest values acquired, the interface has six radio buttons. Through these buttons, it can be selected at a time those six weather stations.

The parameters measured by the meteorological station, selected through the assigned radio button, are displayed to the right of the graphic interface in figure 16.

Identifying the meteorological station selected is highlighted in the graphic interface through the telephone number and the number associated with it (number *k* for the meteorological station *k*). On the other hand, for the user program to know the date and time the last meteorological data were received, the interface has two edit boxes, where the above information is displayed.

The program can be extended very easily for more weather stations.

EXPERIMENTAL RESULTS

With the six weather stations and acquisition program outlined above, it was performed an analysis of the meteorological data measured during the year 2014 in the city of Petrosani.

The six meteorological stations were located in the city of Petrosani at an altitude of about 618 m.

For all weather variables, with the exception of wind direction, the average value was calculated based on values from the six weather stations. The average value of a variable has been calculated in the following way:

$$V_k = \frac{1}{6} \cdot \sum_{i=1}^{6} V_{k,i} \; ; \; k = \{1,2,\ldots,8\} - \{7\} \qquad (3)$$

where:

V_k is the average number of variable weather *k* and V_k the weather variable number *k* measured with the use of the meteorological station *i*. Variations during 2014 of the averages of the meteorological variables are shown in the following figures.

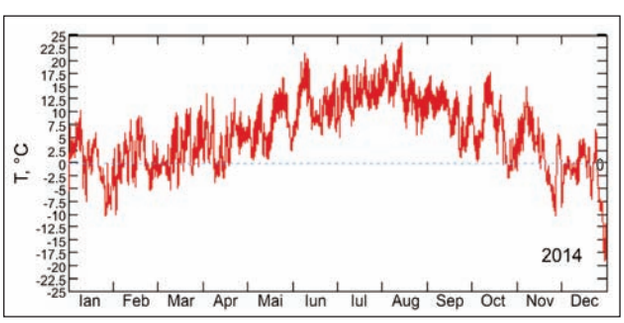

Fig. 17.The temparature variation during year 2014

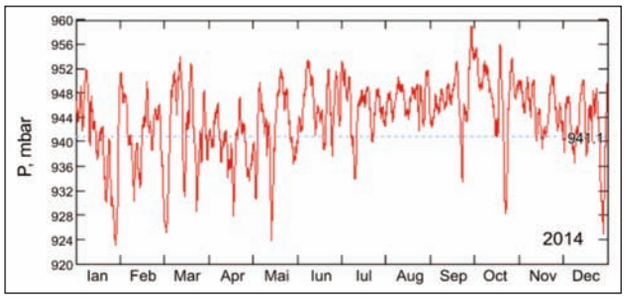

Fig. 18. The pressure variation during year 2014

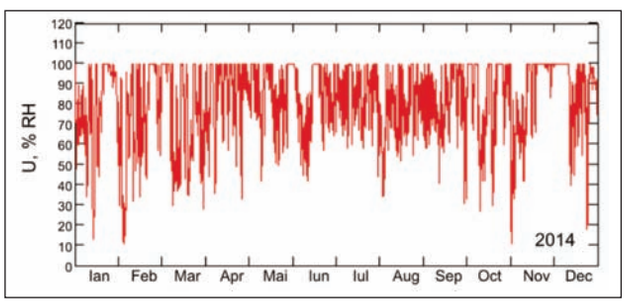

Fig. 19. The humidity variation during 2014

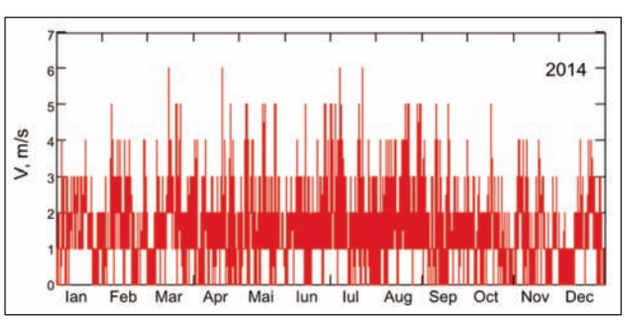

Fig. 20. The wind speed variation during 2014

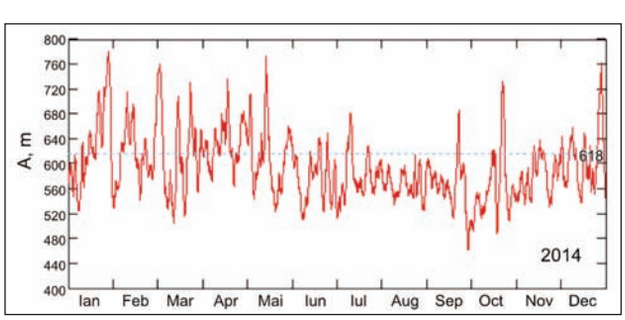

Fig. 21. The altitude calculated with the barometric formula

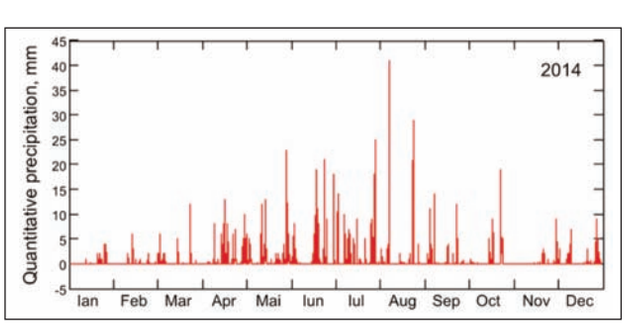

Fig. 22. The quantity of precipitation during year 2014

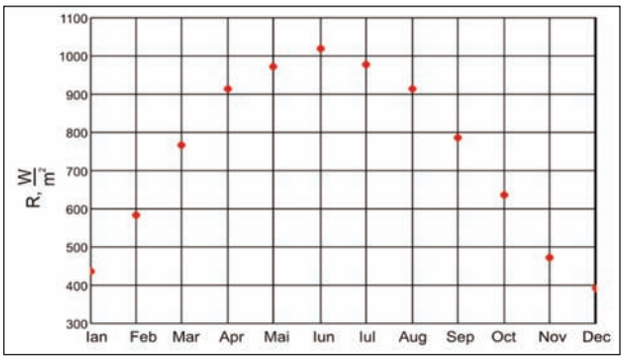

Fig. 23. The variation of the solar global radiation during year 2014

Global solar radiation during year 2014 falls in a horizontal plane, shown in figure 23, is defined by the average monthly value of the maximum solar radiation measured every day.

After analyzing the above presented graphics the following conclusions were drawn:

CONCLUSIONS

1. The cold season in the city of Petrosani takes about 5 months (January, February, March, November and December) where the temperatures below zero degrees Celsius prevail. Winter thermal characteristics are influenced by air masses that are stagnating in Petrosani Depression. On the other hand, the maximum temperature in 2014 was 23.5°C, recorded in August, while the minimum temperature of –19.1°C was recorded at the end of December.
2. The warm season in the Petrosani depression lasts 3 months (June, July and August). During these three months, temperatures reach values above 20°C. The thermal characteristics of the hot season are influenced by thermal inversions, phenomena that typically result in cool summers.
3. The barometric pressure during year 2014, presented variations around 941.1 [mbar], which corresponds to an altitude, calculated using the barometric formula 618 [m].
4. After analyzing the meteorological data measured, it was observed that during year 2014, in the city of Petrosani, south winds prevailed. On the other hand, it was noted that the air masses were stagnant over Petrosani, leading to maintain atmospheric pollutants. The air circuit in the Depression is done through Băniţa-Merisor lane (north) and Jiu Valley (south).
5. After analyzing data on wind speed during 2014, it was observed that the average speed was about 1.5 [m/s], in a southerly direction. On the other hand, it was observed that wind speed in Petrosani depression is increased with together with the altitude. On the mountain tops of Petrosani Depression, wind speed can exceed the 7 [m/s] value.
6. The amount of rainfall during year 2014 was not a uniform one. The maximum level of precipitations was reached in early August and was 41 [mm].

Regarding the average monthly amount of rainfall, we can say that the peak was reached in July and the minimum in January.

7. The average humidity during year 2014 was around 82 [%RH]. The maximum monthly average humidity was in December and the minimum in March.
8. The global solar radiation measured under blue sky in a horizontal plane reaches a maximum of 1020 [W/m^2] in June. On the other hand, the lowest values of solar radiation were recorded at the end and beginning of 2014. Thus, in December the solar radiation was of 391 [W/m^2] , and in January it was 436 [W/m^2].

BIBLIOGRAPHY

[1] Tiţa, M.C. *Atmospheric dispersion modeling of pollutants*, AGIR Scientific Bulletin, 2012, no. 2, pp. 70–75.
[2] ***, *Technical documentation of TPS-103 photovoltaic panel*, www.conrad.com
[3] ***, *Technical documentation of Conrad 12V/4A load controller*, www.conrad.com
[4] ***, *Technical documentation of S12/6.6S solar battery*, www.lpelectric.ro
[5] ***, *Technical documentation of Arduino Uno platform*, www.arduino.cc
[6] ***, *Technical documentation of ATMEL microcontroller, ATMega328P*, www.atmel.com
[7] ***, *Technical documentation of BMP180 sensor*, www.bosch-sensortec.com
[8] ***, *Technical documentation of SHT15 sensor*, www.sensirion.com
[9] ***, *Technical documentation of N96FY anemometer*, www.maplin.co.uk
[10] ***, *Technical documentation of N96FY wind vane,* www.maplin.co.uk
[11] ***, *Technical documentation of N96FY rain gauge*, www.maplin.co.uk
[12] ***, *Technical documentation of LP Silicon – PYRA 04 pyranometer,* www.deltaohm.com
[13] ***, *Technical documentation of HD978TR4 circuit*, www.deltaohm.com
[14] ***, *Technical documentation of a-gsm v2.064 modem*, http://itbrainpower.net
[15] ***, *Technical documentation of BGS25 modem*, www.gemalto.com
[16] ***, *BGS25 AT comands manual,* www.gemalto.com
[17] Petrilean, D. C., Irimie, S. I. *Solutions for the capitalization of the energetic potential of sludge collected in Danutoni Wastewater Treatment Plant,* In: Journal of environmental protection and ecology, ISSN 1311-5065, vol. 16, no. 3, pp. 1203–1211, 2015.
[18] Petrilean, D. C., Popescu F. D. *Temperature determination in hydrotechnical works as a variable of the energy change between air and environment*, In: Wseas Transactions nn Heat and Mass Transfer, ISSN: 1790-5044, Issue 4, Volume 3, pp. 209–218, 2008.
[19] Ghinea, M., Fireteanu, V. *Matlab Numerical calculus. Graphics. Applications*, Teora Publisher, 2004.

Authors:

Dr. Eng. NICOLAE DIACONU[1]
Prof. Dr. Eng. MARIN SILVIU NAN[2]
Assoc. Prof. Dr. Eng. OLIMPIU STOICUTA[3]
PhD student ANDREEA ROXANA UNGUR (POPESCU)[4]
PhD student MARIUS RAZVAN POPESCU[4]
Dr. Eng. DANUT GRECEA[5]

[1]Petrila City Hall
[2]University of Petrosani, Faculty of Mechanical and Electrical Engineering, Department of Mechanical Engineering, Industrial Engineering and Transportation
[3]University of Petrosani, Faculty of Mechanical and Electrical Engineering, Department of Control Engineering, Computers, Electrical Engineering and Power and Power Engineering
[4]Şcoala Doctorală a Universităţii din Petroşani
[5]INCD-INSEMEX Petrosanu

Petrosani – 332006
Str. Universitatii, No. 20, jud. Hunedoara, Romania

e-mail: diaconu_primarie@yahoo.com; nan.marins@gmail.com; stoicutaolimpiu@yahoo.com

Corresponding author:

NICOLAE DIACONU
e-mail: diaconu_primarie@yahoo.com

Neural network based thermal protective performance prediction of three-layered fabrics for firefighter clothing

MÜGE DURSUN
YAVUZ ŞENOL
ENDER YAZGAN BULGUN
TANER AKKAN

REZUMAT – ABSTRACT

Predicția performanței de protecție termică pe baza rețelei neurale a țesăturilor cu trei straturi pentru îmbrăcămintea pentru pompieri

Îmbrăcămintea de protecție pentru pompieri este compusă din trei straturi principale; un strat exterior, o barieră împotriva umezelii și o căptușeală de izolație termică. Această structură de țesături cu trei straturi asigură protecție împotriva incendiilor și mediilor cu temperatură foarte ridicată. Diverși parametri, cum ar fi construcția țesăturii, greutatea, desimea în urzeală/bătătură, grosimea, rezistența la vapori de apă a straturilor de material textil, au efect asupra performanței de protecție, cum ar fi transferul de căldură prin îmbrăcămintea de protecție pentru pompieri. Obiectivul acestui studiu este examinarea predictibilității indicelui de transfer de căldură al țesăturilor cu trei straturi, ca funcție a parametrilor țesăturii, prin utilizarea rețelelor neurale artificiale. Prin urmare, s-au obținut 64 combinații diferite de țesături cu trei straturi pentru îmbrăcămintea de protecție pentru pompieri, iar transferul de căldură prin convecție (HTI) și transferul de căldură radiant (RHTI), prin combinațiile de țesături, au fost măsurate în laborator. Șase rețele neurale cu perceptron multiplu (MLPNN), fiecare cu un singur strat ascuns și aceleași 12 date de intrare, au fost construite separat pentru predicția performanței transferului de căldură prin convecție și a performanței transferului de căldură radiant a țesăturilor cu trei straturi. Rețelele 1–4 au fost instruite pentru predicția HTI_{12}, HTI_{24}, $RHTI_{12}$ și, respectiv, $RHTI_{24}$, în timp ce rețelele 5 și 6 au avut două ieșiri, respectiv HTI_{12} și HTI_{24}, respectiv $RHTI_{12}$ și $RHTI_{24}$. Fiecare sistem indică o bună corelare între valorile estimate și valorile experimentale. Rezultatele demonstrează că MLPNN-urile propuse sunt capabile să estimeze transferul de căldură prin convecție și transferul de căldură radiant eficient. Cu toate acestea, rețeaua neurală cu două ieșiri are o performanță de predicție ușor mai bună.

Cuvinte-cheie: rețele neurale artificiale, predicție, transfer de căldură, țesături cu trei straturi, îmbrăcăminte de protecție pentru pompieri

Neural network based thermal protective performance prediction of three-layered fabrics for firefighter clothing

The firefighter protective clothing is comprised of three main layers; an outer shell, a moisture barrier and a thermal liner. This three-layered fabric structure provides protection against the fire and extremely hot environments. Various parameters such as fabric construction, weight, warp/weft count, warp/weft density, thickness, water vapour resistance of the fabric layers have effect on the protective performance as heat transfer through the firefighter clothing. In this study, it is aimed to examine the predictability of the heat transfer index of three-layered fabrics, as function of the fabric parameters using artificial neural networks. Therefore, 64 different three layered-fabric assembly combinations of the firefighter clothing were obtained and the convective heat transfer (HTI) and radiant heat transfer (RHTI) through the fabric combinations were measured in a laboratory. Six multilayer perceptron neural networks (MLPNN) each with a single hidden layer and the same 12 input data were constructed to predict the convective heat transfer performance and the radiant heat transfer performance of three-layered fabrics separately. The networks 1 to 4 were trained to predict HTI_{12}, HTI_{24}, $RHTI_{12}$, and $RHTI_{24}$, respectively, while networks 5 and 6 had two outputs, HTI_{12} and HTI_{24}, and $RHTI_{12}$ and $RHTI_{24}$, respectively. Each system indicates a good correlation between the predicted values and the experimental values. The results demonstrate that the proposed MLPNNs are able to predict the convective heat transfer and the radiant heat transfer effectively. However, the neural network with two outputs has slightly better prediction performance.

Keywords: artificial neural networks, prediction, heat transfer, three-layered fabrics, firefighter protective clothing

INTRODUCTION

Firefighters are subjected to various fire conditions and extreme thermal environments. Protective clothing provides protection from the thermal hazards, and allows firefighters to work effectively in dangerous thermal environments. This clothing comprises three fabric layers; an outer shell fabric, a moisture barrier, and a thermal liner [1]. The thermal protection of the fabrics is influenced by various properties of these three layers: weight, thickness, construction, water vapour permeability etc. These fabric characteristics are related to each other, and are nonlinear with the thermal protection properties.

Many studies investigated the performance of thermal protective fabrics with the structural features under the laboratory simulated thermal exposures [1, 2–7]. However, it is time consuming and costly to experiment with different fabric characteristics and to evaluate the relation with protective performance.

Moreover, because it is difficult to take account of all fabric parameters simultaneously, and to investigate the effects on the thermal protection performance of three layered fabrics, a new system is required for the effective prediction of the protective performance of such fabrics. An artificial neural network (ANN) is a computational structure and can be used to model the non-linear problems and predict the output values for given input parameters [8, 9]. In this respect, an ANN can be effectively used to evaluate the collective influence of all fabric parameters on the thermal protective performance.

ANN is applied in many field of textile industry such as prediction of yarn and fabric properties, defect detection of textile products, quality control, prediction in garment industry, identification and classification of different textile properties [9–17]. Because many prediction-related problems and textile processes are non-linear, ANNs are considered suitable. Several researchers have investigated on the prediction of the thermal resistance and the thermal performance of the textile fabricsusing artificial neural networks. Bhattacharjee & Kothari used ANN to predict the steady-state thermal resistance and maximum instantaneous heat transfer Q_{max} of a fabric, when the fabric weaving and construction parameters are used as inputs [18]. Cui and Zhang investigated the use of artificial neural networks to predict the thermal protective performance of fabrics [19]. In all these studies, an ANN was used to predict the thermal properties of single layer fabrics.

In the literature, there has been no study regarding the prediction of thermal protective performance of three-layered fabrics used for the firefighter protective clothing. In this study, it is aimed to design an artificial neural network to predict the thermal protective performance of three-layered fabrics. Therefore, six artificial neural networks were constructed to predict the convective heat transfer and the radiant heat transfer of three layered fabrics separately. Four samples from each of outer shell, moisture barrier and thermal liners were selected to create 64 different three-layered fabric assemblies. Six MLPNN were separately trained and tested in a supervised manner, with 12 input fabric characteristics and two actual output experiment values were obtained from the heat transfer instruments. All MLPNNs had the same 12 input fabric characteristics, but a different number of outputs. The outputs of networks were HTI_{12} and HTI_{24} for EN 367 standard and $RHTI_{12}$ and $RHTI_{24}$ for EN ISO 6942 standard. The heat transfer index values were obtained from the trained networks and the results were compared with the actual experimental values captured from the heat transfer instruments.

MATERIALS AND METHODS

Fabric samples and parameters

Four outer shell fabrics, four moisture fabrics and four thermal liners were chosen to represent various combinations of firefighter protective clothing for the performance evaluation of the artificial neural networks. The outer shells are made of Nomex, Polybenzimidazole (PBI) and Kevlar. The moisture barriers are made of polyurethane laminated flame retardant (FR) fabrics. The thermal liners are made of a FR woven fabric quilted to the FR nonwoven or FR felt. The parameters; weave, warp count, weft count, warp density, weft density, weight, thickness, and Limiting oxygen index (LOI) for the outer shell; the weight, thickness and water vapor resistance for the moisture barrier; weight and thickness for the thermal liner were selected to have as ANN inputs. These fabric parameters are related to the thermal protective performance. The warp count and weft count of the outer shells were measured in accordance with standard TS 255. The warp and weft density of the outer shells were measured in accordance with TS 250 EN 1049-2. The thickness of the fabrics was measured pursuant to standard TS 7128 EN ISO 5084 and the weight of the fabrics was measured pursuant to TS 251. The LOI test results values of the outer shells were obtained in accordance with ASTM D-2863. The water vapour resistance of the moisture barriers was obtained from an accredited testing laboratory.

Test methods

To measure thermal protective performance of three-layered fabrics, 64 samples were obtained from combinations of four different outer shells, four different moisture barriers and four different thermal liners. The thermal protective performance of a protective clothing system is related to the radiant and convective heat transfer properties through the fabric layers. In this study, convective heat transfer and radiant heat transfer were measured separately.

Measurement of the convective heat transfer (Heat transfer-flame)

The convective heat transfer can be assessed in respect to Standards No. EN 367 “Protective clothing protection against heat and fire-Method of determining heat transmission on exposure to flame” [20]. The test method in the standard provides thermal performance measures of the component fabrics and therefore, heat transfer within the garment. Figure 1 shows the heat transfer flame tester used during the tests.

The heat protection characteristics of the fabrics are determined by measuring the time to reach a temperature increase of 12 °C or 24 °C in a calorimeter (t_{12} and t_{24}, respectively) covered with the samples when exposed to a convective heat source of 80 kW/m^2 [21]. It is used to measure the time to theoretical pain and second-degree burn through fabric ensembles. These two time values indicate the performance level of the fabrics and are defined as heat transfer index (HTI_{12}, HTI_{24}).

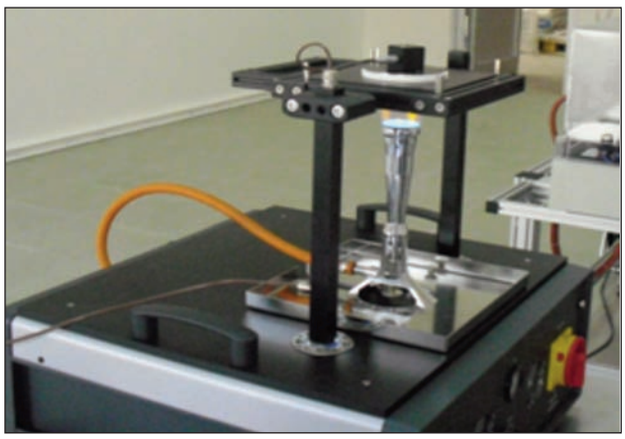

Fig. 1. Heat Transfer Flame tester

Measurement of the radiant heat transfer (Heat transfer radiation)

Radiant heat transfer can be assessed in accordance with Standards No. EN ISO 6942 “Protective clothing protection against heat and fire-Method of determining heat transmission on exposure to flame” [22]. The three-layered fabric is exposed to a radiant heat source of 40 kW/m^2. The time data to reach the temperature increase of 12 °C or 24 °C are recorded pursuant to EN 367 test method. They indicate the performance level of the three-layered fabrics, defined as Radiant Heat Transfer Index ($RHTI_{12}$, $RHTI_{24}$). The heat transfer radiation tester used in the measurements is shown in figure 2.

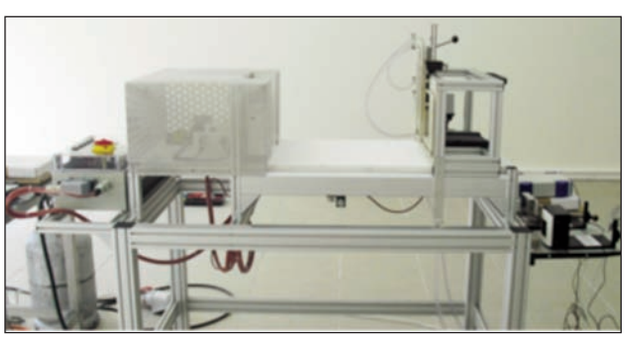

Fig. 2. Heat Transfer Radiation tester

The specifications of each fabric layer and the HTI and RHTI of the three layered fabric combinations are given in table 1.

Artificial neural network (ANN)

MLPNN can be defined as an important class of artificial neural networks, and they find different application areas in various disciplines. The network consists of three layers; input layer, one or more hidden layers and an output layer. Interconnection between the neurons of adjacent layers is provided by weights, and the information flow is in the forward direction from input to output. The input layer has no computation unit; the computation in the overall network takes place only at the hidden and the output layer neurons. The nonlinear mapping from input to output is obtained by weight adjustments through backpropagation algorithm [23]. The backpropagation algorithm aims to reduce the error between the original training output and the actual output. Neurons in the hidden and output layers perform a specific mathematical process, which is called activation function. The output from hidden layer functions goes to the input of adjacent layer neurons. The sigmoid activation function is the common function for most of the applications.

To apply to neural networks, the complete data set were divided into three parts: i) the training set, ii) the validation set, and iii) a test set. The training set is used to train the neural net to obtain a minimum error. The validation set is not used for training purpose. However, this data set provides performance analysis of the network during the training process. The decision to stop the learning is taken based on obtaining at the minimum of the validation set error. After completing the learning phase, the test data set is used to check the performance of the neural network.

In this study, MLPNNs were used to predict the thermal protective performance of three-layered fabrics of firefighter protective clothing from input fabric characteristics. The total of measured fabric parameters were 13. Due to the fact that the warp yarn and weft yarn numbers are equal, and therefore only one of them was used as the input value to ANN. The information of the weaving for Twill or Ripstop was converted into numerical data as 1 and 2, respectively. Finally, 12 input values were selected to train the networks. To find the best network performance, six different multilayer perceptron neural networks (MLPNN) with a single hidden layer were constructed using MATLAB to predict the convective heat transfer and the radiant heat transfer of three-layered fabric assemblies. The only difference among these networks was the number of outputs. Network 1, and 2 produces single output for HTI_{12} and HTI_{24} of EN 367 standard, respectively, and Network 3, and 4 produces single output for $RHTI_{12}$ and $RHTI_{24}$ of EN ISO 6942 standard, respectively. Whereas, Network 5, and 6 produces two outputs for HTI_{12} and HTI_{24} of EN 367 standard and for $RHTI_{12}$ and $RHTI_{24}$ of EN ISO 6942 standard, respectively. Warp count, weft count and their densities are included within the weight input of outer shell. In this consideration, all networks were also trained by exempting warp/weft count and their densities from the network input training set. However, theperformance of these networks was slightly lower than the networks with full input set training. Since previous related studies use the similar data sets, it was decided to use all 12 input date set. Figure 3 shows the block diagram of all networks.

Table 1

Sample No	INPUTS													OUTPUTS			
	Outer Shell (T: Twill, R: Ripstop)								Moisture Barrier			Thermal Liner					
	Weave	Warp count (Nm)	Weft count (Nm)	Warp density (ends/cm)	Weft density (Picks/cm)	Weight (g/m^2)	Thickness (mm)	LOI (%)	Weight (g/m^2)	Thickness (mm)	Water vapour resistance (m^{2}Pa/W)	Weight (g/m^2)	Thickness (mm)	HTI_{12} (EN 367)	HTI_{24} (EN 367)	$RHTI_{12}$ (EN 6942)	$RHTI_{24}$ (EN 6942)
1	T	55	55	26	24	195	0,47	27,04	85	0,15	7,4	270	2,9	10,4	14,5	14,7	20,2
2	T	55	55	26	24	195	0,47	27,04	85	0,15	7,4	240	1,24	10	13,7	12,9	18,7
3	T	55	55	26	24	195	0,47	27,04	85	0,15	7,4	205	1,23	9,6	13,1	10,2	14,8
4	T	55	55	26	24	195	0,47	27,04	85	0,15	7,4	260	3,24	9,8	13,4	15,4	22
5	T	55	55	26	24	195	0,47	27,04	145	0,31	10,7	270	2,9	12,9	17,2	15,5	21,9
6	T	55	55	26	24	195	0,47	27,04	145	0,31	10,7	240	1,24	11,4	15,9	14,9	22,2
7	T	55	55	26	24	195	0,47	27,04	145	0,31	10,7	205	1,23	9,5	12,9	12,1	16,9
8	T	55	55	26	24	195	0,47	27,04	145	0,31	10,7	260	3,24	11,1	14,6	15,3	22
9	T	55	55	26	24	195	0,47	27,04	90	0,35	9,83	270	2,9	11,1	15,2	13,9	20,1
10	T	55	55	26	24	195	0,47	27,04	90	0,35	9,83	240	1,24	14,4	19,1	19,2	25,5
11	T	55	55	26	24	195	0,47	27,04	90	0,35	9,83	205	1,23	11,1	15,1	14,7	20,3
12	T	55	55	26	24	195	0,47	27,04	90	0,35	9,83	260	3,24	12,6	17,4	16,1	22,3
13	T	55	55	26	24	195	0,47	27,04	125	0,89	13,025	270	2,9	14,7	20,8	18,1	24,7
14	T	55	55	26	24	195	0,47	27,04	125	0,89	13,025	240	1,24	12,9	17,6	17,5	24,4
15	T	55	55	26	24	195	0,47	27,04	125	0,89	13,025	205	1,23	12,4	16,7	14,2	20,2
16	T	55	55	26	24	195	0,47	27,04	125	0,89	13,025	260	3,24	14,7	20,2	18,4	25
17	R	55	55	26	24	195	0,46	27,04	85	0,15	7,4	270	2,9	9,9	13,7	13,2	18,5
18	R	55	55	26	24	195	0,46	27,04	85	0,15	7,4	240	1,24	10,5	14,6	13,6	19,9
19	R	55	55	26	24	195	0,46	27,04	85	0,15	7,4	205	1,23	9,6	13,2	10,8	15,8
20	R	55	55	26	24	195	0,46	27,04	85	0,15	7,4	260	3,24	11,1	15,5	15,3	21,3
21	R	55	55	26	24	195	0,46	27,04	145	0,31	10,7	270	2,9	11,7	15,8	14,3	19,9
22	R	55	55	26	24	195	0,46	27,04	145	0,31	10,7	240	1,24	13,9	19,9	15,6	23,2
23	R	55	55	26	24	195	0,46	27,04	145	0,31	10,7	205	1,23	11,1	15,4	12,5	18
24	R	55	55	26	24	195	0,46	27,04	145	0,31	10,7	260	3,24	13	18,1	15	22,5
25	R	55	55	26	24	195	0,46	27,04	90	0,35	9,83	270	2,9	11,7	16,1	13,2	18,5
26	R	55	55	26	24	195	0,46	27,04	90	0,35	9,83	240	1,24	13,1	17,8	16,3	22,1
27	R	55	55	26	24	195	0,46	27,04	90	0,35	9,83	205	1,23	10,8	14,8	12,2	18,1
28	R	55	55	26	24	195	0,46	27,04	90	0,35	9,83	260	3,24	13,3	18,5	16,4	22,2
29	R	55	55	26	24	195	0,46	27,04	125	0,89	13,025	270	2,9	13,4	18,3	17,2	23,6
30	R	55	55	26	24	195	0,46	27,04	125	0,89	13,025	240	1,24	13,9	19,3	17,8	25,3
31	R	55	55	26	24	195	0,46	27,04	125	0,89	13,025	205	1,23	13	17,7	15,8	23,2
32	R	55	55	26	24	195	0,46	27,04	125	0,89	13,025	260	3,24	14,6	19,9	18,8	25,6
33	R	26	26	21	18	200	0,57	44,4	85	0,15	7,4	270	2,9	11,1	15,4	15,7	23,9
34	R	26	26	21	18	200	0,57	44,4	85	0,15	7,4	240	1,24	10,9	15,2	15,3	23,5
35	R	26	26	21	18	200	0,57	44,4	85	0,15	7,4	205	1,23	9,8	13,4	13,3	20,5
36	R	26	26	21	18	200	0,57	44,4	85	0,15	7,4	260	3,24	11,9	16,9	17	24,9
37	R	26	26	21	18	200	0,57	44,4	145	0,31	10,7	270	2,9	11,2	15,8	16,9	24
38	R	26	26	21	18	200	0,57	44,4	145	0,31	10,7	240	1,24	12,7	17,5	16,3	24,2
39	R	26	26	21	18	200	0,57	44,4	145	0,31	10,7	205	1,23	11,1	15,6	14,5	21,3
40	R	26	26	21	18	200	0,57	44,4	145	0,31	10,7	260	3,24	14	19,6	18,7	27,7
41	R	26	26	21	18	200	0,57	44,4	90	0,35	9,83	270	2,9	13,8	20	20,2	29,6
42	R	26	26	21	18	200	0,57	44,4	90	0,35	9,83	240	1,24	10	14,9	21,6	31,0
43	R	26	26	21	18	200	0,57	44,4	90	0,35	9,83	205	1,23	10,9	14,9	15,7	23,3
44	R	26	26	21	18	200	0,57	44,4	90	0,35	9,83	260	3,24	13,4	18,9	20	29
45	R	26	26	21	18	200	0,57	44,4	125	0,89	13,025	270	2,9	15,6	22	20,9	31
46	R	26	26	21	18	200	0,57	44,4	125	0,89	13,025	240	1,24	14,1	19,5	17,6	27,1
47	R	26	26	21	18	200	0,57	44,4	125	0,89	13,025	205	1,23	12,5	17,1	16,4	24,9
48	R	26	26	21	18	200	0,57	44,4	125	0,89	13,025	260	3,24	14,4	20,3	20,6	30,2
49	T	64	64	30	22	165	0,32	33,75	85	0,15	7,4	270	2,9	12,8	18,4	16,4	24,2
50	T	64	64	30	22	165	0,32	33,75	85	0,15	7,4	240	1,24	11,5	15,9	13,5	20,5
51	T	64	64	30	22	165	0,32	33,75	85	0,15	7,4	205	1,23	10,4	14,4	11,9	18,3
52	T	64	64	30	22	165	0,32	33,75	85	0,15	7,4	260	3,24	12,6	17,9	15,6	22,8
53	T	64	64	30	22	165	0,32	33,75	145	0,31	10,7	270	2,9	14,4	20,8	19,2	27,8
54	T	64	64	30	22	165	0,32	33,75	145	0,31	10,7	240	1,24	12,8	17,8	15,1	22,4
55	T	64	64	30	22	165	0,32	33,75	145	0,31	10,7	205	1,23	11,8	16,2	14,4	21,2
56	T	64	64	30	22	165	0,32	33,75	145	0,31	10,7	260	3,24	15,3	21,5	19,9	28,1
57	T	64	64	30	22	165	0,32	33,75	90	0,35	9,83	270	2,9	15	21,6	18,3	26,1
58	T	64	64	30	22	165	0,32	33,75	90	0,35	9,83	240	1,24	12,9	17,9	15,8	22,9
59	T	64	64	30	22	165	0,32	33,75	90	0,35	9,83	205	1,23	11,8	16,1	14,3	21,3
60	T	64	64	30	22	165	0,32	33,75	90	0,35	9,83	260	3,24	14,7	20,2	19,5	26,6
61	T	64	64	30	22	165	0,32	33,75	125	0,89	13,025	270	2,9	14,8	21,3	19,3	27,1
62	T	64	64	30	22	165	0,32	33,75	125	0,89	13,025	240	1,24	14,1	19,7	17,7	25,3
63	T	64	64	30	22	165	0,32	33,75	125	0,89	13,025	205	1,23	12,2	16,3	15,4	22,9

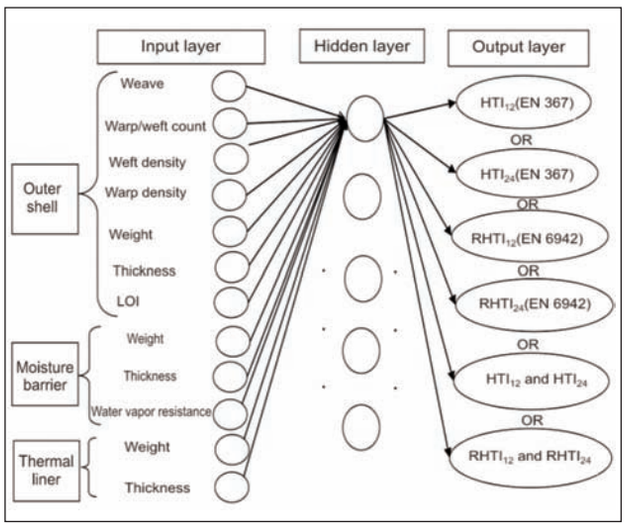

Fig. 3. Block diagram of the networks

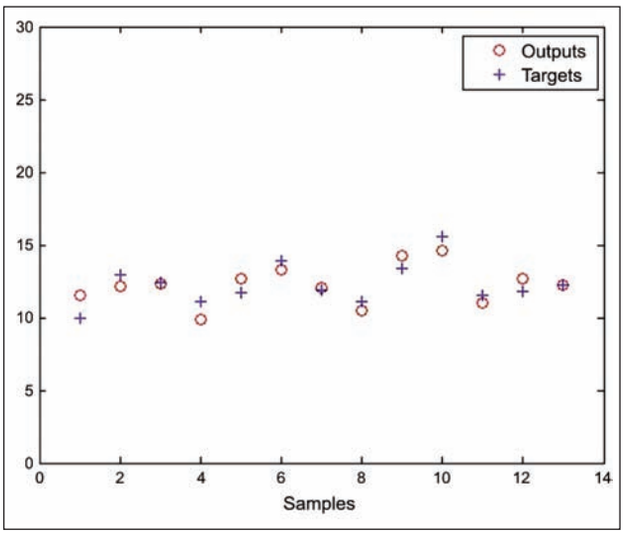

Fig. 4. Comparison between predicted and test sample values for HTI_{12} of EN 367 standard

RESULTS AND DISCUSSION

There are total of 64 data sets, each of which consists of 12 input and 4 outputs. 7 inputs were obtained from the outer shell, 3 inputs from the moisture barrier, and the other 2 from the thermal liner. The outputs are HTI_{12} and HTI_{24} for EN 367 standard and $RHTI_{12}$ and $RHTI_{24}$ for EN ISO 6942 standard.

In this study, all six networks were trained with a different number of hidden layers and neurons in each layer. The best performance was empirically obtained with only one hidden layer having five neurons. Neural networks were trained with Levenberg-Marquardt backpropogation algorithm, which is generally considered the fastest algorithm for providing optimized weight and bias values. Data sets were randomly divided into three sections: 70% for training, 10% for validation, and the remaining 20% to test the networks. To obtain comparable results, all networks were trained and tested with the same data sets.

Network 1 and Network 2, which had only one output, were trained to predict HTI_{12} and HTI_{24} for EN 367 standard, respectively, while Network 3 and 4, which also had only one output, were trained to predict $RHTI_{12}$ and $RHTI_{24}$ for EN ISO 6942 standard. In contrast, Network 5 and 6 were trained to predict two outputs for HTI_{12} and HTI_{24} of EN 367 standard and for $RHTI_{12}$ and $RHTI_{24}$ of EN ISO 6942 standard, respectively. The obtained network output values and the measured target sample values are illustrated in figures 4, 5, 6, 7, 8, and 9, which all show that there are good approximations between network output and corresponding measured target values.

Neural networks were compared with each other by calculating mean absolute percent error (MAPE) between target and predicted values of networks. MAPE is calculated as the average of the unsigned percentage error using the following formula in equation 1. Normally, absolute value of target values,

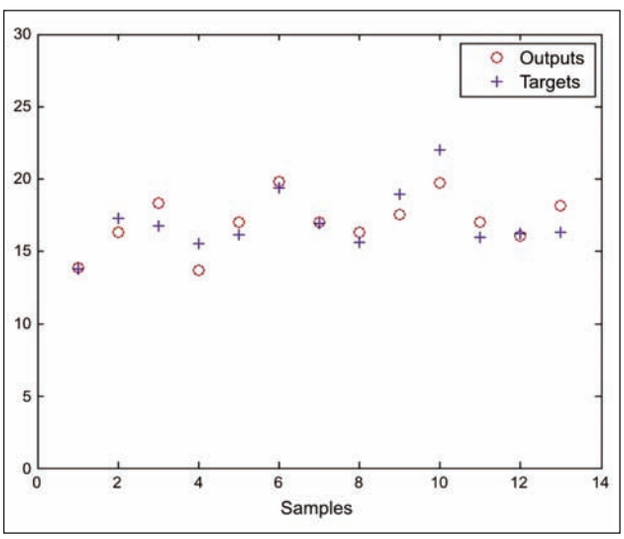

Fig. 5. Comparison between predicted and test sample values for HTI_{24} of EN 367 standard

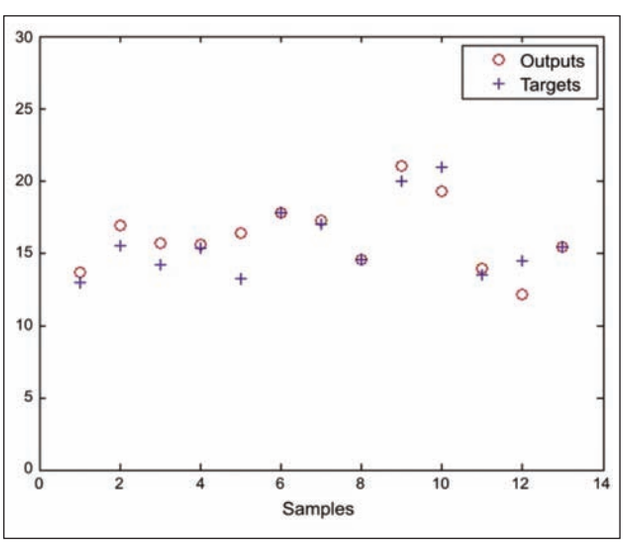

Fig. 6. Comparison between predicted and test sample values for $RHTI_{12}$ of EN ISO 6942 standard

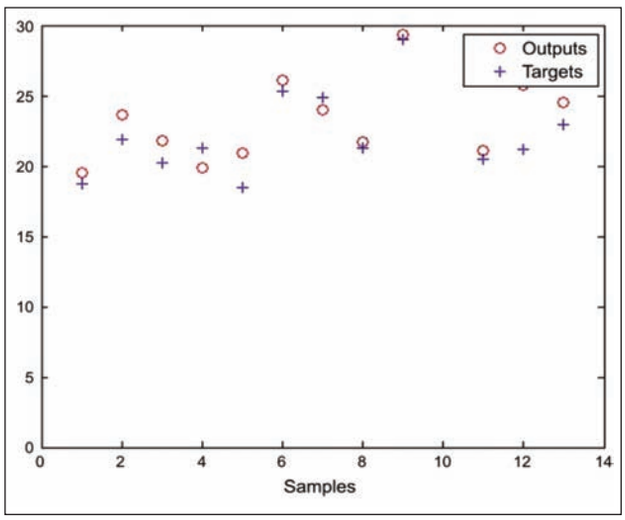

Fig. 7. Comparison between predicted and test sample values for $RHTI_{24}$ of EN ISO 6942 standard

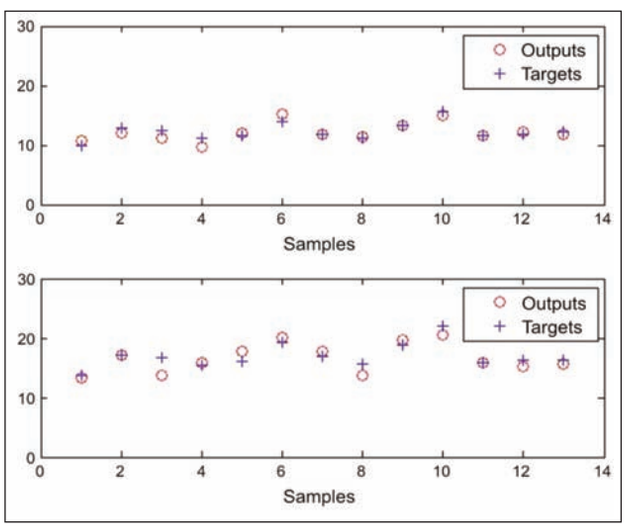

Fig. 8. Comparison between predicted and test sample values for HTI_{12} and HTI_{24} of EN 367standard, respectively

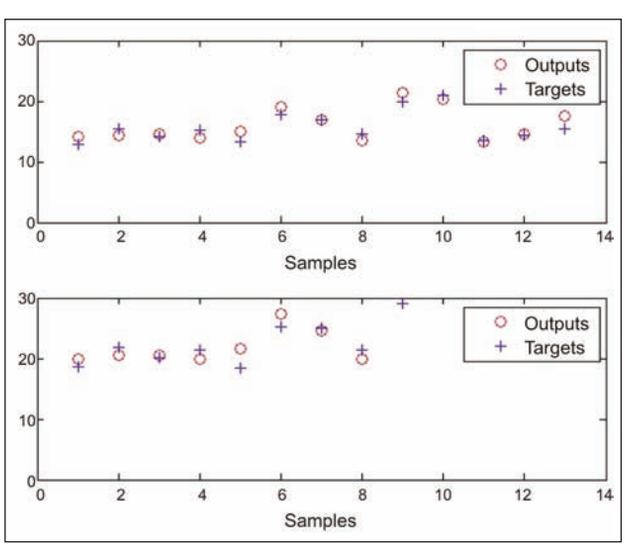

Fig. 9. Comparison between predicted and test sample values for $RHTI_{12}$ and $RHTI_{24}$ of EN ISO 6942 standard, respectively

which is given in the denominator of the equation, is taken. However, the absolute value is not taken here as target value is always positive.

$$MAPE = \frac{|target\ value - predicted\ value|}{target\ value} \times \frac{100\%}{n} \quad (1)$$

where n is total number of samples. Table 2 gives the calculated MAPE values and correlation coefficient of all six networks. Networks 1, 2, 3, and 4 provide single output and Networks 5 and 6 gives two outputs. Therefore, MAPE and correlation coefficient values of last two networks are based on the average of two outputs. From table 2, it is seen that error values of all networks are similar, and the obtained error values varies between 4.95% and 6.87%. However, the networks trained with data obtained in accordance with EN 367 standard provides slightly better error values compared to the networks trained with data obtained in respect to EN ISO 6942 standard. The other outcome of these comparisons is the better result of Network 5 and Network 6 compared to other four networks. The result suggests that prediction of two rather than one output provides less error within the same standard. One possible explanation for this performance improvement would be the reduction of similarities between the output data sets. The consistency of performance of network with two outputs was verified by Networks 5 and 6. In particular, Network 5 gives the best performance among all six networks. The correlation coefficient of target and predicted values gives the strength and direction of the linear relationship. While the correlation coefficients for Network 1 to 4 are similar, Network 5 and Network 6 provide slightly higher values. These results also support lower error values of Network 5 and Network 6.

Table 2

Networks	MAPE	Correlation coefficient	Description
Network 1	5.94%	0.83	HTI_{12} of EN 367 standard
Network 2	5.40%	0.86	HTI_{24} of EN 367 standard
Network 3	6.87%	0.84	$RHTI_{12}$ of EN ISO 6942 standard
Network 4	6.46%	0.88	$RHTI_{24}$ of EN ISO 6942 standard
Network 5	4.95%	0.94	HTI_{12} + HTI_{24} of EN 367 standard
Network 6	6.23%	0.92	$RHTI_{12}$ + $RHTI_{24}$ of EN ISO 6942 standard

CONCLUSIONS

In this study, six different artificial neural networks were studied using MATLAB to predict the convective heat transfer index and radiant heat transfer index of

three-layered fabrics for firefighter protective clothing. Four neural networks; Network 1 to 4 were constructed with 12 inputs data and only one output, corresponding to the index of either convective or radiant heat transfer. Whereas, the Networks 5 and Network 6 were constructed with 12 inputs and two outputs, one for convective heat transfer and one for radiant heat transfer. All networks have one hidden layer with 5 neurons.

The simulation results have shown that all six networks gives similar prediction error values for the corresponding experimentally obtained indexes of convective heat transfer or radiant heat transfer. The results reveal that predicting two rather than one output gave a slight advantage. This performance improvement could possibly the reduction of similarities between two outputs in respect to one output. Moreover, network outputs trained with indexes of convective heat transfer gives less error values independent of number of outputs. The best performance was obtained by Network 5, trained to predict HTI_{12} and HTI_{24} of EN 367 standard.

ACKNOWLEDGEMENTS

This study was funded by Turkish Ministry of Science and Technology SANTEZ (grant number 00782.STZ.2011-1).

BIBLIOGRAPHY

[1] Mandal, S., Song, G., Ackerman, M., Paskaluk, S. and Gholamreza, F. *Characterization of textile fabrics under various thermal exposures*, In: Textile Research Journal, 2013, vol. 83, no. 10, pp. 1005–1019.

[2] Fu, M., Weng, W., Yuan, H. *Effects of multiple air gaps on the thermal performance of firefighter protective clothing under low-level heat exposure*, In: Textile Research Journal, 2013, vol. 84, no. 9, pp. 968–978.

[3] Song, G., Cao, W., Gholamreza, F. *Analyzing stored thermal energy and thermal protective performance of clothing*. In: Textile Research Journal, 2011, vol. 81, no. 11, pp. 1124–1138.

[4] Song, G., Paskaluk, S., Sati, R., Crown, E. M., Dale, J. D., Ackerman, M. *Thermal protective performance of protective clothing used for low radiant heat protection*. In: Textile Research Journal, 2011, vol. 81, no. 3, pp. 311–323.

[5] Kutlu, B. and Cireli, A. *Thermal analysis and performance properties of thermal protective clothing*. In: Fibres & Textiles in Eastern Europe, 2005, vol. 13, no. 3, pp. 58–62.

[6] Sun, G., Yoo, H. S., Zhang, X. S., Pan, N. *Radiant protective and transport properties of fabrics used by wild land fire fighters*, IN: Textile Research Journal, 2000, vol. 70, no. 7, pp. 567–573.

[7] Rossi, R. M., Bolli, W., Staempfli, R. *Performance of firefighters' protective clothing after heat exposure*, In: International Journal of Occupational Safety and Ergonomics (JOSE), 2008, vol. 14, no. 1, pp. 55–60.

[8] Adya, M., Collopy, F. *How effective are neural networks at forecasting and prediction? A review and evaluation*, In: Journal of Forecasting, 1998, vol. 17, pp. 481–495.

[9] Tehran, M. A., Maleki, M. *Artificial neural network prosperities in textile applications*, In: Artificial neural networks – Industrial and Control Engineering Applications, Rijeka, Croatia, InTech, 2011, pp. 35–64.

[10] Gong, R. H., Chen, Y. *Predicting the performance of fabrics in garment manufacturing with artificial neural Networks*, In: Textile Research Journal, 1999, vol. 69, no. 7, pp. 477–482.

[11] Kumar, A. *Neural network based detection of local textile defects*, In: Pattern Recognition, 2003, vol. 36, no. 7, pp. 1645–1659.

[12] Behera, B. K., Mani, M. P. *Characterization and classification of fabric defects using discrete cosine transformation and artificial neural network*, In: Indian Journal of Fibre & Textile Research, 2007, vol. 32, no. 4, pp. 421–426.

[13] Chattopadhyay, R., Guha, A. *Artificial neural networks: Applications to textiles*, In: Textile Progress, 2004, vol. 35, no. 1, pp. 1–46.

[14] Guha, A., Chattopadhyay, R., Jayadeva, *Predicting yarn tenacity: A Comparison of mechanistic, statistical, and neural network models*, In: Journal of the Textile Institute, 2001, vol. 92, no. 2, pp. 139–145.

[15] Fayala, F., Alibi, H., Benltoufa, S., Jemni, A. *Neural Network for predicting thermal conductivity of knit materials*, In: Journal of Engineered Fibers and Fabrics, 2008, vol. 3, no. 4, pp. 53–60.

[16] Matusiak, M. *Application of artificial neural networks to predict the air permeability of woven fabrics*, In: Fıbres & Textıles in Eastern Europe, 2015, vol. 23, no. 1(109), pp. 41–48.

[17] Jhani, Y., Kothari, V. K., Gupta, D. *Development and comparison of artificial neural network and statistical model for prediction of thermo-physiological properties of polyester-cotton plated fabrics*, In: Fashion and Textiles, 2016, vol. 3, no. 19, pp. 1–16.

[18] Bhattacharjee, D., Kothari, V. K. *A neural network system for prediction of thermal resistance of textile fabrics*, In: Textile Research Journal, 2007, vol. 77, no. 1, pp. 4–12.

[19] Cui, Z., Zhang, W. *An adaptive neural network system for prediction of thermal protective performance of fabrics*, In: 3rd International Conference on Intelligent System and Knowledge Engineering, 2008, pp. 837–841.

[20] European Committee for Standardization (CEN). Protective clothing-protection against heat and fire-method of determining heat transmission on exposure to flame (Standard No. EN 367:1992). Brussels, Belgium: CEN; 1992.

[21] Scott, R. A. *Textiles for Protection*, 1st edition. Cambridge, Woodhead Publishing Limited, 2005.

[22] International Organization for Standardization (ISO). Protective clothing-protection against heat and fire-method of test: evaluation of materials and material assemblies when exposed to a source of radiant heat (Standard No. ISO 6942:2002). Geneva, Switzerland: ISO; 2002.

[23] Haykin, S., *Neural network: A Comprehensive foundation*, Second ed. (prentice hall, New Jersey, USA, 1999.

Authors:

MÜGE DURSUN[1], YAVUZ ŞENOL[2], ENDER YAZGAN BULGUN[3], TANER AKKAN[4]

[1]Dokuz Eylul University, Faculty of Engineering, Department of Textile Engineering, Tınaztepe Campus, 35390, Buca, Izmir, Turkey

[2]Dokuz Eylul University, Department of Electrical and Electronics Engineering, Tınaztepe Campus, 35390, Buca, Izmir, Turkey,

[3]Izmir University of Economics, Faculty of Fine Arts and Design, Department of Fashion and Textile Design, 35330, Balçova, Izmir, Turkey,

[4]Dokuz Eylul University, Izmir Vocational School, Department of Mechatronics, 35380, Buca, Izmir, Turkey,

e-mail: muge5678@gmail.com; yavuz.senol@deu.edu.tr; ender.bulgun@ieu.edu.tr; taner.akkan@deu.edu.tr

Corresponding author:

YAVUZ ŞENOL
e-mail: yavuz.senol@deu.edu.tr

Bending strength of intra-ply/inter-ply hybrid thermoplastic composites

GAYE YOLACAN KAYA

REZUMAT – ABSTRACT

Rezistența la încovoiere a compozitelor termoplastice hibride intra-strat/inter-strat

Proprietățile de încovoiere ale compozitelor termoplastice hibride din fibră de carbon/E-glass/polipropilenă (PP) intra/inter-laminare au fost determinate și comparate cu cele ale compozitelor termoplastice nehibride din carbon/PP și E-glass/PP. Compozitele hibride și nehibride au fost fabricate utilizând prepreguri termoplastice țesute uni-direcționale din carbon/ PP, E-glass/PP și carbon/E-glass/PP. Fracțiile de fibre au afectat în mod semnificativ densitatea, rezistența la încovoiere, modulul de elasticitate și îndoirea-deformarea compozitelor hibride termoplastice. Rezistența la încovoiere și modulul compozitelor hibride termoplastice hibride au fost mai mari comparativ cu compozitele termoplastice nehibride. S-a observat că hibridizarea intra-laminară a provocat o deteriorare mai gravă după sarcina de încovoiere atât pe suprafață, cât și pe secțiunea transversală decât hibridizarea inter și intra/inter-laminară. Distribuția uniformă a fibrelor de carbon și E-glass în cadrul și între straturile compozitelor prin utilizarea hibridizării intra-laminare/inter-laminare a rezultat într-un modul de elasticitate mai mare, de până la 65,1% în comparație cu compozitele nehibride.

Cuvinte-cheie: compozite termoplastice, prereg unidirecțional, compozite hibride, rezistența la încovoiere, hibridizare

Bending strength of intra-ply/inter-ply hybrid thermoplastic composites

Bending properties of intra-ply, inter-ply and intra-ply/inter-ply Carbon/Electrical Glass (E-Glass)/polypropylene (PP) hybrid thermoplastic composites were determined and compared with those of non-hybrid Carbon/PP and E-Glass/PP thermoplastic composites. The hybrid and non-hybrid composites were manufactured by using the uni-directional woven carbon/PP, E-glass/PP and carbon/E-glass/PP thermoplastic prepregs. The fiber fractions significantly affected the density, bending-strength, bending-modulus and bending-deflection of hybrid thermoplastic composites. The bending-strength and modulus of the hybrid thermoplastic composites were higher compared to non-hybrid thermoplastic composites. It is observed that the intra-ply hybridization caused a more catastrophic failure after bending load on both surface and cross-section than the inter-ply and intra-ply/inter-ply hybridization. The uniform distribution of Carbon and E-Glass fibers within and between the layers of composites by using intra-ply/inter-ply hybridization resulted as the higher bending modulus up to 65.1% compared to non-hybrid composites.

Keywords: thermoplastic composites, unidirectional prepreg, hybrid composites, bending strength, intra-ply hybridization

INTRODUCTION

Textile structural composites are widely used in various industries due to their high specific strengths, good fatigue and corrosion resistance [1]. Today, thermoplastic polymer based composites have a growing interest due to their easy forming and remolding ability in shorter process-times [2, 3]. Thermoplastic polymers differ from their thermoset counterpart primarily by their melt temperature being lower than their decomposition temperature, while thermoset polymers have melting temperatures higher than their decomposition temperature, meaning that they cannot be reshaped upon melting [4]. However, thermoplastic resins are about 500 to 1000 times more viscous than thermoset resins which restrict the infusion tendency of resins into fibers. A high-pressure requirement in the processing of thermoplastic composites is also considered as another restriction. Semi-crystalline thermoplastic polymers such as PEEK (polyether ether ketone), PPS (polyphenylene sulfide) and LCP (liquid-crystal polymers) are mainly used in aviation due to their mechanical and chemical resistance at relatively high temperatures. Some other thermoplastic polymers such as PP (polypropylene), ABS (acrylonitrile butadiene styrene) and PA (polyamide) find use in the automotive industry. PP is commonly used in the thermoplastic composite production due to its low-cost, high specific strength and re-usability [5–7].

Complex-material requirements in high-technical applications have led to increased use of hybrid materials since the non-hybrid materials do not have adequate performance [8]. Hybridization process can increase the mechanical properties of fiber reinforced composites and reduced its limitations [9]. By using proper material design, it is possible to achieve a balance between cost and performance. Types, orientation and arrangements of fibers mainly determine the properties of hybrid composites [8]. Hybrid composites can be classified as inter-ply and intra-ply. The inter-ply hybrid composite consists of different types of fiber plies bonded together in a matrix while in intra-ply hybrid composite, each ply consists of two or more types of fibers [10]. Thermoplastic prepregs are

one of the most preferred materials in hybrid composite production. They can be stored at room temperature without any time restriction and converted to composites by using appropriate temperature and pressure [11–13]. Hybrid fabrics can be produced in the form of woven, knitted or braided fabric using commingled or wrapped yarns. In either commingled or wrapped yarns, the thermoplastic fibers are melted during the curing process and spread through reinforcing fibers by wetting to form polymeric matrix on solidification/cooling. Some process degradations such as filament breakages may occur in glass and carbon fibers of hybrid yarns which reduces the final composite performance [14]. Hybrid composite performance is dependent on the homogeneity of polymer fibers in yarn [15–19]. Co-weaving is another way to produce hybrid composites and described as weaving at least two different fibers together. Co-weaving can offer a wide variety of fiber material selections for designers and significant improvements in the cost-effectiveness of fabrication [20]. The most critical point in hybrid weaving is to have a uniform fiber distribution and using compatible fibers [21, 22].

Some detailed studies were performed by researchers about the mechanical and impact properties of hybrid composites. It was stated that the hybridization can be used to improve the flexural strength through appropriate fiber selection, geometry and placement [23, 24]. Sorrentino et al. investigated the flexural and impact properties of hybrid thermoplastic composites based on polypropylene and glass fiber woven fabrics by using neat and modified PP films with coupling agent. It was stated that the capability to transfer loads from the matrix to the fibers increased by using coupling agent which improved the flexural modulus and flexural strength [25]. Xu et al. studied the bending behavior of unidirectional glass/PEEK composites manufactured by using wrapped yarns. Bending performances of the composites enhanced by the increase in molding temperature and molding time which also reduced the delamination based failures [26]. Process parameters have also effects on hybrid composite performance. Mechanical properties of hybrid composites molded directly at the process temperature without any preheating are lower than those of preheated molded composites [27]. Shekar et al. investigated the mechanical and thermal properties of glass/PEEK co-woven composites. It was stated that the uniformity in the distribution of resin between various layers of laminate during hybridization plays a major role and have a dominant impact on the mechanical properties of composites especially for aerospace applications [27]. Pandya et al. investigated inter-ply hybrid of E-glass/carbon/epoxy composites. The tensile strengths of the composites where the glass fabric is on the outer layer and the carbon fabric is on the inner layer are higher than those of the composites in which carbon fabric is on the outer layer and the glass fabric is on the inner layer [10]. Zhang et al. produced glass/carbon/epoxy inter-ply hybrid composites. It was stated that when the carbon fabric is on the outer layer and the ratio of the carbon fabric of the hybrid composite is 50%, the structures exhibit high bending strength. On the contrary, the hybrid composites in which the glass fabric is on the outer layer have higher compression strength [28]. The strain in individual fibers also affects the hybrid composite strength and using fibers which have compatible strains resulted as a high strength of hybrid composite [29]. The gain of percentage elongation for hybrid composite is significantly higher than the percentage loss in tensile strength [10]. In addition, hybrid composites have more delamination tendencies, especially between different fiber layers of inter-ply hybrid composites [30].

In most studies of the literature, commercially available fabrics and prepregs were used to manufacture hybrid composites and the thermoplastic fibers are used for toughness purpose in thermoset-based composites. The novelty of this work is investigating mechanical properties of both intra-ply/inter-ply hybrid thermoplastic composites which are produced by using unidirectional (UD) woven thermoplastic prepregs. These prepregs are woven at our laboratory. In the UD woven thermoplastic prepregs, both carbon and E-glass fibers are used as weft while polypropylene fibers are used as warp yarns. Using reinforcement and matrix fibers at warp and weft directions of the prepregs makes it possible to achieve the desired hybridization to withstand the exposed load and provides design flexibility to the composite end-users. This study aims to compare the bending properties of carbon/E-glass/PP intra-ply/inter-ply hybrid thermoplastic composites with non-hybrid carbon/PP and E-glass/PP thermoplastic composites. Bending behavior was studied as considering the bending strength, bending modulus, bending strain and their normalized forms based on both the measured density and fiber volume fraction as specific bending strength, specific bending modulus and specific bending strain. The failures of composites after the bending load were evaluated with optical microscope and SEM (Scanning Electron Microscope) views.

EXPERIMENTAL PART

UD woven thermoplastic prepregs and hybrid thermoplastic composites

Three types of UD thermoplastic prepregs were woven in a manual weaving loom: carbon/PP (PP/C), E-glass/PP (PP/G) and carbon/E-glass/PP (PP/H). BCF (Bulk Continuous Filament) PP fibers (made by Eruslu Textile, Turkey) were used as warp (0°) while carbon fiber (Aksa, Turkey) and E-glass fiber (Cam Elyaf A.S., Turkey) were used as weft (90°). These developed prepregs are defined as the UD woven thermoplastic prepregs since the warp fiber of PP melts at temperature (205 °C) during consolidation process and acts as a matrix. Specifications of the fibers according to producer companies are given in table 1.

PP/C, PP/G and PP/H UD woven thermoplastic prepregs were in a plain weave pattern due to

Table 1

SPECIFICATIONS OF THE FIBRES USED IN HYBRID WOVEN THERMOPLASTIC PREPREGS							
Fibre type	**Measured fibre diameter (μm)**	**Fiber density (g/cm^3)**	**Tensile strength (MPa)**	**Tensile modulus (GPa)**	**Elongation (%)**	**Melting point (°C)**	**Linear density of yarn**
Carbon	6.17	1.78	4200	240	1.8	>1200	3K*
E-Glass	18.34	2.57	2306	81.5	2.97	840	410 tex
Polypropylene	-	0.90	35	14	30	175	150 tex

* K = 1000 filament in TOW.

Table 2

SPECIFICATIONS OF HYBRID WOVEN THERMOPLASTIC PREPREGS										
Prepreg type	**Weave type**	**Yarn sets**		**Density (per cm)**		**Weight (g/m^2)**	**Crimp (%)**		**Thickness (mm)**	**Cover factor (%)**
		Warp	**Weft**	**Warp**	**Weft**		**Warp**	**Weft**		
PP/C	Plain	PP	6 Carbon	4	4.5	794	5.0	2.0	1.35 ± 0.02	99.72
PP/G	Plain	PP	6 E-Glass	4	5.5	1278	16.2	1.0	1.54 ± 0.02	98.30
PP/H	Plain	PP	6 E-Glass/ 3 Carbon	4	5.5	1027	8.8	1.0/2.0	1.46 ± 0.02	97.17

Table 3

DESCRIPTIONS OF THE DEVELOPED HYBRID THERMOPLASTIC COMPOSITES				
Label	**Hybridization**	**Layers**	**Orientation**	**Order of layers***
PP/CC	non-hybrid	4 layers	$[90°/0°]_2$	1: 90° (PP/C), 2: 0° (PP/C), 3: 90° (PP/C), 4: 0° (PP/C)
PP/GC	non-hybrid	4 layers	$[90°/0°]_2$	1: 90° (PP/G), 2: 0° (PP/G), 3: 90° (PP/G), 4: 0° (PP/G)
PP/HC	intra-ply	4 layers	$[90°/0°]_2$	1: 90° (PP/H), 2: 0° (PP/H), 3: 90° (PP/H), 4: 0° (PP/H)
PP/IL1	intra-ply/inter-ply	4 layers	$[90°/0°]_2$	1: 90° (PP/C), 2: 0° (PP/H), 3: 90° (PP/C), 4: 0° (PP/H)
PP/IL2	intra-ply/inter-ply	4 layers	$[90°/0°]_2$	1: 90° (PP/G), 2: 0° (PP/H), 3: 90° (PP/G), 4: 0° (PP/H)
PP/IL3	inter-ply	4 layers	$[90°/0°]_2$	1: 90° (PP/C), 2: 0° (PP/G), 3: 90° (PP/C), 4: 0° (PP/G)

* 1: top layer, 4: bottom layer.

achieve a uniform distribution of polypropylene fibers among the carbon/E-glass fibers with more interlacement. Specifications of PP/C, PP/G and PP/H UD woven thermoplastic prepregs are given in table 2. The thickness of UD woven thermoplastic prepregs was measured using portable thickness gauge (SDL Atlas, J200) according to ISO 5084 standard [31]. Crimp and weights of prepregs were measured according to ISO 7211-3 and ISO 6348 test standards, respectively [32, 33].

As seen in table 2, weights of PP/C, PP/G and PP/H were 794, 1278 and 1027 g/m^2, respectively. Weft crimps of UD woven thermoplastic prepregs were quite lower than the warp crimps since the stiffer structure of carbon and E-glass fibers compare to bulky PP fibers. UD woven thermoplastic prepregs had the similar thicknesses. By using these PP/C, PP/G and PP/H UD woven thermoplastic prepregs, various non-hybrid, inter-ply hybrid, intra-ply hybrid and intra-ply/inter-ply hybrid composites (six types) were developed as described in table 3.

Hot-press (Wermac®-H501, Turkey) was used to consolidate the layered prepregs. Teflon films were used on both top and bottom to prevent any sticking of composites with hot plates of press during consolidation. Prepregs were placed on hot-press at 50°C. Then, the temperature was reached to 205°C in 20 minutes. The process was continued for 40 minutes at this temperature and then cooled down to room temperature. The pressure was fixed to 5.5 bars during all the process. Figure 1 shows the microscopic views of thermoplastic prepregs (figure 1, *a*) and composites (figure 1, *b*). Density measurements of composites were conducted by ASTM D792-13 [34]. Density measurement was performed by using a density meter (Precisa®, XP205) in which the weight of specimen was measured in air at first and then in distilled water at a room temperature. The composite fiber fraction was determined by ASTM D3171-15 [35]. The weight-based fiber fractions of carbon, E-glass and PP were separately determined and the total fiber fractions were calculated as both weight and volume based.

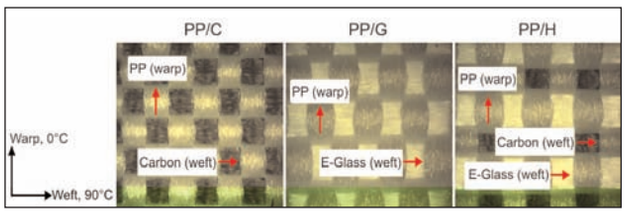

a

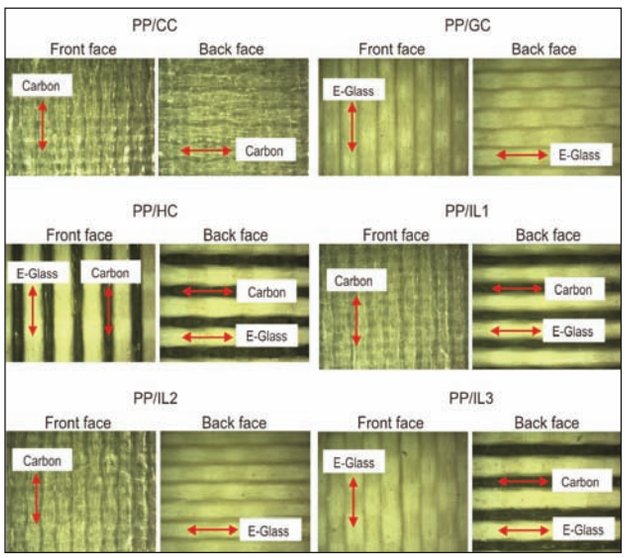

b

Fig. 1. Microscopic views of thermoplastic prepregs (a) and composites (b)

Bending strength test

Bending strengths of hybrid thermoplastic composites were determined according to ASTM D790 by using 3-point bending test method [36]. Schematic view (figure 2, *a*) and photos (figure 2, *b*) of 3-point bending test are shown in figure 2. The bending strength tests of the hybrid thermoplastic composites were performed on a Hounsfield H5KS (UK) tester. Test speed was 1.3 mm/min. The support span length to thickness ratio (L/d) was used as 16/1. The bending load was applied on normal to top-layer of hybrid thermoplastic composites. The dimension of the test specimen was 25 mm × 80 mm. Support span length was 50 mm. Bending strength test was performed on four specimens for each type of samples. The bending strength (1), modulus (2) and strain (3) of hybrid thermoplastic composites were calculated according to the formulations of ASTM D790-90 which are given below:

$$S = 3PL/2bd^2 \quad (1)$$

$$E = L^3m/4bd^3 \quad (2)$$

$$\varepsilon = (l_1 - l_0)/l_0 = \Delta l/l_0 \quad (3)$$

where: S is the stress in the outer fibers at mid-span (N/m^2), P – the load at a given point on the load-deflection curve (N), L – the support span (m), b – the width of beam tested (m), d – the depth of beam tested (m), E – the modulus of elasticity in bending (N/m^2), m – the slope of the tangent to the initial straight-line portion of the load-deflection curve (N/m)

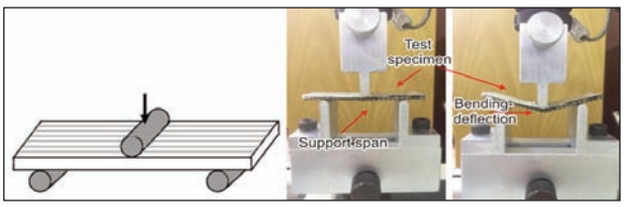

a *b*

Fig. 2. Schematic view (a) and photos (b) of 3-point bending test

of deflection, ε – the bending deflection (%), Δl – the elongation (m) and l_0 – the initial length (m).
The specific-bending strength (4), modulus (5) and deflection (6) were also calculated to evaluate the test results in normalized form based on both the measured density [37] and fiber volume fraction (V_f).

$$S_{spec} = S/\rho, \quad S_{spec} = S/V_f \quad (4)$$

$$E_{spec} = E/\rho, \quad E_{spec} = E/V_f \quad (5)$$

$$\varepsilon_{spec} = \varepsilon/\rho, \quad \varepsilon_{spec} = \varepsilon/V_f \quad (6)$$

where: ρ is the measured-density of hybrid composites (gcm^{-3}), V_f – the fiber volume fraction, S_{spec} – the specific-bending strength, E_{spec} – the specific-bending modulus and ε_{spec} – the specific-bending deflection. Moreover, the surface and cross-sectional failures of thermoplastic hybrid composites after the bending strength test were examined by using an optical microscope (BAB Bs200Doc, Turkey) and SEM (ZEISS EVO® LS10).

RESULTS AND DISCUSSION

Density and fiber fraction test results

Table 4 shows the density and fiber fraction results of the hybrid thermoplastic composites. The thickness values of hybrid thermoplastic composites were varied from 2.65 to 3.26 mm depending on the used prepreg types. Because of the higher fiber density of E-glass compare to carbon, PP/GC had the highest composite density as 1.87 g/cm^3 and followed by the PP/IL2, PP/HC and PP/IL3 hybrid composites depending on the fiber fractions. The lowest composite density was obtained from PP/CC since the lower density of carbon fiber compare to that of E-glass fiber. The densities of hybrid thermoplastic composites were affected by the used fiber ratios. The composite density increased by the increase in E-glass fiber ratio. Generally, the weight-based total fiber fractions were quite high in all types of hybrid composites. The volume-based total fiber fractions were varied depending on the ratios of Carbon and E-glass fibers used. PP/GC had the highest weight-based and volume-based total fiber fractions because of the higher yarn linear density and fiber density E-glass. Fiber fractions can be varied by the constructional arrangements of weaving as using different warp and weft densities, weaving patterns and yarn linear densities. Thus, it is possible to weave prepregs related

Table 4

THE DENSITY AND FIBER FRACTION RESULTS OF THE HYBRID THERMOPLASTIC COMPOSITES							
Label	Thickness (mm)	Density (gcm^{-3})	Fiber fraction (%)				
			Weight-based				Volume-based (V_f)
			Carbon	E-Glass	PP	Total	
PP/CC	3.11 ± 0.02	1.32 ± 0.02	84.40	-	15.60	84.40	62.59
PP/GC	3.26 ± 0.09	1.87 ± 0.02	-	89.94	10.06	89.94	65.44
PP/HC	3.15 ± 0.03	1.62 ± 0.04	17.72	69.38	12.90	87.10	52.92
PP/IL1	2.65 ± 0.04	1.50 ± 0.07	46.79	39.14	14.07	85.93	53.86
PP/IL2	2.98 ± 0.03	1.70 ± 0.01	7.90	80.78	11.32	88.68	46.34
PP/IL3	3.16 ± 0.06	1.61 ± 0.02	32.34	55.48	12.18	87.82	61.81

to load to be exposed and end-use areas of composites which provide design flexibility.

Bending strength test results

The bending strength test results of hybrid thermoplastic composites are presented in table 5 and table 6. Figure 3 shows the load-deflection (figure 3, *a*) and strength-deflection (figure 3, *b*) curves of hybrid thermoplastic composites. As seen in figure 2, the load-deflection curves of all hybrid and non-hybrid composites executed ductile-material behavior as expected due to PP used as matrix. The carbon fibers are used for their high strength in hybridization. The glass fibers have higher strain-to-failure in tension than that of carbon fibers which provides higher strength to hybrid composites. PP/CC composites are generally stiffer than PP/GC and PP/HC composites because of the brittle behavior of carbon fibers. PP/HC intra-ply hybrid composites are more flexible compared to non-hybrid composites since the contribution of higher strain of glass fibers. In addition, intra-ply/inter-ply hybrid PP/IL1 composites behaved as a stiff material according to the load-deflection curves in which they showed a sharp decrease of breaking-point. The breaking loads of hybrid and non-hybrid composites were varied between from 62.50 to 88.87 N. Intra-ply hybrid PP/HC composite showed the highest breaking load since the uniform distribution of carbon and E-glass fibers within the composite layers. Figures 3, 4 and 5 show the bending strength/specific-bending strength, the bending-modulus/specific-bending modulus and the bending-deflection/specific-bending deflection results of hybrid thermoplastic composites, respectively.

Table 5

THE BENDING STRENGTH TEST RESULTS OF THE HYBRID THERMOPLASTIC COMPOSITES			
Label	Strength (MPa)	Modulus (GPa)	Deflection (%)
PP/CC	19.76 ± 0.28	2.95 ± 0.22	75.90 ± 6.94
PP/GC	20.59 ± 0.95	1.30 ± 0.36	134.63 ± 6.40
PP/HC	21.08 ± 1.41	2.34 ± 0.19	85.25 ± 4.61
PP/IL1	24.51 ± 2.64	3.73 ± 1.16	56.00 ± 1.59
PP/IL2	21.85 ± 1.63	3.66 ± 0.16	41.51 ± 6.35
PP/IL3	19.87 ± 2.62	1.93 ± 0.52	99.18 ± 8.68

Bending strength

As presented in tables 5 and 6 and figures 4, the bending strengths of hybrid thermoplastic composites were varied from 19.76 to 24.51 MPa while the specific-bending strengths of hybrid thermoplastic composites were varied from 11.01 to 16.34 MPa/gcm^{-3} and from 0.32 to 0.47 MPa/V_f. PP/IL1 intra-ply/inter-ply hybrid thermoplastic composite showed the highest bending-strength and followed by PP/IL2 which was also an intra-ply/inter-ply hybrid composite. PP/CC had the lowest bending-strength while the specific-bending-strength of PP/CC was higher than those of PP/HC, PP/IL2, PP/IL3 and PP/GC composites. The structure and properties of the fiber-matrix interface is crucial to the mechanical behavior of composite materials [38]. The low bending properties of PP/CC composites may be attributed to weak

Table 6

THE SPECIFIC BENDING STRENGTH TEST RESULTS OF THE HYBRID THERMOPLASTIC COMPOSITES						
Label	Specific strength		Specific modulus		Specific deflection	
	(MPa/gcm^{-3})	(MPa/V_f)	(GPa/gcm^{-3})	(GPa/V_f)	($\%/gcm^{-3}$)	($\%/V_f$)
PP/CC	14.97	0.32	2.23	0.05	57.50	1.21
PP/GC	11.01	0.31	0.70	0.02	71.99	2.06
PP/HC	13.01	0.46	1.44	0.04	52.62	1.61
PP/IL1	16.34	0.39	2.48	0.07	37.33	1.04
PP/IL2	12.62	0.47	2.15	0.08	24.41	0.90
PP/IL3	12.26	0.32	1.19	0.03	61.22	1.60

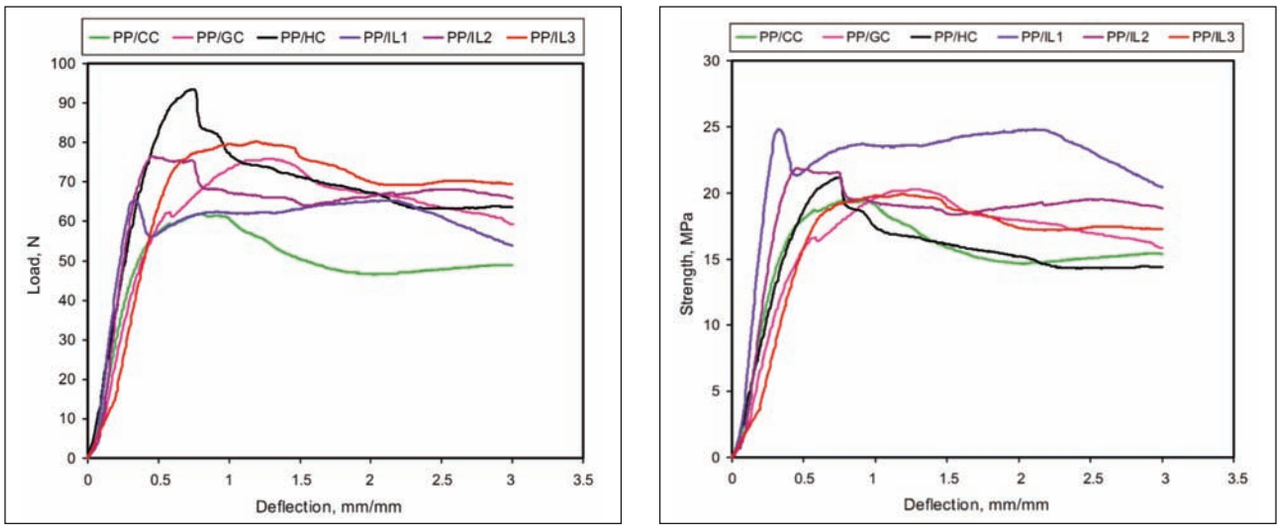

a *b*

Fig. 3. Load-deflection (a) and strength-deflection (b) curves of composites

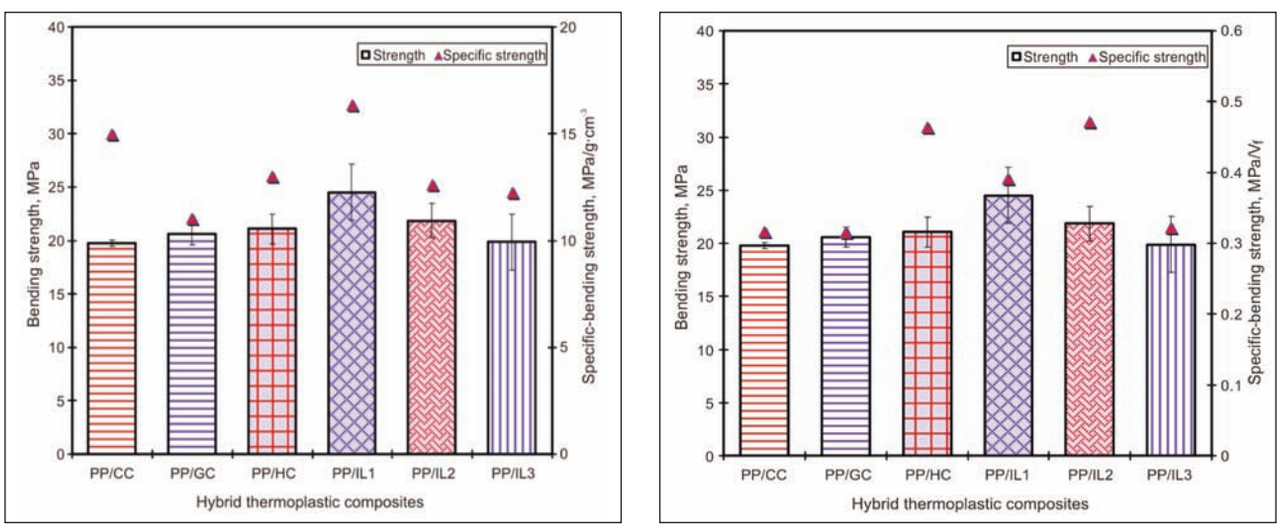

a *b*

Fig. 4. The bending-strength and specific-bending strength of hybrid thermoplastic composites, density based specific-bending-strength (a), volume fraction based specific-bending-strength (b)

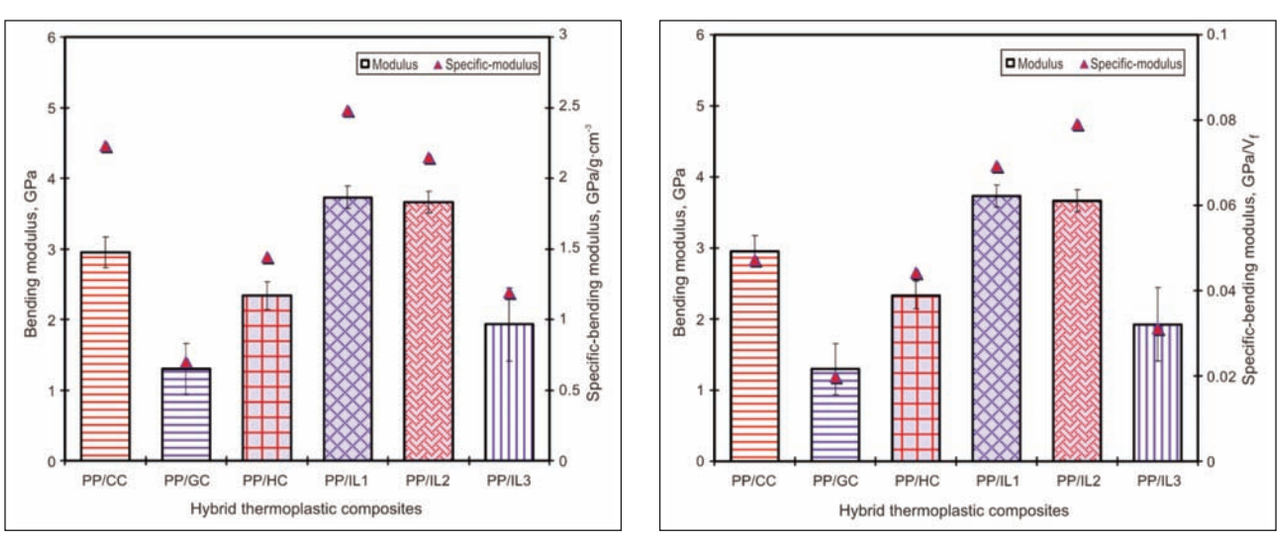

a *b*

Fig. 5. The bending-modulus and specific-bending modulus of hybrid thermoplastic composites, density based specific-bending-modulus (a), volume fraction based specific-bending-modulus (b)

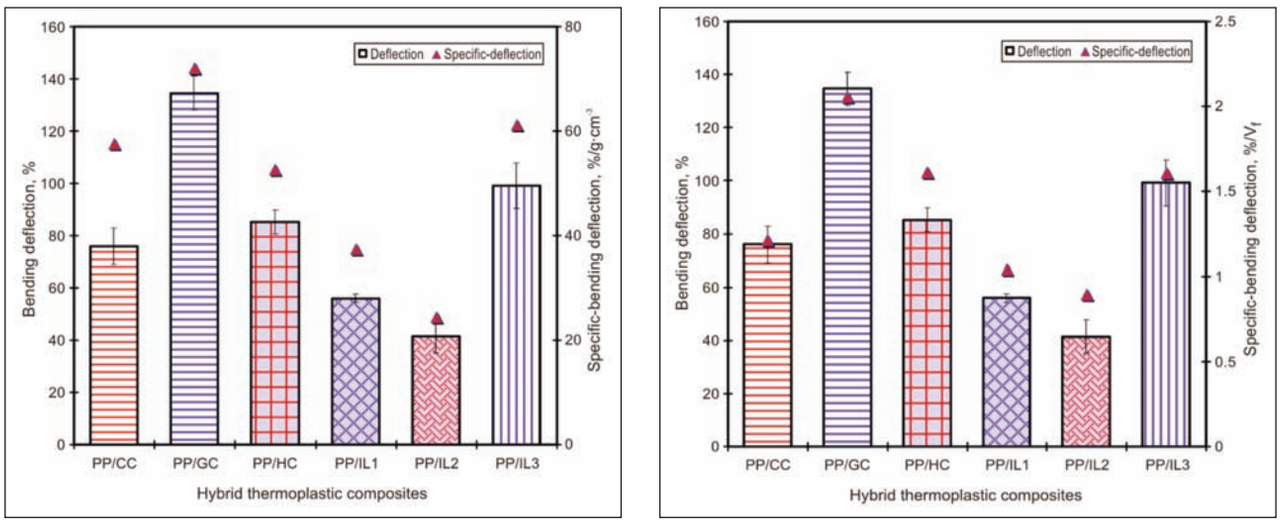

Fig. 6. The bending-deflection and specific-bending deflection of hybrid thermoplastic composites, density based specific-bending-deflection (a), volume fraction based specific-bending-deflection (b)

interface properties of carbon/PP during consolidation process. PP/IL1 and PP/IL2 showed the higher density based and volume fraction based specific-bending-strengths. By using intra-ply/inter-ply hybridization (PP/IL1) increased the bending strength as 19.4% and 17.2% compared to non-hybrid PP/CC and PP/GC composites, respectively. It could be caused by the constraint from the intra-ply and inter-ply E-glass fibers that prevent carbon fiber breakages and formed a considerable hybridization effect due to the delay in failure of the carbon fibers [39]. The uniform distribution of carbon and E-glass fibers within and between the layers the composite structure was also increased the bending strength of composites. However, using different types of reinforcement fibers as carbon and E-glass as layered forms caused an inter-layer delamination under bending load. It was found that the using intra-ply/inter-ply hybridization was a more effective method to obtain higher bending strengths than inter-ply or intra-ply hybridization. The bending-strength of hybrid thermoplastic composites was significantly affected by the intra-ply, inter-ply or intra-ply/inter-ply hybridization. In addition, bending strength is mainly dependent on the fiber-content and fiber-properties of the composites which confirms the synergic effect of hybridization.

Bending modulus

As presented in tables 5 and 6 and figure 5, the bending-modulus of hybrid thermoplastic prepregs was varied from 1.30 to 3.73 GPa while the specific-bending modulus of hybrid thermoplastic composites was varied from 0.70 to 2.48 GPa/gcm^{-3} and from 0.02 to 0.08 GPa/V_f. The bending-modulus of hybrid thermoplastic composites was generally compatible with their specific-bending modulus. The bending-modulus and specific bending-modulus values of PP/IL1 and PP/IL2 were similar and higher than those of PP/CC, PP/HC, PP/IL3 and PP/GC composites. The fiber fractions affected the bending-modulus of composites. It could be concluded that the bending-modulus of hybrid composites generally increased by the increase in carbon fiber fraction because of the higher fiber modulus of carbon compare to E-glass. However, non-hybrid PP/CC showed low bending modulus because of the weak interface properties of carbon/PP during consolidation process.

The carbon fibers are used for their high strength in hybridization. The glass fibers have higher strain-to-failure in tension than that of carbon fibers which provides higher strength to hybrid composites. The intra-ply, inter-ply and intra-ply/inter-ply hybridizations increased the bending modulus of composites by combining the unique specific modulus of carbon and strain of E-glass fibers. The uniform distribution of carbon and E-glass fibers within and between the layers of composites by using intra-ply/inter-ply hybridization resulted in the higher bending modulus. Since the carbon and E-glass fibers have different interface properties with PP during consolidation process in which the interface properties of glass/PP are stronger than that of carbon/PP, it was also important to obtain a balanced Carbon/E-Glass fiber ratio in intra-ply/inter-ply hybridization [38]. PP/IL1 exhibited this balance and thus it had the highest bending-modulus and specific-bending-modulus. PP/IL1 and PP/IL2 showed the higher and density based and volume fraction based specific-bending-modulus. By using both intra-ply/inter-ply hybridization (PP/IL1) increased the bending-modulus as 20.9% and 65.1% compared to non-hybrid PP/CC and PP/GC composites, respectively. The specific-bending modulus of PP/IL1 was higher 10.1% and 71.7% than those of non-hybrid PP/CC and PP/GC composites, respectively. The bending-modulus of hybrid thermoplastic composites was significantly improved by the intra-ply, inter-ply or intra-ply/inter-ply hybridization.

Bending deflection

As presented in tables 5 and 6 and figure 6, the bending-deflections of hybrid thermoplastic prepregs were varied from 41.51% to 134.63% while the specific-bending deflections of hybrid thermoplastic composites were varied from 24.41 to 71.99 %/gcm^{-3} and from 0.90 and 2.06 %/V_f. Generally, non-hybrid and hybrid thermoplastic composites exhibited a quite ductile behavior which means these composite structures absorb energy elastically. PP/CC composites are generally stiffer than PP/GC and PP/HC composites because of the brittle behavior of carbon fibers. PP/HC intra-ply hybrid composites are more flexible compared to non-hybrid composites since the contribution of higher strain of glass fibers. The non-hybrid PP/GC composite showed almost 2-times higher bending deflection compare to non-hybrid PP/CC composite due to the high fiber strain of E-glass. Intra-ply/inter-ply hybrid PP/IL1 and PP/IL2 composites which had the highest bending-modulus showed the lowest bending-deflection/specific-bending-deflection as expected. It can be concluded that the ductility of hybrid thermoplastic composites decreased by the increase in carbon fiber ratio of the composite. The bending-deflection of hybrid thermoplastic composites was significantly decreased by the intra-ply, inter-ply or intra-ply/inter-ply hybridization.

Failure of hybrid thermoplastic composites

Figure 7 shows the surface and cross-sectional microscopic failure analyses of hybrid thermoplastic composites. As seen in figure 7, non-hybrid and hybrid thermoplastic composites generally showed a layer delamination and fiber breakages on their cross-section and fiber undulations on their front faces. The flexure load caused a compression based failure on the top surface and a tension based failure at the bottom surface [40]. The non-hybrid PP/CC composite had an intensive fiber undulation on its front face. This was due to the weak fiber/matrix interface properties of carbon and PP [41]. Fiber breakages, matrix cracks and some local delamination were observed on cross-sectional views. There was an insignificant failure on the back face of PP/CC. A similar tendency of failure was observed for non-hybrid PP/GC composite. However, the fiber undulations on the front face were fewer than that of PP/CC. It could be concluded that the fiber/matrix interface of E-glass/PP was stronger than that of carbon/PP. The intra-ply hybrid PP/HC composite showed an intense fiber undulation on its front face. Moreover, some of the fiber-matrix delaminations were observed on the back face after bending load. This was due to different adhesion properties of carbon/PP and E-glass/PP fibers during consolidation process which caused by the different surface and heat-transfer properties of carbon and E-glass fibers. A wide layer delamination was also observed on the cross-section of PP/HC besides the fiber breakage. The intra-ply hybrid PP/HC exhibited a more catastrophic failure than non-hybrid PP/CC and PP/GC composites on

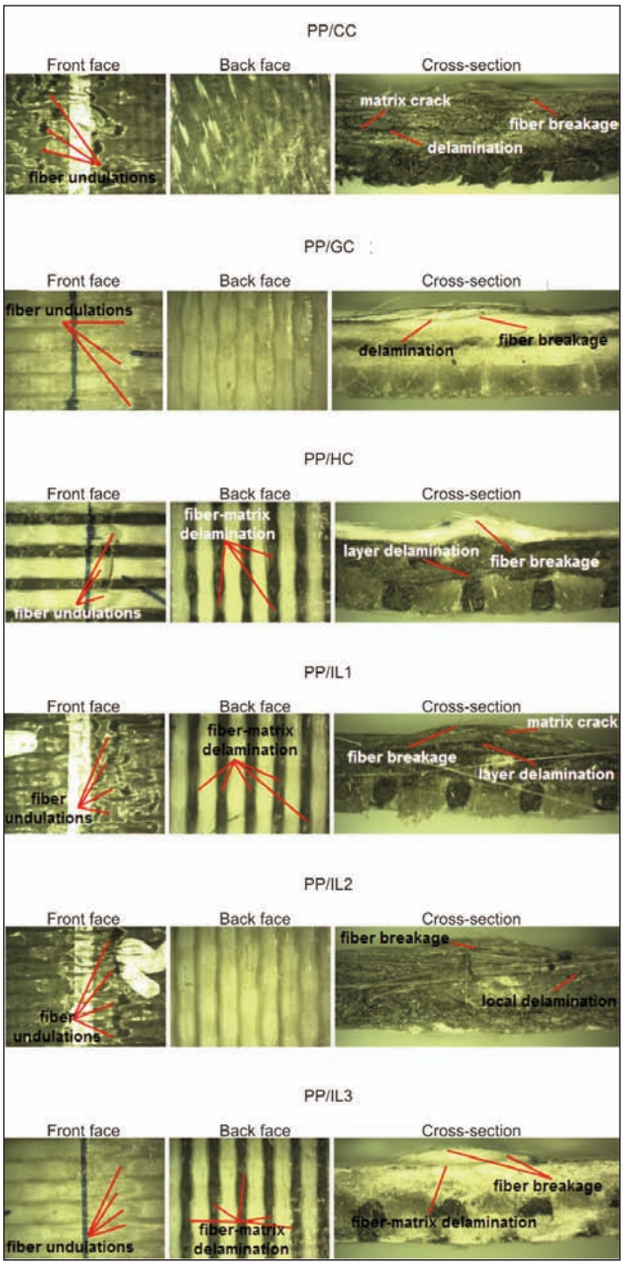

Fig. 7. The surface and cross-sectional microscopic failure analyses of hybrid thermoplastic composites (front-back face: x7, cross-section: x10 magnification)

both its surface and cross-section. The intra-ply/inter-ply hybrid PP/IL1 composite showed the similar front face failure with PP/CC as an intense fiber undulation. The back face failure of PP/IL1 was also similar with PP/HC as the fiber-matrix delamination. Matrix crack, fiber breakage and a layer delamination between PP/C and PP/H layer were also observed. The failure of inter-ply hybrid PP/IL2 composite on the front face was observed as fiber undulations while the back face had an insignificant failure as PP/GC composite. Fiber breakage and a local delamination were observed on the cross-sectional view. The intra-ply/inter-ply hybrid PP/IL3 composite showed a fewer fiber undulation on its front face compare to PP/IL1 and PP/IL2. Fiber-matrix delamination was observed on both its back face and cross-section. The cross-sectional view of PP/IL3 showed a

catastrophic fiber breakage. It was found that the intra-ply hybridization caused a more catastrophic failure on both surface and cross-section than inter-ply and intra-ply/inter-ply hybridization.

Figure 8 shows the surface and cross-sectional SEM failure analyses of hybrid thermoplastic composites. SEM analyses are compatible with optical microscope views. PP/CC showed a deep matrix crack and fiber/matrix delamination on its top face. Inter-ply delamination, intensive fiber breakages and localized kinking zone were observed on cross-sectional view. A fiber undulation, minor matrix crack and fiber/matrix delamination were observed on the front face of PP/GC. Some of the intra-ply and inter-ply delamination were occurred on the cross-sectional view of PP/GC. PP/HC showed a severe fiber/matrix delamination on its top face due to using both carbon and E-glass fiber in intra-ply hybridization. And also, extensive inter-ply/intra-ply delamination and fiber breakages were observed in the cross-sectional view of PP/HC. An intense fiber undulation, a deep matrix crack and multiple fiber breakages were occurred on the top face of PP/IL1. The cross-sectional failure of PP/IL1 was observed as inter-ply delamination. The front face failure of PP/IL2 was observed as fiber undulations while fiber breakages and a local delamination were observed on the cross-sectional view. Fiber/matrix delamination and some fiber breakages were observed on the front face of PP/IL3. A catastrophic fiber breakage was observed on the cross-sectional views of PP/IL3 while the inter-ply and intra-ply delamination was restricted due to the stronger fiber/matrix interface of E-glass/PP.

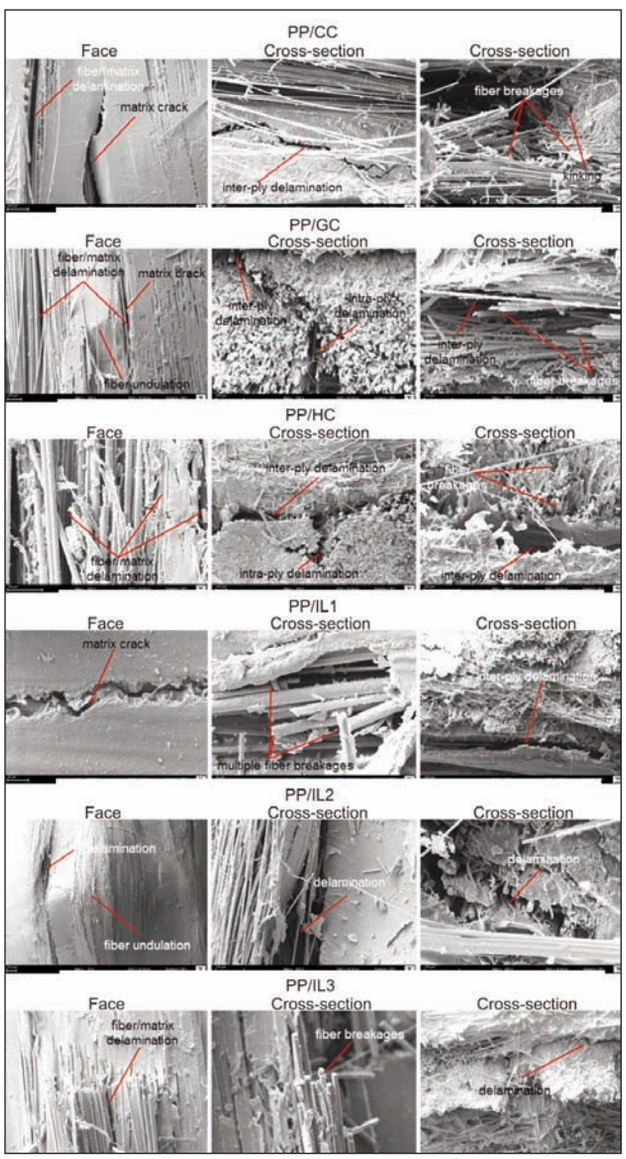

Fig. 8. The surface and cross-sectional SEM failure analyses of hybrid thermoplastic composites

CONCLUSIONS

Bending properties of intra-ply, inter-ply and intra-ply/inter-ply Carbon/E-Glass/PP hybrid thermoplastic composites were compared with those of non-hybrid Carbon/PP and E-Glass/PP thermoplastic composites. The conclusions are:

- UD woven thermoplastic prepregs are suitable materials to achieve the desired hybridization related to load to be exposed and end-use areas of composites which provides design flexibility.
- The densities of hybrid thermoplastic composites were affected by the ratios of different fiber types used in hybridization. The composite density was increased by the increase in E-Glass fiber ratio. The lowest composite density was obtained from PP/CC since the lower density of carbon fiber compare to that of E-glass fiber. Fibre fractions can be varied by the constructional arrangements of weaving as using different warp and weft densities, weaving patterns and yarn linear densities.
- The carbon fibers are used for their high strength in hybridization. The glass fibers have higher strain-to-failure in tension than that of carbon fibers which provides higher strength to hybrid composites. PP/CC composites are generally stiffer than PP/GC and PP/HC composites because of the brittle behavior of carbon fibers. PP/HC intra-ply hybrid composites are more flexible compared to non-hybrid composites since the contribution of higher strain of glass fibers.
- The bending-strength of hybrid thermoplastic composites was significantly improved by the intra-ply, inter-ply or intra-ply/inter-ply hybridization. The intra-ply/inter-ply hybridization (PP/IL1) increased the bending strength as 19.4% compared to non-hybrid composites. It could be caused by the constraint from the intra-ply and inter-ply E-glass fibers that prevent carbon fiber breakages and formed a considerable hybridization effect due to the delay in failure of the carbon fibers [39]. The uniform distribution of carbon and E-glass fibers within and between the layers the composite structure was also increased the bending strength of composites. Bending strength is mainly dependent on the fiber-content and fiber-properties of the composites which confirms the synergic effect of hybridization.
- The fiber fractions affected the bending-modulus of composites. The bending-modulus of hybrid com-

posites generally increased by the increase in Carbon fiber fraction because of the higher fiber modulus of Carbon compared to E-Glass fiber. However, non-hybrid PP/CC showed low bending modulus because of the weak interface properties of carbon/PP during consolidation process.

- The intra-ply, inter-ply and intra-ply/inter-ply hybridizations increased the bending modulus of composites because of the combining the unique specific modulus of Carbon and strain of E-Glass fibres.
- The uniform distribution of Carbon and E-Glass fibers within and between the layers of composites by using intra-ply/inter-ply hybridization resulted as the higher bending modulus up to 65.1% compared to non-hybrid composites.
- The bending-deflection of hybrid thermoplastic composites was significantly affected by the intra-ply, inter-ply or intra-ply/inter-ply hybridization and fiber ratios used. The ductility of hybrid thermoplastic composites decreased by the increase in Carbon fiber ratio of the composite.
- The Carbon/PP and E-Glass/PP fibers showed different adhesion properties during consolidation process which caused by the different surface and heat-transfer properties of Carbon and E-Glass fibers. The non-hybrid and hybrid thermoplastic composites generally showed a layer delamination and fiber breakages on their cross-section and fiber undulations on their front faces. The intra-ply hybridization caused a more catastrophic failure on both surface and cross-section than those in inter-ply and intra-ply/inter-ply hybridization.
- It is evaluated that using Carbon fiber at the top layer makes the hybrid thermoplastic composites stiff and increases the bending strength and modulus.

ACKNOWLEDGEMENTS

The author would like to thank Kahramanmaras Sutcu Imam University Scientific Research Unit, Turkey for supporting this study (2016/3-76 M).

BIBLIOGRAPHY

[1] Hoa, S. V. *Principles of the manufacturing of composite materials*, DEStech Publications, Inc., Lancaster, 2009, pp. 3–15.
[2] Offringa, A.R. *Thermoplastic composites-rapid processing applications*, In: Composites Part A: Applied Science and Manufacturing, 1996, vol. 27, pp. 329–336.
[3] Iyer, S.R., Drzal, L.T. *Manufacture of powder-impregnated thermoplastic composites*, In: Journal of Thermoplastic Composite Materials, 1990, vol. 3, pp. 325–355.
[4] Joncas, S., M. Sc. Dissertation, *Thermoplastic composite wind turbine blades: An integrated design approach*, Université du Québec, Canada, 2010.
[5] Brandrup, J., Immergut, H., Grulke, A. *Polymer Handbook*, 4th ed., John Willey & Sons, Inc., New York, 1999, pp. 171–186.
[6] Mazumdar, S. K. *Composites manufacturing, materials, product and process engineering*, CRC Press, USA, 2002, pp. 45–60.
[7] Choi, B. D., Diestel, O., Offermann, P. *Commingled CF/PEEK hybrid yarns for use in textile reinforced high performance rotors*, 19th International Conference on Composite Materials (ICCM), Montreal, 2013.
[8] Thwe, M.M., Liao, K. *Durability of bamboo-glass fiber reinforced polymer matrix hybrid composites*, In: Composite Science Technology, 2003, vol. 63, pp. 375–387.
[9] Gupta, M. K., Srivastava, R. K., *Mechanical properties of hybrid fibers reinforced polymer composite: A review*, In: Polymer-Plastics Technology and Engineering, 2016, vol. 55, pp. 626–642.
[10] Pandya, K. S., Veerraju, Ch., Naik, N. K. *Hybrid composites made of carbon and glass woven fabrics under quasi-static loading*, In: Materials and Design, 2011, vol. 32, pp. 4094–4099
[11] Mallick, P. K. *Fiber reinforced composites materials, manufacturing and design*, CRC Press, USA, 2007, pp. 55–70.
[12] Mader, E., Rausch, J., Schmidt, N. *Commingled yarns – processing aspects and tailored surfaces of polypropylene/glass composites*, In: Composites Part A: Applied Science and Manufacturing, 2008, vol. 39, pp. 612–623.
[13] Long, A. C., Wilks, C. E., Rudd, C.D. *Experimental characterization of the consolidation of a commingled glass/polypropylene composite*, In: Composites Science and Technology, 2001, vol. 61, pp. 1591–1603.
[14] Alagirusamy, R., Fangueiro, R., Ogale, V., Padaki, N. *Hybrid yarns and textile preforming for thermoplastic composites*, In: Textile Progress, 2006, vol. 38, no. 4, pp. 1–71.
[15] Wakeman, M. D., Cain, T. A., Rudd, C. D., Brooks, R., Long, A.C. *Compression moulding of glass and polypropylene composites for optimised macro and micro mechanical properties of commingled glass and polypropylene*, In: Composites Science and Technology, 1998, vol. 58, pp. 1879–1898.
[16] Lariviere, D., Krawczak, P. *Interfacial properties in commingled yarn thermoplastic composites, part i: characterization of the fiber/matrix adhesion*, In: Polymer Composites, 2004, vol. 25, pp. 577–587.
[17] Ye, L., Friedrich, K., Kastel, J., Mai, Y.W. *Consolidation of unidirectional CF/Peek composites from commingled yarn prepreg*, In: Composites Science and Technology, 1995, vol. 54, pp. 349–358.
[18] Alagirusamy, R., Ogale, V. *Commingled and air jet-textured hybrid yarns for thermoplastic composites*, In: Journal of Industrial Textiles, 2004, vol. 33, no. 4, pp. 223–243.
[19] Schafer, J., Stolyarov, O., Ali, R., Greb, C., Seide, G., Gries, T. *Process-structure relationship of carbon/polyphenylene sulfide commingled hybrid yarns used for thermoplastic composites*, In: Journal of Industrial Textiles, 2016, vol. 45, no. 6, pp. 1661–1673.

[20] Ishikawa, T., Chou, T. W. *Elastic behavior of woven hybrid composites*, In: Journal of Composite Materials, 1982, vol. 16, pp. 2–19.
[21] Baghaei, B., Skrifvars, M., Berglin, L. *Characterization of thermoplastic natural fibre composites made from woven hybrid yarn prepregs with different weave pattern*, In: Composites Part A: Applied Science and Manufacturing, 2015, vol. 76, pp. 154–161.
[22] Baghaei, B., Skrifvars, M. *Characterisation of polylactic acid biocomposites made from prepregs composed of woven polylactic acid/hemp–lyocell hybrid yarn fabrics*, In: Composites Part A: Applied Science and Manufacturing, 2016, vol. 81, pp. 139–144.
[23] Dong, C., Davies, I. J. *Flexural and tensile strengths of unidirectional hybrid epoxy composites reinforced by S-2 glass and T700s carbon fibres*, In: Materials and Design, 2014, vol. 54, pp. 955–966.
[24] Khatria, S. C., Koczak, M. J. *Thick-Section as 4-Graphite/E-Glass/PPS hybrid composites: Part II. Flexural response*, In: Composites Science and Technology, 1996, vol. 56, no. 4, pp. 473–482.
[25] Sorrentino, L., Simeoli, G., Iannace, S., Russo, P. *Mechanical performance optimization through interface strength gradation in PP/Glass fiber reinforced composites*, In: Composites Part B, 2015, vol. 76, pp. 201–208.
[26] Xu, Z., Zhang, M., Wang, G., Luan, J. *Bending property and fracture behavior of continuous glass fiber-reinforced peek composites fabricated by the wrapped yarn method*, In: High Performance Polymers, 2018, DOI: 10.1177/0954008318767500.
[27] Shekar, R. I., Kotresh, T. M., Krishna Prasad, A. S., Damodhara Rao, P. M., Satheesh Kumar, M. N., Siddaramaiah, *Hybrid fiber fabric composites from poly ether ether ketone and glass fiber*, In: Journal of Applied Polymer Science, 2010, vol. 117, pp. 1446–1459.
[28] Zhang, J., Chaisombat, K., He, S., Wang, C.H. *Hybrid composite laminates reinforced with glass/carbon woven fabrics for lightweight load bearing structures*, In: Materials and Design, 2012, vol. 36, pp. 75–80.
[29] Sreekala, M. S., George, J., Kumaran, M. G., Thomas, S. *The mechanical performance of hybrid phenol-formaldehyde-based composites reinforced with Glass and Oil Palm fibers*, In: Composites Science and Technology, 2002, vol. 62, pp. 339–353.
[30] Sevkat, E., Liaw, B., Delale, F., Raju, B.B. *Drop-weight impact of plain-woven hybrid glass-graphite/toughened epoxy composites*, In: Composites Part A: Applied Science and Manufacturing, 2009, vol. 40, pp. 1090–1110.
[31] ISO 5084-1996 Determination of thickness of textiles and textile products, 1996
[32] ISO 7211-3-1984 Woven fabrics – construction – methods of analysis – Part 3: Determination of crimp of yarn in fabric, 1984.
[33] ISO 6348-2011 Determination of Mass – Vocabulary, 2011.
[34] ASTM D792-2013 Standard test methods for density and specific gravity (relative density) of plastics by displacement, 2013.
[35] ASTM D3171-2015 Standard test methods for constituent content of composite materials, 2015.
[36] ASTM D790-1990 Standard test methods for flexural properties of unreinforced and reinforced plastics and electrical insulating materials, 1990.
[37] Bilisik, K., Yolacan, G. *Warp-weft directional bending properties of multistitched biaxial woven E-Glass/Polyester nano composites*, In: Journal of Industrial Textiles, 2015, vol. 45, no. 1, pp. 66–100.
[38] Mukhopadhyay, S., Deopura, B. L., Alagiruswamy, R. *Interface behavior in polypropylene composites*, In: Journal of Thermoplastic Composite Materials, 2003, vol. 16, pp. 479–495.
[39] Wisnom, M.R., Czél, G., Swolfs, Y., Jalalvand, M., Gorbatikh, L., Verpoest, I. *Hybrid effects in thin ply carbon/glass unidirectional laminates: Accurate experimental determination and prediction*, In: Composites: Part A, 2016, vol. 88, pp. 131–139.
[40] Bilisik, K., Ozdemir, H., Yolacan Kaya, G. *Interlaminar shear strength properties of multistitched preform nano composites*, In: Industria Textila, 2016, vol. 67, no. 2, pp. 127–131.
[41] Spragg, C. J., Drzal, L. T., *Fiber, matrix, and interface properties*, *ASTM*, 1996, USA, pp. 168–180.

Authors:

GAYE YOLACAN KAYA

Department of Textile Engineering, Faculty of Engineering and Architecture
Kahramanmaras Sutcu Imam University
46040 Kahramanmaras,Turkey

Corresponding author:

GAYE YOLACAN KAYA
e-mail: gkaya@ksu.edu.tr

Non-conventional textile structures with technical destination, designed and developed at S.C. Cora Trading & Service S.R.L.

MARIAN-CATALIN GROSU ALEXANDRU ALEXAN

REZUMAT – ABSTRACT

Structuri textile neconvenționale cu destinație tehnică, proiectate și dezvoltate la S.C. Cora Trading & Service S.R.L.

Fibrele de lână sunt o resursă naturală, regenerabilă, durabilă, cu un impact redus asupra mediului și un potențial enorm pentru omenire. În conditiile în care populația Terrei se înmulțește exponențial, materiile prime sunt din ce în ce mai puține, o afacere bazată pe prelucrarea materiilor prime regenerabile, în special a fibrelor de lână, are mari șanse de supraviețuire și dezvoltare.

România, cu o economie agrară foarte dezvoltată, are o populație de aproape 10 milioane de ovine și o producție de peste 16.000 tone de lână medie și grosieră. Având în vedere necesitatea de a stabili cerințe minime de performanță energetică pentru clădirile noi și pentru renovarea majoră a celor existente la nivelul Uniunii Europene, este necesară dezvoltarea de noi materiale și tehnologii, astfel încât posibilitatea de a valorifica lâna pentru domeniul construcțiilor să poată fi un element funcțional pe termen lung.

Această lucrare prezintă rezultatele experimentale ale caracteristicilor a 4 structuri textile neconvenționale (STN) realizate din fibre de lână 100%, proiectate și dezvoltate la S.C. Cora Trading & Service SRL, pe tehnologia proprie, existentă și adaptată. Amestecul fibros utilizat, care constă atât din lână de tăbăcărie, cât și din lână de tunsoare, permite dezvoltarea unor structuri inovatoare, cu potențial de utilizare pentru capacitatea lor de izolare termică și cu un mare potențial de dezvoltare durabilă pentru producător.

Cuvinte-cheie: lână grosieră de tunsoare, lână de tăbăcărie, structuri textile neconvenționale, conductivitate termică

Non-conventional textile structures with technical destination, designed and developed at S.C. Cora Trading & Service S.R.L.

Wool fibers are a natural, renewable, sustainable, low impact on the environment, with huge potential for humanity. Given the exponential growth of the Earth's population, raw materials are getting less and less, a business based on the processing of renewable raw materials, especially wool fibers, has a high chance of survival and development.

Romania, with an overwhelming agrarian economy, has a population of nearly 10 million sheep and a production of over 16,000 tons of medium and coarse wool. Given the need to set minimum energy performance requirements for new buildings and for the major renovation of existing ones at European Union level, the development of new materials and technologies is necessary, so that the opportunity to capitalize on wool for buildings be a workable item on long term.

This paper presents the experimental results of the characteristics of 4 non-conventional textile structures (UTS) made of 100% wool fibers, designed and developed at S.C. Cora Trading & Service SRL, on their existing adapted technology. The fibrous blend used, consisting of both tanning wool and coarse shared wool allow development of innovative structures, with potential of use for their thermal insulation capacity and great potential of sustainable development of the manufacturer.

Keywords: coarse wool fibers, tanned wool fibers, non-conventional textile structures, thermal conductivity

INTRODUCTION

European Union targets by 2030 include creating a cleaner and healthier climate. Investments for improving energy efficiency in buildings, related to ensuring a clean, non-polluting environment in a sustainable way are a priority of the governments of the European Union countries, in the context of the reduction of greenhouse gases [1, 2, 3].

Under the Energy Performance of Buildings Directive, EU countries have to set minimum energy performance requirements for new buildings and major renovation of existing ones [3]. In this directive, the action „Accelerating the European Energy System Transformation" refers to "Developing new materials and technologies, energy efficiency solutions for buildings". It is estimated that Romania will become one of the largest European sheep breeders, sheep reared for meat, so the opportunity to exploit wool in construction can be a long-term exploitable item.

Wool has a huge potential for the use of technical textiles [5, 6], thanks to its essential and unique characteristics such as: thermal resistance of high values, even in humidity conditions; capacity to minimize thermal and heat variation in humidity conditions; moisture management capacity; capacity to minimize condensation (does not favor mold growth), absorption capacity of volatile organic compounds, formaldehyde, sulfur dioxides, nitrogen oxides and carbon dioxide in the atmosphere; hypoallergenic and non-toxic character [7]; airborne and surface noise reduction capacity (reduction factor ≥ 90%), heat transfer capacity, self-extinguishing capacity in contact with

fire sources, biodegradable and compostable character [8, 9, 10].
The paper proposes the presentation of experimental results of non-conventional textile structures (NTS) from 100% wool fibers, designed and developed at S.C. Cora Trading & Service SRL, on their existing adapted technology, with potential for use in the field of construction, thanks to the thermal insulation properties [11, 12, 13, 14]. The particularity of these structures is the presence in the fibrous blend of both tanned wool fibers and sheared thick wool fibers, with a low degree of valorization, currently, in Romania.

EUROPEAN CONSTRUCTION MATERIAL MARKET

Thermal insulation materials in buildings, which amounted to ~ 7.4 million tons in 2014, corresponding to a volume of ~ 234 million m^3, are essential for increasing energy efficiency in buildings, as construction consumes more than 40% of the amount of energy of the European Union and account for about 35% of all greenhouse gases [3]. Old buildings have the greatest potential for increasing energy efficiency (~ 36% by 2030). The annual compound growth rate of the production and consumption of thermal insulation materials is projected to be 4.5% by 2027 [3]. The market of thermal insulation materials in buildings is vast, with several identified classes, which are presented in the table 1.
The competitiveness of the thermal insulating material market is affected by the increasing demand, the improvement of the standards in the field, the requirements for improving the quality of insulating materials and the reconfiguration of the European construction industry [3, 4, 15]. The distribution chain of thermal insulation materials is shown in figure 1.
The essential parameters that are taken into account both by manufacturers and by the end users of thermal insulation are: the thermal insulation potential, the environmental relation, the protection factors (fire resistance) and the price.

Fig. 1. Distribution chain of insulation materials [3]

An element that plays a significant role in calculating the cost of an insulation material is the provided safety and the quality of the insulated interior air [1, 16]. In this context, fire behavior is carefully studied, both in terms of damage in the event of a fire, but especially because of the toxic gases that it discharges during combustion. These gases can cause serious illness or even death [2].
Although the structures derived from organic, vegetal and animal materials occupy a secondary place in the thermal insulation market in the European Union (thermal insulation of wool occupying 1%), their development potential is very developed in the conditions of sustainable development [4]. Thermal wool insulation does not support burning. Due to the nitrogen (16%) and sulfur (3–4%) content, in the chemical structure, wool fibers show the highest fire resistance of natural fibers (flame resistant fibers) (table 2). The assessment of the degree of flammability (the ability to ignite and burn) in textile materials is done by determining the limiting oxygen index (LOI – %) [16]. Wool textiles protect (temporarily) the propagation of outside fire inside a home or vice versa, and when exposed to the flame they do not release toxic substances [1, 16].

MATERIALS AND METHODS

In order to obtain an experimental model (EM) of non-conventional textile structures (NTS) [18], a fibrous blend was designed, as shown in table 3 [17, 20, 21].

Table 1

INSULATION MATERIAL AT EU LEVEL [3]		
No.	**Class**	**Type**
1	Inorganic mineral fibrous	Stone wool; glass wool; slag wool
2	Organic fossil fuel derived	Polyurethane (PU); Expanded polystyrene (EPS); Extruded polystyrene (XPS); Polyisocyanurate (PIR); Phenolic foam
3	Organic plant/animal derived	Cellulose; Woodfibre; Cork; Sheep's wool; Cotton; Hemp; Flax; Compressed straw
4	Innovative	Biopolymers; Nano-coatings; Aerogel; Vacuum insulation panels; Nano-cellular foam; Phase change materials (PCM); Advanced insulation foams
5	Other	Cellular Glass; Aerated glass; Vermiculite; Expanded clay pellets; Foil products

Table 2

LIMITING OXYGEN INDEX OF SHEEP'S WOOL [16]		
LOI limiting oxygen index (%) – minimum oxygen quantity to burn	Materials with LOI>25% burn quickly	Materials with LOI<25% do not support burning
Sheep wool	25.2	

Table 3

BLEND RECIPE (BR) – SHARES OF THE COMPONENTS		
Components, P1	**Fibre fineness**	**Weight percentage wt. %**
1. Sheared/virgin wool	Medium, coarse wool	50
2. Tanned wool		50

The main characteristics of blend recipe are presented in table 4.

The designed fiber blend was processed on two adapted technological flows, available at SC Cora Trading & Service (figure 2), which includes 5 preliminary processing operations, web and batt forming operations, mechanical bonding operations (to obtain NTs) and final finishing operations [10, 19, 20] (table 5). The high degree of impurities imposed the use of 5 primary processing operations, which can eliminate about 50–60% of these matters (vegetable matter and dirt) [21].

Table 4

TECHNICAL SPECIFICATION ON THE VARIATION LIMITS OF THE FIBER BLEND CHARACTERISTICS		
Fiber characteristics	**Value**	
	Average	**CV, %**
Diameter, μm	32,986	36,855
Length, mm	64,33	74,97
Elongation to break, %	29,675	0,460
Breaking force, cN	30,825	0,637
Content of impurities, % (vegetable + mineral)	0,8	-
Soluble substances in organic solvents, %	4,06	-
Index of solubility in alkali, %	12,69	-

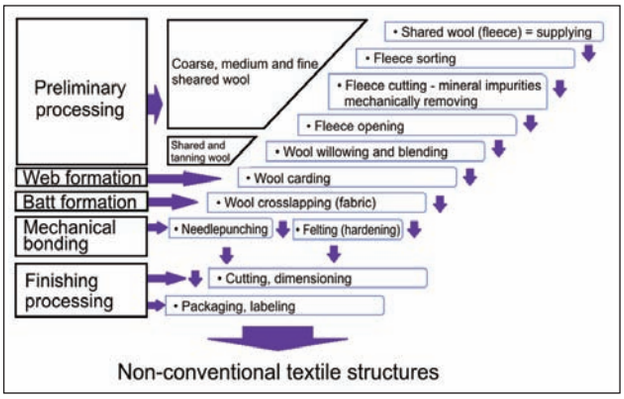

Fig. 2. Technological flow of non-conventional textile structures for thermal insulation [22]

EXPERIMENTAL

Using the technologies presented in figure 2, four experimental models (EM) of NTS, encoded S1 (figure 3, *a*), S2 (figure 3, *b*), S3 (figure 3, *c*) and S4 (figure 3, *d*) were made. The four NTS vary function of thickness, specific mass (density) and bonding/felting technology.

The NTS experiment matrix (identified in figure 3, *a* – S1, figure 3, *b* – S2, figure 3, *c* – S3 and figure 3, *d* – S4) is shown in table 6.

Table 5

TECHNOLOGICAL PARAMETERS FOR NON-CONVENTIONAL TEXTILE STRUCTURES PRODUCTION, AVAILABLE TO SC CORA TRADING & SERVICE SRL [22]			
Technological Flow stage	**Technological operation**	**Equipment**	**Characteristic**
Preliminary processing	Fleece supplying	-	Bales, sacks
	Fleece sorting	-	Manual operation
	Fleece cutting, mineral impurities mechanical removing	2 knifes rotary cutter – invention	Productivity: 200 kg/h – one pass; Cutting length: 100 mm
	Fleece opening	Fleece opening equipment – invention	Productivity: 50 kg/h – one pass
	Willowing	Technological adapted opening willow	Productivity: 200kg/h – one pass
Web formation	Carding	HBD Card	Productivity: 40 kg/h; Web's specific mass: 20g/m^2; Web's width: 1.80 m
Batt formation	Cross-lapping	Technological adapted transversal crosslaper	Web layers/m: 15; Batt's specific mass: 240 g/m^2; Batt's width: 180 cm – 250 cm
Mechanical bonding	Needle-punching	Asselin single board needle loom	Maximum width: 6,5 m; Maximum thickness after needle-punching: 4 cm; Maximum specific mass: 7 kg/m^2; Maximum density: 0,35 g/cm^3
	Felting – hardening	Hardener – Technologically adapted flat installation	Maximum width: 220 cm; Streaminglength: 3 m; Top platen length: 3m;
Finishing processing	Cutting, dimensioning	Circular knife, guillotine	Panels, rolls
	Packaging, labelling	-	PE foil

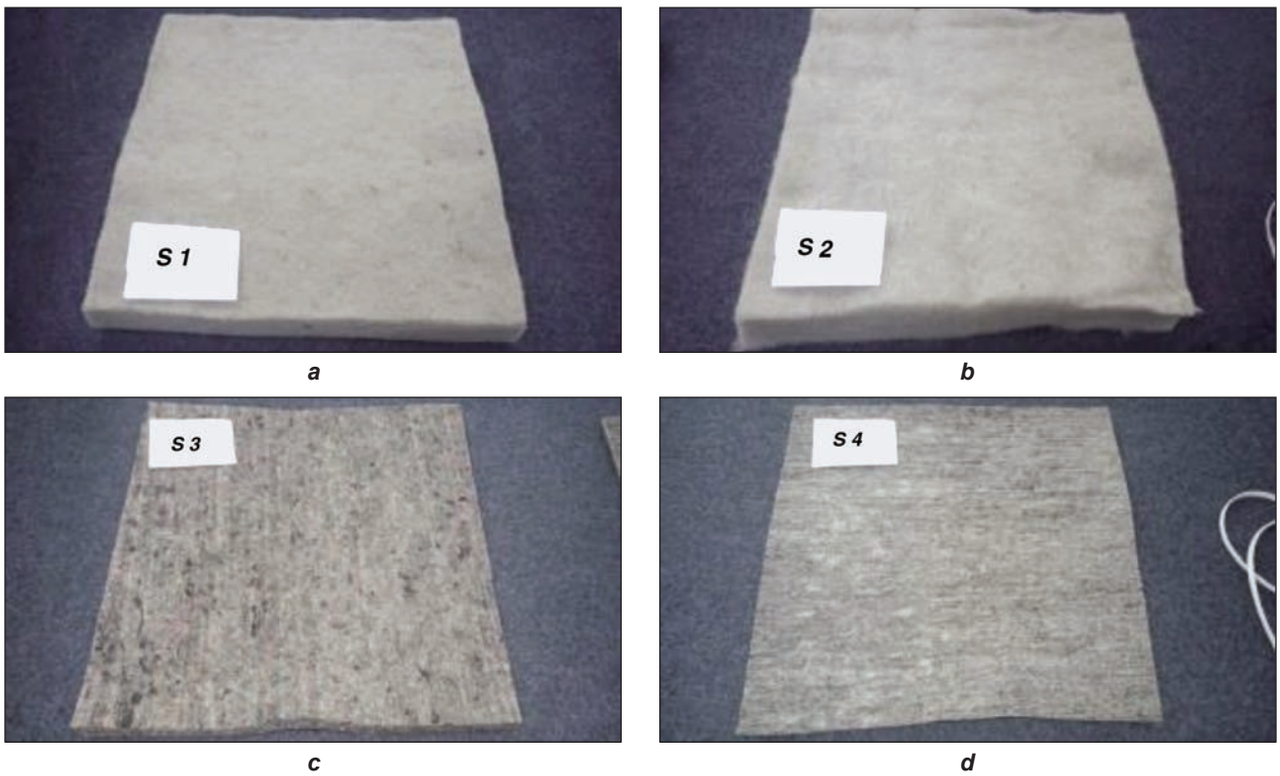

a *b* *c* *d*

Fig. 3. STN a) S1, b) S2, c) S3, d) S4

Table 6

EXPERIMENTAL MATRIX			
Experimental matrix		**Obtaining technology**	
		T1	**T2**
Obtained structure	**S1**	x	
	S2	x	
	S3		x
	S4		x

Legend:

T1 – technology to obtain voluminous STNs, bonded by hardening; T2 – technology for obtaining STN with low degree of volume, bonded by needle punching; S1 – STN with specific mass imposed in the range 2100 g/m^2 ± 5%, made by T1 technology; S2 – STN with specific mass imposed in the range of 1700 g/m^2 ± 5%, made by T1 technology; S3 – STN with specific mass imposed in the range of 2700 g/m^2 ± 5%, made by T2 technology; S4 – STN with specific mass imposed in the 900 g/m^2 ± 5% range, made by T2 technology.

The technological variants of EM: S1, S2, S3 and S4, in the form of fibrous panels, have been analysed in terms of field of use specific functionalities: physical analysis (mass/unit area, thickness) and functional (thermal conductivity, fire behaviour, electrical resistivity).

RESULTS

Mass per unit area

The mass/unit area of the structures was obtained by overlapping the fibrous batts obtained from cross-laping, weighed in advance.

A number of batts have been folded successively until aim posed specific mass and weight, possible to consolidate, is reached. The values obtained are shown in table 7.

Regarding the specific mass of S1, S2 S3 and S4 NTS, for the obtained values it can be mentioned that S2 has a specific mass by 17,29% lower than S1, this being the minimum specific mass, possibly obtained by this bonding technology. Below this value, keeping the consolidation conditions constant (including the height), the mechanical bonds between the fibers are not secured, so the structure does not get mechanical resistance. In the case of S3 and S4, the consolidation technology allows obtaining large specific masses at smaller thicknesses than the S1 and S2

Table 7

STATISTICAL INDICATORS ON EM SPECIFIC MASS					
Characteristics	**Reference document**	**ME Technological sample**			
		S1	**S2**	**S3**	**S4**
Average mass/ unit area, g/m^2	SR EN 12127:2003	2141.81	1771.40	2659.22	877.20
CV, %		2.55	3.91	2.48	3.65

Fig. 4. Top view of the STN, with emphasis on thickness differences

structures. S3 has a specific mass greater than 203.15% over S4. The four technological variants are potentially different for recovery in the construction area, given the specific mass differences.

Thickness

The mechanical bonding by steam hardening allows high-porosity structures to be obtained (higher volumes than bonded reinforced structures by other modes) (figure 4). For structures S1 and S2 a height of the oscillating table of the hardening equipment has been calibrated at 60 mm. The results obtained from the measurements are presented in table 8.

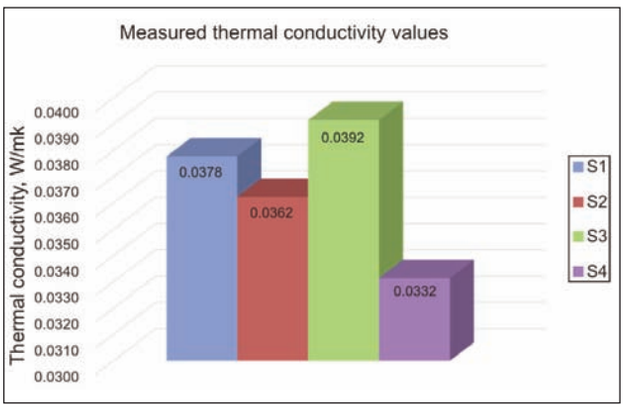

Fig. 5. Thermal conductivity of S1, S2, S3 and S4 EM [22]

Celsius [23]. The value of λ is a material constant, and its decrease leads to an increase in the level of thermal insulation that the material can provide. Values of λ for STN S1-4 are presented in the table 9. Figure 5 shows that the λ value of structure S2 is 4.07% smaller than S1, which means that structure S2 is better isolator than structure S1 (structure S2 has a larger air volume than structure S2, which allows a higher convective transfer that structure S1). Structure S4 shows an λ value of 15.34% lower than S3.

Burning behaviour of NTS

Fire behaviour test: Determination of flame propagation properties on vertically oriented specimens consists of two procedures: A. ignition of the surface, B. ignition of the lower end. The results of the fire

Table 8

STATISTICAL INDICATORS OF EM THICKNESS					
Characteristics	**Reference document**	**EM technological sample**			
		S1	**S2**	**S3**	**S4**
Average thickness, mm	SR EN ISO 9073-2-2000	39,744	48,669	19,173	9,102
CV, %		1,019	1,742	3,424	1,210
Calculated density, kg/m^3		53.89	36.35	133.03	96.76

Due to the different specific mass, after the bonding operation, the S1 and S2 structures did not remain at the calibrated height but decreased by 33.76% (S1) and 18.8% (S2), respectively. The thickness of S2 is 22% greater than S1. The S3 and S4 structures are more compact, with smaller thicknesses than the S1 and S2 structures, as the bonding technology allows barbed needles to train the fibers in order to fix them through the interstices of said fibrous batt (rendering compactness). Structure S4 is 55% thicker than S3.

Thermal conductivity

The thermal conductivity λ [W/mK] is equal to the amount of heat that passes for 1 hour through a 1 m thick material with a surface area of 1 m^2 and a temperature difference on the two faces of its 1 degree

Table 9

STATISTICAL INDICATORS OF EM'S THERMAL CONDUCTIVITY				
Characteristics	**EM technological sample**			
	S1	**S2**	**S3**	**S4**
Average thermal conductivity, W/mK	0.0378	0.0362	0.0392	0.0332
CV, %	0.1186	0.1425	0.8697	0.1590

tests of the S1, S2, S3, S4 structures (the height of the footprint) are shown in table 10.

By comparing the data obtained from table 10, it is found that: NTS S1-4 are hard to ignite, so the area subjected to flame releases unpleasant odour,

Table 10

THE TRACE HEIGHT OF THE BURNED AREA AFTER TESTING									
EM technological sample		**S1**		**S2**		**S3**		**S4**	
Procedure	**Trace height, mm**	**L**	**T**	**L**	**T**	**L**	**T**	**L**	**T**
A		87	87	95	85	72	60	65	57
B		103	112	143	147	108	115	100	105

L – longitudinal testing; *T* – transversal testing.

burned hooves; The trace dimensions due to the initiation flame of 40 ± 2 mm (procedure A) and 25 ± 2 mm (procedure B) are higher in high-volume structures (S1 and S2) than in high density structures (S3 and S4), both longitudinally and transversally, for both procedures. The smallest trace shows the S4 structure in fire testing by both procedures.

Electrical resistivity

Testing the electrical resistivity of wool fiber panels confirms their dielectric character. The average resistivity test values are shown in table 11.

From the analysis of the experimental values we find that the values are ranged between 10^{13} (Ω) to 10^{14} (Ω), both for surface resistivity and for the resistivity of the volume, values above the resistivity values of dielectric insulating materials (10^{11} Ω), comparable to the prexiglas, teflon, air etc. [12]. It can be appreciated that the use of structures S1, S2, S3 and S4 in construction structures traversed by electric cables does not pose additional risk in case of short electric circuits.

Table 11

EM ELECTRICAL RESISTIVITY		
EM technological sample	**Surface resistivity, (Ω)**	**Volume resistivity, (Ω*cm)**
S1	$4{,}81*10^{13}$	$5{,}54*10^{13}$
S2	$1{,}08*10^{13}$	$1{,}56*10^{13}$
S3	$9{,}35*10^{13}$	$2{,}51*10^{13}$
S4	$1{,}84*10^{14}$	$1{,}67*10^{14}$

CONCLUSIONS

The study reveals the potential for the use of wool fibers in non-conventional textile structures for thermal insulation in construction. The experimental fibrous blend consists of tanning wool, considered as tannery waste and sheared coarse wool.

For the experiments two existing technological flows, at S.C. Cora Trading & Service SRL, for processing the fibrous blend were selected, which contain preliminary processing operations, web and batt formation and final operations. Due to the high content of impurities of mineral, animal and vegetal origin, the fleece has been subjected to 5 preliminary processing operations, where the manufacturer's own invented or with specific technological adaptations equipment was used.

For the experiments 4 technological samples of non-conventional textile structures, formed by two ways of bonding/felting (hardening – structures S1 and S2), needle punching – structures S3 and S4) have been used.

The 4 non-conventional textile structures designed and developed represent a sustainable developing potential for the manufacturer particularly and for the Romanian textile industry generally.

ACKNOWLEDGEMENTS

This work was carried out under the PNIII, Programe 2: P2 – Increasing the Romanian economic competitiveness through RDI, Subprograme 2.1. Research, development and inovation, Innovation Checks 2018, Program implemented with the support of the Executive Agency for Higher Education, Research, Development and Innovation Funding, project no. PN-III-P2-2.1-CI-2018-0870and the publication is funded by the Minister of Research and Innovation through the Program 1 – Development of the National Research and Development System, Subprogram 1.2 – Institutional Performance – RDI excellence funding projects, Contract no. 6PFE/ 16.10.2018.

BIBLIOGRAPHY

[1] Stec, A. A., & Hull, R. T. (2011). *Assessment of the fire toxicity of building insulation materials*. In: Energy and Buildings, 43(2–3), 498–506.

[2] Woolley, T. (2016). *Building materials, health and indoor air quality: No breathing space?* Routledge.

[3] Pavel, C. C., & Blagoeva, D. T. (2018). *Competitive landscape of the EU's insulation materials industry for energy-efficient buildings* – JRC Technical Reports. Joint Research Center. Luxembourg: Publication Office of the European Union.

[4] European Commission (2018). Energy.

[5] Johnson, N., Wood, E., Ingham, P., McNeil, S., & McFarlane, I. (2003). *Wool as a technical fibre*. In: The Journal of The Textile Institute, 94 (Part 3: Technical Textiles).

[6] Baillie, C., & Jayasinghe, R. (2017). *Green composites: Nature and waste-based materials for a sustainable*

[7] Mansour, E., Loxton, C., Elias, R. M., & Ormondroyd, G. A. (2014). *Assessment of health implications related to processing and use of natural wool insulation products*. In: Environment International, 73, pp. 402–412.

[8] Giuliano, F., Riccardo, I., Takayuki, A., Hideki, S., & Masuhiro, T. (2003). *Physical properties of wool fibers modified with isocyanate compounds*. In: J. App. Sc., 89, pp. 1390–1396.

[9] Asandei, N., & Grigoriu, A. (1983). *Chimia și structura fibrelor*. București, Editura Academiei Republicii Socialiste România.

[10] Stevens, J. R. & Co. Inc. (1970). *Wool Handbook* – Third Enlarged Edition (Vol. 2 (2)). London: Interscience.

[11] Patnaik, A., Mvubu, M., & Muniyasamy, S. (2015). *Thermal and sound insulation materials from waste wool andrecycled polyester fibers and their biodegradation studies*. In: Energy and Buildings, 92, pp. 161–169.

[12] Savio, L., & Bosia, D. (2018). *Application of Building indulation products based on natural wool and hemp fibers, advances in natural fibre composites: raw materials, processing and analysis*, Springer International Publishing.

[13] Zach, J., Korjenic, A., & Petránek, V. (2012). *Performance evaluation and research of alternative thermal insulations based on sheep wool*. In: Energy Build., 49, pp. 246–253.

[14] Pennacchio, R., Savio, L., & Bosia, D. (2017). *Fitness: Sheep-wool and hemp sustainable insulation panel*. In: Energy Procedia, 111, pp. 287–297.

[15] Chaupin, M. T. (2013). *Regional projects valuing wool in Europe*. Symposium on South American Camelids and other Fibre Animals. Nantes.

[16] Kim, N. K., Lin, R. J., & Bhattacharyya, D. (2015). *Flammability characteristics of wool fibre polypropylene composites using halogen-free fire retardants*. The 38th Polymer Conference & Annual Meeting of the Polymer Society Taiwan 2015. Taipei.

[17] Caraiman, M., Netea, M., & Taras, I. (1998). *Filatura de lână – Fire – Materii prime – Amestecuri*. Iasi: BIT.

[18] W. Albrecht, H. F. (Éd.). (2003). *Nonwoven fabrics – raw materials, manufacture, applications, characteristics, testing processes*. Weinheim: WILEY-VCH Verlag GmbH & Co. KGaA.

[19] Preda, C. (1996). *Structuri și tehnologii de obținere a materialelor textile neconvenționale*, Iaşi: BIT.

[20] Visileanu, E. (2004). *Prelucrarea mecanică a fibrelor de lână și tip lână*, Certex, București.

[21] Dodu, A. (Éd.). (2003). *Manualul Inginerului Textilist – Tratat de inginerie textilă* (Vol. 2, Partea A), AGIR, București.

[22] *Optimizarea gamei de nețesute din lână pentru termo și fono izolații – RO-IZOLANA* – Raport științific și tehnic, 2018, Cod proiect: PN-III-P2-2.1-CI-2018-0870, Cecuri de Inovare.

[23] Horga, G.; Horga, M; Hossu, I.; Avram, D. (2013). *Investigation on determining the coefficient of thermal conductivity to textile materials recoverable, used for thermal protection of hot pipelines*, In: Journal of Textile & Apparel, vol. 23, Issue 2, pp. 94–100.

Authors:

MARIAN-CATALIN GROSU[1]
ALEXANDRU ALEXAN[2]

[1]National R&D Institute for Textiles and Leather, Bucharest
Lucrețiu Pătrășcanu street, no. 16, sector 3, postal code 030508, Bucharest, Romania
e-mail: certex@certex.ro

[2]S.C. CORA TRADING & SERVICE S.R.L.,
Mehadiei street, no. 43, sector 6, Bucharest, Romania
e-mail: a.alexan@romfelt.ro

Corresponding author:

MARIAN-CATALIN GROSU
e-mail: catalin.grosu@certex.ro

Essential mint oil-based emulsions: preparation and characterization

ANGELA DĂNILĂ
CARMEN ZAHARIA
DANIELA ŞUTEU
EMIL IOAN MUREŞAN
GABRIELA LISĂ
SINEM YAPRAK KARAVANA
ALI TOPRAK
ALINA POPESCU
LAURA CHIRILĂ

REZUMAT – ABSTRACT

Emulsii obținute pe bază de ulei esențial de mentă: obținere și caracterizare

Scopul acestei lucrări este de a prezenta pe scurt metodologia de obținere a patru tipuri de emulsii (M_2, M_3, M_6 și M_7) pe bază de ulei esențial de mentă (Mentha Piperita) și proprietățile fizico-chimice și calitative ale acestora (pH, densitate, indice de aciditate, indice de peroxid, conținutul de diene și triene conjugate, stabilitatea în timp, conținutul de apă și materie grasă), cu scopul de a selecta varianta optimă de formulare a emulsiei pentru aplicare în domeniul textil. Această lucrare subliniază, de asemenea, faptul că cea mai stabilă este emulsia M_6 urmată de emulsia M_3.

Cuvinte-cheie: ulei esențial de mentă, ceară de albine, emulsie, proprietăți fizico-chimice și calitative

Essential mint oil-based emulsions: preparation and characterization

The aim of this work is to present briefly the preparation methodology of four emulsions (named M_2, M_3, M_6, and M_7) based on extracted mint oil (Mentha Piperita) and their physical-chemical properties and quality characteristics (pH, density, acidity index, peroxide index, diene and triene content, in-time stability, humidity and fatty matter content), in order to select the most recommendable emulsion to be used in textile field. This work also underlines that the most stable emulsion is M_6 emulsion followed by M_3 emulsion.

Keywords: mint essential oil, beeswax, emulsion; physical-chemical properties; quality characteristics

INTRODUCTION

Researches from last years have shown that aromatherapy textiles are increasingly used because of the benefits offered as: environmentally friendly and beneficial effects on wellbeing and human health.

Essential oils are a common source of bioactive ingredients and are used for their various functional properties (anti-inflammatory, anti-microbial, organoleptic, antioxidant, anti-arrhythmic, anti-thrombotic, anti-vasoconstrictive, anti-hypertension, anti-ulcerous, anti-aging, anti-carcinogen, anti-diabetic, anti-depressant, anti-pyretic, and insect repellent) [1]. In textile field, most essential oils are used for their antimicrobial effect [2].

Although skin is not a common way of managing biologically active principles due to difficult absorption especially for water-soluble substances, in recent years, more attention has been paid to the benefits of transdermal administration: controlled release of biologically active principles leading to reduced invasiveness; reduction of the metabolic stages in the liver; avoiding stomach trauma [3, 4].

Losses by evaporation and difficulties in controlling releases make the application of essential oils to be limited. In this case, carrier systems (lipid particles, nano-emulsions, biocompatible polymer particles) can provide an ideal solution to achieve a controlled and targeted distribution of essential oil.

Natural waxes are suitable for essential oils embedding [5]. Also, natural waxes are of food grade purity (insect waxes – bees wax and plant waxes – candelilla wax, carnauba wax) and exhibit interesting rheology and microstructure [5].

In last years have been reported a series of researches on successful applications of beeswax in preparing diverse biodegradable films and coatings [6].

Bees wax is soft, biodegradable and a considerable viable absorbent. It is used to create a cover around the materials as a hydrophobic layer [7].

The study aims to produce the beeswax/mint essential oil emulsions and to analyze a few of its physical-chemical and quality characteristics.

EXPERIMENTAL PART

Materials and methods

▪ *Basic materials for emulsions preparation: raw and auxiliary materials*

For all experimental researches, it was used as basic raw matter the essential mint oil received from the Turkish company Doğal Destek.

As auxiliary materials, there were used: (*i*) beeswax purchased from a private apiary in the Northeast region of Romania; (*ii*) glycerin purchased from SC Elemental SRL, Romania, and (*iii*) Tween 80 (Merck, Germany).

All other chemical reagents used for analytical analysis were of analytical purity (p.a.), being purchased from Romanian companies (e.g., Chemical Company S.A., Iasi, RO), or from abroad (Sigma Co., or Merck Co.).

▪ *Emulsion preparation methodology*

The beeswax was melted with a 700 rpm rate at a temperature of 65°C, over which distilled water was added at 63°C to form the wax/water system. Tween 80 emulsifier was added to the wax/water system, and the system was maintained under stirring for 10 minutes at 63°C, after which glycerol was added. After complete homogenization, the system was cooled to 40°C, over which the mint essential oil was added dropwise.There were prepared series of emulsions (M_i) which are different due to varying ratios of wax/essential oil used (there were selected as representative series – M_2, M_3, M_6 and M_7 emulsions having the ratio wax/oil varying in range of 1:2; 1:1.3; 1:5; and 1:6).

The prepared esential mint oil-based emulsions were analyzed and characterized further especially for its stability and transformation degree.

Analysis methods

▪ *Emulsions appearance*

The appearance of the four prepared emulsions was visually and microscopically analyzed using a KRÜSS optical microscope equipped with a NIKON Coolpix P 5100 photo digital camera.

▪ *pH determination*

Emulsion *pH* was directly measured using a HANNA portable pH-meter immersed in the prepared non-diluted emulsion (M_i).

▪ *Density determination*

All measurements were performed directly using an Anton Paar DMA 4500 Density Meter (Anton Paar GmbH, Granz, Austria) at three different temperatures of 19°, 20° and 25°C. For each temperature, there were performed at least six till eleven measurements and calculated the mean value of density at specific temperature. This mean value was reported in our work.

▪ *Determination of the acidity index (AI)*

Around 2.5 g of emulsion sample (weighted with precision of 0.001 g) was contacted with 12.5 mL of chloroform and 12.5 mL of ethylic alcohol. After stirring, there were added a few drops of phenolphthalein indicator and the obtained solution was titrated under stirring with potassium hydroxide (0.1 M KOH) till a pink color obtained, stable at least 1 min. For calcula - tion of the acidity index (*AI*) it was used the relation (1):

$$AI = \frac{V_{KOH} \cdot M_{KOH} \cdot 56.11}{m} \left[\frac{\text{mg of KOH}}{\text{g of emulsion}}\right] \quad (1)$$

where: *AI* – the acidity index (mg KOH/g of emulsion); V_{KOH} – the volume of KOH consumed at titration (mL); M_{KOH} – the concentration of KOH solution (mol/L); 56.11 – molecular weight of KOH (g/mol) and *m* – sample mass (g).

▪ *Determination of the peroxide index (PI)*

In a closed glass vessel was weighed around 1–2 g of emulsion which was contacted with 5 mL of chloroform, 7.5 mL of glacial acetic acid and 1 mL of 10% KI. The closed vessel was stirred for 1 min and after set in a dark place for 15 min. It was added 37.5 mL of distilled water and, after stirring, was introduced starch solution till a dark stable blue color appears. The formed iodine is titrated with sodium thiosulfate (0.05 N $Na_2S_2O_3$). A control titration is performed in parallel with the basic determination. For calculation of the peroxide index (*PI*) it was considered the following relation:

$$PI = \frac{(V_{ref} - V) \cdot 1000}{m} \left[\frac{\text{mmol of peroxide}}{\text{g of emulsion}}\right] \quad (2)$$

where: *PI* is the peroxide index (mol of peroxide/kg of emulsion), V_{ref} – volume of $Na_2S_2O_3$ solution consumed at titration of control sample (mL), *V* – volume of $Na_2S_2O_3$ solution consumed at titration of analyzed emulsion sample (mL), $N_{Na_2S_2O_3}$ – normal concentration of sodium thiosulfate solution (val/L), 1000 – recalculation coefficient of [mol of peroxide/g] in [mol of peroxide/kg] and *m* – sample mass (g).

▪ *Determination of conjugated diene or triene concentration*

The method is based on the absorbance measurement at a fixed wavelength in UV field for a constant mass of emulsion sample, *i.e.* 236, or 267 nm for diene and 273 nm for conjugated triene [8]. A emulsion sample of 0.1 g was diluted with distilled water till 25 mL in a volumetric flask. The absorbance measurement of emulsion sample was performed at Camspecspectrophotometer M 500. The value for conjugated diene (CD) and triene (CT) concentration is calculated as in relation (3) or (4):

$$C_{CD} = \frac{A_{236/267} \cdot (2.5 \cdot 10^4)}{(\varepsilon \cdot l)/m} \quad (3)$$

$$C_{CT} = \frac{A_{273} \cdot (2.5 \cdot 10^4)}{(\varepsilon \cdot l)/m} \quad (4)$$

where: C_{CD} – molar concentration of conjugated diene (mol/kg, or mmol/g of emulsion), C_{CT} – molar concentration of conjugated triene (mmol/cm^{-3}), $A_{236/267}$ or A_{273} – absorbance of diluted emulsion at 236, or 267 nm, and 273 nm, ε – molar absorbance (extinction coefficient) for linoleic acid hydroperoxide ($\varepsilon = 2.525 \cdot 10^4$ M^{-1}·cm^{-3}), *l* – cuvette length (l = 1 cm) and *m* – sample mass (g).

RESULTS AND DISCUSSIONS

Emulsion appearance

Emulsions appearance is presented in figure 1.

According to microscopic images, the dispersed molecule phase is presented as a compact, dense small globule mass. Related to visual images, emulsions M_2 and M_3 are homogeneous, white, without agglomerations of particles and easily handle. Emulsions M_6 and M_7 are translucent and free of particles in suspension.

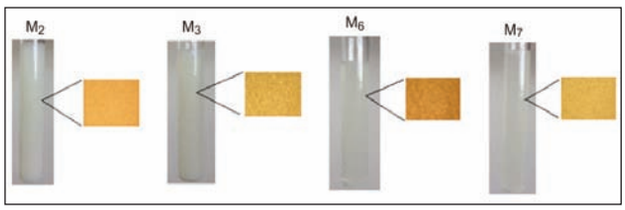

Fig. 1. Emulsions appearance

Physical-chemical analysis of emulsions

The physical-chemical properties of emulsions play a special role in preparation and further utilization of M_i emulsions based on mint essential oil and are dependent of the chemical and structural composition. Therefore, there are necessary serious investigations for selection of a few emulsion compositions with increased value and physical, oxidative and microbiological stability. In this context, there were determined a few basic quality indices of prepared M_i emulsions according with the international approved standard norms for cosmetic and food products.

The quality indices were determined at room temperature (19–22°C) during the period of emulsions storage for at least 4 weeks.

The selection of emulsion composition was performed for obtaining an optimal ratio of poly unsaturated fatty acids in triglycerides with curative-prophylactic properties, good application on textile fabrics and assurance of emulsion resistance to different oxidations and also obtaining of an acceptable acidity (aggression) on contact with skin.

In table 1 are presented some values of physical-chemical quality indicators of the investigated M_i emulsions.

The general physical-chemical quality indicators of the four investigated M_i emulsions were analyzed being in range of 67.26–78.9% for separated aqueous phase, 21.21–32.26 % for separated fatty phase (organic phase), 3.5–4.9 for pH, 1.0204–1.0310 g/cm^3 for average absolute density at 19°C, 1.0193–1.0307 g/cm^3 for mean density at 20°C and 1.0171–1.0299 g/cm^3 for mean density at 25°C. All these characteristics are corresponding to the standardized norms in cosmetic products.

During the storage period, the prepared M_i emulsions are supposed to possible degradation processes which can affect their quality. Usually, the emulsions can be slowly oxidized and converted in a complex organic system with a high number of components due to all oxidation steps (*i.e.* initiation, development and breaking of different macromolecular chains).

To analyze the in-time variation of prepared emulsions' quality is one of the important aim of this work. That is why it is important to establish the dynamic of primary oxidation products formed (*i.e.* hydroperoxides) during the storage of M_i emulsions, considering especially the acidity index (*AI*), peroxide index (*PI*), conjugated diene (*CD*) and triene (*CT*) concentrations. The analysis is performed for a period of 4 weeks at room temperature (19–23°C), in absence of light only in the night period.

The experimental results are summarized in table 2.

In period of emulsions storage can take place the oxidative and hydrolytic degradation which is characterized by formation of oxidation and hydrolysis products, expressed by the value of free fatty acids or fatty phase separation, and acidity index.

The value of acidity index in the four investigated M_i emulsions was varied in 4 weeks between 1.121 and

Table 1

SOME PHYSICAL-CHEMICAL QUALITY INDICES OF INVESTIGATED EMULSIONS

Physical-chemical quality indicators	**M_2**	**M_3**	**M_6**	**M_7**
Aqueous phase, [%]	78.79	69.70	67.26	77.50
Fattyphase (organic phase), [%]	21.21	30.30	32.26	22.50
pH (room temperature, t = 23.7°C)	3.5±0.3	4.8±0.2	5.0±0.2	4.9±0.2
Density (absolute, mean value), [g/cm^3]				
19°C	1.0310	1.0294	1.0204	1.0252
20°C	1.0307	1.0294	1.0193	1.0240
25°C	1.0299	1.0283	1.0171	1.0225
Acidity index, [mg KOH/g of emulsion]	1.1420	2.2716	0.8672	0.8944
Peroxide index, [mmol/g of emulsion]	6.7895	6.1627	5.7306	2.8020
Diene concentration, [μmol/g of emulsion]	2.998	9.370	3.840	1.856
Conjugated triene concentration, [μmol/g]	2.539	8.125	2.674	1.248
Stability in a month, [%]				
1-3 days	Stable	Stable	Stable	Stable
4 days	78.89	Stable	Stable	78.89
1 week	50.00	69.70	Stable	50.00
2 weeks	31.30	50.00	Stable	30.30
3 weeks	21.21	30.21	Stable	22.21

Table 2

ACCUMULATION OF PRIMARY LIPIDIC OXIDATION PRODUCTS IN PERIOD OF EMULSIONS STORAGE					
Physical-chemical quality indicators	**Storage period**	**M_2**	**M_3**	**M_6**	**M_7**
Acidity index (*AI*), [mg KOH/g of emulsion]	1 week	1.121	2.263	0.862	0.885
	2 weeks	1.123	2.268	0.863	0.889
	3 weeks	1.136	2.270	0.865	0.892
	4 weeks	1.142	2.272	0.867	0.894
Peroxide index (*PI*), [mmol/g of emulsion]	1 week	6.7884	6.1611	5.7297	2.7002
	2 weeks	6.7890	6.1613	5.7298	2.8005
	3 weeks	6.7894	6.1625	5.7306	2.8018
	4 weeks	6.7895	6.1627	5.7306	2.8020
Diene concentration (*CD*), [μmol/g of emulsion]	1 week	2.686	9.302	3.834	1.611
	2 weeks	2.712	9.325	3.836	1.618
	3 weeks	2.834	9.354	3.841	1.787
	4 weeks	2.998	9.370	3.840	1.856
Conjugated triene concentration (*CT*), [μmol/g of emulsion]	1 week	2.358	8.109	2.645	1.104
	2 weeks	2.404	8.118	2.659	1.116
	3 weeks	2.512	8.123	2.668	1.203
	4 weeks	2.539	8.125	2.674	1.248

1.142 mg KOH/g of emulsion for M_1, 2.263 and 2.272 mg KOH/g of emulsion for M_2, 0.862 and 0.867 mg KOH/g of emulsion for M_6 and 0.885 and 0.895 mg KOH/g of emulsion for M_7. Analyzing these AI_i values of prepared mint oil-based M_i emulsions in the period of their storage at room temperature, it can conclude that all AI_i values increase, fact which demonstrates the accumulation of free fatty acids. The values of acidity indices (AI_i) differ significantly, the highest being obtained for M_3 emulsion and the lowest for M_7. In addition, the fatty phase separated was the highest in the case of M_7 emulsion followed by M_3 emulsion. This fact can be explained by the high content of fatty acids with double and triple bonds, which are degraded much faster in the storage activity (at room temperature).

It is known that the presence of peroxide (hydroperoxide) in emulsion determines the degree of emulsion stability during the storage process (at room temperature). The values of peroxide index were not significantly changed after 4 weeks, varying for M_2 emulsion in range of 6.7884–6.7895 mmol/g, 6.1611–6.1627 mmol/g for M_3 emulsion, 5.7297–5.7306 mmol/g for M_6 emulsion and 2.7002–2.8020 mmol/g for M_7 emulsion. Based on the resulted experimental data, the highest peroxide concentration was performed in the case of M_2 which was found also with lowest stability in time at room temperature, followed by M_7 emulsion.

For the study of lipids oxidation, it must be analyzed the variation of conjugated diene and triene concentration which are produced from unsaturated fatty acids as result of hydroperoxide formation due to rearrangements of double bonds. The formed conjugated diene presents an intense absorption at the wave length of 234 nm or 267 nm, and in case of triene the intense absorption is registered at 273 nm. An increase of UV absorption indicates the formation of primary oxidation products in the investigated M_i emulsions. This fact concludes clearly that the storage of M_i emulsion at room temperature acts in direction of increasing the conjugated diene and triene concentrations. The highest value during 4 weeks of storage at room temperature was achieved for M_3 emulsion, *i.e.* 9.303–9.370 μmol/g of emulsion for diene concentration and 8.109–8.125 μmol/g of emulsion for triene concentration, and the lowest for M_7 emulsion, *i.e.* 1.611–1.856 μmol/g of emulsion for the diene concentration and 1.104–1.248 μmol/g of emulsion for the triene content.

In addition, the peroxides are instable compounds, but in the process of emulsion storage these can be decomposed forming secondary oxidation products as aldehydes, ketones and its derivates with carbonyl chain of different lengths. The peroxides have no direct influence on sensory indices of emulsions, but if aldehydes and ketones are formed, these have rancid odor. In the case of M_i emulsions it was found no such a rancid odor, being indicated that secondary oxidation products were not formed during the period of 4 weeks of emulsion storage at room temperature.

CONCLUSIONS

The physical-chemical quality indices of investigated M_i emulsions based on mint essential oil were indicated that the highest stability had the M_6 emulsion followed by M_3 emulsion.

The comparative analysis of experimental results performed for the acidity index, peroxide index, conjugated diene and triene concentration were permitted some preliminary information concerning the dynamic of M_i emulsion degradation during the storage activity at room temperature for a time period of 4 weeks. The results indicated the formation of primary oxidation products (hydroperoxides), but no formation of secondary oxidation products (aldehydes and ketones) with their specific rancid odor.

The general physical-chemical indicators of investigated M_i emulsions were found corresponding with

the standardized norms in cosmetics and textiles for topical applications.

ACKNOWLEDGEMENTS

This work was supported by a grant of the Romanian National Authority for Scientific Research and Innovation, CCCDI – UEFISCDI, project number 29/2018 COFUND-MANUNET III-AromaTex, project title *"Manufacturing of value-added textiles for aromatherapy and skin care benefits"*, within PNCDI III.

BIBLIOGRAPHY

[1] Bakry, A.M., Abbas, S., Ali, B., Majeed, H., Abouelwafa, M.Y., Liang, L. *Microencapsulation of oils: A Comprehensive review of benefits, techniques, and applications*. In: Bioengineering, 2017, vol. 4, p. 74.

[2] Horrocks, A.R., Anand, S.C. *Hand-book of Technical Textiles*. Published by Woodhead Publishing Limited in association with The Textile Institute, 2010.

[3] Montenegro, L., Lai, F., Offerta, A., Sarpietro, M.G., Micicche, L., Maccioni, A.M., Valenti, D., Fadda, A.M. *From nanoemulsions to nanostructured lipid carriers: A relevant development in dermal delivery of drugs and cosmetics*. In: Journal of Drug Delivery Science and Technology, 2016, vol. 32, p. 100.

[4] Radu, C.D., Cerempei, A., Salariu, M., Parteni, O., Ulea, E., Campagne, C. *The potential of improving medical textile for cutaneous diseases*. In: IOP Conference Series: Materials Science and Engineering, 2017, vol. 254, pp. 1–8.

[5] Milanovic, J., Manojlovic, V., Levic, S., Rajic, N., Nedovic, V., Bugarski, B. *Microencapsulation of flavors in Carnauba Wax*. In: Sensors, 2010, vol. 10, p. 901.

[6] Khanzadi, M., Jafari, S.M., Mirzaei, H., Chegini, F.K., Maghsoudlou, Y., Dehnad, D. *Physical and mechanical properties in biodegradable films of whey protein concentrate–pullulan by application of beeswax*. In: Carbohydrate Polymers, 2015, vol. 118, p. 24.

[7] Namdariyan, R., Farahbakhsh, A., Golestani, H.A. *Encapsulation ZnO nanoparticles by using beeswax*. In: Proceedings of the 2nd International Conference on Oil, Gas and Petrochemical Issues(ICOGPI'2013), 2013, Kuala Lumpur (Malaysia), p. 67.

[8] Capcanari, T. *Technologies of preparation of food emulsions from mixtures of sunflower oils and graves oil.* In: *Ph.D. Thesis*, Technical University of Republic of Moldova, 2012, p. 47.

[9] Banu, C., *Quality and quality control of food products*. AGIR Ed., Bucureşti, Romania, 2002, p. 55.

Authors:

Lecturer PhD. Eng. ANGELA DĂNILĂ[1]
Associate Prof. PhD. Eng. CARMEN ZAHARIA[2]
Prof. PhD. Eng. DANIELA ŞUTEU[2]
Lecturer PhD. Eng. EMIL IOAN MUREŞAN[2]
Prof. PhD. Eng. GABRIELA LISĂ[2]
SINEM YAPRAK KARAVANA[3]
ALI TOPRAK[4]
PhD. Eng. ALINA POPESCU[5]
PhD. Eng. LAURA CHIRILĂ[5]

[1] "Gheorghe Asachi" Technical University of Iasi, Faculty of Textile Leather Engineering and Industrial Management, Iasi, 29 Prof. Dr. Doc. Dimitrie Mangeron street, Romania

[2] "Gheorghe Asachi" Technical University of Iasi, Faculty of Chemical Engineering and Environmental Protection, Department of Environmental Engineering and Management, 73 Prof. Dr. Docent D. Mangeron Blvd, 700050 – Iasi, Romania

[3] Ege University, Faculty of Pharmacy, Department of Pharmaceutical Technology, 35100 Bornova, Izmir, Turkey

[4] DoğalDestekÜrünleriAraştırmaSanayiveTicaret A.Ş., AtburgazıMah. Abdiİpekçi Cad. No:70 Söke-AYDIN Turkey

[5] The National Research-Development Institute for Textiles and Leather Research, Bucuresti, Romania

e-mail: angela.cerempei@yahoo.com; czah@ch.uiasi.ro;dsuteu@ch.tuiasi.ro; eimuresan@yahoo.co.uk; gapreot@ch.tuiasi.ro;sinem.yaprak.karavana@ege.edu.tr; atoprak@dogaldestek.com.tr; alina.popescu@certex.ro; laura.chirila@certex.ro

Corresponding author:

CARMEN ZAHARIA

email: czah@ch.uiasi.ro or czaharia2003@yahoo.com

Indoor air quality of museums and conservation of textiles art works. Case study: Salacea Museum House, Romania

LILIANA INDRIE
DORINA OANA
MARIN ILIEȘ
DORINA CAMELIA ILIEȘ
ANDREEA LINCU
ALEXANDRU ILIEȘ

ȘTEFAN BAIAS
GRIGORE HERMAN
AURELIA ONET
MONICA COSTEA
FLORIN MARCU
LIGIA BURTA
IOAN OANA

REZUMAT – ABSTRACT

Calitatea aerului din interiorul muzeelor și conservarea operelor de artă din materiale textile. Studiu de caz: Casa-muzeu Sălacea, România

Prezenta lucrare analizează calitatea aerului (temperatură, umiditate, lumină, contaminare cu fungi) în interiorul Casei-muzeu din Sălacea, județul Bihor, și influența acestor factori asupra materialelor textile expuse în interior, în contextul necesității de a proteja elementele patrimoniului și de a diminua riscurile legate de sănătatea umană: locuitorii, turiștii, muzeografii și toți cei care au acces în interior. Monitorizarea temperaturii și a umidității a fost efectuată in perioada 03.06.2018 și 02.07.2018 și a fost utilizat termo-higrometrul KlimaLogg Pro (șapte senzori) cu funcția data logger, iar pentru ceilalți parametri analizați: loggerul de date Luxmeter Extech SDL400 și contorul de oxigen Extech SDL150. Contaminarea fungică a fost determinată folosind metoda de sedimentare Koch. Din cauza temperaturii scăzute și a umidității ridicate a aerului din mediul înconjurător, are loc dezvoltarea microorganismelor și a mucegaiului, iar temperaturile înalte pot duce la deshidratarea fibrelor, prin diminuarea rezistenței și scăderea elasticității acestora; de aceea este necesar să se mențină microclimatul standard al temperaturii și umidității în interiorul casei-muzeu.

Cuvinte-cheie: textil, patrimoniu cultural, casă-muzeu, microclimat, fungi, România

Indoor air quality of museums and conservation of textiles art works. Case study: Salacea Museum House, Romania

The present paper is analyzing the quality of the air (temperature, humidity, light, contamination with fungi) inside the Museum House from Salacea, Bihor county, and the influence of such factors on textile materials that are exposed inside it in the context of the need to protect the heritage elements and in order to diminish the risks related to human health: the inhabitants, the tourists, museographers and all those who have access to the interior. Monitoring of the temperature and humidity was carried out between 03.06.2018 and 02.07.2018 and we used the thermo-hygrometer with data function logger KlimaLogg Pro (seven sensors), and for other analyzed parameters: Luxmeter data logger Extech SDL400 Oxygen meter Extech SDL150. The fungal contamination was determined using Koch sedimentation method. Due to the fact that the low temperature together with the high air humidity of the ambient environment stimulates the formation of microorganisms and mold and high temperatures can dehydrate the fibers by diminishing their strength and decreasing their elasticity, therefore it is necessary to maintain the standard micro climate of temperature and humidity inside the museum house.

Keywords: textile, cultural heritage, museum house, microclimate, fungi, Romania

INTRODUCTION

Understood as a connection between the past and the future, cultural heritage is unique, vulnerable and irreplaceable, so its preservation connects with the legacy that each generation receives and transmits to the next.

Conserving and preserving cultural heritage is an interdisciplinary field that requires, on one side, a close collaboration between restorers, archaeologists, art historians, museum curators and conservators on the other side. This fact represents an important issue and many scientific works were prepared in this field of research [1–3].

A big responsibility in order to conserve, research, and exhibit cultural heritage lies with the museums.

Therefore, the goal of the present paper is to highlight the role of museums in conservation of the textile artwork, so we will further focus on the factors causing deterioration of the textiles inside museums.

Most of museum textiles are made of organic fibers, so they are exposed to different factors of degradation: human intervention/incompetence (such as

mishandling, improper storage and displaying, neglect) and environmental factors (light, temperature, humidity, pests, pollutants), and thus their vulnerability is huge.

There are some agents of deterioration that affect the museum textiles [4]:

a) Organic (pests and mold)

There are various rodents and insects (moths, silverfish, firebrats, carpet beetles) which can damage the fibers. The mold is another significant threat to museum textiles, being well known that there is no real cure once this is located in a fabric. Also, the dust can contain soil particles, fragment of human/animal skin and hair, soot and ash, spores, pollen which, in time, gets embedded between fibers and, in majority of cases, it is impossible to remove.

b) Physical

Light exposure (being natural or ultra violet light), high/ low humidity and heat progressively damage the textiles. Not only the colors change, but also the fibers lose their flexibility, becoming weak and fragile.

c) Chemical

The airborne pollution represents a high risk for textiles. Exposed to some noxious gases (Sulphur dioxide, nitrogen dioxide), to acidic or oxidizing substances the fibers can be damaged beyond repair.

d) Mechanical factors can refer to unappropriated procedures of storing and packing (e.g. textiles can be torn because they are stored folded, hung heavy embroidered dresses will eventually break on the shoulder area).

Therefore, conservation is not only the prime function of a museum, but a great challenge.

Among the researches concerning monitoring, controlling and prevention of the fungal deterioration of textile artifacts in the museum we mention those of Lazaridis et al., 2015 [3] and Kareem-Bbdel, 2010 [10] for Jordanian heritage and from Egypt; Spiros Zervosa et al., 2013 [11], about experimental design for the investigation of the environmental factors' effects on organic materials. Cavicchioli et al., 2014 [12] does a research on the particulate matter in the indoor environment of museum in the mega city of Sao Paolo; Kavkler et al., 2015 [13], about contamination of textile objects preserved in Slovene museums and religious institutions. Lech et al., 2015 [14], analyses microflora present on historical textiles with the use of molecular techniques. Di Carlo et al., 2016 [15], wrote about fungi and bacteria in indoor cultural heritage environments: microbial-related risks for artworks and human health.

CASE STUDY

The case study was carried out in the Museum House (figure 1) in Sălacea, Bihor county. It is located in the southern central part of the Sălacea village (according to http://www.cimec.ro/) and represents a servant peasant household from the second half of the 19th century; The material of the house is a beaten-cob construction and the roof is made of reed. The partition of the house includes a small room without natural lighting and a living room with 2 small windows (about 13 m^2). Inside the museum, the owner, Kéri Gáspár, exhibited ethnographic objects, such as furniture, traditional fabrics and other household items, various tools (figure 2). The purpose of this paper was to analyze and correlate the quality of the air (temperature, humidity, fungi content) inside the museum house and the influence of these factors on the objects exhibited inside the museum house, in the context of the need to protect the heritage elements and to reduce the risks related to human health: visitors, museographers, etc.

Our country is located in a geographical area with a temperate climate. Due to the existing topography, the tradition of growing plants containing bast fibers (flax, hemp, jute) and of growing sheep (for getting wool) over the years was transmitted from generation to generation. These are the reasons why in the past the Romanian folk costumes and the articles for decorating the peasant dwellings were made in their own households. So the textiles exhibited in the Museum House in Sălacea are majorly woven textiles such as Romanian traditional clothing, tapestries, textile furnishings, upholstery. The main group of material compositions consist of natural fibers such as hemp, flax, jute and wool.

The first step in conserving and preserving cultural and historic objects is to control the environmental conditions in which they are stored and exhibited. Our task was to find the external factors that have a corrosive effect on the textiles museum's collections. The microclimate factors that influence the physical-mechanical characteristics of textile fibers are mainly

a *b*

Fig. 1. Exterior (a) and interior (b) Museum House Sălacea (19th century), Bihor county

Fig. 2. The ethnographic collection inside the museum house:
a – Jute (the strap of the Romanian traditional bag); *b* – Wool; *c* – Flax; *d* – Hemp

temperature, relative humidity and sunlight. These are destructive factors of textile fibers, especially natural textile fibers. These natural fibers found in the composition of the materials exhibited in the museum house (figure 2) have appropriate hygienic-functional properties under standard microclimate conditions (air temperature 20 °C ± 2 °C and relative air humidity 65% ± 5%), the variation of these factors lead to the degradation of products made of natural fibers over time.

The microclimate inside the museum house was monitored during 03.06.2018 – 02.07.2018. The following equipment was used: thermo-hygrometer with data function logger Klimalogg Pro (seven sensors), Oxigenometer Extech SDL150; Luxmeter data logger Extech SDL400; Piranometer digital Voltcraft PL-110SM [5–9]. For isolation of fungi air sampling techniques were used. The fungal contamination was determined using the conventional techniques of open plates called Koch sedimentation method [6–9, 16, 17].

As a result of the air temperature and humidity analysis (figure 3) it was found that the average air temperature was 23.3 °C and the average relative humidity was 65%. The temperature should not exceed 22 °C (HG no. 1546/2003), always following its correlation with relative humidity (U.R.), and U.R. should generally be between 50% and 65%.

Concerning the fungal structures identified, the average values of fungi colonies inside the house museum there are 73 in the middle of the museum house, 63 in the corner and 39 in the ceiling level. Geotrichum can give risk factor related to immunosuppression, especially in haematological malignancies (e.g. acute leukaemia, associated with profound and prolonged neutropenia) [18]. Exposures to fungi

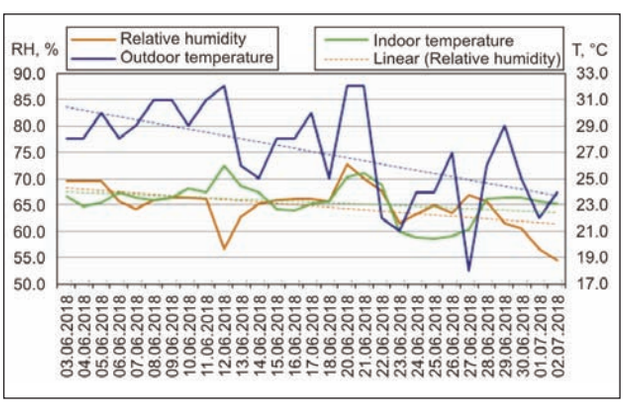

Fig. 3. Variation of air temperature and relative humidity inside and outside of Sălacea Museum House, during the period 03.06.2018 – 02.07.2018

and spores may cause allergic reactions such as sneezing, rhinorrhoea, coughing, eye irritation, skin rash. Fungi such as Cladosporium due to increased allergenic potential may represent a threat to human health if it is present in an increased concentration in closed environments without ventilation [19]. Rarely it is pathogenic to humans, but there have been reported infections of the skin, nails, sinuses and lungs [20–21]. From ascomycete fungi we found Alternaria [15], known as major aeroallergens, representing a major risk factor for the development, worsening and persistence of asthma and allergic rhinitis. Growing indoors can cause hypersensitivity reactions and fever or sometimes it can constitute a potential risk for asthma.

The following figure shows the position of sensors in order to monitor the microclimate and the locations of the fungi colonies inside the museum house.

The intensity measured indoors: 10 to 20 lux (and outside 85,000 lux).

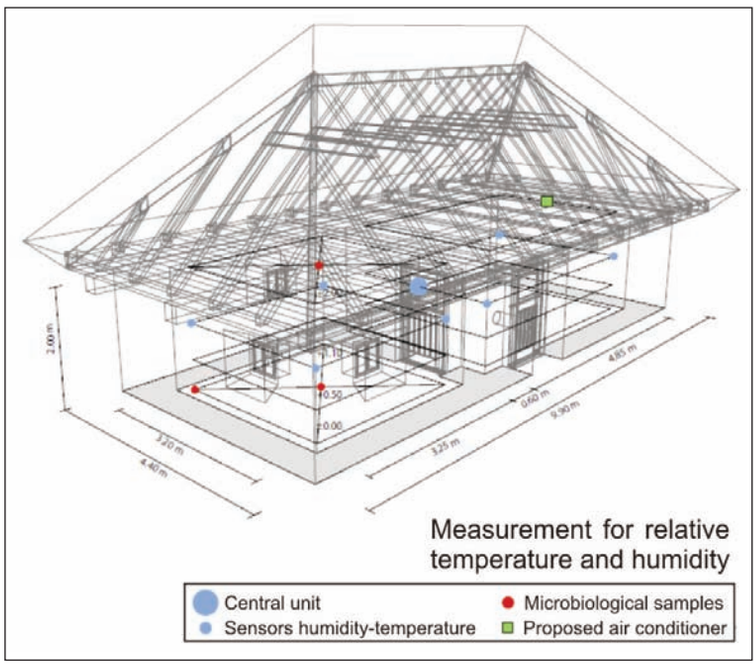

Fig. 4. 3D sketch microclimate monitoring sensors location and microbiological samples

Most of the products exhibited in the museum are flax, hemp and jute and are part of the Liberian fiber category. These fibers have similar properties with small specific differences due to their morphological structure and cellulosic chemical composition. Liberian fibers (flax, hemp, jute) are processed in the form of beads called technical fibers. These are made up of several cells joined together by means of medium-sized blades containing hemicellulose, lignin, etc. These fibers consist of several concentric layers of cellulose, arranged in three distinct areas. The specific morphological structure and chemical composites (cellulose) determine their properties [22–23].

Further on we will show how these fibers are influenced by the microclimatic factors inside the museum house.

Flax fibers can absorb moisture up to 30% of their own mass, hemp between 25% – 30% and jute up to 33%. Oxidative substances, including sunlight, have destructive effects on flax, hemp and jute fibers, resulting in yellowing the materials and reducing their strength over time. Flax is resistant to the attack of microorganisms, it dries quickly and is less affected by the action of light. It absorbs and gives off moisture easily, is a good heat conductor. Unlike flax, hemp textiles are not heat resistant because the fibers are breaking due to high temperature. Under the influence of air and light, the color of the jute turns dark brown. This fiber is less resistant than flax and hemp. Light, air and, above all, humidity make it breakable and reduce its resistance.

Another product exhibited in the museum house is made of harsh wool from Turcana sheep, a type of sheep specific to this area. Turcana sheep wool is a harsh type of wool from a morphologic point of view, of inferior quality, which has barely noticeable curls. The wool is a morphologically pluricelullar fiber, the fiber having 3 layers presenting a medullary canal, the scales of the fiber's structure are thick just like the roof tiles on top of a house. Due to the fact that the medullary layer is developed in the case of Turcana sheep wool, it has a reduced mechanical and chemical resistance as well as a low affinity for dyes. The specific behavior of Turcana sheep wool products is determined by this morphological structure and by the chemical (protein) composition [22–23].

Wool fibers are considered the most resistant to the action of light and atmospheric agents. This is considered the most hygroscopic natural textile fiber. Under normal conditions, wool absorbs from the air 15–18% water. In a humid atmosphere (ie relative air humidity higher than 70%) it can absorb up to 40% water. The water exchange is replenished faster than to fine wool. In wet condition, the strength of the wool decreases by approximately 10%. This decrease is due to the fact that water penetrates the macromolecules of keratin, weakening the forces of mutual attraction. As the temperature rises, the wool becomes fragile, its rigidity increases and the fibres become yellow. In conditions of increased humidity, the wool is attacked by microorganisms (fungi and bacteria) leading to fiber degradation. A much greater danger for wool is moths, heat is a determining factor in their development.

Because the majority of textile objects exhibited inside the museum house are made of natural fibres (flax, hemp, jute, wool) they are a target of microbial attack and degradation, resulting in the loss of structural strength, discoloration and the appearance of some stains. Uncontrollable microclimatic conditions can lead to contamination with fungi of the natural fiber due to their hygroscopic difference. Textile objects that are contaminated with fungi will produce undesirable effects on air quality that will negatively affect human health as they can generate or lead to accentuation of some respiratory diseases, allergic rhinitis, etc.

CONCLUSIONS

As a result of the results obtained during the analysis (average air temperature 23.3 °C; the mean value of relative humidity 65%, it was found that inside the museum house the two fundamental conditions necessary to ensure the optimal conditions of the microclimate are not fully met (air temperature 20 °C ± 2 °C and relative air humidity 65% ± 5%) in order to maintain the physico-mechanical and aesthetic properties of textile materials.

Low temperature together with the high air humidity of the ambient environment stimulate the formation of microorganisms and mold and high temperatures can dehydrate the fibers by diminishing their strength and decreasing their elasticity, so that it is necessary to maintain the standard microclimate of temperature and humidity. Poor air quality caused by pollution leads to dust and dirt. The light can cause the greatest damage, gradually causing colors to fade and turning uncolored textiles to yellow. These external changes are accompanied by a degradation of the fiber. To reduce the growth of fungi in the room, the installation of an air conditioner (figure 4) is recommended in order to ventilate the chambers twice a day for 30 minutes and to provide good ventilation because high humidity stimulates fungal growth.

ACKNOWLEDGEMENTS

The monitoring and sampling are not invasive for the museum house. The research was possible by equal scientific involvement of all authors. The authors wish to thank to anonymous reviewer for their thoughtful suggestions and comments and to acknowledge the support of the grant PN-III-P1-1.2-PCCDI-2017-0686.

BIBLIOGRAPHY

[1] Turcu, M. *Conservarea pieselor de muzeu* [Online]. Available: https://www.spiruharet.ro/facultati/istorie/biblioteca/f1b4945e65341cbf6962ca5a19e96351.pdf.

[2] *** *Selecting carpets and floor coverings for exhibit galleries and visitor centers*, In: Conserve O Gram series, Vol. 1/11, June 2001, [Online]. Available: https://www.nps.gov/museum/publications/conserveogram/01-11.pdf.

[3] Lazaridis, M., Katsivela, E., Kopanakis, I., Raisi, L., Panagiaris, G. *Indoor/outdoor particulate matter concentrations and microbial load in cultural heritage collections*, In: Heritage science, Lazaridis et al. Herit Sci (2015) 3:34, DOI 10.1186/s40494-015-0063-0.

[4] Donny Hamilton, L. *Methods of conserving underwater archaeological material culture*. In: Conservation Files: ANTH 605, Conservation of Cultural Resources I. Nautical Archaeology Program, Texas A&M University, World Wide Web, College Station, Texas 77807, 1998, p. 34 [Online]. Available http://nautarch.tamu.edu/CRL/conservationmanual/ConservationManual.pdf.

[5] Ilieș, A., Wendt, J.A., Ilieș, D.C., Herman, G.V., Ilieș, M., Deac, A.L. *The patrimony of wooden churches, built between 1531 and 2015, in the Land of Maramureș, Romania*. In: Journal of Maps, Nov 4; 12(sup1), pp. 597–602, 2016.

[6] Onet, A., Ilies, D.C., Buhas, S., Rahota, D., Ilies, A., Baias, S., Marcu, F., Herman, G.V., *Microbial air contamination in indoor environment of university Sport Hall*. In: Journal of Environmental Protection and Ecology 19 (2), pp. 694–703, 2018.

[7] Ilieș, D.C., Oneț, A., Marcu, F., Gaceu, O.R., Timar, A., Baias, Ș., Ilieș, A., Herman, G.V., Costea, M., Țepelea, M., Josan, I., Wendt, J. *Investigations regarding the air quality in the historic wooden church in Oradea City, Romania*. In: Environmental Engineering and Management Journal, 2018 (http://www.eemj.icpm.tuiasi.ro/pdfs/accepted/204_294_Ilie%C8%99_17.pdf).

[8] Ilieș, D.C., Buhaș, R., Ilieș, A., Gaceu, O., Oneț, A., Buhaș, S., Rahotă, D., Dragoș, P., Baiaș, Ș., Marcu, F., Oneț, C. *Indoor air quality issues. Case study: the multipurpose sports hall of the University of Oradea*. In: Environmental Engineering and Management Journal, 2018, (http://www.eemj.icpm.tuiasi.ro/pdfs/accepted/213_544_Ilies_17.pdf).

[9] Ilieș, D.C., Oneț, A., Wendt, J.A., Ilieș, M., Timar, A., Ilieș, A., Baias, Ș., Herman, G.V. *Study on microbial and fungal contamination of air and wooden surfaces inside of a historical Church from Romania*. In: Journal of Environmental Biology, 39, pp. 1–5, 2018.

[10] Kareem-Bbdel, O. *Monitoring, controlling and prevention of the fungal deterioration of textile artifacts in the museum of Jordanian heritage and from Egypt*. In: Mediterranean Archaeology and Archaeometry, Vol. 10, No. 2, pp. 85–96, 2010.

[11] Zervos, S., Choulis, K., Panagiaris, G. *Experimental design for the investigation of the environmental factors effects on organic materials (Project INVENVORG), The case of paper*. In: Procedia-Social and Behavioral Sciences, Aug 25; 147, pp. 39–46, 2014.

[12] Cavicchioli, A., Morrone, E.P., Fornaro, A. *Particulate matter in the indoor environment of museums in the megacity of São Paulo*. In: Química Nova, 37(9), pp. 1427–35, 2014.

[13] Kavkler, K., Gunde-Cimerman, N., Zalar, P., Demšar, A. *Fungal contamination of textile objects preserved in Slovene museums and religious institutions*. In: International Biodeterioration & Biodegradation, Jan 1;97, pp. 51–9, 2015.

[14] Lech, T., Ziembinska-Buczynska, A., Krupa, N. *Analysis of microflora present on historical textiles with the use of molecular techniques*. In: International Journal of Conservation Science, Apr 1;6(2), 2015.

[15] Di Carlo, E., Chisesi, R., Barresi, G., Barbaro, S., Lombardo, G., Rotolo, V., Sebastianelli, M., Travagliato, G., Palla, F. *Fungi and bacteria in indoor Cultural Heritage environments: microbial-related risks for artworks and human health.* In: Environment and Ecology Research, 4(5), pp. 257–64, 2016.

[16] Asadi, E., Costa, J.J., da Silva, M.G. *Indoor air quality audit implementation in a hotel building,* in Portugal. In: Building and Environment, 46 (8), pp. 1617–1623, 2011.

[17] Cernei, E.R., Maxim, D.C., Mavru, R., Indrei, L. *Bacteriological analysis of air (aeromicroflora) from the level of dental offices in Iaşi County Romanian*. In: Journal of Oral Rehabilitation, 5 (4), 2013.

[18] Alper, I., Michel, F., Labrie, S. *Ribosomal DNA Polymorphisms in the Yeast Geotrichum candidum*. In: Fungal Biology, 115 (12), pp. 1259–1269, 2011.

[19] Ogórek, R., Lejman, A., Pusz, W., Miłuch, A., Miodyńska, P. *Characteristics and taxonomy of Cladosporium fungi.* In: Mikologia Lekarska, 19 (2), pp. 80–85, 2012.

[20] Kirk, P.M., Cannon, P.M., Minter, P.F., Stalpers, D.W., Stalpers, J.A. *Ainsworth & Bisby's Dictionary of the Fungi*, 10th Edition, Cabi, 2008.

[21] Ranalli, G., Zanadini, E., Sorlini, C. *Biodeterioration – including cultural heritage*. In: M. Schaechter (Ed.), Encyclopedia of microbiology (pp. 191–205). Amsterdam: Elsevier, 2009.

[22] Bordeianu, D.L. *Fibre textile*, Ed. Universității din Oradea, 2005.

[23] Gribincea, V., Bordeianu, L. *Fibre textile – proprietăți generale*, Ed. Performantica, Iași, 2002.

Authors:

LILIANA INDRIE[1], DORINA OANA[1], MARIN ILIES[2], DORINA CAMELIA ILIEȘ[3], ANDREEA LINCU[3], ALEXANDRU ILIEȘ[3], ȘTEFAN BAIAS[3], GRIGORE VASILE HERMAN[3], AURELIA ONET[4], MONICA COSTEA[4], FLORIN MARCU[5], LIGIA BURTA[5], IOAN OANA[1]

[1]University of Oradea, Faculty of Energy Engineering and Industrial Management, Department of Textile, Leather and Industrial Management, B.St. Delavrancea Str. No. 4, 410058, Oradea, Romania

[2]University "Babes Bolyai", Faculty of Geography, Extension Sighetu Marmatiei, Cluj Napoca, Romania

[3]University of Oradea, Faculty of Geography, Tourism and Sport, 1st University Street, Oradea, 410087, Romania

[4]University of Oradea, Faculty of Environmental Protection, 26, Gen. Magheru Street, Oradea, Romania

[5]University of Oradea, Faculty of Medicine and Pharmacy, Oradea, Romania

e-mail: liliindrie@yahoo.com; oanaioanpavel@yahoo.com; marin_ilies@yahoo.com; iliesdorina@yahoo.com; lincu_andreea@yahoo.com; alexandruilies@gmail.com; stefanbaias.gts@gmail.com; grigoreherman@yahoo.com; tudor.caciora@yahoo.com; aurelia_onet@yahoo.com; costea.monica@yahoo.it; mfmihai27@yahoo.com; oliviaburta@gmail.com

Corresponding author:

LILIANA INDRIE

e-mail: liliindrie@yahoo.com

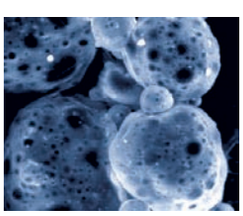

Validity of Washburn's equation in sericin treated polyester fabric

DASARATHAN KAMALRAJ VENKATRAMAN SUBRAMANIAM

REZUMAT – ABSTRACT

Valabilitatea ecuației lui Washburn în cazul țesăturii din poliester tratate cu sericină

Aplicarea sericinei pe țesăturile de poliester și bumbac aduce avantaje, prin faptul că materialele devin mai hidrofile și sunt capabile să confere un efect antimicrobian. De asemenea, materialele pot fi vopsite utilizând coloranți reactivi. S-a efectuat o analiză foarte amănunțită cu privire la aplicarea sericinei pe țesăturile din poliester și bumbac. Higroscopicitatea țesăturilor tratate a fost studiată și s-a demonstrat că a existat o îmbunătățire. O analiză detaliată a studiului este justificată în ceea ce privește higroscopicitatea, deoarece analiza efectuată a fost limitată. În acest studiu, a fost necesară validarea ecuației lui Washburn, care constituie o componentă importantă a cineticii higroscopicității. Este studiată valabilitatea ecuației lui Washburn pentru un set de date privind higroscopicitatea țesăturilor din poliester tratate cu sericină. Stratul de poliester netratat și cel tratat cu sodă caustică și plasmă, urmat de tratamentul cu sericină utilizând DMDHEU și glutaraldehida, a fost prelevat pentru studiile privind higroscopicitatea. Au fost utilizate două modele. Din analiza gradienților, s-a constatat că este utilizată ecuația lui Washburn.

Cuvinte-cheie: substanțe alcaline, intercept, tratament cu plasmă, gradient, higroscopicitate

Validity of Washburn's equation in sericin treated polyester fabric

Application of sericin to polyester and cotton fabrics will bring about a number of advantages in that the materials become hydrophilic and are capable of imparting antimicrobial effect. Also, the materials can be dyed using reactive dyes. A considerable amount of work has been carried out on the application of sericin to polyester and cotton fabrics. Wickability of treated fabrics has been studied and it was demonstrated that there was an improvement. A detailed analysis of study is warranted on wickability as the work done on it was scant. It is necessary to validate Washburn's equation which constitutes an important component of kinetics of wicking in this paper. The validity of Washburn's equation for a set of data on wickability of sericin treated polyester fabrics is studied. Untreated polyester fabric and treated with caustic soda and plasma followed by sericin treatment using DMDHEU and Glutaraldehyde were taken for wicking studies. Two models were used. From the slopes it is found that Washburn's equation is followed.

Keywords: alkali, intercept, plasma treatment, slope, wickability

INTRODUCTION

Wickability of fabrics has become an important test as it discloses information on comfort, dyeability and usefulness as a sportswear. A number of papers on the wickability of yarns and fabrics have been published and reviews have appeared [1]. The role of water in transporting moisture has been appreciated for a very long time. A considerable amount of work has been done on the application of sericin to polyester and cotton fabrics with a view to conferring antimicrobial property to them [2–4]. From the papers published it is found that wickability test, although was performed on the fabrics, has not been studied in detail.

Wicking is the spontaneous transport of a liquid driven into a porous system by a capillary force [5]. Wicking height is proportional to root of time.

Lucas-Washburn equation, which is a very popular one, includes properties such as surface tension, radius of the capillary, contact angle and viscosity of the liquid which has been used to study wickability. It is reported that the weft density pore size and the arrangement of void spaces in fabric have a significant effect on the wicking performance [6]. It is also reported that the motion of liquid in the void spaces between fibers in a yarn impacts the mechanism of fabric wicking critically [7]. It is found that the rate of movement of liquid is governed by the fibre arrangement in yarn which control the capillary size and continuity [8].

Validity of Washburn's equation can be checked by two models, namely

$$h^2 = c^2 t \quad \text{or} \quad h = c\sqrt{t} \tag{1}$$

$$h = c' t^k \tag{2}$$

Where h is wicking height, t – time and k – time exponent, c and c' are constants.

In this communication, the wickability of sericin treated polyester fabrics is dealt with. Although some data on wickability have been provided, they were not examined in detail. The applicability of Washburn's equation is discussed for a series of polyester fabrics that have been treated with sericin.

MATERIALS AND METHODS

Sericin was obtained from CSTRI Bangalore. Polyester fabric with plain weave having the specification of 133 g/m^2 weight with 55 ends per cm and 33 picks per cm was used for the study.

Modification of polyester fabric

Polyester fabric sample was scoured to remove any impurities and it was pretreated with alkali 1M (40 g/l) NaoH at 80°C for 45 min with 1:100 material to liquor ratio to create functional groups on its surface, before applying sericin to the fabrics.

Application of sericin

Sericin was applied on modified polyester fabric with and without the use of a crosslinking agent.
20 g/l of sericin solution was used. Alkali treated fabric were padded with the sericin solution in a laboratory padding mangle by a 2 dip 2 nip process. The padded fabric was dried at 80°C for 3 min and cured at 130°C for 2 min. Cured samples were then washed and dried. Glutaraldehyde was used as a crosslinking agent to attach sericin to alkali modified polyester.

Plasma treated with DMDHEU

The polyester fabric was prepared in the required dimension of 54×54 cm and weighed. This fabric was clamped to the frame and inserted in the plasma chamber between the two plates and pressure in the chamber was brought to 0 bar then the oxygen gas was passed to the chamber with the flow rate of 2 bar pressure. Initially the top side of the fabric was exposed to the plasma current 1.06 amp, plasma voltage 350 volt at temperature 29°C this was continued for 5 min. Then the bottom side of the fabric was exposed to the plasma current 1.53 amps, plasma voltage 300 volt at a temperature of 29°C for 5 min. After the process, the fabric was weighed again to determine the weight loss percentage.
The plasma treated fabric was then wetted in water along with Turkey Red Oil 2 g/l and immersed in the prepared solution (sericin 25% (owf) and Dimethylol Dihydroxy Ethylene Urea 150% (owf), polyethylene emulsion 2g/l based on weight of the sample) for dipping process and was carried out using material-to-liquor ratio of 1:9. This fabric was then padded in the 2dip-2nip padding mangles and curing process carried at the temperature of 140°C for 3 min. Plasma treatment changes the surface properties of the fabric [9].

Plasma treated with Glutaraldehyde (GA)

The required dimension of the plasma treated fabric was weighed and the fabric was wetted in water along with wetting agent (TRO) and then treated with the solution of Sericin 25% (owf),GA 20 g/l,magnesium chloride 10 g/l and acetic acid 1.0 ml/l using material-to-liquor ratio of 1:9. The above procedure was followed for both padding and curing.

Alkali treatment with DMDHEU and Glutaraldehyde

The same untreated polyester fabric was treated with 15% NaOH (owf) with the material-to-liquor ratio kept at 1:40, at 60°C for 30 min. This alkaline treated polyester fabric was then treated with sericin, Glutaraldehyde, magnesium chloride and acetic acid and sericin, DMDHEU, polyethylene emulsion combination as in the same manner above and then padded and then cured.

Untreated polyester with DMDHEU and Glutaraldehyde

Untreated polyester fabric was directly treated with DMDHEU with other chemicals and Glutaraldehyde with the above mentioned chemicals. Drying and curing were carried out at 140°C for 3 min.

Experimental

In this study, seven samples of polyester fabric such as polyester fabric treated with alkali (PA), untreated polyester treated with sericin and Glutaraldehyde (USG), polyester fabric with sericin and DMDHEU (USD), Polyester fabric treated with alkali followed with Sericin and Glutaraldehyde (ASG), polyester fabric treated with alkaline followed with sericin and DMDHEU (ASD), Polyester fabric treated with plasma followed with sericin and Glutaraldehyde (PSG), Polyester fabric treated with plasma followed with sericin and DMDHEU (PSD). Details of the polyester fabrics used are given in table 1.

Table 1

GEOMETRICAL PROPERTIES OF UNTREATED AND TREATED POLYESTER FABRIC

S.No.	Particulars	Ends/cm	Picks/ cm	GSM	Thickness (mm)
1	Polyester fabric treated with alkali (PA)	55	33	133	0.32
2	Untreated Polyester fabric with sericin and DMDHEU (USD)	54	32	134	0.31
3	Untreated polyester fabric with sericin and glutaraldehyde (USG)	55	34	135	0.32
4	Alkali treated polyester fabric with sericin and DMDHEU (ASD)	54	33	137	0.33
5	Alkali treated polyester fabric with sericin and glutaraldehyde (ASG)	55	34	138	0.32
6	Plasma treated polyester fabric with sericin and DMDHEU (PSD)	54	33	131	0.32
7	Plasma treated polyester fabric with sericin and glutaraldehyde (PSG)	54	33	133	0.32

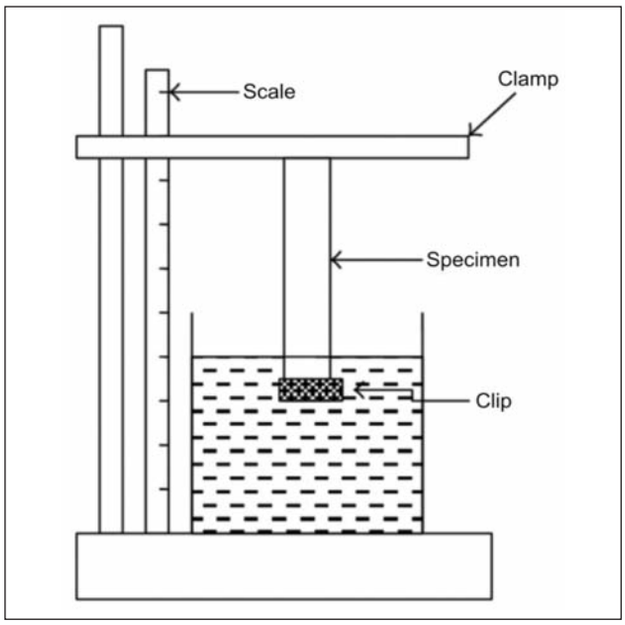

Fig. 1. Wicking test instrument

Determination of Wickability of treated and untreated fabrics

Wickability was studied by using vertical wicking method (DIN 53924 standard) as shown in figure 1.

RESULTS AND DISCUSSION

By plotting h^2 against t and using regression model passing through origin it will be possible to obtain values of K and check the applicability of Washburn's equation.

The evaluation of the h^2 as a function of time is determined for given times in the region of 0–600 s and the slopes are given in table 2. The curve obtained is linear and the experimental values lead to a linear regression coefficient of R^2 exceeding 0.99. It is necessary to get a correlation coefficient of more than 0.99, as only then will the Lucas Washburn's equation is followed.

The results of the wicking test are shown in tables 2 and 3.

Model A

Plotting height in cm^2 against the time sec gives the following values which are given in table 2.

Regression analysis has been done to get slope and intercept.

Model B

Values of slopes and intercepts are given in table 3, following model $h = c't^{k.}$

There are two models which are used to find out the validity of Washburn's equation. The first model is

$$h^2 = c^2t \quad \text{or} \quad h = c\sqrt{t} \tag{3}$$

$$h = c't^k \tag{4}$$

Where h is wicking height in cm and t – time in second. By plotting h^2 against t and using regression model passing through origin it will be possible to obtain values of k and check applicability of Washburn's equation. Values are shown in table 2.

The second model B is $h = c't^k$. This was proposed by Laughlin et al. [10] who suggested the following equation and Deboer [11] has also used this equation. It is interesting to note that Deboer [11] has not referred to Laughlin etals [10] paper in his study.

By taking logarithm on both sides

$$\ln(h) = k\ln(t) + \ln(c') \tag{5}$$

This model has been used by Nyoni [12] and Zhuang et al. [13] in their studies.

Table 3 gives the results, in this equation, there are strange units ln(c') of k and c parameters. c' is not intercept but equal to value of ln(h) for time t = 1. When h = 0, t = 0 and this leads to difficulties because ln(0) is minus infinity. Hence, while in X-axis the curve starts from zero, in Y-axis a finite value is

Table 2

VALUES OF THE SLOPE AND INTERCEPT USING MODEL $h^2 = c^2t$

Time (sec)	UT (cm)	USD (cm)	USG (cm)	ASD (cm)	ASG (cm)	PSD (cm)	PSG (cm)
Slope (cm^2/s)	0.02	0.06	0.05	0.05	0.06	0.04	0.06
Intercept	–1.15	1.03	–0.20	1.48	0.44	0.95	0.13
R^2	0.99	0.98	0.99	0.99	0.99	0.99	0.99

Table 3

VALUES OF THE TIME EXPONENT USING MODEL $h = c't^k$

Time (Sec)	PA (cm)	USD (cm)	USG (cm)	ASD (cm)	ASG (cm)	PSD (cm)	PSG (cm)
Slope (cm/min)	0.83	0.53	0.52	0.43	0.48	0.47	0.49
Intercept	–3.93	–1.57	–1.61	–1.05	–1.27	–1.37	–1.38
R^2	0.98	0.98	0.99	0.99	0.99	0.99	0.99

obtained by taking logarithm of wicking height values. Thus at 0 time, there is wicking which looks absurd. Another problem with regard to this model is that when wicking height and time have values less than 1, negative values are obtained. In this model when $K = 0.5$, it is taken that Washburn's equation is valid. Alternatively, the model $h^2 = c^2t$ is sound as for 0 time, 0 is the wicking [14–16]. This model is devoid of the deficiency as mentioned above.

CONCLUSION

Using the model $h^2 = c^2t$ the experimental results have shown that the wicking height square had a positive and high correlation with time in the warp direction ($R^2 = 0.99$) indicating that the Lucas – Washburn's equation was suitable for evaluating the wicking property of sericin treated polyester fabrics. This other model namely, $h = c't^k$ is not sound as there are strange units.

Acknowledgements

We sincerely thank Shri Mayavan Mills Erode and Csrti Bangalore for providing the polyester fabric and sericin respectively. One of the authors dr. V. Subramaniam would like to thank prof. Jiri Militky (technical university liberec) Czech Republic for his advice.

BIBLIOGRAPHY

[1] Subramaniam, V., Pramod, Raichurkar, *A review on wicking of yarn and fabrics,* In: International Journal of Textile Engineering and Processing, In: 2015, vol. 1, no. 2, pp. 1–4.
[2] Deepti Gupta, Harshita Chaudhary, Charu Gupta, *Sericin based bioactive coating for polyester fabric*, In: Indian Journal of Fibre Textile Research, 2015, vol. 40, no. 1, pp. 70–80.
[3] Deepti Gupta, Harshita Chaudhary, Charu Gupta, *Sericin-based polyester textile for medical applications*, In: The Journal of the Textile Institute, 2015, vol. 106, no. 4 , pp. 366–376.
[4] Deepti Gupta, Somes Bhaumik, *Antimicrobial treatments for textiles*, In: Indian Journal of Fibre Textile Research, 2007, vol. 32, no. 2, pp. 254–263.
[5] Harnett, P.R., Mehta, P.N., *A survey and comparison of laboratory test methods for measuring wicking*, In: Textile Research Journal, 1984, vol. 54, no. 7, pp. 471–478.
[6] Saricum, C., Kalaoglu, F. *Investigation of the wicking and drying behavior of polyester woven fabrics*, In: Fibres & Textile in Eastern Europe, 2014, vol. 22, no. 3, pp. 73–78.
[7] Rajagopalan, D., Aneja, A. *Modeling capillary flow in complex geometries*, In: Textile Research Journal, 2001, vol. 71, no. 9, pp. 813–821.
[8] Hollies, N.R.S., Kaessinger, M.M., Watson, B.S., Bogaty, H. *Water transport mechanisms in textiles materials. Part II: Capillary-type penetration in yarns and fabrics*, In: Textile Research Journal, 1957, vol. 27, no. 1, pp. 8–13.
[9] Loghin, C., Muresan, R., Ursache, M., Muresan, A. *Surface treatments applied to textile material and implications on their behavior in wet conditions*, In: Industria Textila, 2010, vol. 61, no. 6, pp. 284–290.
[10] Laughlin, R.D., Davies, J.E. *Some aspects of capillary adsorption in fibrous textile wicking*, In: Textile Research Journal, 1961, vol. 31, no. 10, pp. 904–910.
[11] DeBoer, J.J. *The wettability of scoured and dried cotton fabrics*, In: Textile Research Journal, 1980, vol. 50, no. 10, pp. 624–631.
[12] Nyoni, A.B., Brook, D. *Wicking mechanism in yarns – the key to fabric wicking performance*, In: The Journal of Textile Institute, 2006, vol. 97, no. 2, pp. 119–128.
[13] Zhuang, Q., Harlock, S.C., Brook, D.B. *Transfer wicking mechanisms of knitted fabrics used as undergarments for outdoor activities*, In: Textile Research Journal, 2002, vol. 72, no. 8, pp. 727–734.
[14] Kamath, Y.K., Hornby, S.B., Weigmann, H.D., Wilde, M.F. *Wicking of spin finishes and related liquids into continuous filament yarns*, In: Textile Research Journal, 1994, vol. 64, no. 1, pp. 33–40.
[15] Ansari, N., Kish, M.H. *The wicking of water in yarn as measured by an electrical resistance technique*, In: Journal of Textile Institute, 2000, vol. 91, no. 3, pp. 410–419.
[16] Sharabaty, T., Biquenct, F., Dupus, D., Viallier, P. *Investigation on moisture transport through polyester/cotton fabrics*, In: Industrial Journal Fiber Textile Research, 2008, vol. 33, no. 4, pp. 419–425.

Authors:

DASARATHAN KAMALRAJ[1], VENKATRAMAN SUBRAMANIAM[2]

[1] Anna Univeristy, Textile Technology, Department of Handloom &Textile Technology, Indian Institute of Handloom Technology, Foulke's Compound, Thillai Nagar, Tamilnadu, Salem – 636001, India

[2] Anna University, Textile Technology, Department of Textile Technology, Jaya Engineering College, CTH Road, Thiruninravur, Chennai – 602024, Tamilnadu, India

e-mail: kamalraj3448@gmail.com; vsubram@hotmail.com

Corresponding author:

DASARATHAN KAMALRAJ

e-mail: kamalraj3448@gmail.com

INFORMATION FOR AUTHORS

Industria Textila magazine is an international peer-reviewed journal published by the National Research & Development Institute for Textiles and Leather – Bucharest, in print editions.

Aims and Scope: *Industria Textila* magazine welcomes papers concerning research and innovation, reflecting the professional interests of the Textile Institute in science, engineering, economics, management and design related to the textile industry and use of fibres in consumer and engineering applications. Papers may encompass anything in the range of textile activities, from fibre production through textile processes and machines, to the design, marketing and use of products. Papers may also report fundamental theoretical or experimental investigations, practical or commercial industrial studies and may relate to technical, economic, aesthetic, social or historical aspects of textiles and the textile industry.

Submission of Manuscripts
The paper submitted for publication shall concern problems associated with production and application of fibers and textiles.

Please include full postal address as well as telephone/ fax/e-mail details for the corresponding author, and ensure that all correspondence addresses are included. Also include the scientific title of the authors.

Industria Textila magazine considers all manuscripts on the strict condition that they have been submitted only to the *Industria Textila* journal, on this occasion, and that they have not been published already, nor are they under consideration for publication or in press elsewhere. Authors who fail to adhere to this condition will be charged with all costs which *Industria Textila* magazine incurs and their papers will not be published.

Manuscripts
Manuscripts of the following types are accepted:
Research Papers – An original research document which reports results of major value to the Textile Community
Notes – see below
Book Reviews – A brief critical and unbiased evaluation of the current book, normally invited by the Editor
Correspondence – Communications based on previously published manuscripts

Manuscripts shall be submitted in English in double-spaced typing, A4 paper, size font 10, Arial, margins 2 cm on all sides, under electronic version in Word for Windows format.

The volume of the submitted papers shall not exceed 10 pages (including the bibliography, abstract and key words), typescript pages including tables, figures and photographs.

All articles received are reviewed by a reviewer, renowned scientist and considered expert in the subject the article concerns, which is appointed by the editorial board. After the article has been accepted, with the completions and the modifications required by the reviewer or by the editorial staff, it will be published.

The submission of the above-mentioned papers is by all means the proof that the manuscript has not been published previously and is not currently under consideration for publication elsewhere in the country or abroad.

There may also be published papers that have been presented at national or international scientific events, which have not been published in volume, including the specification related to the respective event.

The articles assessed as inappropriate by the reviewer or by the editorial staff, concerning the subject matter or level, shall not be published.

The manuscript shall be headed by a concise title, which should represent in an exact, definite and complete way the paper content. Authors should also supply a shortened version of the title, suitable for the running head, not exceeding 50 character spaces.

The manuscript shall also be headed by complete information about the author(s): titles, name and forename(s), the full name of their affiliation (university, institute, company), department, city and state, as well as the complete mailing address (street, number, postal code, city, country, e-mail, fax, telephone).

Tables and figures (diagrams, schemes, and photographs) shall be clear and color, where possible.

The photographs shall be sent in original format (their soft), or in JPEG or TIF format, having a resolution of at least **300 dpi**.

All tables and figures shall have a title and shall be numbered with Arabic numerals, consecutively and separately throughout the paper, and referred to by the number in the text.

Generally, symbols and abbreviations shall be used according to ISO 31: specifications for quantities, units and symbols. SI units must be used, or at least given comprehensive explanations or their equivalent.

Cited references shall be listed at the end of the paper in order of quotation and contain: **for a paper in a periodical** – the initials and surname of the author(s), title of journal and of the article, year and number of issue, number of volume and page numbers; **for a book** – the initial and surname of the author(s), full name of the book, publisher, issue, place and year of publishing, and the pages cited; **for patents** – the initial and surname of the author(s), the title, the country, patent number and year.

[1] Popescu, D., Popa, I., Cicea, C., Iordănescu, M. *The expansion potential of using sales promotion techniques in the Romanian garments industry*. In: Industria Textilă, 2013, vol. 64, issue 5, pp. 293-300

Authors are requested to send an abstract of the paper, preferably no longer than 100 words and a list of 5-6 key words (preferably simple, not compound words, in alphabetical order). Avoid abbreviations, diagrams and direct reference to the text.

All manuscripts with the material proposed for publication, shall be sent to:

certex@certex.ro

Complimentary issue – The corresponding author will receive a complimentary print copy of the issue in which his/her article appears. It will be up to the corresponding author if he/she decides to share or route his/her copy to his/her co-author(s).